



Durham E-Theses

Point discharge pulse measurements in atmospheric electricity

Stromberg, I. M.

How to cite:

Stromberg, I. M. (1968) *Point discharge pulse measurements in atmospheric electricity*, Durham theses, Durham University. Available at Durham E-Theses Online: <http://etheses.dur.ac.uk/8750/>

Use policy

The full-text may be used and/or reproduced, and given to third parties in any format or medium, without prior permission or charge, for personal research or study, educational, or not-for-profit purposes provided that:

- a full bibliographic reference is made to the original source
- a [link](#) is made to the metadata record in Durham E-Theses
- the full-text is not changed in any way

The full-text must not be sold in any format or medium without the formal permission of the copyright holders.

Please consult the [full Durham E-Theses policy](#) for further details.

POINT DISCHARGE PULSE MEASUREMENTS
IN ATMOSPHERIC ELECTRICITY.

by

I.M. STROMBERG, B.Sc.

A Thesis Presented In Candidature for the Degree of
Doctor of Philosophy in the University of Durham.

September 1968.

The copyright of this thesis rests with the author.
No quotation from it should be published without
his prior written consent and information derived
from it should be acknowledged.



CONTENTS

	Page
FOREWORD	(i)
ABSTRACT	(iii)
<u>CHAPTER 1. POINT DISCHARGE IN ATMOSPHERIC ELECTRICITY</u>	
1.1 <u>An outline of atmospheric electricity</u>	
1.1.1 Introduction	1
1.1.2 The electrosphere and the fine weather potential gradient.	1
1.1.3 Conduction currents	2
1.1.4 The electrification of clouds	4
1.1.5 Point discharge and lightning discharge currents.	5
1.2 <u>The Importance of point discharge in atmospheric processes.</u>	
1.2.1 The maintenance of the earth's charge	6
1.2.2 The potential of the Electrosphere	6
1.2.3 The charge on the Electrosphere	7
1.2.4 The charge balance	9
1.2.5 Fine weather conduction currents	9
1.2.6 Precipitation currents	9
1.2.7 Lightning discharge currents	10
1.2.8 Point discharge currents	10
1.2.9 Conduction currents above storm clouds	11
1.3 <u>The pulsed nature of point discharge currents</u>	
1.3.1 The process of ionization by collision	12
1.3.2 Characteristics of positive pulses	13
1.3.3 Characteristics of negative pulses	13.

	Page
1.4 <u>The relation between point discharge and other parameters.</u>	
1.4.1 Potential gradient	14
1.4.2 The effect of wind speed	15
1.4.3 The "effective separation" of points	16
1.4.4 Space Charge considerations.	17
1.5 <u>Previous measurements of natural point discharge</u>	
1.5.1 Measurements with isolated points	18
1.5.2 Direct measurements of point discharge on trees.	18
1.5.3 Indirect measurements of point discharge on trees.	19
1.6 <u>Outstanding problems in the measurement of natural point discharge.</u>	
1.6.1 Limitations of measurements from isolated points.	20
1.6.2 Limitations of previous measurements	21
1.6.3 The measurement of point discharge on representative trees.	22

CHAPTER 2. APPROACH TO THE PRESENT WORK

2.1 <u>Introduction</u>	24
2.2 <u>Preliminary observations of point discharge Pulses.</u>	
2.2.1 Introduction	25
2.2.2 Negative Point	25
2.2.3 Positive Point	27
2.2.4 Pulses from a small tree	28
2.2.5 The d.c. levels in pulse waveforms	29

2.3	<u>Theoretical considerations on the pulse shape</u>	
2.3.1	An idealized form for the pulse shape	29
2.3.2	The d.c. levels in pulse waveforms	30
2.3.3	The input time constant and rise time of the measuring equipment.	31
2.4	<u>Conclusion</u>	36
<u>CHAPTER 3.</u>	<u>INSTRUMENTATION FOR LABORATORY MEASUREMENTS OF POINT DISCHARGE PULSES.</u>	
3.1	<u>Introduction</u>	38
3.2	<u>Choice of measuring techniques</u>	
3.2.1	Amplitude measurement	38
3.2.2	Measurement of pulse repetition frequency	39
3.2.3.	Performance required from the system	41
3.3	<u>General description of the system used</u>	41
3.4	<u>The electronic circuitry</u>	
3.4.1	The time constant and galvanometer circuit	42
3.4.2	Variable attenuator	43
3.4.3	Pulse Inverter	43
3.4.4	The pulse amplifiers	44
3.4.5	Differential Pulse Height Selector	45
3.4.6	Integrating frequency meter	46
3.4.7	Control Unit	46

	Page
3.4.8 1 MHz scaler	48
3.4.9 100 kHz scalers	49
3.4.10 3 kHz Scaling Unit	51
3.4.11 Power Supplies	51
3.5 <u>Performance of the system</u>	51

CHAPTER 4. LABORATORY MEASUREMENTS WITH METAL POINTS

4.1 <u>Introduction</u>	53
4.2 <u>Apparatus</u>	53
4.3 <u>Techniques of measurement</u>	
4.3.1 Positive Currents	55
4.3.2 Negative Currents	56
4.4 <u>Results for Positive Currents</u>	
4.4.1 Potential - Current Characteristics.	57
4.4.2 Frequency - Current Characteristics.	58
4.4.3 Pulse amplitude - Current Characteristics	58
4.4.4 The standard deviation of pulse intervals	59
4.4.5 The distribution of pulse amplitude	61
4.5. <u>Results for Negative Currents</u>	
4.5.1 Potential - Current Characteristics	61
4.5.2 Frequency - Current Characteristics	62
4.5.3 Pulse amplitude measurements	63
4.6 <u>Conclusion</u>	64

<u>CHAPTER 5.</u>	<u>LABORATORY EXPERIMENTS WITH NATURAL POINTS</u>	
5.1	<u>Introduction</u>	65
5.2	<u>Apparatus</u>	66
5.3	<u>Techniques of Measurement</u>	66
5.4	<u>Results for positive currents</u>	
5.4.1	Potential - current characteristic	67
5.4.2	Frequency - current characteristic	67
5.4.3	Pulse amplitude - current characteristic	68
5.4.4.	The standard deviation of the pulse intervals.	68
5.4.5.	The distribution of pulse amplitude	69
5.5	<u>Results for negative currents</u>	
5.5.1	Potential - current characteristic	69
5.5.2	Pulse frequency measurements	70
5.5.3	Pulse amplitude measurements	70
5.6	<u>The Capacitative Electrode</u>	
5.6.1	Electrical connection of measuring equipment to natural points	71
5.6.2	Design of a capacitative electrode	72
5.6.3	Performance of a trial electrode	73
5.7	<u>Conclusion</u>	73
<u>CHAPTER 6.</u>	<u>THE APPLICATION OF THE LABORATORY EXPERIMENTS TO THE MEASUREMENT OF NATURAL POINT DISCHARGE</u>	
6.1	<u>The pulsed nature of point discharge as a basis for measurement</u>	75
6.2	<u>The capacitative electrode on full-size trees</u>	75
6.3	<u>Measurement of positive and negative currents in trees.</u>	76
6.4	<u>Conclusion</u>	77

	Page
<u>CHAPTER 7. THE FIELD EXPERIMENT AT LANEHEAD</u>	
7.1 <u>Initial considerations</u>	78
7.2 <u>The site and facilities at Lanehead</u>	79
7.3 <u>The parameters measured</u>	
7.3.1 Measurements on trees	81
7.3.2 Potential gradient	82
7.3.3. Point discharge on an elevated metal point	82
7.3.4 Other Parameters	83
7.4 <u>A summary of the aims of the experiment</u>	83
<u>CHAPTER 8. INSTRUMENTATION AT LANEHEAD</u>	
8.1 <u>Introduction</u>	85
8.2 <u>The general difficulties of field work at Lanehead.</u>	85
8.3 <u>Layout of equipment at Lanehead</u>	87
8.4 <u>The instrument housing</u>	88
8.5 <u>Power Supplies</u>	89
8.6 <u>Earthing</u>	90
8.7 <u>The automatic recording system</u>	90
8.8 <u>The field mill</u>	91
8.9 <u>The elevated metal point</u>	94
8.10 <u>Windspeed and direction</u>	94
8.11 <u>Wet and dry bulb temperature</u>	94
8.12 <u>Allocation of recording channels</u>	95

	Page
<u>CHAPTER 9. THE DETECTOR FOR POINT DISCHARGE ON TREES</u>	
9.1 <u>Introduction</u>	96
9.2 <u>Initial considerations on electrode design</u>	96
9.3 <u>Construction of the electrodes on four trees</u>	98
9.4 <u>Early versions of the detector</u>	99
9.5 <u>The addition of a selective radio frequency filter</u>	100
9.6 <u>The new approach</u>	101
9.7 <u>Further improvements</u>	103
9.8 <u>First successful measurements of point discharge pulses</u>	104
9.9 <u>Performance and calibration of final form of detector.</u>	105
9.10 <u>Conclusion</u>	106
<u>CHAPTER 10. THE POINT DISCHARGE CURRENT MEASUREMENTS AT LANEHEAD.</u>	
10.1 <u>Introduction</u>	107
10.2 <u>Analysis of recorded data</u>	
10.2.1 Objects of the analysis	108
10.2.2 Potential gradient measurements	108
10.2.3 Point discharge on the elevated metal point	109
10.2.4 Point discharge on trees	110

	Page
10.3 <u>Results for potential gradient and point discharge on the elevated metal point</u>	
10.3.1 Monthly distributions for potential gradient and point discharge.	111
10.3.2 Potential gradient and point discharge distributions for the total period	112
10.3.3 The duration and mean values of the potential gradient	113
10.4 <u>Results for point discharge on trees</u>	
10.4.1 A single tree on the edge of the plantation	114
10.4.2 Point discharge on a tree inside the plantation	116
10.5 <u>Signals other than point discharge pulses received by the trees.</u>	118
<u>CHAPTER 11. DISCUSSION OF THE RESULTS OF THE LANEHEAD FIELD EXPERIMENT</u>	
11.1 <u>The techniques of measurement of natural point discharge</u>	120
11.2 <u>The transfer of charge by point discharge on trees at Lanehead</u>	127
<u>CHAPTER 12. SUGGESTIONS FOR FURTHER WORK</u>	
12.1 <u>The improvement of measuring equipment</u>	134
12.2 <u>Further experiments</u>	135
<u>REFERENCES</u>	137

FOREWORD

The work in this thesis falls into two distinct parts. Laboratory experiments conducted at Durham are first described, followed by an account of field work in Weardale.

The S.I. system of units is used exclusively in the theoretical work and in most other cases.

Throughout the thesis, the sign of the atmospheric potential gradient is taken as positive if a small positive charge would tend to move towards the earth in the fine weather potential gradient. The term "field" is not used where its sign is important. Currents are taken as positive if they tend to neutralise the Earth's negative bound charge, i.e. transfer positive charge downwards or negative charge upwards.

I wish to express my sincere thanks to my supervisor for the last year and a half, Dr. W.C.A. Hutchinson, and also to the late Professor J.A. Chalmers, who supervised the first part of the work and continued to take an active interest up to the time of his death. Thanks are also due to Professor G.D. Rochester, F.R.S., for the provision of the research facilities in the Department, to the Physics Department workshop staff, especially Mr. Jack Moralee, for their assistance, and to the United States Office of Naval

Research for financial support under contracts numbers N62558-4299 and F61052-68-C-007(NR082-199). It is a pleasure to thank Professor W.B. Fisher for the use of the Department of Geography's field station in Weardale. I must also thank my fellow research students in the Atmospheric Physics Group, particularly Mr. G.T. Sharpless, for their interest in, and useful suggestions towards the work.

Finally, the typescript was prepared by Mrs. J. Popplewell, to whom I am very grateful for her speed and efficiency.

ABSTRACT

Previous methods for estimating the charge transferred to earth by point discharge are reviewed. It is concluded that point discharge on trees may well make a large contribution to this transfer of charge but that no reliable method of measurement has previously been devised.

A laboratory study of the pulsed nature of the point discharge currents produced at metal points and natural points has been made. It is concluded from these measurements that the amplitude and repetition frequency of these current pulses can be used to give the total discharge current.

A new method for measuring point discharge currents in trees has now been developed and the apparatus successfully calibrated. This takes the form of a capacitative electrode, attached to a branch at the top of a tree, which detects pulses of point discharge current in the tree. The electrode is connected to an electronic pulse detector which gives a measure of the point discharge current in the tree.

Measurements of point discharge currents have been made in two trees over a period of three months in a plantation of conifers in Weardale. The potential gradient and the point discharge current through a metal point were measured outside the plantation over a period of eleven months. The charge transferred to earth by point discharge on one tree in three months was found to be $4.3 \times 10^{-4} \text{ C}$ whereas for the metal point in the same period the charge transferred was $72 \times 10^{-4} \text{ C}$. It is concluded that this difference is a result of the higher potential gradients necessary to initiate point discharge on the tree compared with those for the metal point. The point discharge measurements for two trees, one on the edge and one inside the plantation, are compared and found to be of similar magnitudes. The charge per unit area transferred to earth by point discharge on all the trees in the plantation is estimated to be $270 \text{ C km}^{-2} \text{ yr}^{-1}$.

CHAPTER 1.Point Discharge in Atmospheric Electricity1.1 An outline of atmospheric electricity1.1.1 Introduction

Atmospheric electricity is in general concerned with the study of the electrical phenomena in the atmosphere between two conducting surfaces, those of the earth and the lower region of the ionosphere. The surfaces form the two plates of a spherical capacitor, which has as a dielectric the poorly conducting atmosphere.

1.1.2 The electrosphere and the fine weather potential gradient.

The existence of a conducting layer in the upper atmosphere was first suggested by KELVIN (1860) and later by HEAVISIDE (1902) and KENNELLY (1902). Experiments involving the reflection of radio waves from regions of the upper atmosphere have given definite evidence of a conducting region, known as the ionosphere, at altitudes greater than about 100 km. From the point of view of atmospheric electricity the atmosphere becomes a good conductor at altitudes above 50 km. This lower region is often referred to as the "electrosphere".



In fine weather the potential in the atmosphere, with respect to the earth, rises with increasing height. We therefore have a positive potential gradient in the atmosphere under fine weather conditions. It has always been considered that the electrosphere and the earth, from the point of view of electrostatics, are both good conductors, so that there is practically no variation in potential over each of the two surfaces. However, this assumption is now in question. It has been found that the electrosphere is at a positive potential with respect to the earth. The potential of the electrosphere shows annual and diurnal variations and has an average value of about 2.9×10^5 V.

1.1.3 Conduction currents.

The fact that there is a potential difference between the earth and the electrosphere and that the air between the two surfaces is a poor conductor means that a small positive conduction current flows through the atmosphere to earth in fine weather. The conduction current in the atmosphere consists of the flow of ions which have been produced mainly by the effects of cosmic radiation or by radioactivity at the earth's surface.

If V is the potential of the electrosphere with respect to the earth and R is the resistance of a column of air, of unit cross-sectional area, between the earth and the electrosphere, then:-

$$i = V/R$$

As i is a current density R must have the dimensions $\Omega \text{ m}^2$. If r is the resistance of, for example, the lowest metre of this column of air and F is the potential drop over this section, then, if the effect of any space charge can be neglected, we have

$$F = ir = Vr/R$$

F will be the average potential gradient over the lowest metre of the column. If we use the specific conductivity of the air \mathcal{K} ($\Omega^{-1} \text{ m}^{-1}$) instead of r , we have:-

$$F = i/\mathcal{K} = V/R$$

$$\text{or } i = \mathcal{K}F$$

Typical values for the above parameters in fine weather are given below.

PARAMETER	VALUE
Air earth conduction current (i)	$+2.4 \times 10^{-12} \text{ A m}^{-2}$
Specific conductivity (ρ)	$1.8 \times 10^{-14} \Omega^{-1} \text{ m}^{-1}$
Potential gradient (F)	$+130 \text{ V m}^{-1}$

1.1.4 The electrification of clouds.

It was thought, first by FRANKLIN (1752) and later by WILSON (1925) that storm clouds often have a concentration of positive charge in their upper regions and a lower negative charge. The existence of a separation of charge in a storm cloud, which one can consider in a simplified way as an electrostatic dipole, may give rise to high values of both positive and negative potential gradients at the earth's surface in disturbed weather. This means that air-earth conduction currents in disturbed weather may be either positive or negative with respect to the fine weather conduction current, and up to two orders of magnitude greater than the fine weather value.

1.1.5 Point discharge and lightning discharge currents.

The ions present in the atmosphere are normally produced by radioactivity or by cosmic radiation. If the potential gradient in the air is sufficiently large, then there may be fresh ionization caused by the ions already present. This is the process of ionization by collision. The potential gradient in the region beneath a thundercloud can reach values of many thousands of volts per metre. When ionization by collision occurs over a large distance a lightning discharge takes place. The process is of course much more complex than this, see CHALMERS (1967) and MALAN (1963). If the ionization by collision is confined to a small volume of air surrounding an earthed point, where the potential gradient is locally enhanced, there is the phenomenon of point discharge, which is also known as corona discharge or St. Elmo's Fire. The magnitude of point discharge currents can be of the order of a few micro-amperes, whereas the current in a lightning discharge may be many thousands of amperes. However, the duration of the lightning discharge is only a fraction of a second whereas point discharge may continue for periods as long as an hour.

1.2 The importance of point discharge in atmospheric processes

1.2.1 The maintenance of the earth's charge.

As was mentioned in 1.1.2, there is usually a positive potential gradient in the air in fine weather giving a negative bound charge on the surface of the earth below. However, there is also a positive air-earth conduction current coming to earth tending to neutralise the negative bound charge. It was shown by SCRASE (1933) that, under typical fine weather conditions, a positive charge equal in magnitude to the negative bound charge would be brought to earth by the conduction current in about 50 minutes. The problem is to explain how the earth's bound charge remains constant under fine weather conditions. The answer must be that, as the earth is a conductor, an equal negative charge has arrived over some other region of the earth's surface.

1.2.2 The potential of the Electrosphere.

CLARK (1958) showed that the best value for the mean potential of the electrosphere with respect to the earth is $2.9 \pm 0.3 \times 10^5$ V. CLARK (1958) and FISCHER (1962) found that diurnal and annual variations about the mean amounted to about $\pm 20\%$.

1.2.3 The charge on the Electrosphere.

If the electrosphere is a conducting spherical surface, it must be impervious to lines of force and the sum of all charges inside it and on its inner surface must be zero. These charges being those in the atmosphere, in clouds, on the surface of the earth and on the inner surface of the electrosphere.

CHALMERS (1953) showed that the total charge on the inner surface of the electrosphere was zero. Consider a surface in the atmosphere surrounding the earth at a level above all thunder clouds. Let the surface be composed of points of equal specific conductivity \mathcal{R} . Considering unit area of this surface, let the lines of force crossing this area have charge σ at their upper ends. It can be shown that the potential gradient F across this unit area of surface is:-

$$F = \sigma / \epsilon_0$$

where ϵ_0 is permittivity of free space. The current density through the surface is given by:

$$i = \mathcal{R}F = \sigma \mathcal{R} / \epsilon_0$$

Since the current flows along the lines of force then

$$i = \mathcal{R} \sigma / \epsilon_0 = -d\sigma / dt$$

Integrating for the whole surface we have

$$\sum \frac{d\sigma}{dt} = - \sum \frac{\eta\sigma}{\epsilon_0}$$

Let Q be the total charge above the surface.

$$\therefore \sum \sigma = Q$$

$$\therefore \sum \frac{d\sigma}{dt} = \frac{dQ}{dt}$$

STERGIS, REIN and KANGAS (1957) found that the specific conductivity, η , of air above a thunder cloud is no different from that at the same place in fine weather.

$$\therefore \frac{dQ}{dt} = - \frac{\eta Q}{\epsilon_0}$$

Let $Q = Q_0$ at $t = 0$; then it follows that

$$Q = Q_0 e^{-\frac{\eta}{\epsilon_0} t}$$

Thus the charge on the inner surface of the electrosphere falls rapidly to zero and remains there. The rate at which it falls is given by the time constant η/ϵ_0 which is known as the "relaxation time of the atmosphere" and is of the order of 30 minutes. Thus the net charge on the inner surface of the electrosphere is zero and it therefore follows that the sum of the charges in the atmosphere in clouds and on the surface of the earth is zero.

1.2.4 The charge balance.

The fact that the bound charge on the surface of the earth in fine weather is maintained indicates that there should be a balance between positive and negative charges arriving at the earth. The known processes by which charge can reach the earth are:-

- a) Air-earth conduction and convection currents.
- b) Precipitation currents.
- c) Lightning discharge currents.
- d) Point discharge currents.

1.2.5 Fine weather conduction currents.

Measurements of the air-earth current in fine weather at various places have given values of charge reaching the earth, due to conduction, in the range +30 to +100 coulombs per square kilometre per year. For the world as a whole KRAAKEVIK's (1961) results give a value of about $+86 \text{ C km}^{-2} \text{ yr}^{-1}$.

1.2.6 Precipitation currents.

It has been found that precipitation plays an important part in the transfer of charge in the atmosphere. CHALMERS and LITTLE (1947) obtained a total vertical current density of $+100 \text{ C km}^{-2} \text{ yr}^{-1}$ of which they attributed +60 C to conduction, leaving +40 C for precipitation.

1.2.7 Lightning discharge currents.

It has been found that lightning discharges to ground on balance bring negative charge to earth. ISRAEL (1953) used BROOK'S (1925) value of 1800 for the total number of storms active at one time, to estimate the total charge brought to 1 km^2 of the earth's surface in a year. He assumed a value of 60 lightning flashes to ground per hour for each storm, and accepted the value of 20 C per flash. He estimated that 80% of the flashes bring negative and 20% of the flashes bring positive charge to ground. He obtained a mean value, for the current density due to lightning discharges, of $-20 \text{ C km}^{-2} \text{ yr}^{-1}$ for the earth as a whole.

1.2.8 Point discharge currents

Point discharge currents down elevated metal points have been measured by various workers. WORMELL (1930), over a period of four years, obtained an average value, of the annual resultant charge passing due to point discharge, of about -0.12 C . He estimated that there would be an equivalent of about 800 such points per square kilometre. This gave a value of $-100 \text{ C km}^{-2} \text{ yr}^{-1}$ as the contribution of point discharge currents to the maintenance of the negative charge on the earth. WORMELL (1953) showed that this estimate was probably too low and suggested that the value should be increased to $-170 \text{ C km}^{-2} \text{ yr}^{-1}$.

It is thought that trees may be the most important natural objects at which point discharge occurs.

SCHONLAND (1928) supported a tree on insulators and measured currents through it during thunderstorms. He estimated the total current below a thunderstorm, due to point discharge to be $-2A$. His figure is probably a little high since the tree he used was more exposed than those in the surrounding area. GISH and WAIT (1950) measured the conductivity and potential gradient above storm clouds and deduced a value of $-0.5A$ for the average total current below a thunderstorm. In the past it has been thought that point discharge may be the most important process in the transfer of charge between thunder clouds and earth.

1.2.9 Conduction currents above storm clouds.

It was shown by GISH and WAIT (1950) that the total current from the top of a thunder cloud to the electrosphere must, on average, be equal to the total upward current within the cloud and also equal to the total current between the cloud and earth. GISH and WAIT measured the total current above thunder clouds by flying over storms and measuring the specific conductivity of the air and the potential gradient at various points. They found that the total current above thunder clouds was between 0 and $-1.4A$, the average value being $0.5A$. Similar results were obtained by STERGIS, REIN and KANGAS (1957).

1.3 The pulsed nature of point discharge currents

1.3.1 The process of ionization by collision.

Consider the simplified case of a horizontal storm cloud, giving a uniform potential gradient between it and the surface of the earth, so that the lines of force are vertical in the atmosphere over a wide area. If a pointed conductor is erected on the earth's surface then the lines of force will be deflected from their vertical direction and will tend to concentrate at the point. Thus the potential gradient in the air at and near the point will be considerably increased above the value in the surrounding air and ionization by collision may occur in the small volume of air around the point. Thus ionization can occur under conditions which ordinarily would be prohibitive. When the potential gradient in the atmosphere is negative, electrons will move towards the point and positive ions away. When the potential gradient is positive, positive ions will move towards it and electrons away from it. The electrons will attach themselves to molecules to form negative ions. In both cases the process of ionization by collision produces ions or electrons moving towards the point and ions of the opposite sign moving away. The latter form a space charge around the point. This will reduce the

potential gradient near the point. As more space charge is produced the potential gradient near the point will be reduced until ionization by collision ceases. Thus the current into the point will fall to zero. As the space charge is removed by the potential gradient ionization by collision can again occur. Thus, under suitable conditions, point discharge currents will flow down the point as a series of pulses.

1.3.2 Characteristics of positive pulses.

TRICHEL (1938) performed laboratory experiments which showed that, when the point is negative in a positive potential gradient, the pulses occur fairly regularly and each pulse carries approximately the same amount of charge which is of the order of 10^{-10} C. LARGE and PIERCE (1955) found similar results for natural point discharge on a 7m metal point in positive potential gradients.

1.3.3 Characteristics of negative pulses.

When the point is in a negative potential gradient, AMIN (1954) found that, at low values of discharge current, the pulses often occurred in short bursts. At higher currents the discharge was often more stable. AMIN's results were confirmed by LARGE and PIERCE (1955) for natural point discharge on a metal point, in negative potential gradients.

1.4 The relation between point discharge and other parameters.

1.4.1 Potential gradient.

For any discharging point there is a minimum value of potential gradient at the earth's surface nearby, depending on the nature and location of the point, at which point discharge will commence. As the potential gradient increases above this minimum value, the discharge current will increase, as a result of the intensification of the ionization by collision at the point. It was shown by WHIPPLE and SCRASE (1936) that, under laboratory conditions, the relation between point discharge current, I , and the potential gradient, F , nearby, is of the form

$$I = a(F^2 - M^2),$$

where a and M are constants for a given system. WHIPPLE and SCRASE (1936) measured point discharge currents into an elevated metal point and the potential gradient at the ground nearby. They were able to fit their results to the above formula. KIRKMAN and CHALMERS (1956) analysed the results of WHIPPLE and SCRASE (1936) and HUTCHINSON (1951) to fit a formula

$$I = A (F - M)^n$$

where A and M are constants. They found the best value of n to be 1.1.

1.4.2 The effect of wind speed.

DAVIS and STANDRING (1947) observed an increase in point discharge current with wind speed. CHALMERS and MAPLESON (1955) found an empirical relation

$$I = K W^{\frac{1}{4}} V^{\frac{7}{4}}$$

where W is the wind speed, K is a constant and V is the potential difference between the point and its surroundings. KIRKMAN and CHALMERS (1956) using an isolated point at 30m found the relation

$$I = k (F - M)(W + b)$$

where k , b and M are constants. CHAPMAN (1956) suggested that the correct relation should be

$$I = a(V - V_0)v$$

where v is the velocity at which ions are removed from the neighbourhood of the point and a and V_0 are constants. If there is no wind

$$v \propto F$$

and assuming that the effects of any space charge, below the point but above the instrument for measuring potential gradient, can be neglected, then

$$V = Fh \quad \text{and} \quad V_0 = F_0h$$

where h is the height of the point; thus

$$I = A(F - F_0)F$$

where A and F_0 are constants. This formula is similar to that of WHIPPLE and SCRASE (1936).

If however wind is the main factor for the removal of ions from the point, then

$$I = a(V - V_0)W = ah(F - F_0)W$$

which is similar to the formula of KIRKMAN and CHALMERS (1956).

LARGE and PIERCE (1957) measured currents from a point raised to high potentials and exposed to wind. At the suggestion of CHALMERS they considered the velocity, v , at which ions are removed from the point, as the vector sum of wind speed and a term involving V . They obtained the relation

$$I = a(V - V_0)(W^2 + c^2V^2)^{\frac{1}{2}}$$

where a , V_0 and c are constants.

1.4.3 The "effective separation" of points.

If the natural point discharge current down a metal point is used as a measure of the amount of natural point discharge current flowing to ground in the surrounding area, then, to obtain an estimate of the latter, it is necessary to convert from the current down a point to the current density over an area. To do this one needs to know the "effective separation" of similar points in the area. CHALMERS (1953) using the electrical model of a thunder cloud proposed by SIMPSON and ROBINSON (1940) and the relation between point discharge current and potential gradient, of WHIPPLE and SCRASE (1936),

found the total point discharge current below a thunder cloud in terms of the effective separation of points. Assuming that the total current below a thunder cloud is equal in magnitude to the average current of 0.5A above the cloud, found by GISH and WAIT (1950), then a value of 11m was obtained for the effective separation of points at Kew.

1.4.4 Space Charge considerations.

The process of point discharge produces a current down the point to earth and an ionic current away from the point. If the potential gradient remains constant and there is a wind, the ions leaving the region around the point will travel downwind and cause the potential gradient at the ground downwind of the point to be reduced. LUTZ (1941) and HUTCHINSON (1951) observed time lags between a change in sign of potential gradient and of point discharge currents. This was explained in terms of space charge, produced by neighbouring points, in the region below the point but above the apparatus for measuring potential gradient.

1.5 Previous measurements of natural point discharge

1.5.1 Measurements with isolated points

WORMELL (1953) obtained an estimate for point discharge of $-170 \text{ C km}^{-2} \text{ yr}^{-1}$. WHIPPLE and SCRASE (1936) estimated it to be $-100 \text{ C km}^{-2} \text{ yr}^{-1}$. CHALMERS and LITTLE's (1947) estimate was $-90 \text{ C km}^{-2} \text{ yr}^{-1}$. All these estimates necessitated the assumption of a value for the effective separation of points. Herein lies the main difficulty. From measurements with a single isolated metal point, it is difficult to deduce the currents flowing in an irregular configuration of metal points of similar exposure. When we attempt to deduce the currents for trees, the problem becomes even more complex. It is doubtful whether it is possible to obtain reliable estimates of charge transfer, due to point discharge currents, by using measurements of currents down isolated metal points.

1.5.2 Direct measurements of point discharge on trees.

SCHONLAND (1928) made measurements of point discharge currents with a tree supported on insulators. He was able to make an estimate of -2A for the total current to earth from a thundercloud. MILNER and CHALMERS (1961) measured point discharge currents down a lime tree by inserting two

electrodes into the trunk at different heights and bypassing some of the current through a galvanometer. They found that the current through the lime tree was comparable with that through an isolated point of the same height, but the tree begins to discharge at a higher value of potential gradient. ETTE (1966) showed that the bypassed current was only a fraction of the total current through the tree. JHAWAR and CHALMERS (1967) applied artificial potential gradients to small trees and found

$$I = a V(V - V_0)^2$$

whereas for an isolated point they found

$$I = b(V - V_0')$$

where a , b , V_0 and V_0' are constants and V is the voltage applied to the plate above the tree or point.

1.5.3 Indirect measurements of point discharge on trees.

MAUND and CHALMERS (1960) attempted to measure the point discharge current down a tree, using two field mills to give the potential gradient at the ground upwind and downwind of the tree. If the tree is discharging, ions will be blown from the tree downwind and the potential gradient at the ground downwind will be reduced. Thus the difference in potential gradient, at the ground, upwind and downwind of the tree, should give a measure of the current down the tree.

They found that, even when the potential gradient reached 5000 Vm^{-1} , a tree in full leaf did not discharge. However, for ash and poplar trees not in leaf, discharge commenced at about 1000 Vm^{-1} . Ions, produced at trees by point discharge, have been detected as space charge by BENT, COLLIN, HUTCHINSON and CHALMERS (1965).

1.6 Outstanding problems in the measurement of natural point discharge

1.6.1 Limitations of measurements from isolated points.

The fact that it is relatively simple to measure the point discharge current down an elevated metal point is perhaps the main reason why it has so often been used as a measure of natural point discharge. However, the ease of measurement by this method is offset by the difficulty of obtaining the effective separation of points for the area. It has been shown by JHAWAR and CHALMERS (1967) that the relation between current and potential gradient for a tree contains a cubic factor, whereas the relation for an isolated point contains a squared factor. To obtain the effective separation of points for an area, it would be necessary to allow for the different heights of the trees in that area as well as their different behaviour when compared with a single metal point. This is probably not possible to any reasonable degree of accuracy.

1.6.2 Limitations of previous measurements.

Measurements using electrodes in the trunk of a tree are subject to the effects of displacement currents, caused by changes in potential gradient. ETTE (1966) found the effective area of a tree and showed that displacement currents could be as large as the point discharge currents, in periods of rapidly varying potential gradient.

Electrochemical action and contact potentials, in the region of the tree-electrode interface, can give rise to spurious current which can vary with the state of the tree. Again, these currents can be of the same order as the point discharge current itself.

Measurements of point discharge on trees have usually been concerned with isolated trees rather than trees in a wood. This means that the measurements would not be representative of typical wooded countryside since an isolated tree will start to discharge at lower values of potential gradient.

The method of MAUND and CHALMERS (1960) does not suffer from the disadvantages of displacement or spurious electrode currents and is probably a good method for isolated trees.

However, if it is used on a larger scale for a wood, difficulties could arise in connection with the turbulent transfer of space charge. It would be difficult to establish that a difference in potential gradient at the ground, upwind and downwind, was caused only by point discharge ions from the trees.

1.6.3 The measurement of point discharge on representative trees.

If a reliable method could be devised for the measurement of point discharge currents down living trees, under natural conditions, which would not disturb the tree or its surroundings, then it should be possible to obtain representative measurements of point discharge. If several trees in a wood were instrumented by this method and measurements made over a period, it has been suggested that it would be possible to deduce the average annual current density for the wood. It is thought that trees in leaf discharge less readily than those not in leaf and experiments could be conducted to establish whether or not this is so. It is also important to know to what extent the exposure of a tree effects the discharge. There is a need to establish whether most trees will discharge or only isolated trees and perhaps trees on the edge of a wood.

To obtain a value for the contribution of point discharge to the transfer of charge in the atmosphere, reliable and representative measurements of natural point discharge are needed.

CHAPTER 2.Approach to the present Work2.1 Introduction

Of the known processes by which charge transfer occurs in the atmosphere, the contribution made by point discharge is probably the most uncertain. The limitations of the various methods, that have been used by previous workers to estimate the amount of point discharge, have been discussed in 1.6.1 and 1.6.2. These methods were intended to give the integrated value of the discharge current and were not dependent on the pulsed nature of the discharge. There is obviously a need for the development of new techniques of measurement so that more reliable estimates of widespread point discharge can be made. Comprehensive experimental studies of the characteristics of point discharge pulses have been made by AMIN (1954) and PIERCE, NADILE and McKINNON (1960). LOEB (1965) gave an account of the basic physical mechanisms involved in the discharge. However, it appears that hitherto the pulsed nature of the current has had no part in measuring techniques. The present work is intended as a contribution to that study.

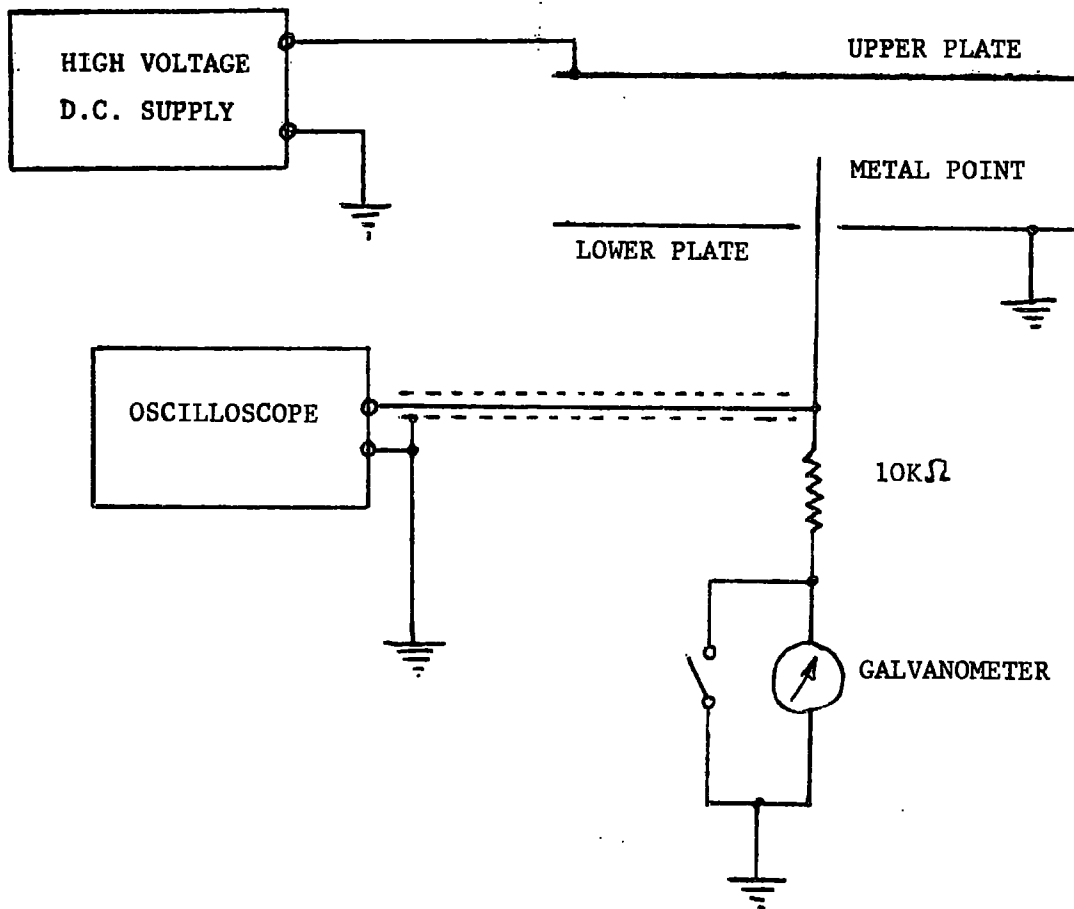


Fig. 2.1 Apparatus for preliminary observations of point discharge.

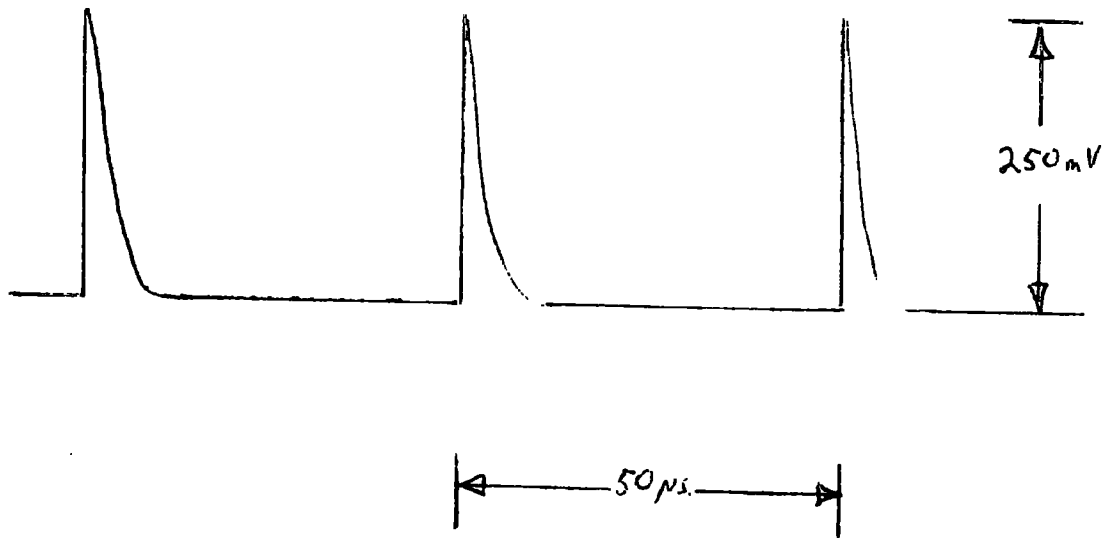
2.2. Preliminary observations of point discharge pulses.

2.2.1. Introduction.

The observations described below were made to obtain a general idea of the size, shape and frequency range of point discharge pulses, for cases when the point was both positive and negative with respect to the potential of the air surrounding it. The apparatus used, consisted of two parallel circular plates, 50cm in diameter (Fig. 2.1). The lower plate was earthed and the upper plate was connected to a stabilised d.c. voltage source which was variable from 0 V to ± 10 kV. The separation of the two plates could be varied by adjusting the position of the lower plate.

2.2.2. Negative Point

The plate separation used was 15 cm and a steel point protruding 10 cm above the earthed plate was connected to earth, via a $10\text{ K}\Omega$ resistor in series with a galvanometer. The point was also connected to the input of an oscilloscope to display the voltage waveform at the point. The voltage source was adjusted to positive polarity and the plate voltage was gradually increased from zero. A certain plate voltage was reached which was just sufficient to cause



$$RC = 10\text{K}\Omega \times 200\text{pF} = 2\mu\text{sec.}$$

Fig. 2.2. Typical voltage waveform for Trichel Pulses.

the discharge to commence. The galvanometer current at this stage was less than $0.1 \mu\text{A}$. The current could be seen on the oscilloscope screen as single positive pulses occurring at very irregular intervals. As the plate voltage was gradually increased the galvanometer current and pulse repetition frequency (p.r.f.) both increased. The pulses also became more regularly spaced. At a current of $1 \mu\text{A}$ the p.r.f. was about 10 kHz and it was possible to observe the shape of the pulses. A rapid rise to the maximum pulse height was followed by a slower exponential fall-off to zero. The time constant of this fall-off was the same for each pulse and roughly equal to the combined input time constant of the oscilloscope and input cables. (See Fig. 2.2). At a current of $10 \mu\text{A}$ the pulses were very regularly spaced with a p.r.f. equal to about 200kHz. As the plate voltage had been increased up to this point, the amplitude of the pulses had remained roughly constant at about 250mV. However, for frequencies above about 200 kHz, the amplitude gradually decreased. At 1MHz the current was about $60 \mu\text{A}$ and the amplitude had fallen to 180 mV. At currents of $100 \mu\text{A}$ or more, corresponding to a p.r.f $\geq 1.5 \text{ MHz}$, the amplitude of the pulses approached zero and the discharge current no longer appeared to flow in

CURRENT (μ A)	P.R.F. (kHz)	PULSE HEIGHT (mV)	VARIATION IN PULSE INTERVAL
< 0.1	< 1	250	Large
1	10-20	250	Moderate
10	200	< 250	Small
60	1000	180	Small
> 100	-	-	No pulses

Fig. 2.3 Summary of preliminary observations of Trichel pulses

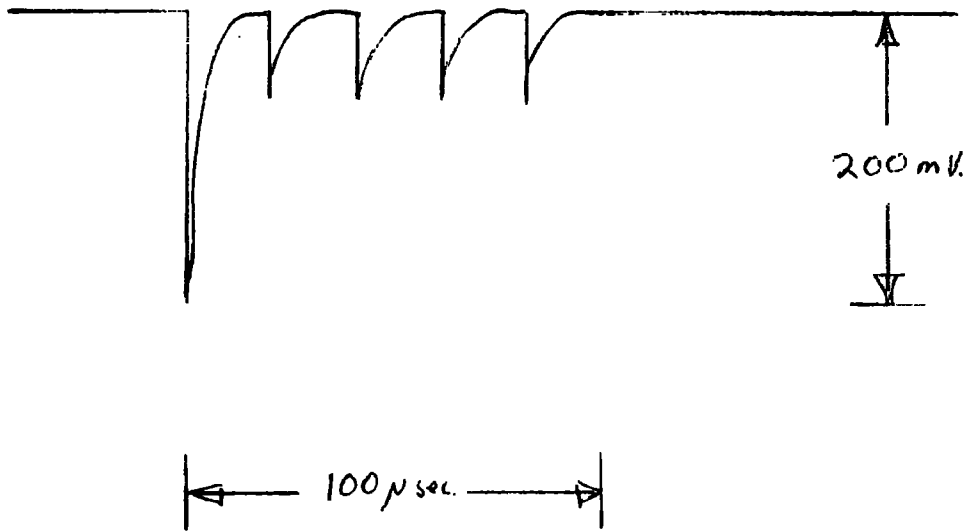


Fig. 2.4. Primary and secondary pulses from a positive point.

a series of pulses. The observations described above are summarised in Fig. 2.3. The pulses which occur when the point is at a negative potential with respect to its surroundings, were first investigated by TRICHEL (1938), and are often referred to as Trichel pulses. Trichel found that the pulses contained a quantity of charge, of the order of 10^{-10} C, which remained roughly constant as the current and frequency increased.

2.2.3. Positive point

The same apparatus was used as for the negative point observations but the polarity of the voltage source was made negative. In this case the current pulses were in the form of short bursts of pulses occurring at irregular intervals. The pulses within a single burst were all negative. The first pulse was about three times the height of the secondary pulses which followed. As the plate voltage was increased the interval between consecutive bursts decreased to a certain minimum value and then began to increase again. The interval between the secondary pulses decreased and also their amplitude increase as the plate voltage was increased. (see Fig. 2.4). It was found difficult to make precise observations from the oscilloscope since the pulses occurred at irregular intervals and therefore did not give a clear waveform on the screen. However the

magnitudes of currents and frequencies were found to be similar to those for the negative point. As in the case of the negative point, the currents above $100\mu\text{A}$ no longer appeared to be in the form of pulses.

2.2.4 Pulses from a small tree

The earthed plate was lowered to the bench and the metal point replaced by a small (50 cm) spruce tree growing in soil in a plant pot. The plant pot was insulated from the lower earthed plate and electrical connection made to the soil by means of a metal rod. The clearance between the top of the tree and the upper plate was 5 cm. The plate voltage needed to initiate point discharge on the tree was higher than that needed for the metal point. However, currents through the tree of up to $10\mu\text{A}$, both positive and negative, were measured. Oscilloscope observations clearly showed that the current was pulsed. It was not possible to use the oscilloscope for frequency measurements because of the large irregularities in pulse interval. However, it could be seen that an increase in plate voltage caused a corresponding increase in the number of pulses on the screen, indicating that an increase in p.r.f. was occurring.

2.2.5 The d.c. levels in pulse waveforms

At values of pulse repetition frequency greater than about 100 kHz , the presence of a d.c. level was observed in the pulse waveform from the metal point. The input time constant was approximately $10 \text{ K}\Omega \times 200 \text{ pF}$, i.e. $2 \mu\text{sec}$. Thus the pulse amplitude could not fall to zero at high values of p.r.f. and so a d.c. level would build up until a quasi-equilibrium was reached.

2.3. Theoretical considerations on the pulse shape

2.3.1. An idealized form for the pulse shape

TRICHEL (1938) found that for discharge at a point negative with respect to its surroundings, the pulses of current each contain approximately the same amount of charge. In the preliminary observations described in 2.2 it was mentioned that the rise time of the pulses was very rapid. In fact the rise time is certainly less than $5 \times 10^{-8} \text{ sec}$.

If we can assume that the charge per pulse Q_0 is constant and the rise time of the pulse T to be much less than the instrumental time constant RC , we can write an expression for the current I through the point in terms of Q_0 , RC and time t . Thus:-

$$I = Q_0/RC \exp(-t/RC)$$

where charge Q_0 arrives instantaneously at the point at $t = 0$, i.e. assuming $T = 0$.

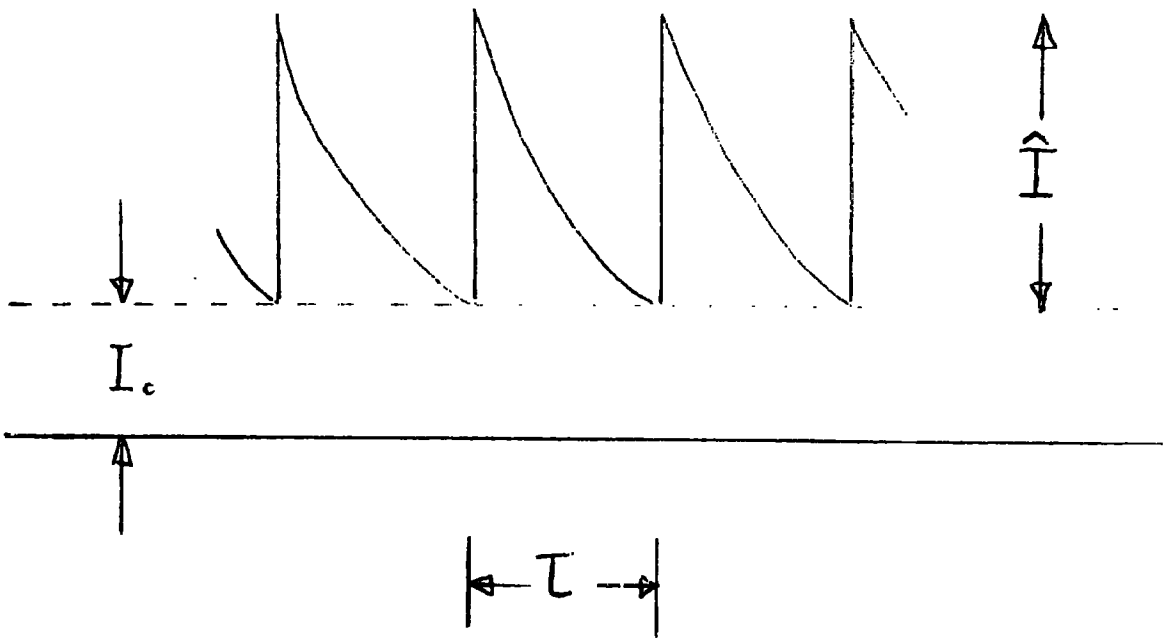


Fig. 2.5. The d.c. levels in pulse waveforms.

The maximum value of I is

$$\hat{I} = Q_0/RC$$

occurring at $t = 0$. Therefore the maximum voltage on the point is

$$\hat{V} = Q_0/C$$

also occurring at $t = 0$. The voltage on the point will then decay exponentially to zero with a time constant equal to the input time constant RC . The equation

$$I = Q_0/RC \exp(-t/RC)$$

gives an idealized form for the shape of a single current pulse. In practice the observed pulse shape will be modified since the rise time T is not zero. The oscilloscope will also have a significant rise time T_R and this will further modify the pulse shape.

2.3.2. The d.c. levels in pulse waveforms.

It was mentioned in 2.2.5 that under certain conditions a d.c. level was found to be present in the waveform. Let this d.c. level be a current I_0 (Fig. 2.5). If the charge per pulse Q_0 and the interval between pulses T remain constant, a quasi-equilibrium will be reached and I_0 will become constant. The d.c. amplitude is given by

$$\hat{I} = Q_0/RC, \text{ assuming } T \ll RC.$$

Thus the total amplitude of the waveform will be $(I_o + \hat{I})$. This will decay by an amount \hat{I} in time τ . So we have

$$\hat{I} = (I_o + \hat{I})(1 - \exp(-\tau/RC))$$

$$\therefore I_o = \hat{I}/(\exp(\tau/RC)-1)$$

As an example, when $RC = \tau$, the d.c. level I_o will be approximately 60% of \hat{I} . However if $RC = \tau/5$, I_o will be only 0.7% of \hat{I} .

2.3.3. The input time constant and rise time of the measuring equipment.

Since the arrival of charge at the point cannot be instantaneous, it is not surprising that we find the rise time of the pulses is not zero. Furthermore, as the ionization process is quenched by space charge, the rate of arrival of charge at the point will fall to zero over a finite period of time. Let us consider a single pulse and let the charge begin to accumulate at the point at time $t = 0$. Now, if we assume that at $t = t$ the charge Q which has arrived at the point is given by

$$Q = Q_o (1 - \exp(-t/T))$$

where Q_o is the total charge per pulse and T is the time constant for the fall-off in the rate of arrival of charge at the point.

Thus: $dQ/dt = Q_0/T \exp(-t/T)$

However, the rate at which charge accumulates on the input capacitor also depends on the input time constant RC . If there is charge q on C at time t , the rate at which charge flows through R is q/RC . This is the rate at which charge is lost from C . The resultant rate at which charge accumulates on C is therefore

$$dq/dt = dQ/dt - q/RC$$

$$\therefore dq/dt = Q_0/T \exp(-t/T) - q/RC$$

$$\therefore q + RC dq/dt = RC Q_0/T \exp(-t/T)$$

The solution of this differential equation is of the form

$$q = A \exp(-t/RC) + B \exp(-t/T)$$

where A and B are constants.

At $t = 0$; $q = 0$

$$\therefore A = -B$$

Also, at $t = 0$ we have

$$dq/dt = dQ/dt = Q_0/T$$

and $dq/dt = -A/RC \exp(-t/RC) - B/T \exp(-t/T)$

at $t = 0$;

$$dq/dt = Q_0/T = -A/RC - B/T$$

$$A = -B$$

$$\therefore Q_0/T = A(1/T - 1/RC)$$

$$\therefore A = Q_0/(1 - T/RC) \text{ and } B = -Q_0/(1 - T/RC)$$

$$\therefore q = (Q_0/(1 - T/RC))(\exp(-t/RC) - \exp(-t/T))$$

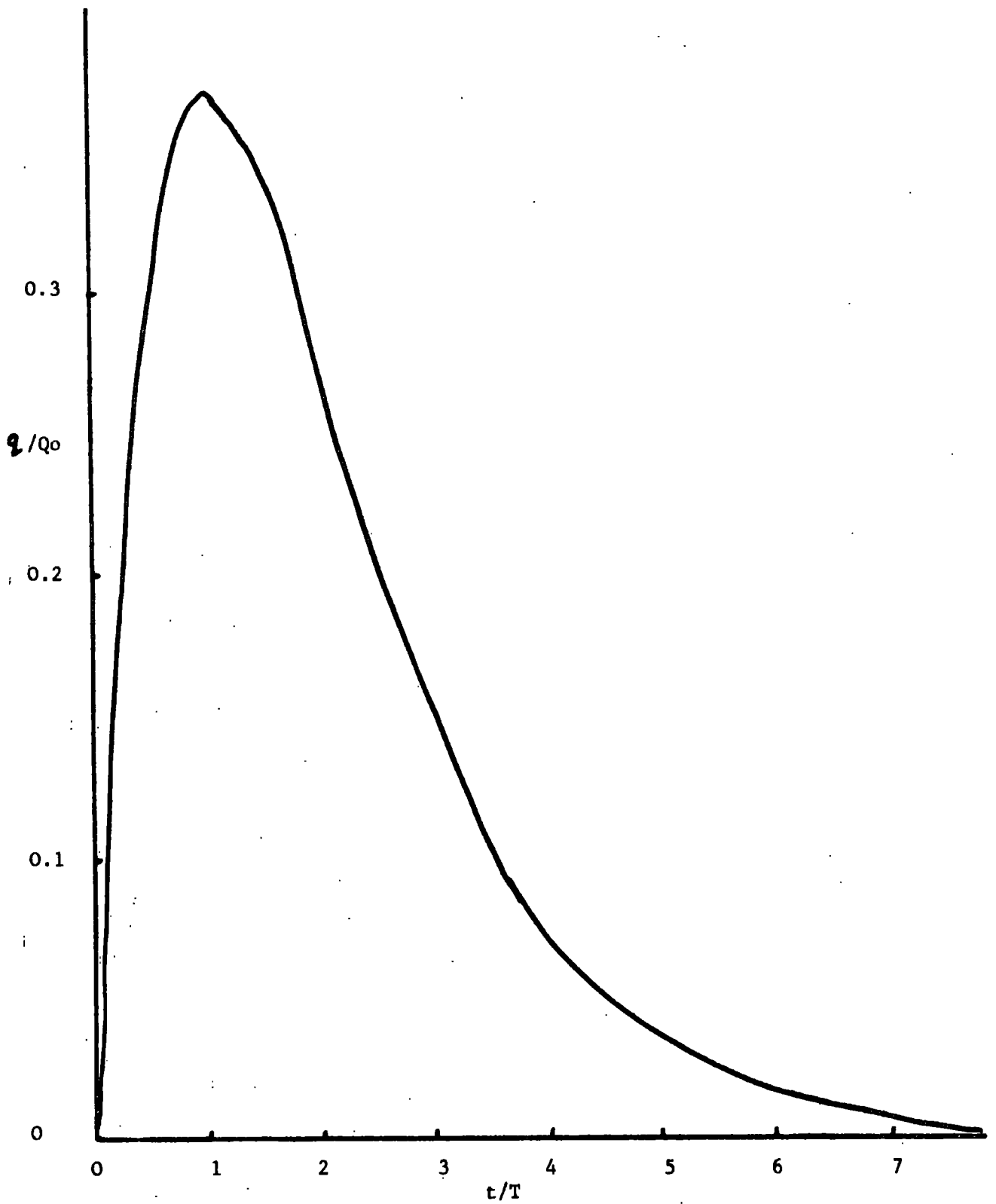


Fig. 2.6 Pulse shape for $RC = T$ and $T_R = 0$

If we put $T = 0$, we obtain

$$q = Q_0 \exp(-t/RC)$$

which is the equation for the idealized pulse derived in 2.3.1. However, when $T = RC$ (Fig. 2.6) we find that the maximum charge on the point occurs, not at $t = 0$, but at $t = T$. Also the maximum charge \hat{q} is not equal to Q but Q/e . This means that the observed pulse height will be reduced from the theoretical maximum voltage of, $\frac{Q}{C}$ by a factor $\frac{1}{e}$, when $T = RC$.

If we now consider the effect of the rise time T_R , of the measuring equipment, it is evident that this will have an integrating effect on the pulse given by

$$q = Q_0 \frac{1}{(1 - \frac{T}{RC})} \left[e^{-\frac{t}{RC}} - e^{-\frac{t}{T}} \right]$$

If we express this pulse in terms of voltages we obtain:

$$V = \frac{Q_0}{C} \frac{1}{(1 - \frac{T}{RC})} \left[\exp(-t/RC) - \exp(-t/T) \right] \quad (1)$$

where V is equal to q/C . Let V' be the voltage at the output of the measuring equipment after integration by the rise time T_R .

$$\text{Then:} \quad \frac{dV'}{dt} = \frac{(V - V')}{T_R}$$

$$\therefore \frac{dV'}{dt} + \frac{V'}{T_R} = \frac{V}{T_R} \quad (2)$$

$$\therefore \frac{dV'}{dt} + \frac{V'}{T_R} = \frac{Q_0}{CT_R(1-T/RC)} \left[\exp(-t/RC) - \exp(-t/T) \right] \quad (3)$$

The solution of this differential equation is of the form

$$V' = E \exp(-t/RC) + F \exp(-t/T) + G \exp(-t/T_R) \quad (4)$$

where E, F and G are constants.

Now $V' = V = 0$, at $t = 0$. Therefore from (4)

we have

$$E + F + G = 0 \quad (5)$$

Also from (2) we have

$$dV'/dt = 0 \quad \text{when } t = 0$$

$$\therefore E/RC + F/T + G/T_R = 0 \quad (\text{from (4)}) \quad (6)$$

To obtain a third equation for E, F and G we can use the fact that the area of the pulse before integration by T_R will be equal to the area of the pulse after integration.

Thus

$$\int_0^{\infty} V \cdot dt = \int_0^{\infty} V' \cdot dt$$

From (1) and (4) we therefore obtain

$$E \cdot RC + F \cdot T + G \cdot T_R = \frac{Q_0(RC - T)}{C(1 - T/RC)} \quad (7)$$

The solution of equations (5), (6) and (7) for E, F and G

gives:

$$E = \frac{Q_0}{C(1 - T/RC)} \left[\frac{1}{1 - T_R/RC} \right] \quad (8)$$

$$F = \frac{Q_0}{C(1 - T/RC)} \left[\frac{1}{T_R/T - 1} \right] \quad (9)$$

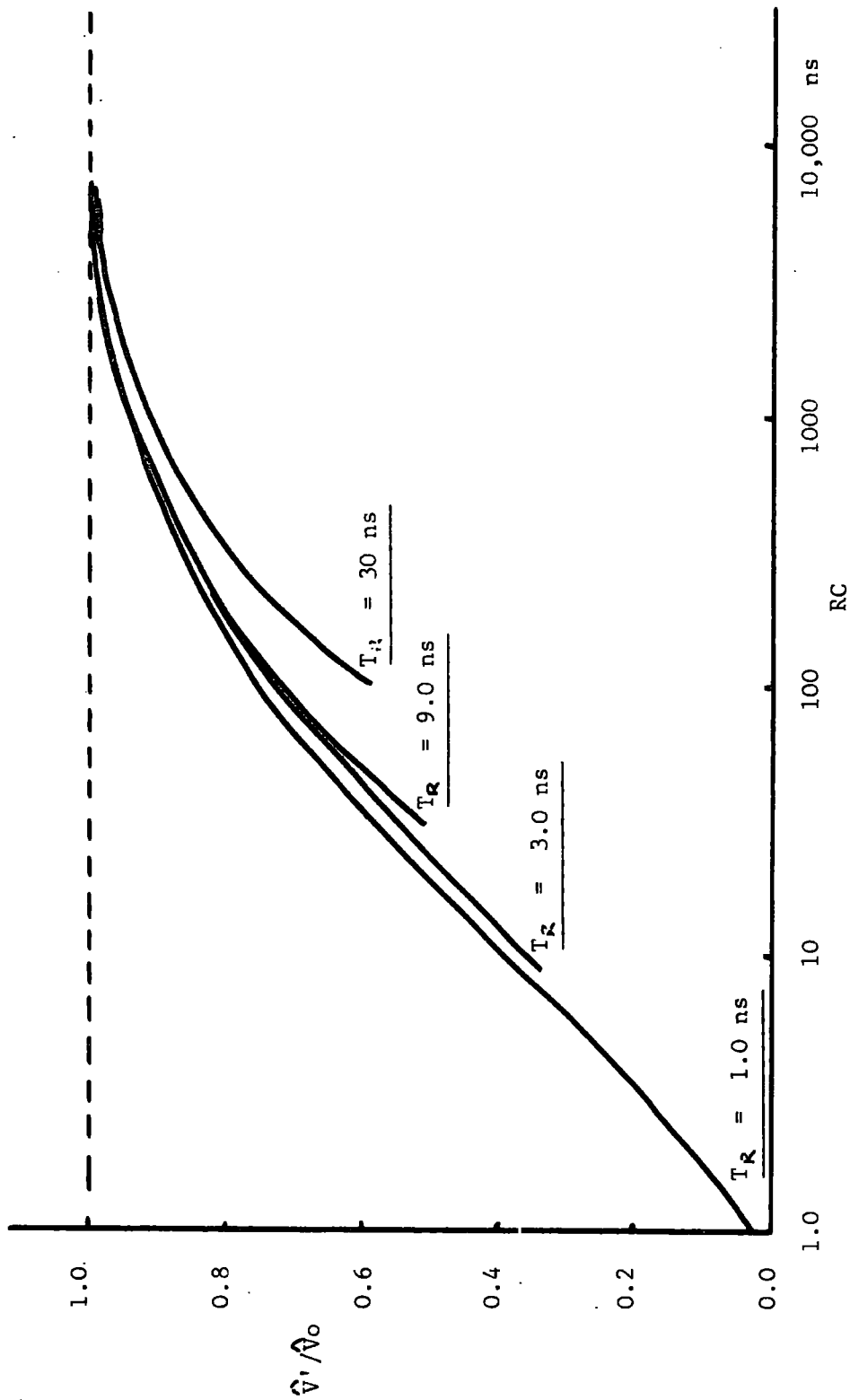


Fig. 2.7 Fractional variation of observed pulse height with RC for $T = 10$ ns

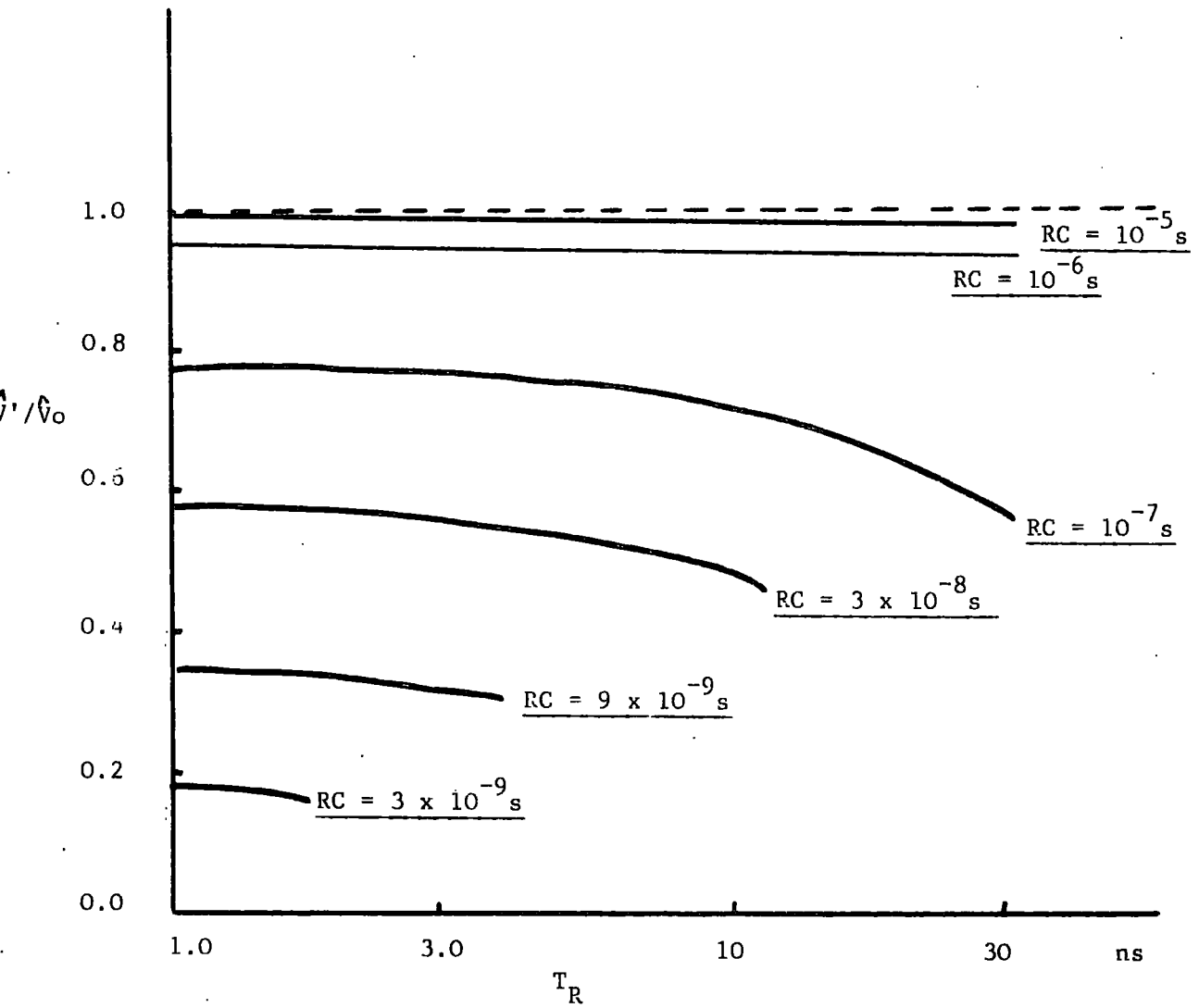


Fig. 2.8 Fractional variation of observed pulse height with T_R

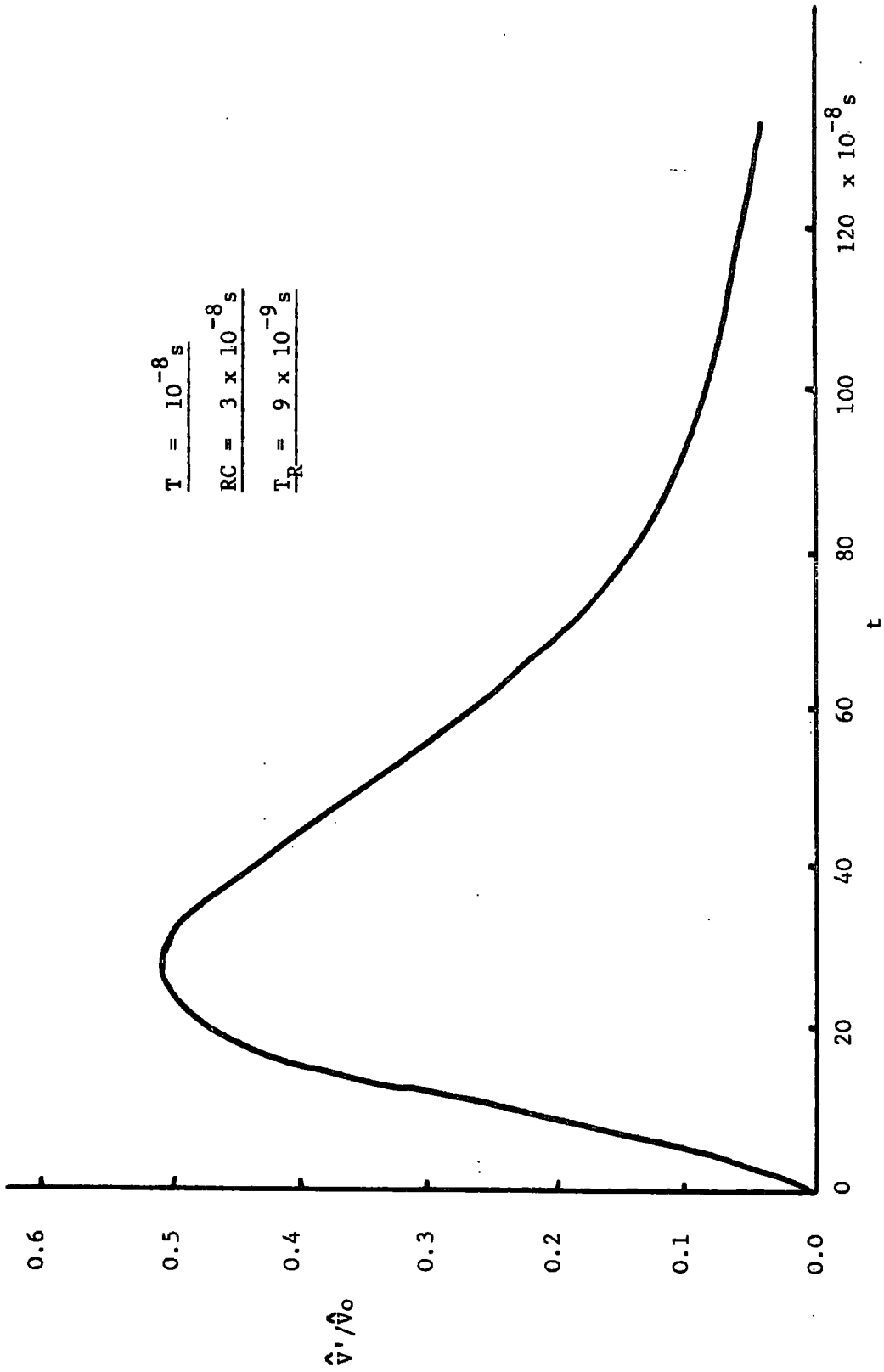


Fig. 2.9 A typical calculated pulse shape.

$$G = \frac{Q_0}{C(1-T/RC)} \left[\frac{1}{(1-RC/T_R)} + \frac{1}{(T/T_R - 1)} \right] \quad (10)$$

So putting Q_0/C equal to \hat{V}_0 , the expression for the pulse after integration by the measuring equipment is

$$V' = \frac{\hat{V}_0}{(1-T/RC)} \left\{ \frac{1}{(T/T - 1)} \exp(-t/T) + \frac{1}{(1-T_R/RC)} \exp(-t/RC) + \left[\frac{1}{(1-RC/T_R)} + \frac{1}{(T/T_R - 1)} \right] \exp(-t/T_R) \right\} \quad (11)$$

Now if T and T_R are both zero we obtain the idealised pulse shape which was derived in 2.3.1. Thus

$$V' = \hat{V}_0 \exp(-t/RC)$$

where the maximum value of this idealized pulse is

$$\hat{V}_0 = Q_0/C$$

The relation (11) was evaluated by computer for several values of RC/T and T_R/T , assuming a value for T of 10^{-8} sec. The results are shown in Figs. 2.7, 2.8 and 2.9. It is evident that the conditions for the observed pulse height to be close to the maximum possible value \hat{V}_0 , are

$$(i) \quad RC \geq 100T$$

$$(ii) \quad T_R \leq 3T$$

$$\text{for } \hat{V}' \geq 0.95\hat{V}_0$$

If these conditions are satisfied, small variations in T will not appreciably affect the height of the pulses and so the height of the pulses will be directly proportional to the charge per pulse. Under these conditions the pulse height will therefore be within 5% of that found for the

idealised form of pulse shape. In both cases we have the extra condition that

$$RC \leq \frac{T}{5}$$

where T is the interval between pulses, for there to be no d.c. level in the waveform.

2.4 Conclusion

Some of the characteristics of point discharge pulses from a metal point have been observed. It was found that the point discharge current down a small tree was also in the form of pulses, but that deviations in pulse interval and amplitude about their respective mean values were larger than those for a single metal point.

The effect of measuring equipment on the size and shape of the observed pulses has been found theoretically. It has been shown that if the input time constant RC is within a certain range, the effects on the pulse height of non-zero values of T and T_R will be negligible.

It was concluded that it should be possible to measure natural point discharge on trees, by measuring the frequency and possibly the amplitude of the pulses, provided that a satisfactory method for detecting the pulses could be found. However, it was thought necessary initially to make laboratory measurements under controlled conditions before attempting field experiments.

CHAPTER 3.Instrumentation for Laboratory Measurements of Point Discharge Pulses.3.1 Introduction

This chapter describes the instruments which were constructed for making laboratory measurements of point discharge pulses. These measurements are described in Chapters 4 and 5.

The amplitude and time interval between point discharge pulses are both variable quantities even when the integrated value of the discharge current is constant. With this fact in view, a system was developed which would measure, not only the mean pulse amplitude and the mean pulse interval over a period, but also the distribution of these quantities about their respective means.

3.2 Choice of measuring techniques.3.2.1 Amplitude measurement.

To obtain the distribution of pulse amplitude for any given current it is necessary to obtain the number of pulses which fall in each range of amplitude or channel.

This can be achieved by using a multi-channel pulse height selector, often called a kicksorter, which simultaneously counts the pulses arriving in each channel. Thus the distribution of amplitude is obtained directly. The alternative approach is to use a single channel pulse height selector. With this method the pulses are counted over a short period for each channel in turn. In view of the high cost of a kicksorter, and as the single channel pulse height selector was sufficient for the requirements of the present work, it was decided to use the latter technique for amplitude measurements.

3.2.2 Measurement of pulse repetition frequency (p.r.f)

Three methods were considered for measuring the mean p.r.f. and the distribution of pulse interval.

a) Photographic techniques. If the pulses are displayed on an oscilloscope and photographs of single sweeps of the screen are taken, then measurements of individual pulse intervals can be made.

b) Counting techniques. Point discharge pulses can be amplified and then counted by a high frequency scaler.

If the pulses are counted over a known period of time, a measure of the average p.r.f. for that period is obtained. By varying the counting period, it is possible to find the distribution of pulse interval.

c) The integrating frequency meter. This instrument gives an average value for the p.r.f. and has the advantage that the latter can be read directly from a meter. However, it does not give information on the deviation of pulse interval about the mean value.

It is clear that the three methods described above all give the mean p.r.f. However, method (a) gives detailed information about a small number of pulses and method (c) gives a continuous integrated value for the mean p.r.f. of a large number of pulses. Method (b) can be used to sample a small number of pulses or it can be used to give a measure of the mean p.r.f. It was therefore decided to use (b), the counting method, as the main technique with (c), the frequency meter, as a subsidiary method.

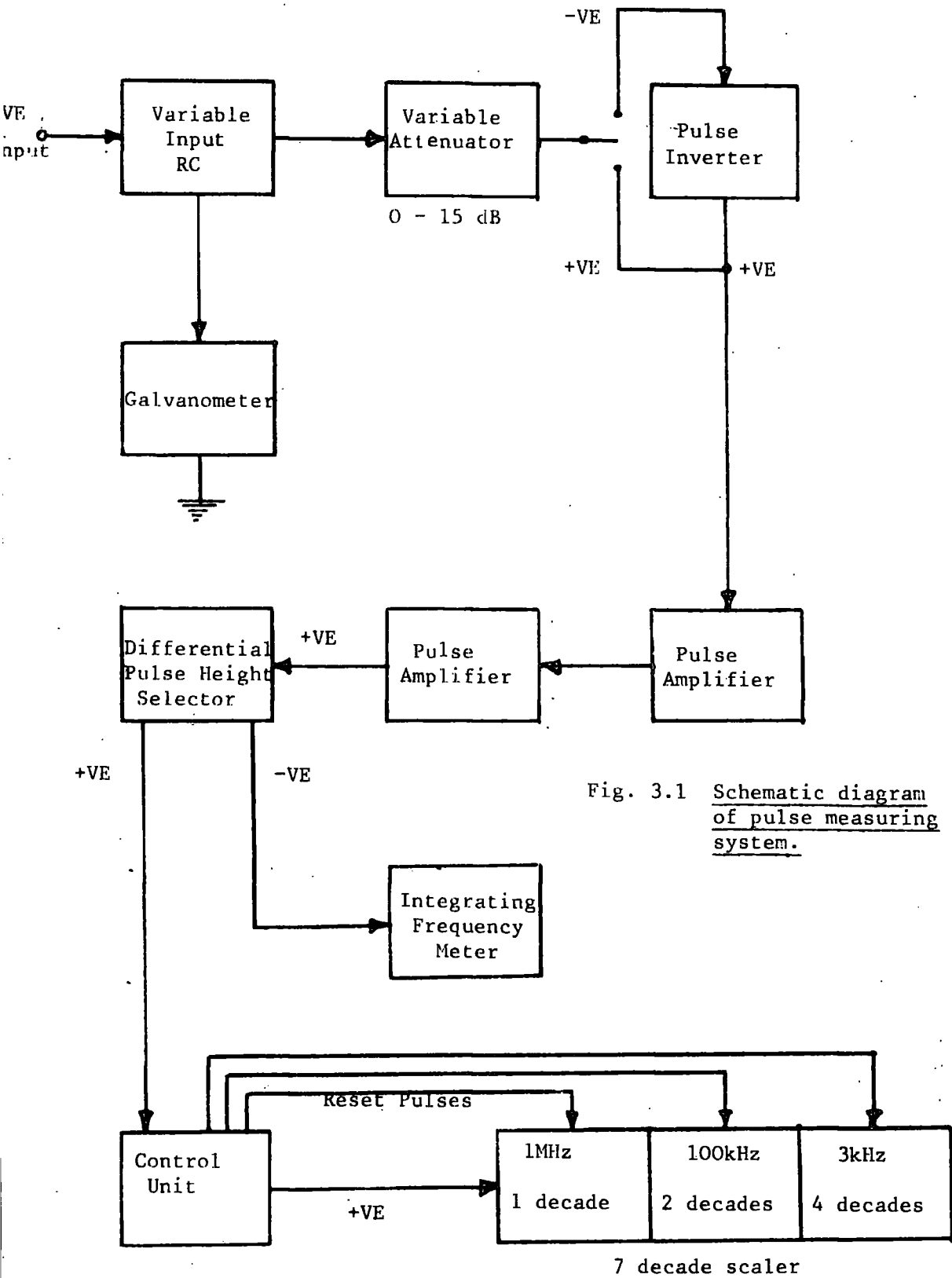


Fig. 3.1 Schematic diagram of pulse measuring system.

3.2.3 Performance required from the system

Preliminary observations of point discharge pulses showed that the equipment should be able to count pulses of amplitude ranging from 1 mV to 1 V. The maximum counting rate required would be about 1 MHz_2 . To obtain the standard deviation of pulse interval, the counting interval would need to be variable from about 50 μ sec to 1 sec.

3.3 General description of the system used.

The system is shown schematically in Fig. 3.1. The source of point discharge pulses is applied to the input. The input time constant can be varied over a wide range and the pulses can also flow to earth through a galvanometer. After this first stage, the pulses pass through a variable attenuator and a pulse inverter. The pulse inverter is necessary only when negative pulses are being applied to the input of the system. After voltage amplification the positive pulses are applied to the input of the Differential Pulse Height Selector. The two outputs from this unit are in the form of standard positive and negative pulses which are produced simultaneously. Whenever the input pulse has an amplitude lying between two preset threshold values, which can both be varied, one positive and one negative pulse are

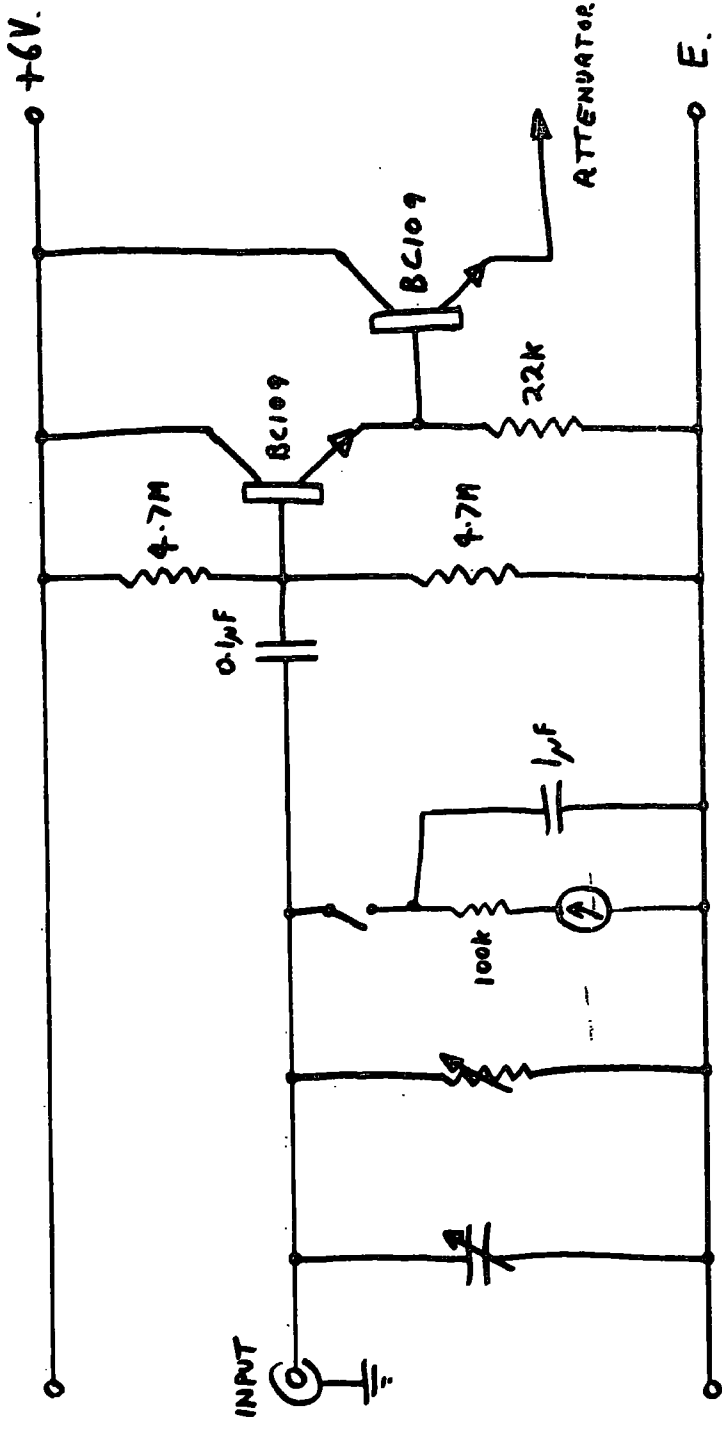


Fig. 3.2 The Time Constant and Galvanometer Circuit

produced at the outputs. The negative output pulses go to an integrating frequency meter whilst the positive pulses go to the control unit. The function of the control unit is to allow the pulses to be counted by the scalers for short periods of time. Thus in operation, pulses are counted, the count is then displayed and the scalers are finally reset to zero. This process is then automatically repeated every few seconds. As the counting time is known, the mean count will give the mean p.r.f. The variation between counts will be a measure of the variation in pulse interval.

3.4 The electronic circuitry

3.4.1 The time constant and galvanometer circuit

The shape of point discharge pulses is affected by the input time constant of the measuring system. The circuit (Fig. 3.2) has switched resistors from $1\text{ K}\Omega$ to $100\text{ K}\Omega$ together with switched capacitors from 0 pF to 100 pF . This can therefore give a range of input time constant from 50 n.sec up to $100\text{ }\mu\text{sec}$. The capacitance of the input lead must be included when the time constant is calculated. The two emitter follower stages act as a buffer amplifier between the input circuit and the attenuator.

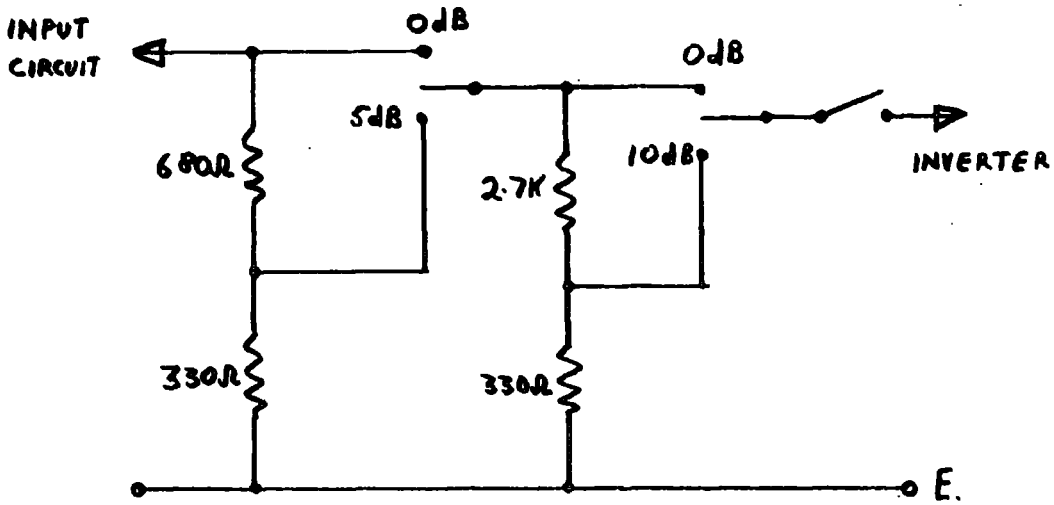


Fig. 3.3. The Variable Attenuator

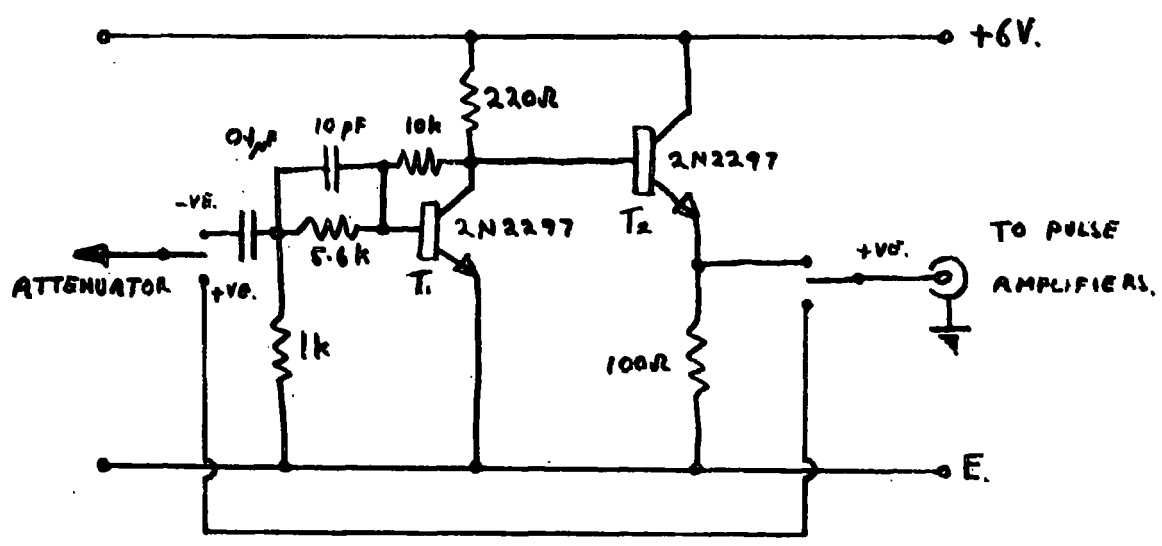


Fig. 3.4. The Pulse Inverter

When the galvanometer is switched into the circuit the switched resistors are set to open circuit. To avoid non-linear effects on the pulse shape it is necessary to use high frequency transistors and also to reduce stray capacitance in the wiring to a minimum.

3.4.2 Variable attenuator.

The purpose of the attenuator (Fig. 3.3) is to permit a wide range of pulses, ranging from 1 mV to 1V, to be amplified, by fixed gain amplifiers, up to a level suitable for the Differential Pulse Height Selector. The two pulse amplifiers each have a voltage gain of 20 dB, so that the attenuator introduces a certain amount of flexibility into the system. By using one or both of the pulse amplifiers in conjunction with the attenuator, the overall gain can be varied from 5 dB to 40 dB. As with the input circuitry it is important to minimise stray capacitance.

3.4.3 Pulse Inverter

The pulse inverter (Fig. 3.4) is used to invert negative point discharge pulses without changing their height or shape. This is necessary since the pulse height selector will only accept positive pulses. Thus it

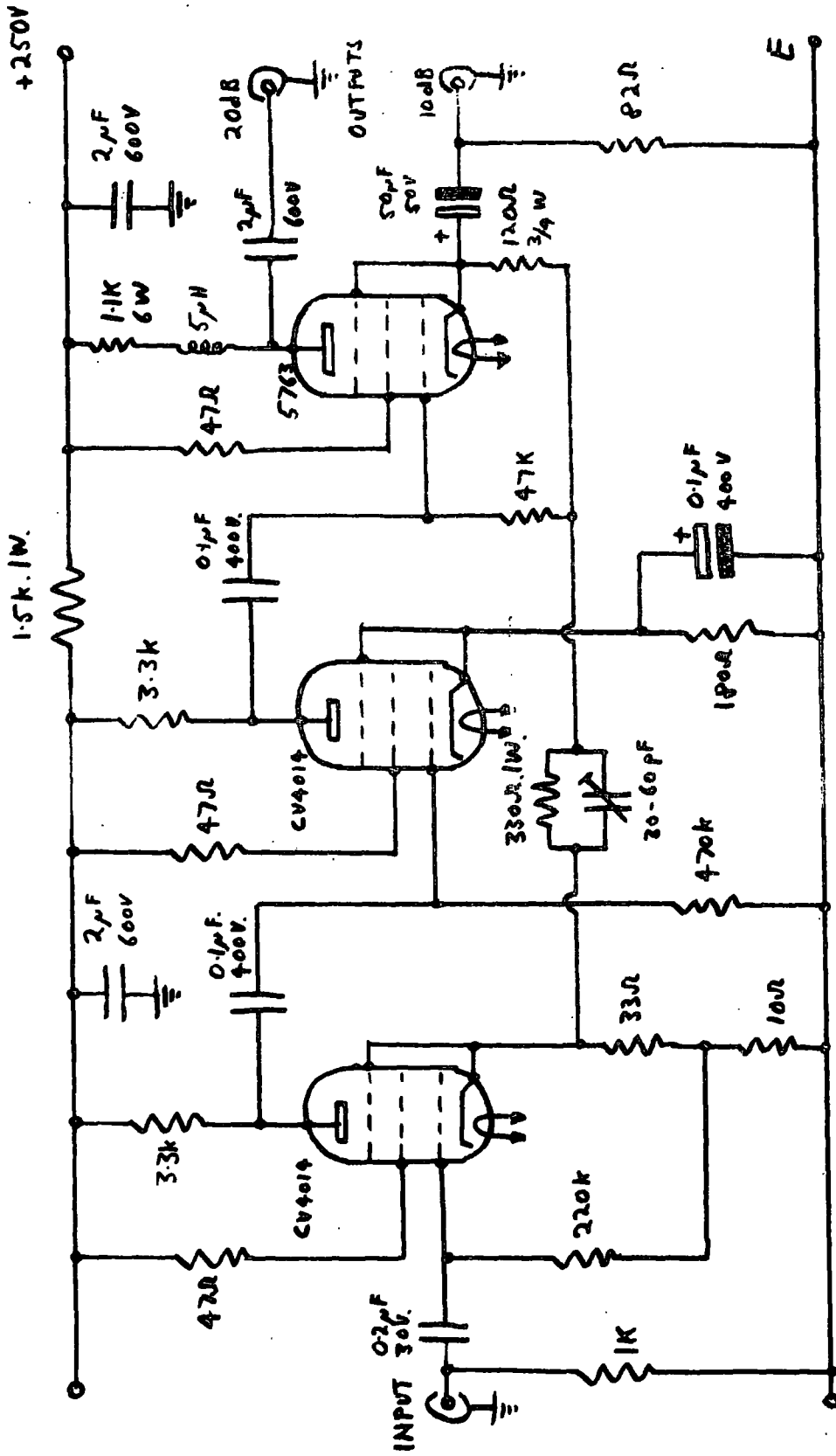


Fig. 3.5. The Pulse Amplifier Circuit

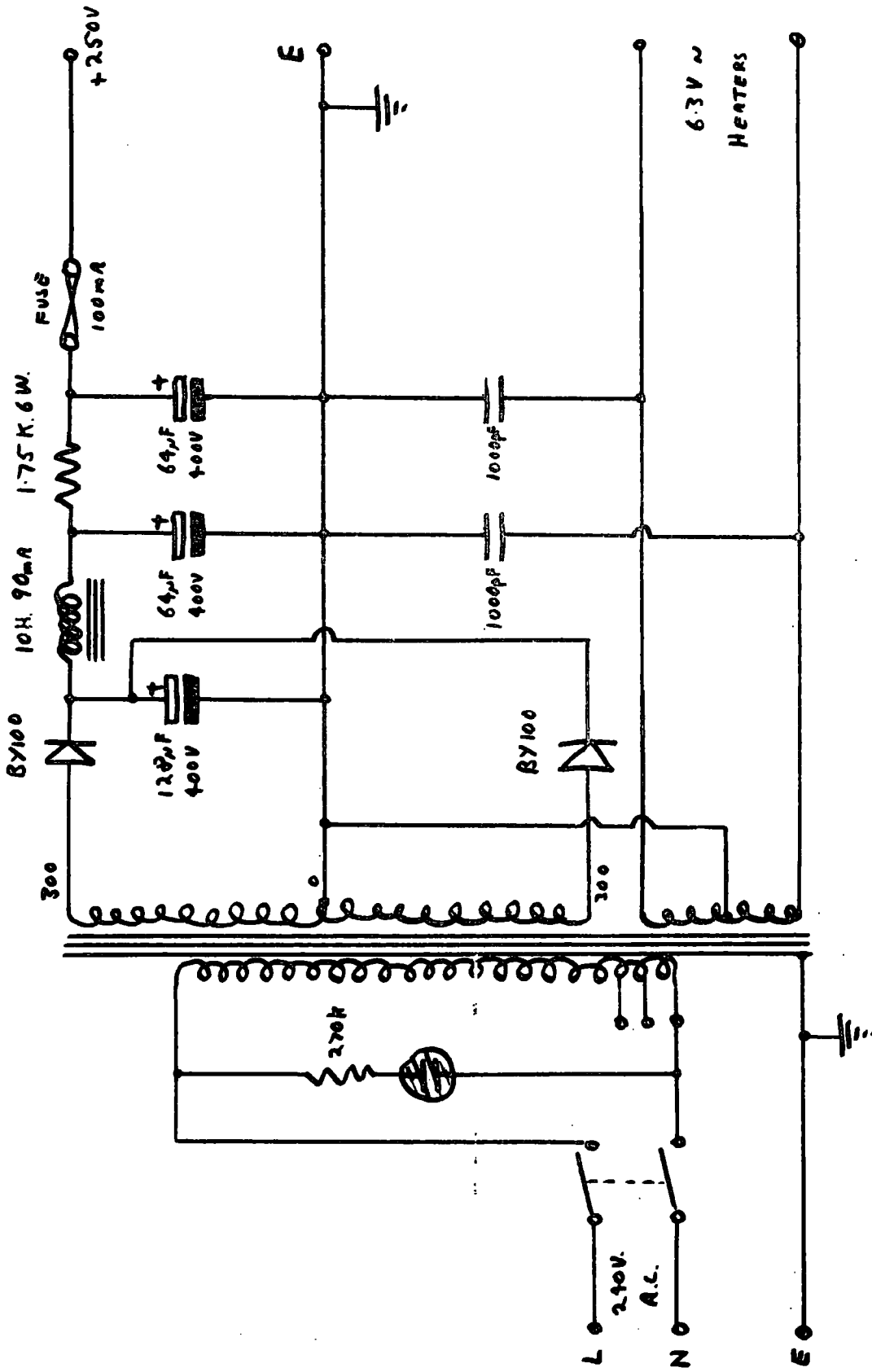


Fig. 3.6 Power Supply for the Pulse Amplifier.

is required that the inverter has a voltage gain of -1 over a wide frequency range. By using high frequency and high current transistors together with low resistance values, the shunting effect of stray capacitance is minimised. The feedback resistor for transistor T_1 was adjusted to give a voltage gain of -1 for the circuit as a whole, i.e. (T_1 and T_2). It was found necessary to incorporate a 10 pF capacitor into the feedback network to give high frequency compensation.

3.4.4 The pulse amplifiers

The voltage amplification required is about 30 dB together with a bandwidth of 15 MHz. A considerable amount of time was spent attempting to construct transistor pulse amplifiers to this specification. Several of the amplifiers constructed achieved one or other of the two requirements but they were all characterised by instability, in the form of oscillations, when the gain was increased above 20 dB. It was decided that the design and construction of a 30 dB wideband transistor feedback amplifier was too difficult and a valve circuit was sought. The circuit finally adopted (Figs. 3.5 and 3.6) (FEINBERG 1966) has a gain of 20 dB and 15 MHz bandwidth. Two such amplifiers were constructed, each with its own independent power supply. Thus a gain of 40 dB was achieved without instability. The rise time of the amplifiers is about 10 n Sec.

3.4.5 Differential Pulse Height Selector

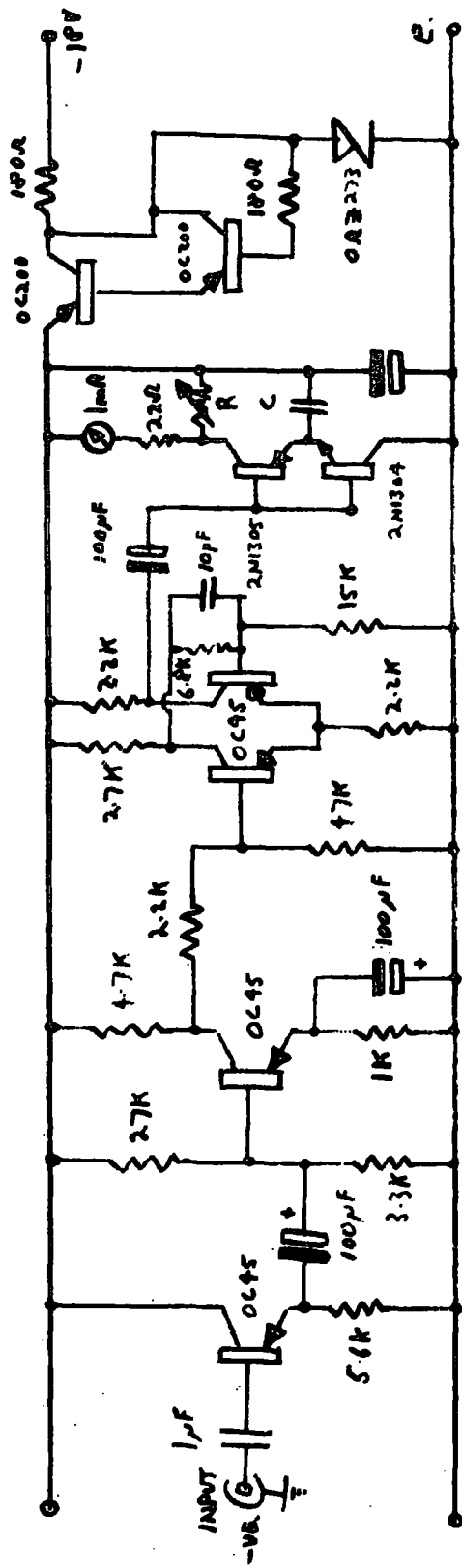
A single-channel differential pulse height selector (Type NE5103) was purchased from Nuclear Enterprises Ltd.

The specification of the unit is given below:-

NE5103 Specification

Discriminator operating range	:	3 to 100 V
Reset accuracy of range	:	0.1 V
Discriminator gate width	:	0 to 30 V
Reset accuracy of gate width	:	0.01 V
Resolving time	:	1.2 μ sec.
Maximum counting rate	:	2×10^5 per sec
Output pulse amplitude	:	9 V positive and 9 V negative
Output impedance	:	150 Ω
Pulse height drift	:	Less than 0.05 volts per day.
Gate width drift	:	Less than 0.01 volts per day

This unit was found to be more than adequate for the measurements which were made.



Range	R	C
0.1 kHz	100F	5 . F
1 kHz	100F	0.5 . F
10 kHz	100F	0.05 μ.F
100 kHz	100F	0.005 μ.F

Fig. 3.7. The integrating frequency meter

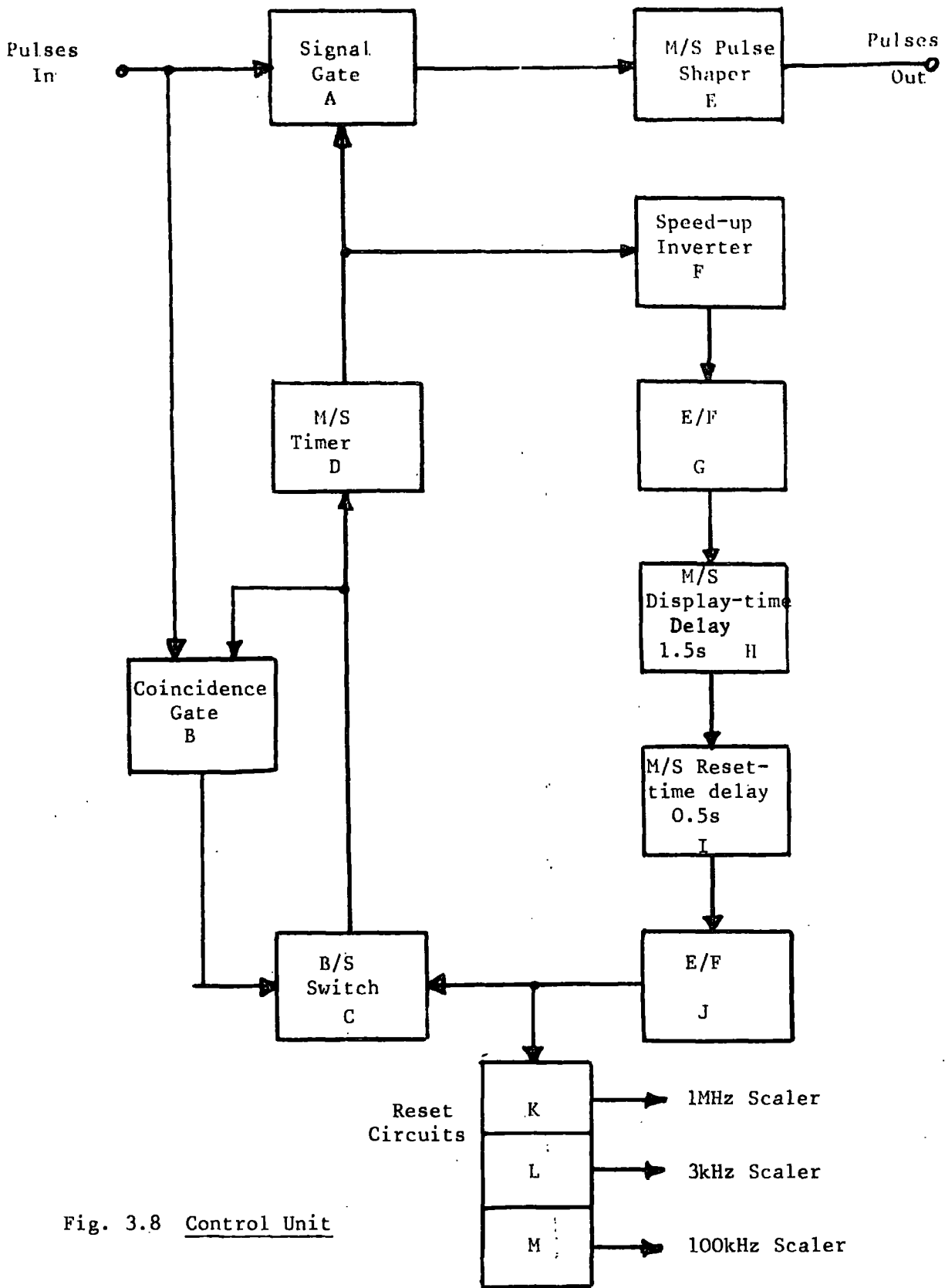


Fig. 3.8 Control Unit

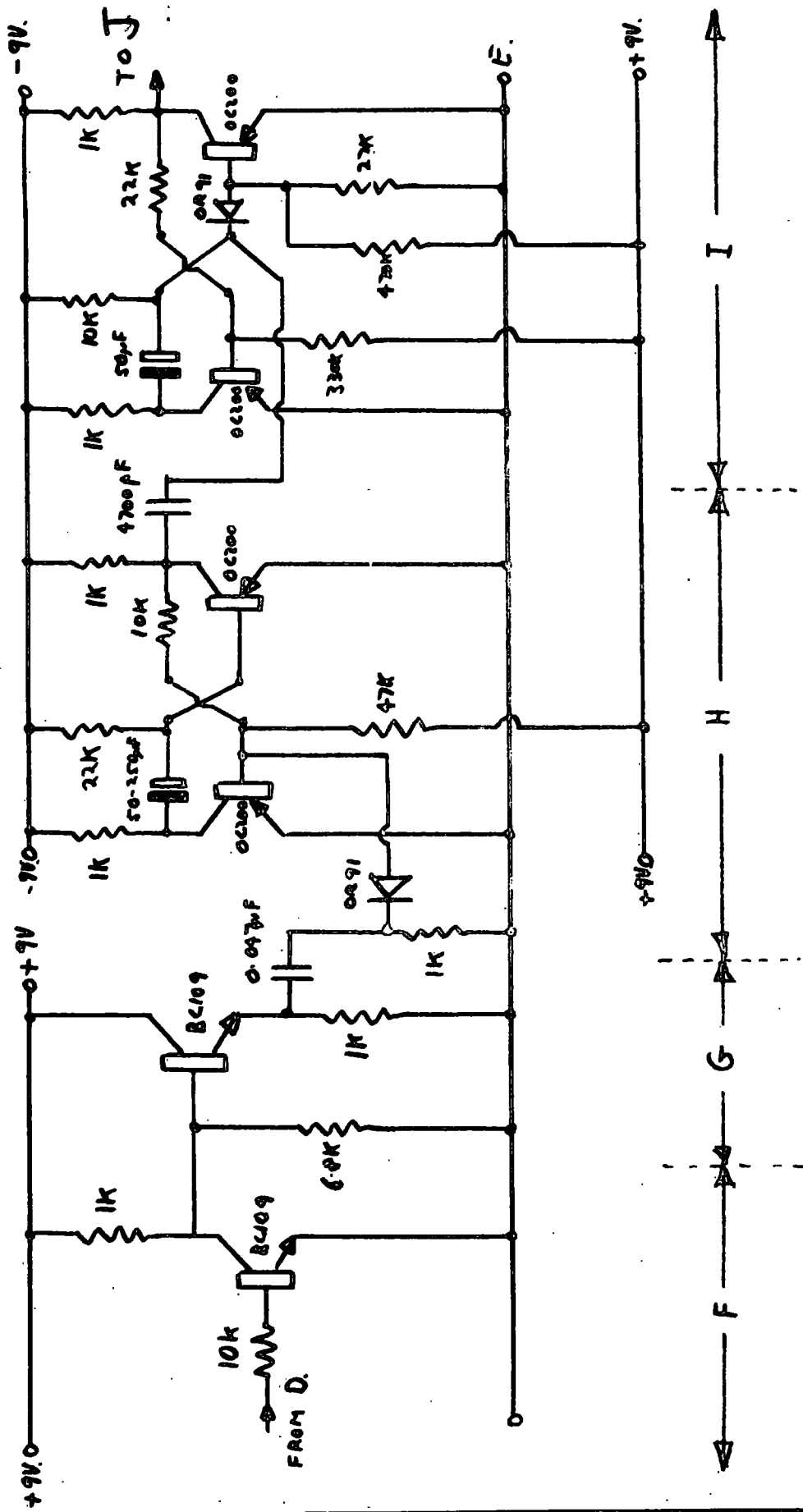


Fig. 3.9. Sections F, G, H, and I of Control Unit

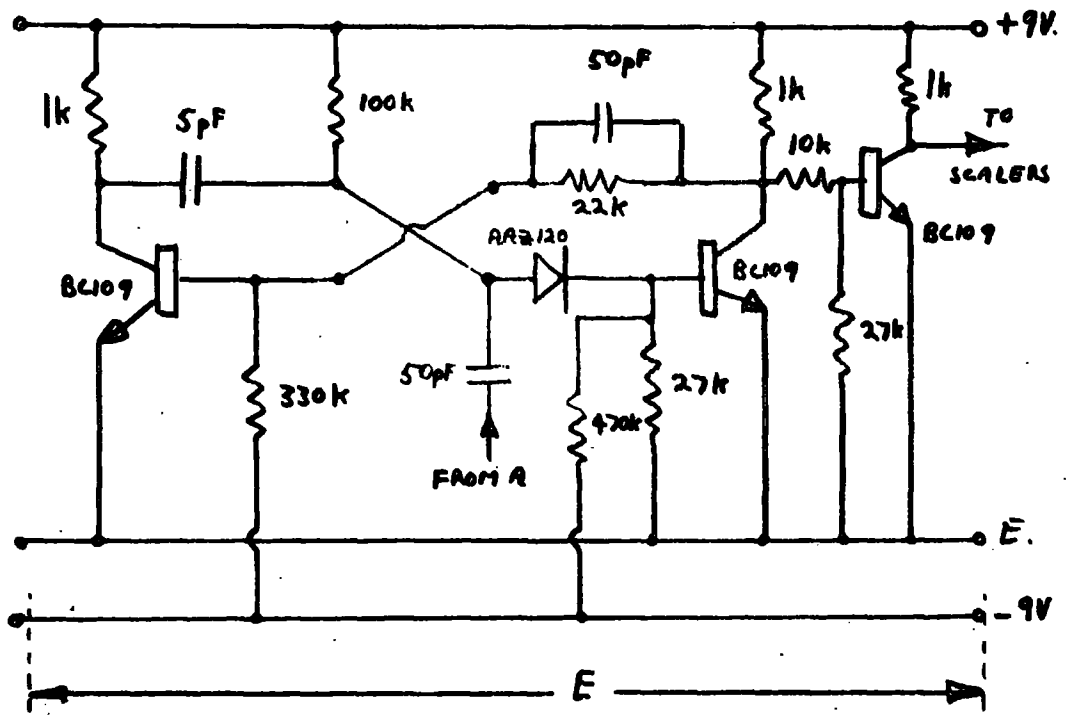
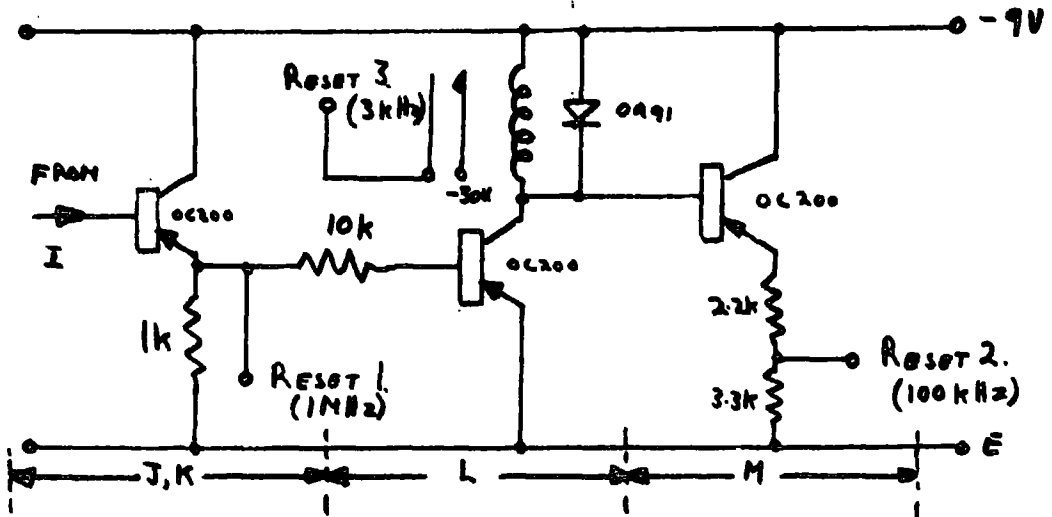


Fig. 3.10. Control Unit, Sections E, J, K, L and M.

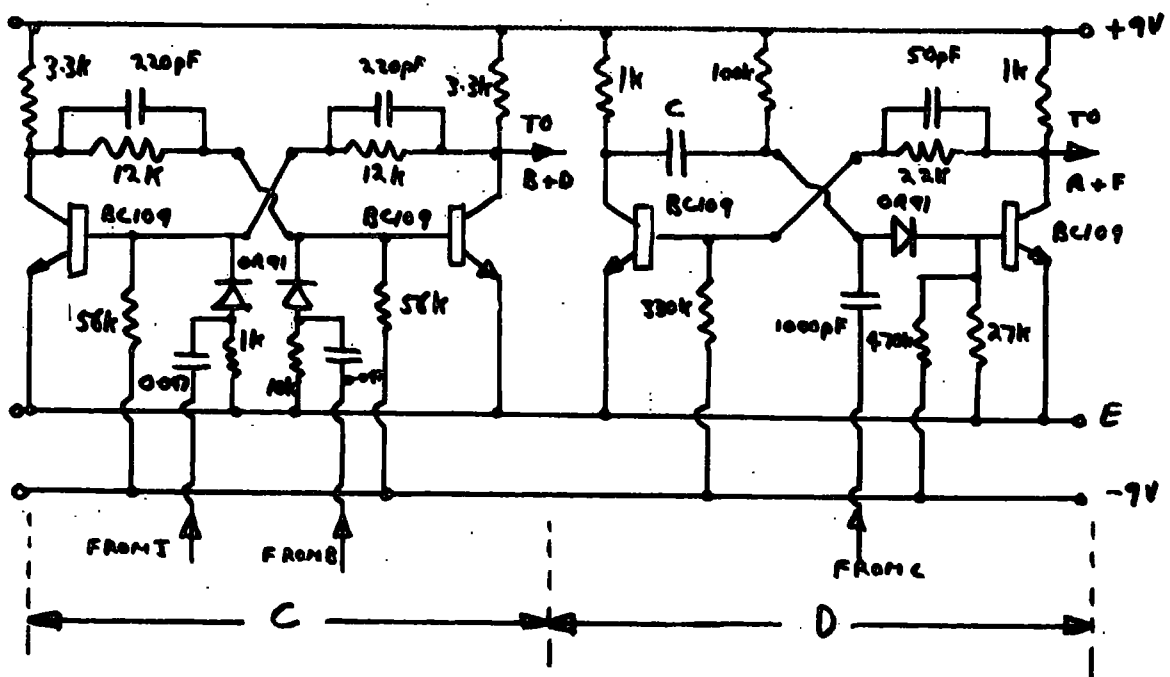
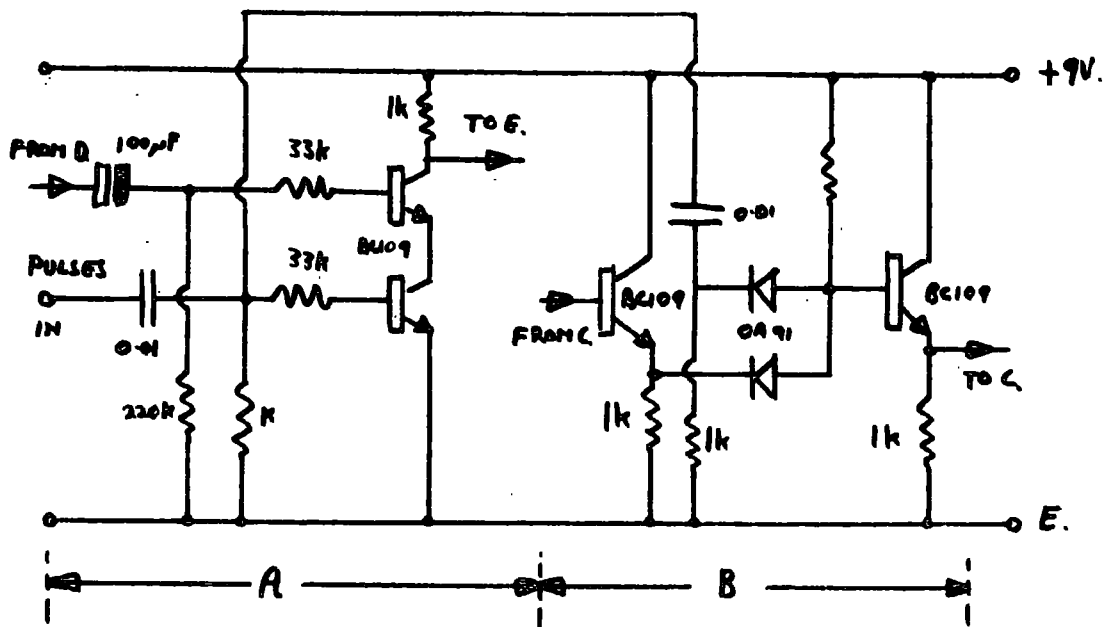


Fig. 3.11. Control Unit, Sections A, B, C and D

3.4.6 Integrating frequency meter

This unit is driven from the negative output of the pulse height selector. The circuit used (Fig. 3.7) is a fairly standard one. The use of complementary transistors in the final stage gives good linearity (1%) in the output. The output is displayed on a 0-1 mA meter. The unit has four frequency ranges; 0 - 0.1, 0 - 1, 0 - 10 and 0 - 100 kHz. The output meter has a response time of about 1 second so that the frequency reading is an integration over a period of this order.

3.4.7 Control Unit

This unit was constructed in order that the measuring system as a whole would run automatically. It controls the passage of pulses to the scalars and returns the scalars to zero after each count has been displayed. The length of time for which the pulses are counted can be varied from 10 μ sec to 1 sec. The display time can be adjusted to 1, 3 or 5 sec. The circuit is shown schematically in Fig. 3.8 and in detail in Figs. 3.9, 3.10 and 3.11. The control unit was designed using conventional pulse circuit elements such as monostable circuits and coincidence gates. Detailed description of these elements will not be given as their design and operation are

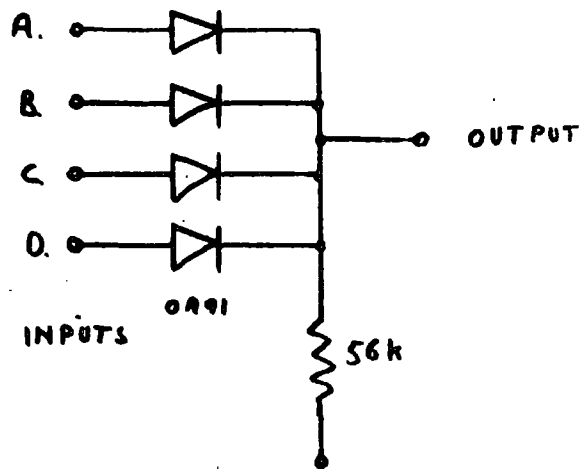
adequately covered in standard textbooks (e.g. TOWERS. 1965). However, a description of the operation of the unit as a whole may be of use.

The +9V pulses entering the control unit, after the scalars have been reset to zero, cannot pass through the signal gate A, as it is closed. However, the pulses are also being applied to one input of the coincidence gate B. The second input of this gate B is being held at +9V by the bistable switch C. The first +9V pulse to arrive at B causes coincidence and a single +9V output pulse is generated which changes the state of bistable C. No further pulses are generated, as the bistable C is now no longer maintaining +9V on one input of B. The change of state of C also triggers the monostable timer D, which in turn opens the signal gate A for the selected time. Pulses now pass through A to the monostable pulse shaper E. This shortens the rise time of the pulses so that they are sufficiently sharp to drive the 1 MHz scaler. When the monostable timer D closes the signal gate A, it also triggers the monostable display time delay H, via an inverter F, and an emitter follower G. The purpose of the inverter F is to speed up the negative face of the pulse from D. At the end of the

display time delay, which can be set to 1, 3 or 5 sec, the monostable reset time delay I is triggered. The output from I immediately causes the reset circuits K, L and M to generate the reset pulses for the 1 MHz, 100 kHz and 3 kHz scalars. At the end of the reset time delay of 0.5 sec, the bistable C is switched, by I, to its original state. Thus C once again maintains one input of the coincidence gate B at +9V. The system has now completed one cycle and the next pulse to arrive will cause the process to be repeated.

3.4.8 1 MHz scaler

For this scaler, a 1 MHz decade counter module, type DCM 703, was purchased from Quarndon Electronics Ltd. The module consists of four saturating bistable elements a binary-to-decimal decoding network and driver circuits to control the numerical indicator tube. This scaler forms the first decade of a seven-decade counter and also produces the necessary output pulses for the next decade. The input of the scaler is connected to the output from the control unit. The reset pulse is also obtained from the control unit.



4 ENTRY AND-GATE.

AND GATE		OUTPUTS OF D.C.M. USED			
DECIMAL	0	Q_1	Q_2	Q_3	Q_4
"	1	Q_1	Q_2	Q_3	Q_4
"	2	Q_1	Q_2	Q_3	Q_4
"	3	Q_1	Q_2	Q_3	Q_4
"	4	Q_1	Q_2	Q_3	Q_4
"	5	Q_1	Q_2	Q_3	Q_4
"	6	Q_1	Q_2	Q_3	Q_4
"	7	Q_1	Q_2	Q_3	Q_4
"	8	Q_1	Q_2	Q_3	Q_4
"	9	Q_1	Q_2	Q_3	Q_4

Fig. 3.12. Binary-to-Decimal Conversion

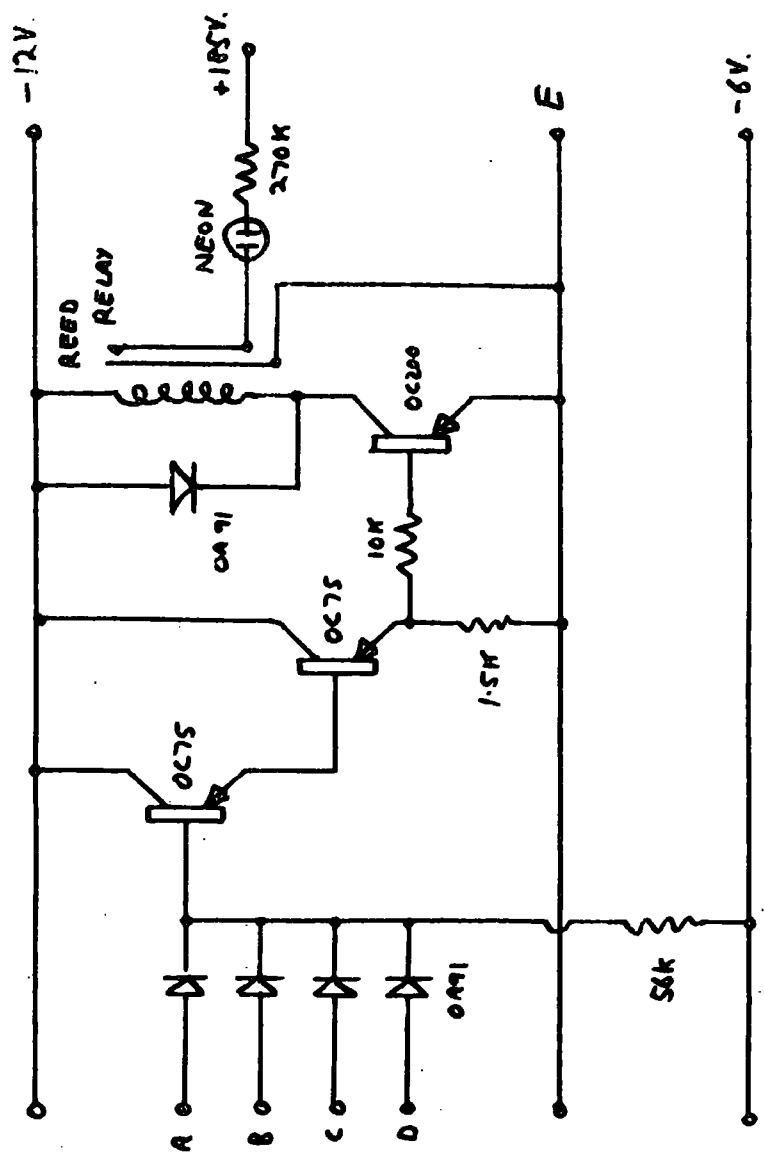


Fig. 3.13. Readout Display for one Digit

3.4.9 100 kHz scalars.

Two Mullard 100 kHz decade counter modules form the second and third decades of the scaler. These modules give a binary output and so it was necessary to construct the binary-to-decimal converters and the read-out displays. (Figs. 3.12 and 3.13). The state of the binary output from the module, A, B, C and D and their inverses \bar{A} , \bar{B} , \bar{C} and \bar{D} , gives the decimal count. The loading of the counter is 1 - 2 - 4 - 2, thus

$$\begin{array}{ll}
 A = 0 \text{ or } 1 & \bar{A} = 1 \text{ or } 0 \\
 B = 0 \text{ or } 2 & \bar{B} = 2 \text{ or } 0 \\
 C = 0 \text{ or } 4 & \bar{C} = 4 \text{ or } 0 \\
 D = 0 \text{ or } 2 & \bar{D} = 2 \text{ or } 0
 \end{array}$$

The decimal output is therefore obtained by decoding the eight binary outputs. This can be achieved by using an electronic logic element known as an "AND" Gate. This gate can have any number of inputs and usually has one output. If we let +6V represent binary 1 and 0V represent binary 0, then we can say that the output from an "AND" gate will be +6V when, and only when, all the inputs are at +6V. The "truth table" given below illustrates the properties of an AND gate.

e.g. Three-entry AND gate

TRUTH TABLE			
INPUT'S			OUTPUT
A	B	C	
1	1	1	1
0	0	0	0
0	0	1	0
0	1	0	0
0	1	1	0
1	0	0	0
1	0	1	0

The decoding of the decade counters is achieved using ten four-entry AND gates. Each gate is connected to four of the eight outputs from the module (Figs. 3.12 and 3.13) e.g. Decimal 7 The AND gate is connected to A, B, C and \bar{D} as all these are in the binary 1 state when the counter is in a state representing decimal 7.

The outputs from each of the ten AND gates are connected to gate amplifiers, which drive neon indicator bulbs via reed relays. Thus an output from the decimal 7 AND gate, for example, will illuminate the 7th neon bulb (Fig. 3.13) for that decade.

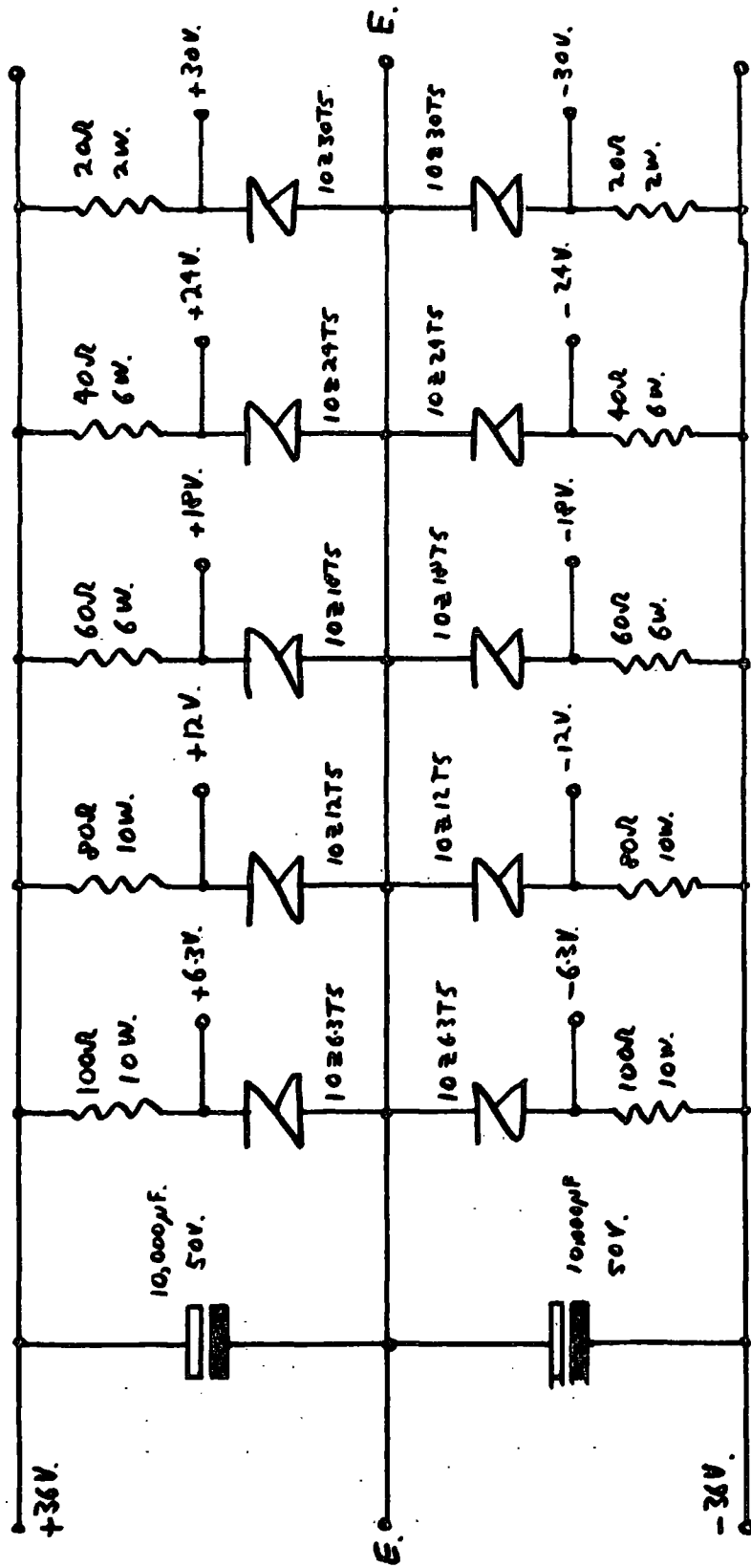


Fig. 3.14 Basic Circuit for the Stabilised Power Supply

3.4.10 3 kHz Scaling Unit

The remaining four decades of the pulse counter consisted of a decatron scaling unit TYPE 2026A. This scaler will count reliably only up to a p.r.f. of 3.3 kHz. However, the maximum p.r.f. it can have at its input is 1 kHz since the frequency limit of the first decade is 1 MHz.

3.4.11 Power Supplies.

The control unit, frequency meter, scalars, etc. require stabilised supplies at various voltages. A power supply was constructed to give $+6$, $+12$, $+18$, $+24$ and $+30$ V (Fig. 3.14). The maximum available current for each voltage is 300 mA. Stabilisation of the voltages is achieved by using Zener diodes. The ripple on the output due to 50 Hz is less than 20 mV.

3.5 Performance of the system

The accuracy in pulse height selection is determined mainly by the constancy of gain of the pulse amplifiers. The gain of the amplifiers was found to vary by less than 5% for a 10% change in the mains supply and wide variation in ambient temperatures.

Measurements of pulse repetition frequency are limited by the accuracy and constancy of the timing interval. Temperature variations caused the biggest changes in timing interval. In extreme cases these amounted to 5%

Over period of a few hours the variations in pulse height selection and frequency measurement amounted to 1%. On each occasion before measurements of point discharge pulses were made, the system was calibrated with a signal of known amplitude and frequency.

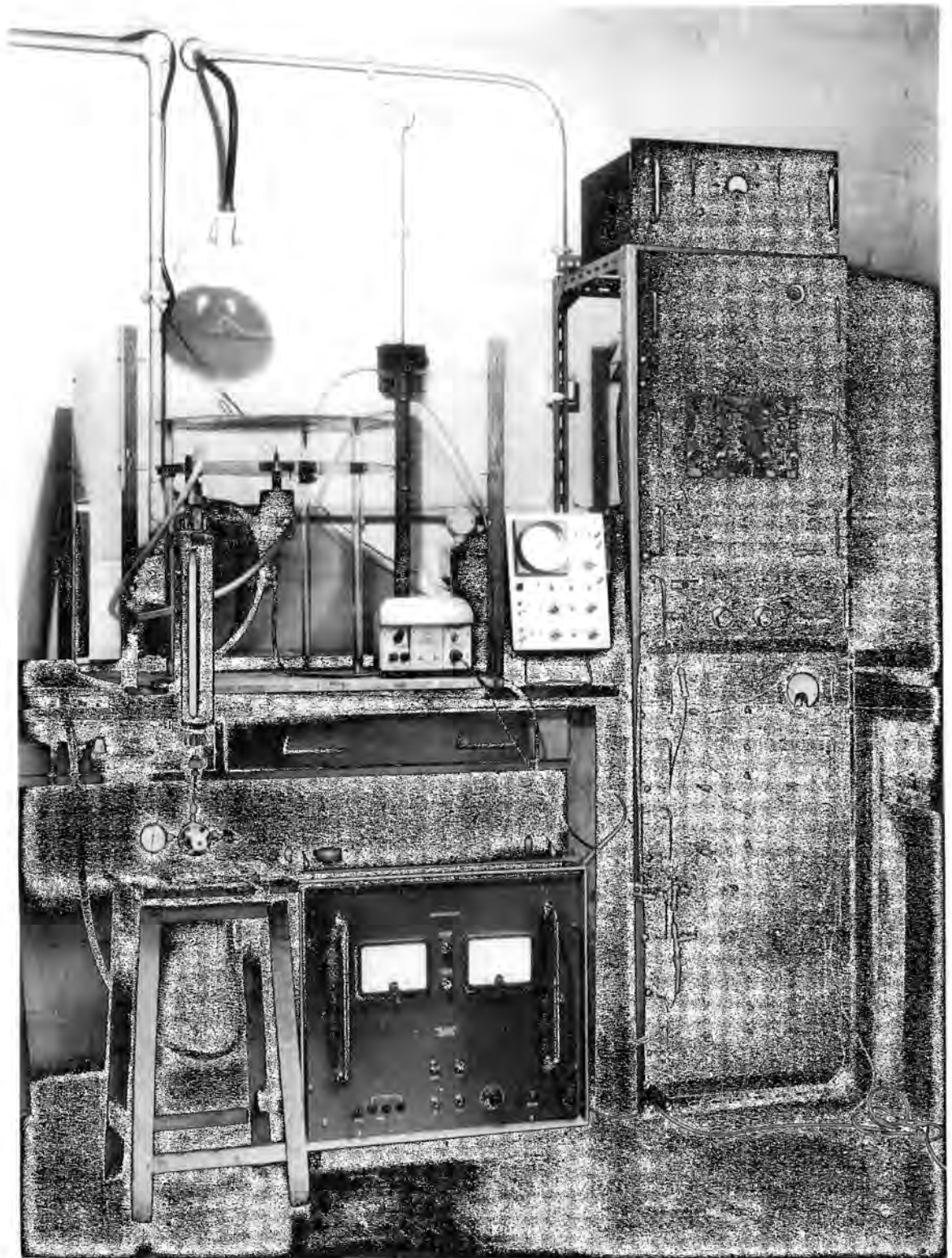


FIG. 4.1 APPARATUS USED FOR LABORATORY MEASUREMENTS
OF POINT DISCHARGE

CHAPTER 4.

Laboratory Measurements with Metal Points

4.1 Introduction

The experiments described in this Chapter give information about the characteristics of point discharge pulses from single metal points of different tip radii. The characteristics of the pulses from an array of five metal points were also investigated. The purpose of these experiments is to find the distributions of pulse interval and pulse amplitude and to see how these are affected by the nature and number of points.

4.2 Apparatus

The point-plane apparatus which was used consisted of two circular aluminium plates mounted on insulating legs (Fig. 4.1). The fixed top plate is connected to a variable E.H.T Supply (Brandenburg Type M.R.50A) giving up to 50 kV at 1 mA. The lower earthed plate can be moved to give the required plate separation. The two plates are surrounded by a perspex safety screen. The single metal points which were used had tip radii of 0.05, 0.15, 0.40, 0.8 and 1.5 mm. The points were made from 0.125" silver

steel rod. To obtain the required tip radii the rods were ground and polished, until examination under a microscope showed that the radius was correct. The multiple point array consisted of five steel needles, each with a tip radius of approximately 0.1mm. The single points can be mounted in a holder in the lower earthed plate and the arrangement allows air to be blown past the point in a direction parallel to the point (Fig. 4.1). In all the experiments with single metal points an air flow of 10 l min^{-1} was maintained past the points. When multiple points were being used the single point holder was replaced by the base plate for the five points. In this case an air flow of approximately 25 l min^{-1} was maintained past the points in a direction parallel to the plates.

The electrical connection between the point and the measuring equipment was by means of a coaxial cable having a total shunt capacitance of 500 pF. The input resistance of the equipment was adjusted to $10 \text{ K}\Omega$ so that the input time constant was $10 \text{ K}\Omega \times 500 \text{ pF}$, i.e. $5 \mu\text{s}$. An oscilloscope, Phillips Type 3102, was used to monitor the pulse waveforms. The rise time of this instrument is 30 ns .

The conditions stated in 2.3.3. are therefore satisfied, i.e.

$$RC \geq 100 T$$

$$T \leq 3 T$$

where RC is the input time constant, T_R is the rise time of the oscilloscope or the pulse amplifiers and T is the minimum possible rise time for the pulses.

4.3 Techniques of measurement

4.3.1 Positive Currents

With all the points used, the height of the point above the earthed plate and the point-plane gap were both adjusted to be 5 cm. The measurements described below were made for each of the five single points and then for the set of multiple points. In each case the measurements were made in three stages.

Stage 1. The voltage V_p on the upper plate was increased and the discharge current I , pulse frequency f and maximum pulse height \hat{V} were measured. The discharge current I was found simply by allowing the current to flow to earth through the galvanometer. The integrating frequency meter gave the pulse repetition frequency f and the maximum pulse amplitude \hat{V} was obtained from oscilloscope measurements.

Stage 2. To obtain the distribution of pulse interval the frequency of the pulses was measured using the pulse counters. The counting time was adjusted so that approximately 100 pulses were counted. About 25 such counts were recorded for each of several different currents.

Stage 3. The distribution of pulse height was obtained by varying the setting of the differential pulse height selector and observing the corresponding reading on the integrating frequency meter. Thus as the minimum pulse height threshold is gradually increased, the observed pulse repetition frequency f will at some point begin to fall from its maximum value and eventually reach zero.

4.3.2 Negative Currents

The technique of measurement for negative currents was essentially the same as that described above. One difference was that in some cases there was a range of current I , where the discharge was continuous and thus no pulses were observed. However, measurements were made in the three stages described in 4.3.1.

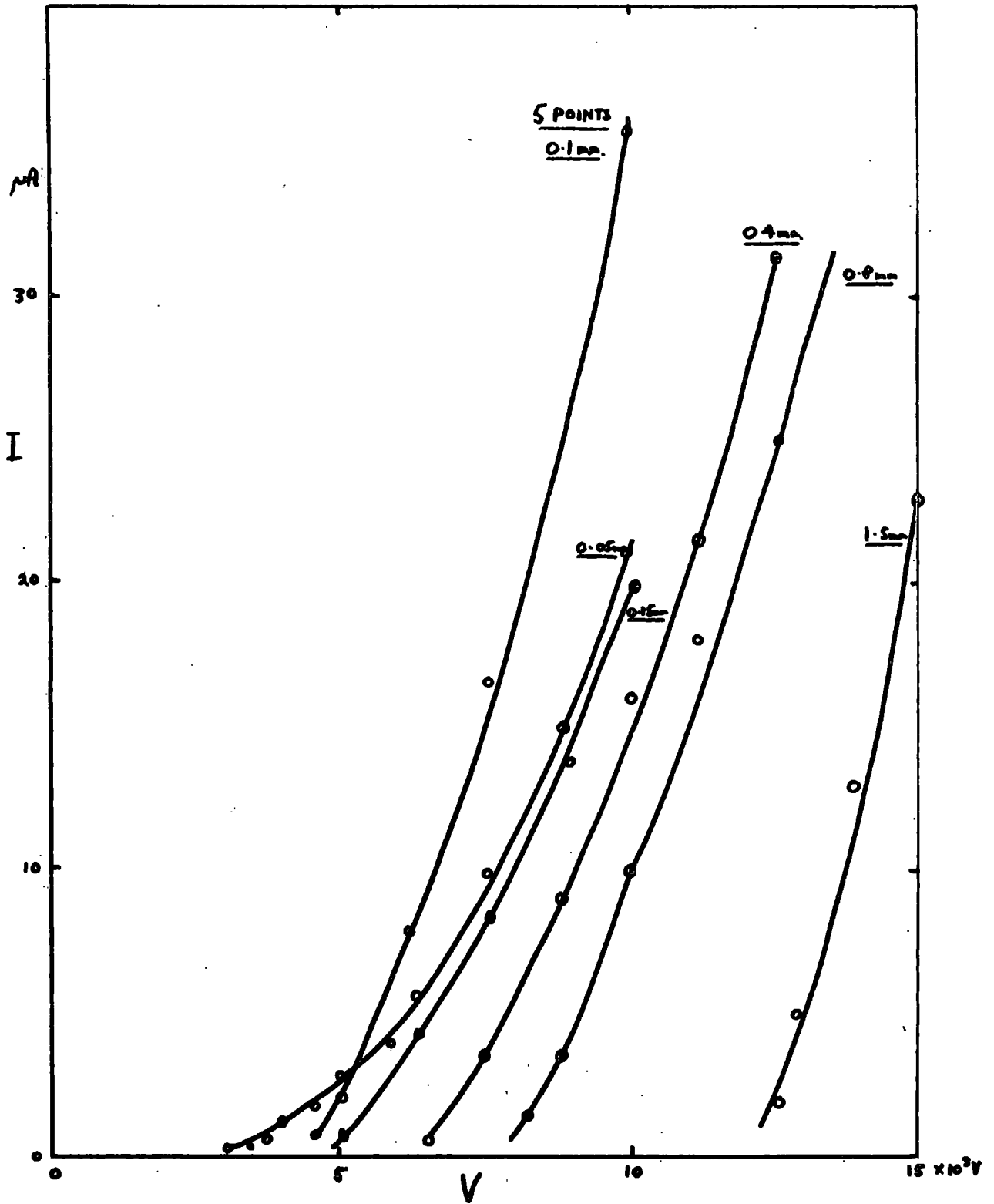


Fig. 4.2. Potential V and Positive Current I for metal points.

4.4 Results for Positive Currents

4.4.1 Potential - Current Characteristics.

The potential V in a region between the plates, at a height h above the lower plate, where the field is not disturbed appreciably by the presence of the point is given by:-

$$V = hV_p/D$$

where D is the plate separation and V_p is the plate voltage. If h is the height of the point then V will be the potential in the air near the point. Fig. 4.2 shows a plot of V against I for five single points and also the array of five points.

It can be seen that the value of the potential V , at which the discharge commences, increases as the tip radius increases. This is to be expected since, for a given plate voltage, the potential gradient is greatest at the surface of the sharpest point. Thus the discharge will commence first at the sharpest point. The curve for the array of five points (Fig. 4.2) has a greater slope than the other curves for single points and it also crosses the curve for $r = 0.05$ mm. This is in agreement with the results of JHAWAR (1967).

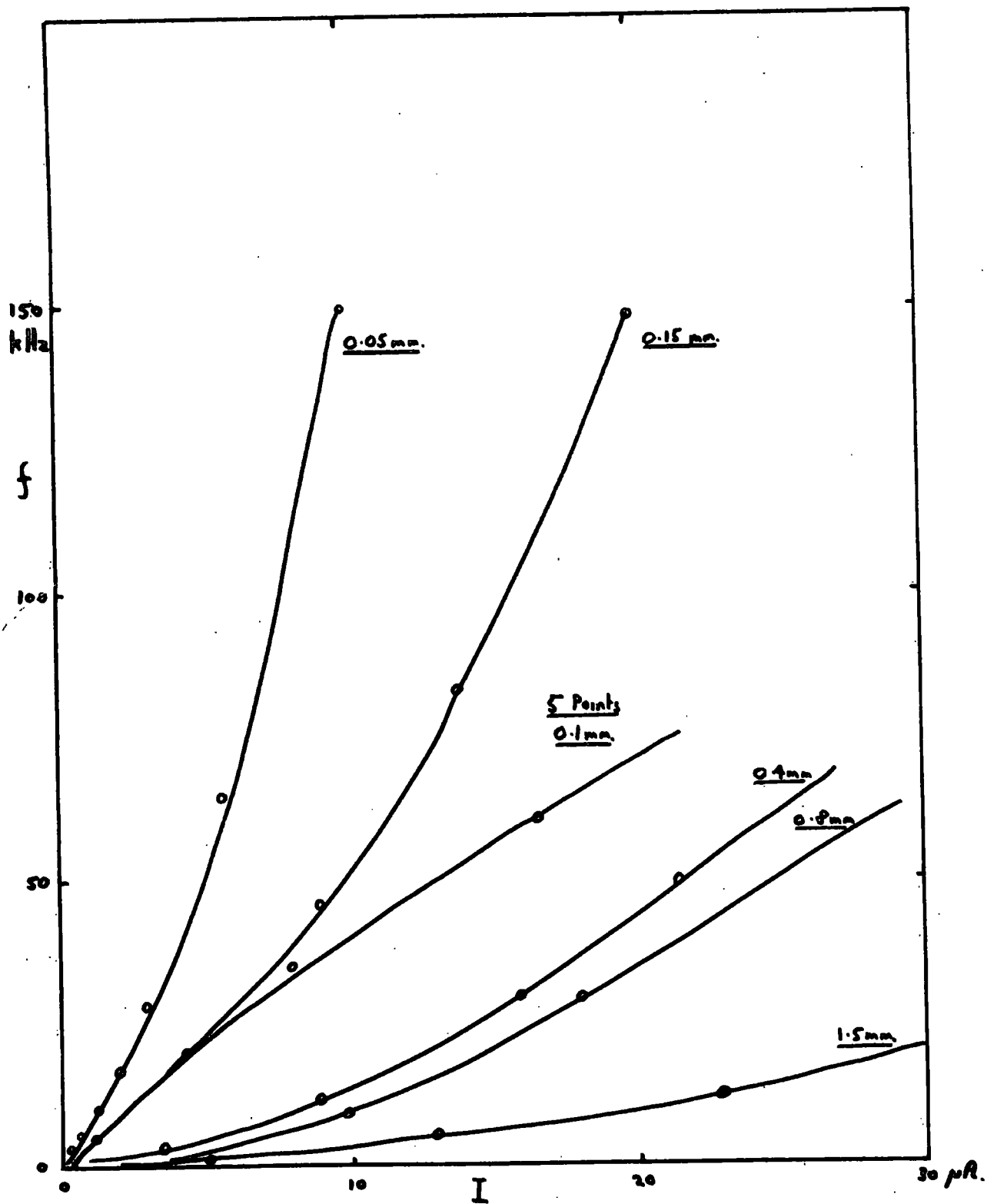


Fig. 4.3. Frequency f and Positive Current I for Metal Points

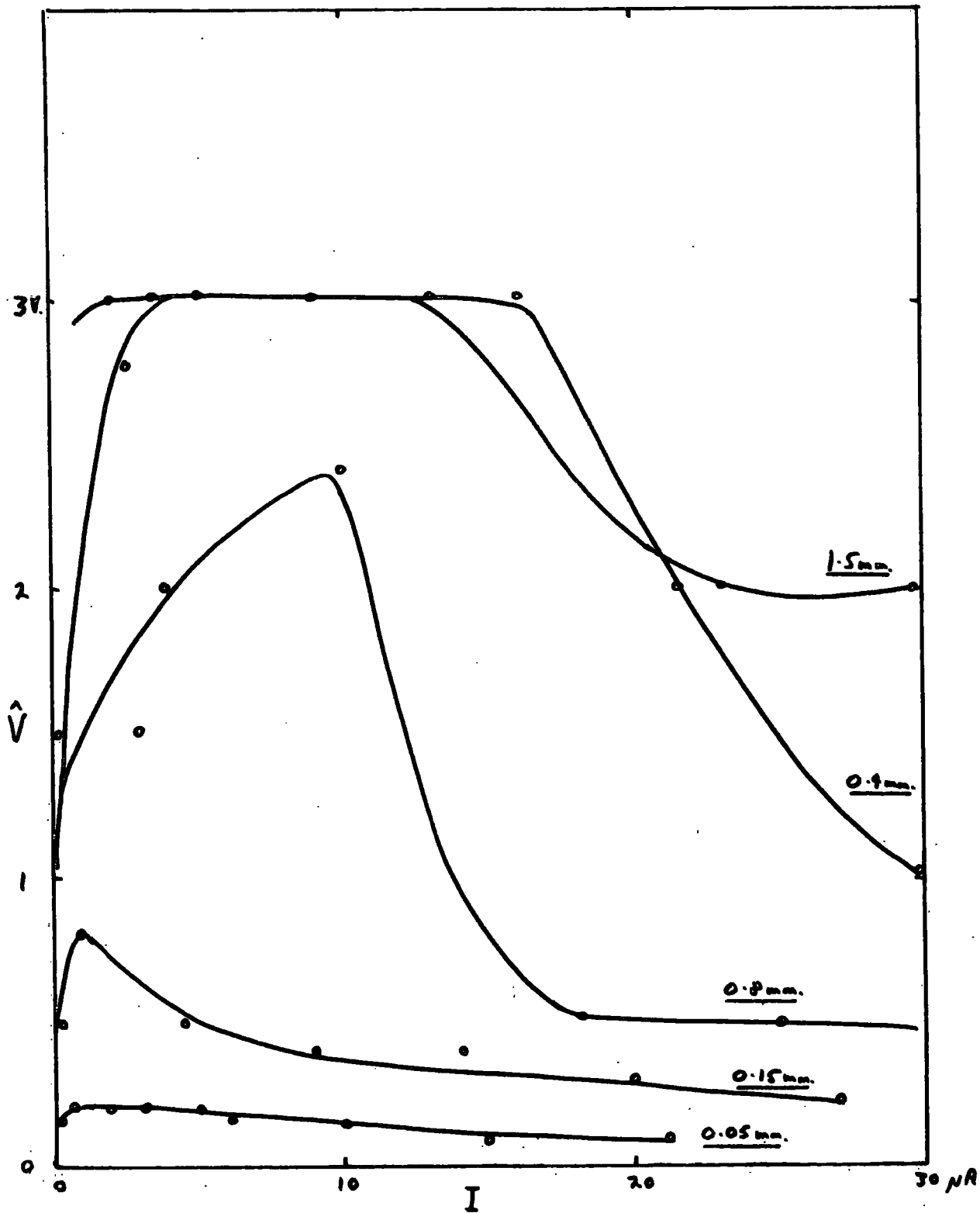


Fig. 4.4 Pulse Amplitude \hat{V} and Positive Current I for single metal points

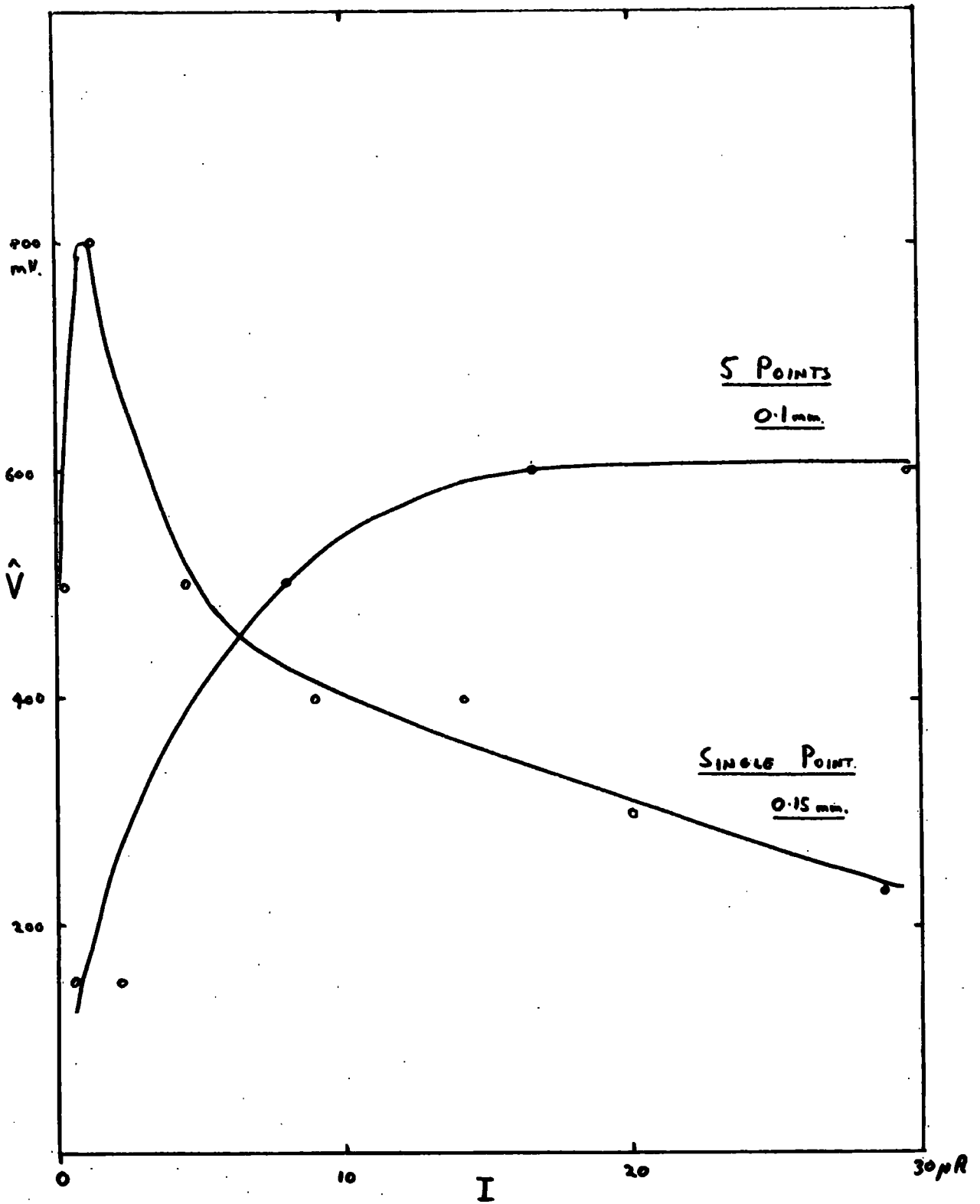


Fig. 4.5. Pulse Amplitude \hat{V} and Positive Current I for 5 Points

4.4.2 Frequency - Current Characteristics

A plot of the pulse repetition frequency f versus current I is shown in Fig. 4.3. It can be seen from this that the slope of the curves for the single points decreases as the tip radius increases. This indicates that the charge per pulse is larger for points with larger tip radii.

The slope of the curve for the multiple points was smaller than was expected. The cause of this is probably that, with an input time constant of $5 \mu\text{s}$, the pulses from the five points will begin to coincide at higher frequencies. Thus it can be seen that the curve for five points follows the curve for a single point of 0.15 mm radius to begin with, and then falls away.

4.4.3 Pulse amplitude - current characteristics

The maximum observed amplitudes \hat{V} are shown plotted against current I in Figs. 4.4 and 4.5. A higher charge per pulse for points of larger tip radii can be inferred from these graphs as the pulse amplitude is directly related to the charge per pulse. In fact, in the ideal case where $T_R = 0$ and $RC \gg T$

$$\hat{V} = Q/C$$

where Q is the charge per pulse and C is the total input

capacitance. It can also be seen from the graphs that \hat{V} is more variable for larger values of tip radius r . The reason for this is that the discharge spot can move about on the surface of points of large r . This causes a change in the charge per pulse Q . With sharp points the discharge spot does not move appreciably and Q remains approximately constant. The effect of pulse coincidence in the multiple point case is shown as an increase in the observed amplitude \hat{V} at higher frequencies. (Fig. 4.5.)

4.4.4. The standard deviation of pulse intervals

If the standard deviation of the interval between consecutive pulses can be obtained, we have a measure of the irregularity of occurrence of the pulses. The measurements using the pulse counter give the number of pulses n , occurring in each of N equal periods of time t_c . Thus \bar{f} , the mean p.r.f., for a given period t_c , will be:

$$\bar{f} = n/t_c$$

The average p.r.f. for all the periods, is given by

$$f = \bar{n}/t_c$$

where \bar{n} is the mean pulse count, given by

$$\bar{n} = \sum_1 n/N$$

The average pulse interval τ will therefore be

$$\tau = t_c/\bar{n}$$

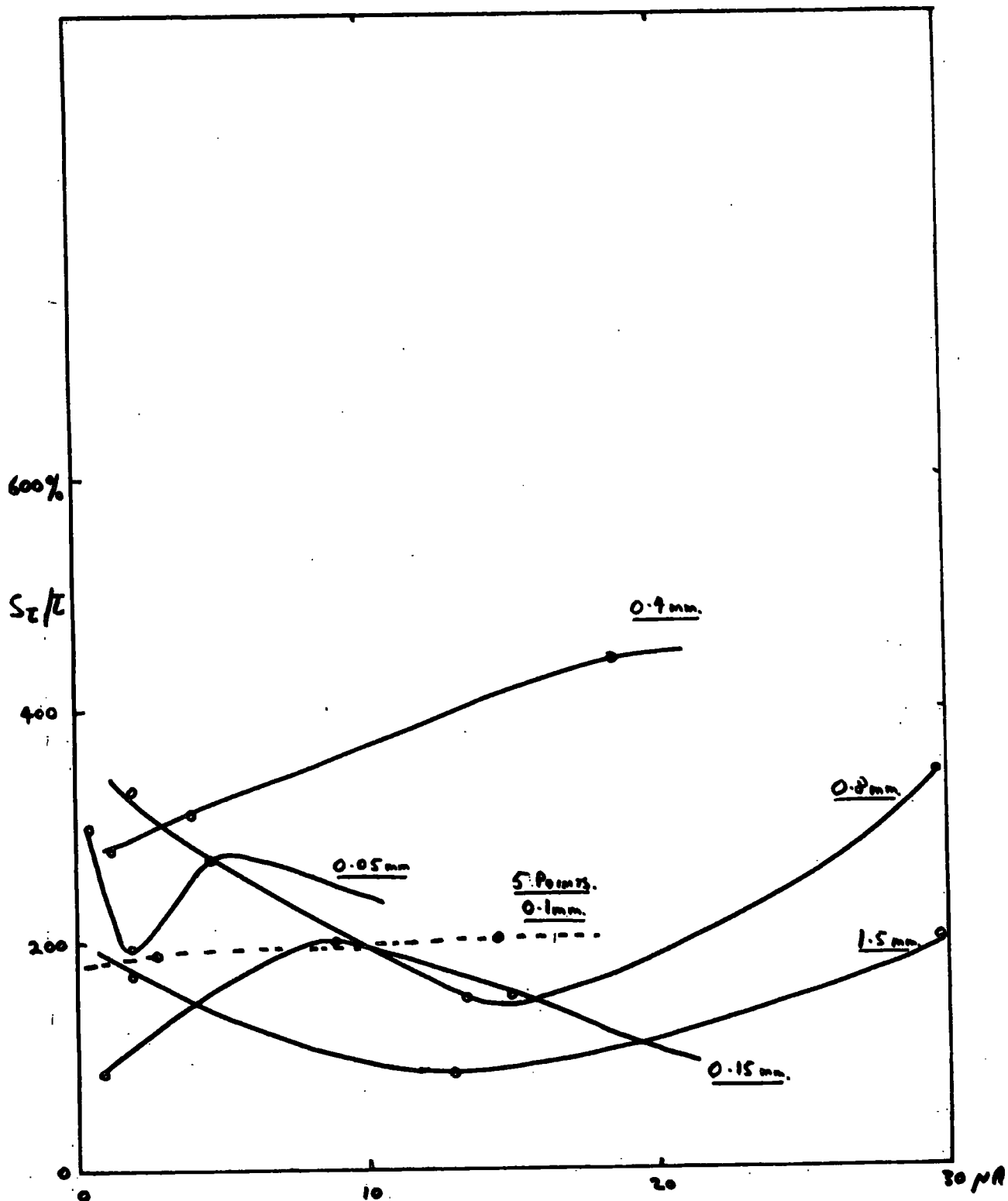


Fig. 4.6 Irregularity of Pulse Intervals S_T/T and Positive Current I for metal points.

Let the standard deviation of the N values of n be S_n and the standard deviation of the pulse interval for the N periods of time t_c , be S_τ . Now the magnitude of S_n will decrease as \bar{n} increases. In fact S_n will be inversely proportional to the square root of \bar{n} . Therefore we can write:-

$$(1)^{\frac{1}{2}} S_\tau / \tau = (\bar{n})^{\frac{1}{2}} (S_n / \bar{n})$$

$$\therefore S_\tau / \tau = S_n / (\bar{n})^{\frac{1}{2}}$$

$$\text{where } S_n = (\sum (n - \bar{n})^2 / N)^{\frac{1}{2}}$$

From the observed values of n , values of S_τ / τ were obtained and expressed as a percentage for each of the points at various currents. The results are shown graphically in Fig. 4.6. A low value of S_τ / τ signifies high pulse regularity. It can be seen that, for the sharpest points, the pulses become more regular at higher currents. The other points reached a maximum in regularity at about 15 μ A and then became more irregular for higher currents. The reason for this difference is probably that "families of pulses" occur for the less sharp points at higher currents. Thus the discharge may be occurring at two or three places on the surface of the point giving pulses with differing charge. The pulses were also observed on the oscilloscope to be much more irregular when more than one pulse was present in each family. In most cases the number of

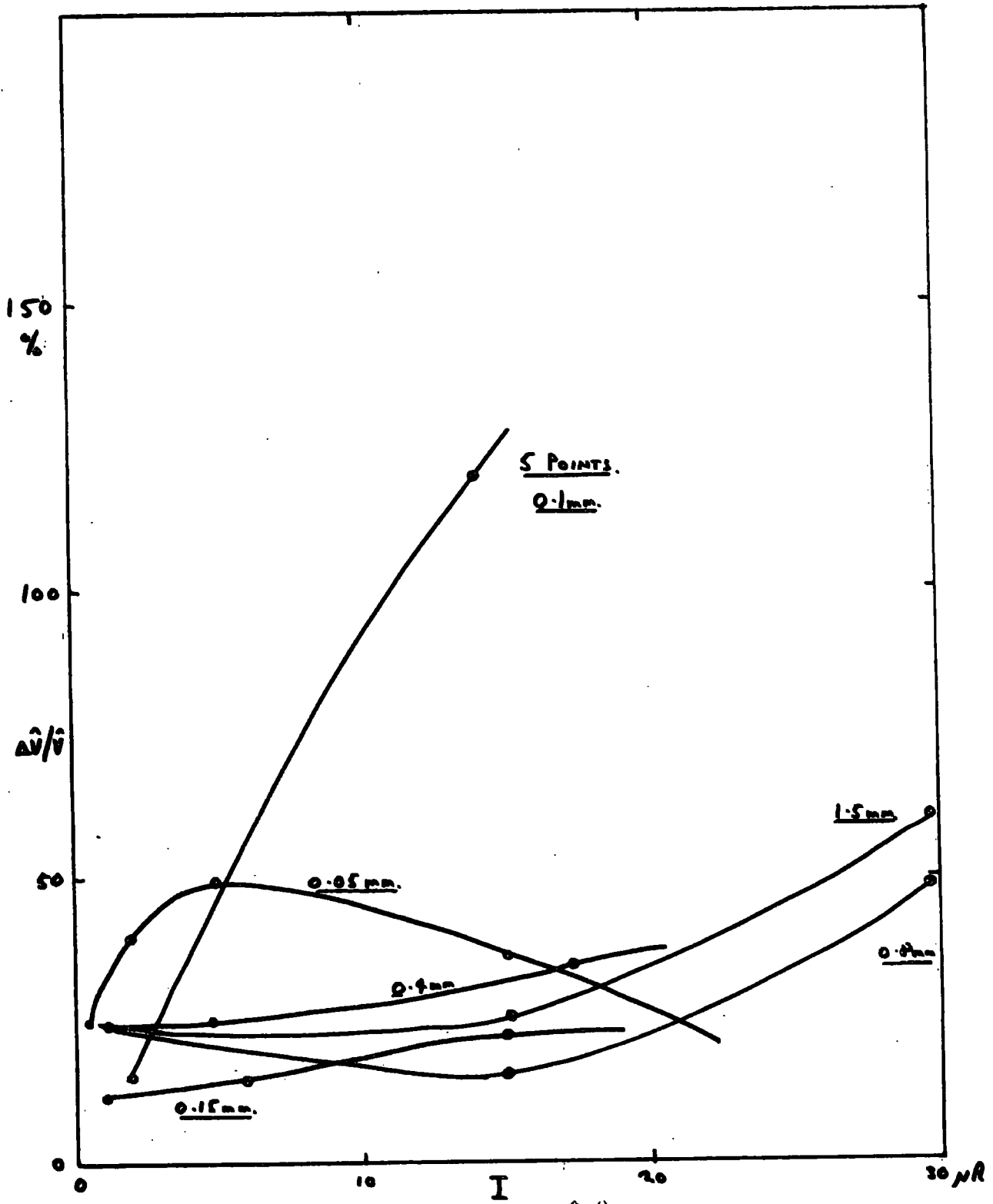


Fig. 4.7. Pulse amplitude irregularity $\Delta\hat{V}/\hat{V}$ and Positive Current I for metal points

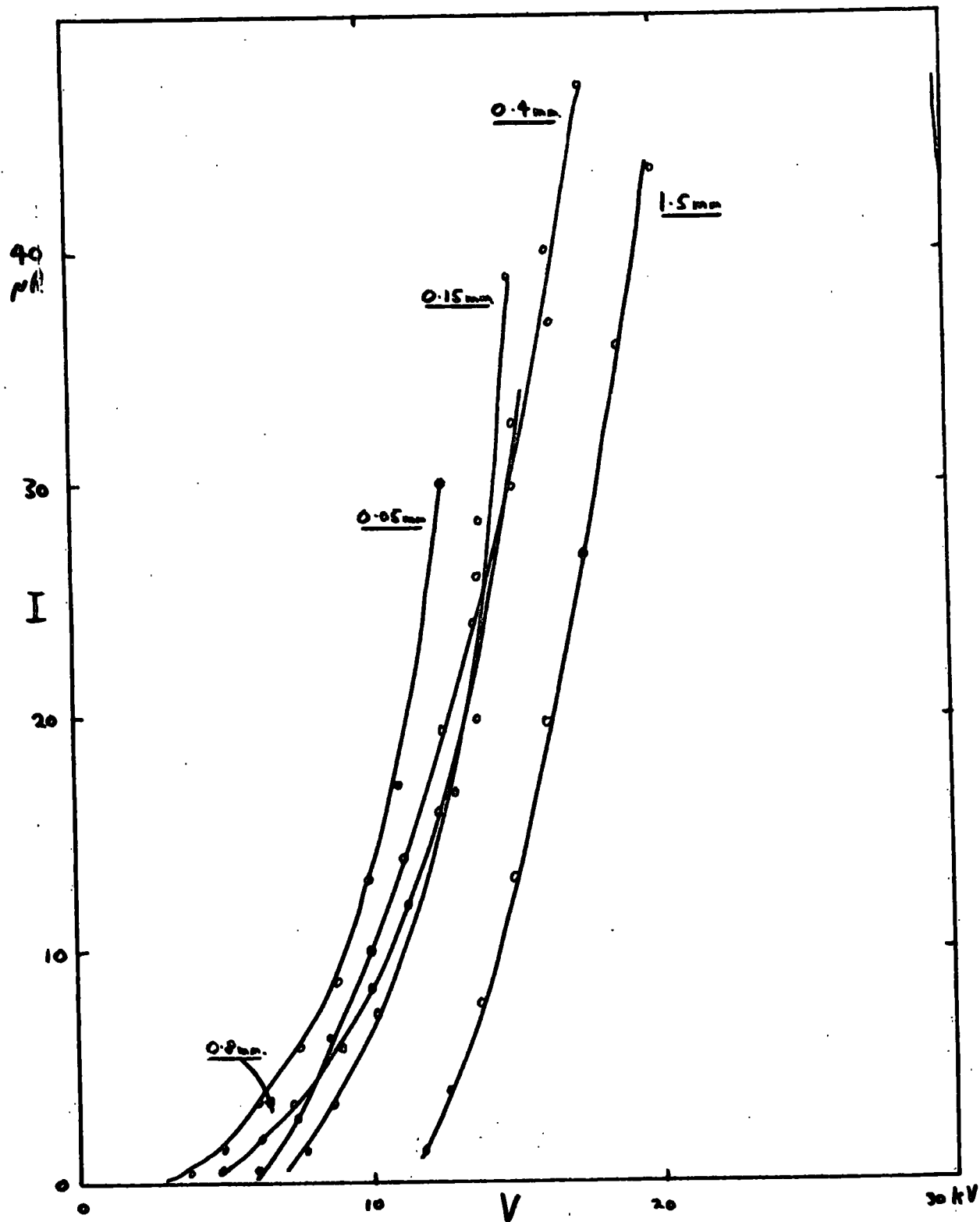


Fig. 4.8. Potential V and Negative Current I for single metal points

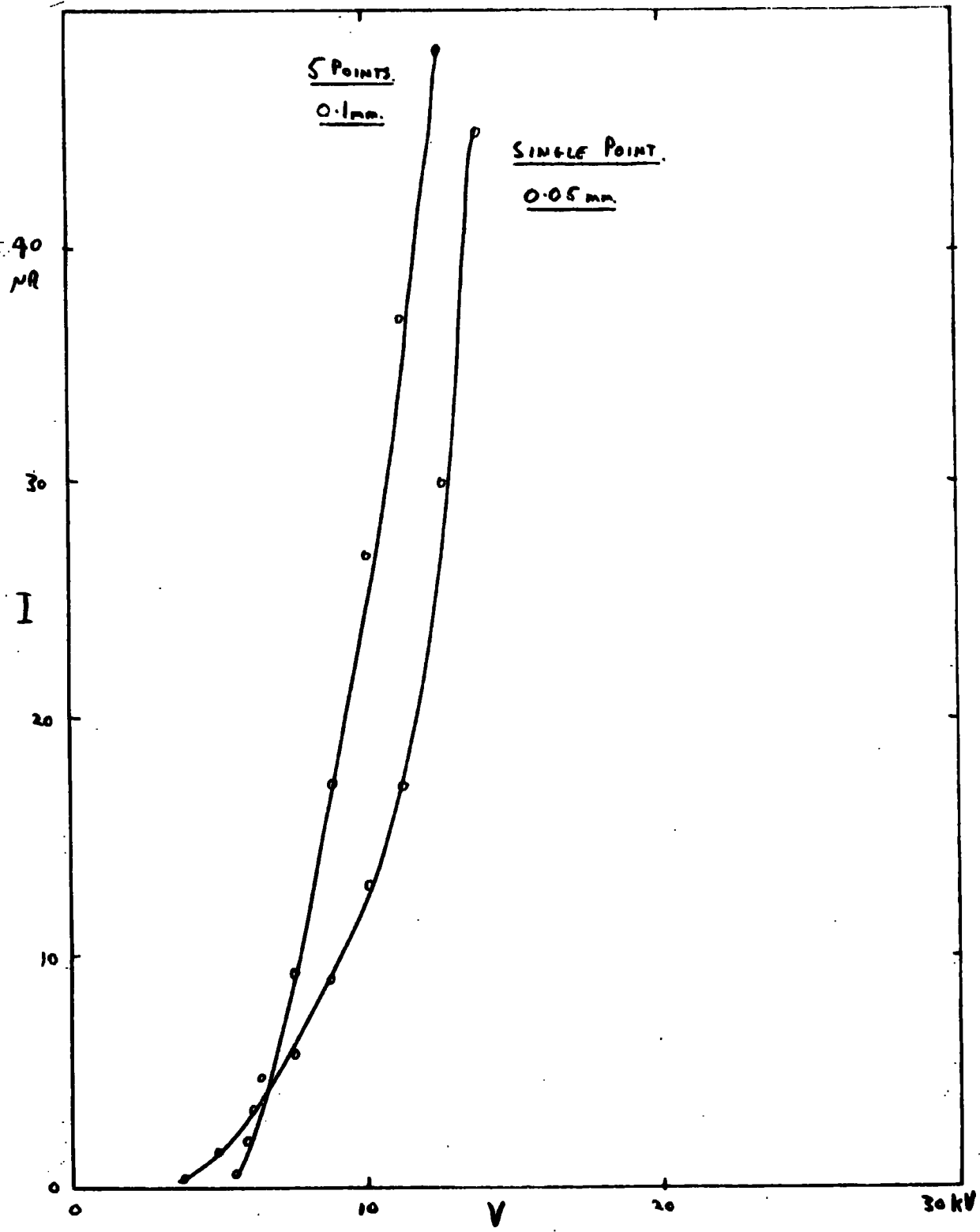


Fig. 4.9. Potential V and Negative Current I for 5 points

pulses per family increased as the current increased. For sharp points, such as $r = 0.05$ and 0.15 mm, only one pulse per family was usually observed.

4.4.5 The distribution of pulse amplitude.

From the measurements made with the differential pulse height selector, the total spread of pulse amplitude $\Delta\hat{V}$ was calculated. Fig. 4.7 shows a plot of $\Delta\hat{V}/\hat{V}$ against I for the various points. In general it can be seen that the spread in pulse amplitudes is about 30%. A special case is that of the multiple point array where coincidence of pulses at higher frequencies gives deviations about the average value of over 100%.

4.5 Results for negative currents

4.5.1 Potential - current characteristics

The potential V was calculated, as in 4.4.1, and Figs 4.8 and 4.9 show the relation between V and I for negative currents. The curves are similar to those for positive currents except that the starting value of the potentials are a little higher in some cases. As in the case for positive currents the slope of the current potential curve for the multiple points rises the most rapidly.

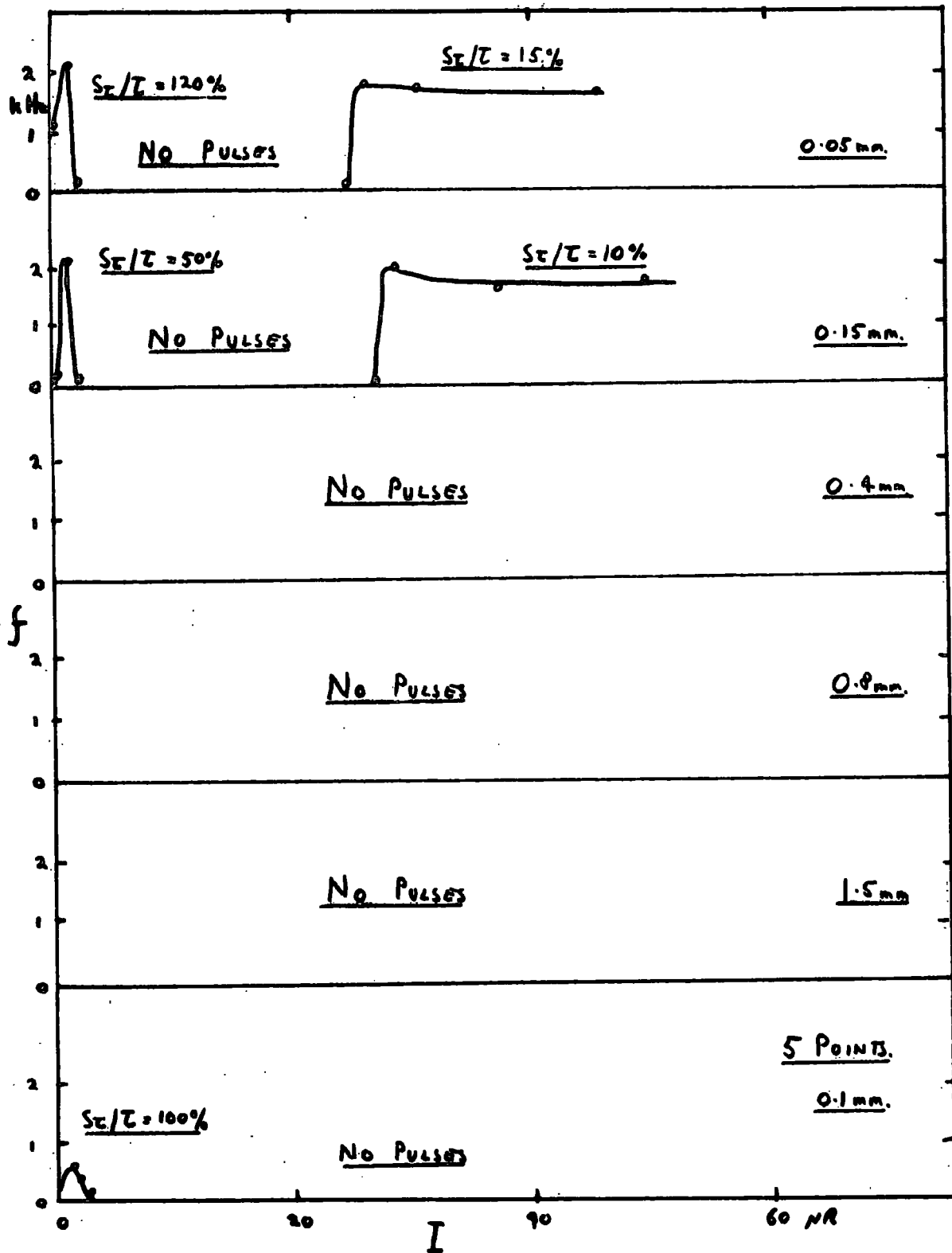


Fig. 4.10. Pulse frequency characteristics f and S_T/I and negative current I for metal points.

4.5.2 Frequency - current characteristics

The relation between the mean pulse frequency and negative current I is quite different from that for positive currents. Fig. 4.10 shows the frequency characteristics together with values for the standard deviation of the pulse intervals S_{τ} , expressed as a percentage of τ the mean pulse interval. It can be seen that for the three single points with the largest radii, the current was not pulsed. In the cases of the remaining two single points with radii of 0.05 and 0.15 mm, the nature of the currents can be divided into three distinct parts. First, there is a narrow range of current, at and above the onset potential, where the current is pulsed. In this region, as the current increases, the p.r.f. rapidly increases to a maximum and then falls to zero. At this point the current has reached about $1\mu\text{A}$. Above $1\mu\text{A}$ the current is not pulsed. This is the second distinctive range of current. At about $25\mu\text{A}$ the current again becomes pulsed but an initial increase in f is followed by a region of constant or slightly diminishing frequency. The pulses in this the third distinctive range of current were very much larger than the initial pulses occurring at potentials close to the onset value. The multiple points gave pulses, in the range $0 - 1\mu\text{A}$,

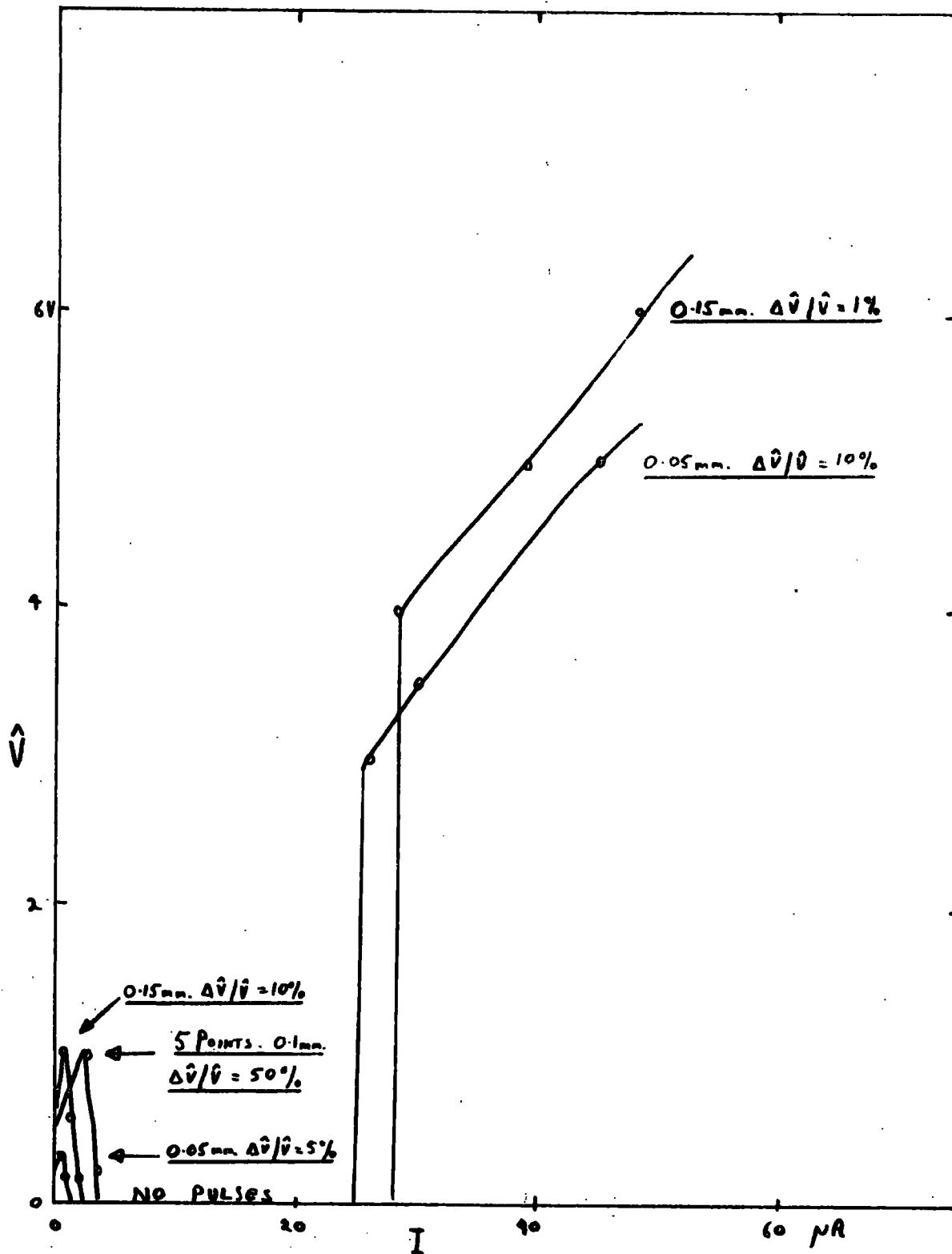


Fig. 4.11. Pulse amplitude characteristics \hat{V} and $\Delta \hat{V}/\hat{V}$ and negative current I for metal points.

similar in frequency to those for single points. However, the region of steady current extended beyond $25 \mu\text{A}$ and a second series of pulses was not observed for currents up to $100 \mu\text{A}$. The standard deviations of the pulse intervals were in the range 50 - 120% for the initial series of pulses. The pulses which occurred above $25 \mu\text{A}$ for the two single points were extremely regular, For these pulses the standard deviation of pulse interval was 10-15%.

4.5.3 Pulse amplitude measurements,

The pulse amplitude \hat{V} and its spread $\Delta\hat{V}$ was measured in the same way as for positive pulses. The results are shown in Fig. 4.11 as a plot of \hat{V} against I together with values of $\Delta\hat{V}/\hat{V}$. As was mentioned in 4.5.2 the current was not pulsed in the cases of three of the points. In the remaining cases, the pulse amplitudes \hat{V} and the spread $\Delta\hat{V}$ were initially of the same order as those for the corresponding positive currents. However \hat{V} was observed to fall to zero at about $1 \mu\text{A}$. The amplitudes of the pulses occurring after the continuous current region were much larger than those for the corresponding positive currents. Furthermore, the amplitude increased as the current increased, whilst the frequency remained approximately constant. In the case of positive currents the amplitude remained approximately constant, whilst the frequency increased with increasing current. The spread in amplitude of the large negative pulses was found to be small (1 - 10%).

4.6 Conclusion

It has been found for both single and multiple points that the pulse structure of positive currents is quite different from that for negative currents. For the positive Trichel pulses the main effect which occurs as the current increases is an increase in frequency. For negative currents, pulses do not occur over the entire current range. When they do occur, it is mainly the amplitude which increases with current, whilst the frequency remains approximately constant. These negative pulses are more regular in separation and height than the positive Trichel pulses at corresponding currents.

CHAPTER 5.Laboratory Experiments with Natural Points5.1 Introduction

It was decided, after making preliminary observation of point discharge on various plants and tree branches, to use small branches cut from a spruce tree as the subject of the observations described below. These preliminary observations were of a qualitative nature but it was nevertheless apparent that most foliage produced similar pulses of point discharge current when subjected to high potential gradients. The reasons for choosing branches from a conifer were twofold. Firstly it is thought that the pointed foliage gives rise to point discharge at lower potential gradients than those for foliage from deciduous trees. Secondly, a small plantation of conifers exists adjacent to the Lanehead Field Station of the University of Durham's Department of Geography. It was hoped to attempt the measurement of natural point discharge on these trees. Thus, a knowledge of the behaviour of this type of foliage under laboratory conditions would be of use.

5.2 Apparatus

Essentially the same apparatus was used here as for metal points. The plate separation was kept at 10 cm and the metal points were replaced with a small spruce twig. This was adjusted in height so that the minimum gap between the twig and the upper plate was 5 cm. The twig was subjected to a horizontal air flow of approximately 25 l min^{-1} as was used for the multiple metal points. Electrical connection to the twig was made by means of a "crocodile clip". This was clipped onto the stem of the twig in such a way that contact was made with the conducting sapwood. It should be mentioned here that the twigs were cut from a living tree immediately before measurements were made. The coaxial cable from the pulse measuring equipment was connected to the crocodile clip. Care was necessary to ensure that the stem of the twig was insulated from the lower earthed plate.

5.3 Techniques of Measurement

Measurements were made in the same way as was described for metal points in 4.3. The main difference was that the observed pulses were much smaller than for metal points, no doubt because they were attenuated and integrated in their passage through the twig. For this reason it is not very meaningful to make comparisons between the pulse amplitudes for metal points and those for the spruce twigs.

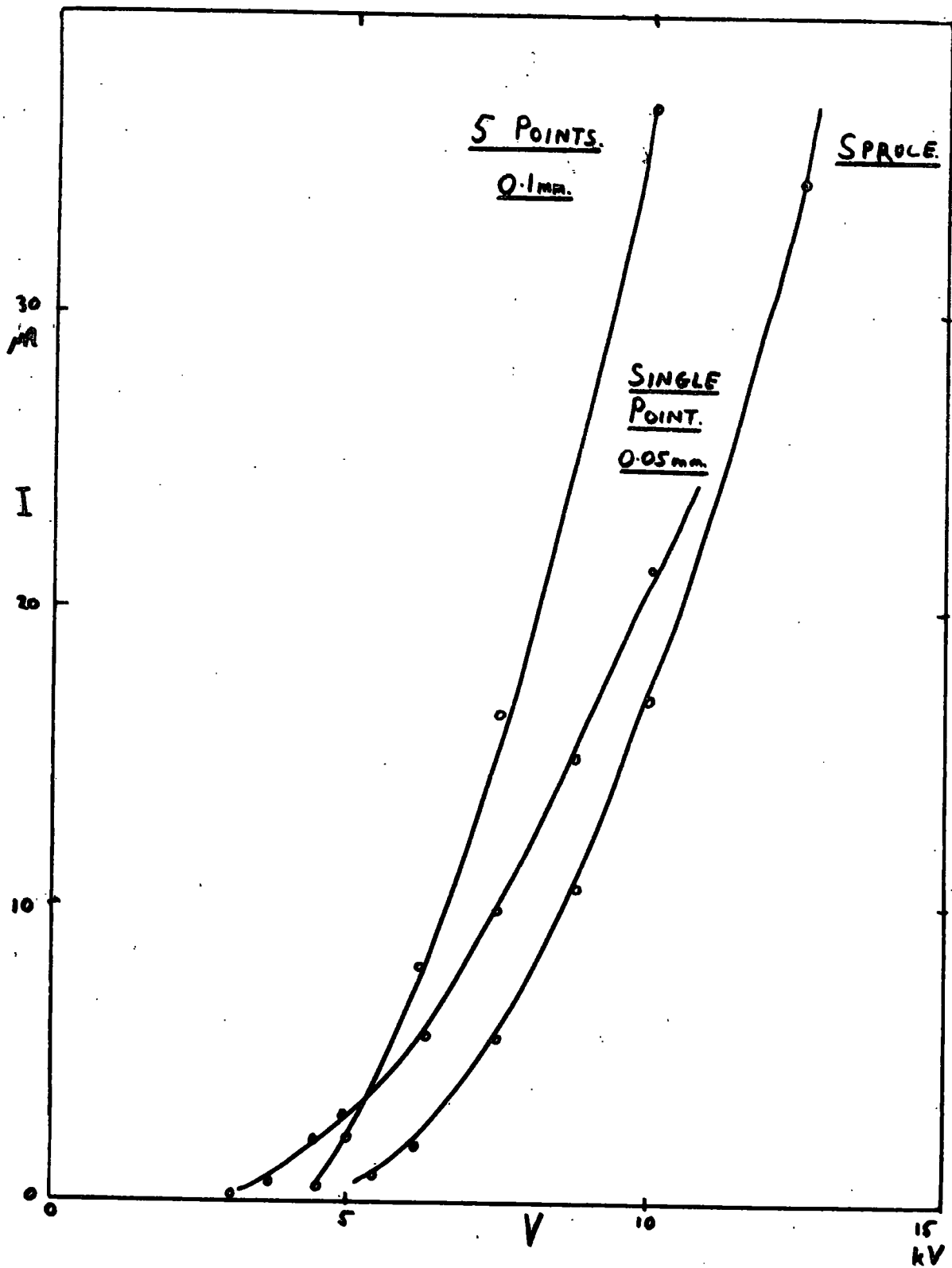


Fig. 5.1. Potential V and positive current I for a Spruce Twig.

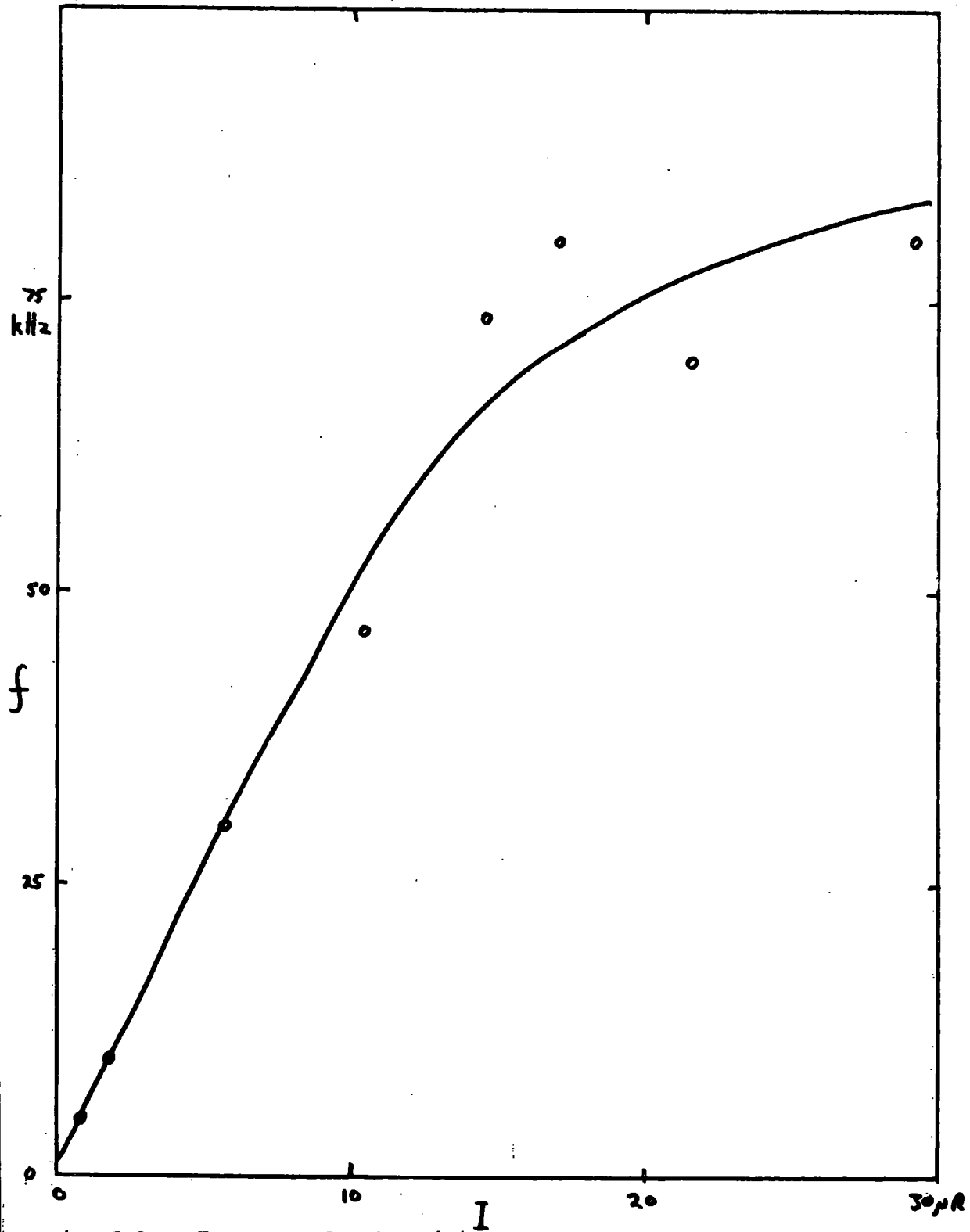


Fig. 5.2. Frequency f and positive current I for a Spruce twig

5.4 Results for positive currents

5.4.1 Potential - current characteristic

The potential at a height h above the lower earthed plate is, as before,

$$V = hV_p/D$$

where V_p is the plate voltage, h is the height of the spruce twig, and D is the plate separation. The relation between V and the discharge current I is shown in Fig. 5.1. The slope of this curve is, initially, closer to that for a single point rather than that for multiple points. At higher currents when the discharge occurs at more points on the twig the slope of the curve approaches that for the multiple points. The fact that a higher potential than that for multiple points is necessary to initiate a discharge on the spruce twig indicates possibly that the points on the twig have a tip radius greater than 0.1 mm.

5.4.2 Frequency - current characteristic

This is shown in Fig. 5.2. The decrease in the slope of this curve as the current increases is probably caused by the two effects simultaneously. Firstly, as the potential increases, points below the top of the twig may begin to discharge. Thus the number of points discharging may

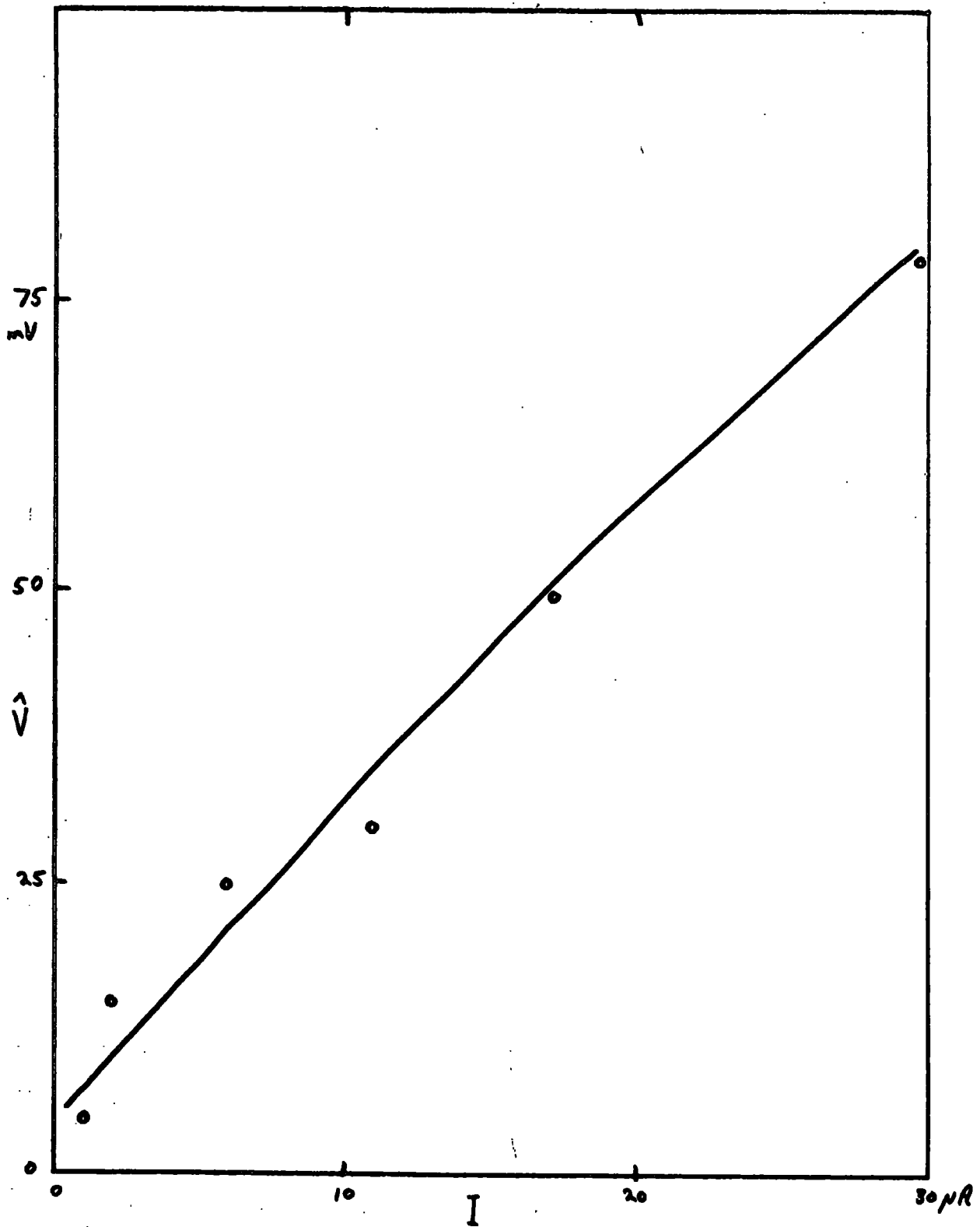


Fig. 5.3. Pulse amplitude \hat{V} and positive current I for a Spruce twig.

increase with potential. Secondly, points on the twig with greater tip radii may begin to discharge at higher potentials. Thus these points will give pulses with a greater charge per pulse. Both these effects will result in a decrease in the slope of the frequency versus current curve. It is also likely, at the higher pulse frequencies, that coincidence of pulses may occur. This will also give a decrease in the slope of the frequency characteristic.

5.4.3. Pulse amplitude - current characteristic.

The increase in pulse amplitude with current, Fig. 5.3 indicates that the average charge per pulse may increase with current. This may be caused by the less sharp points discharging at higher potentials giving the increase in charge per pulse, or by coincidence of pulses giving an apparent increase in the charge per pulse. In practice both these effects may occur together.

5.4.4 The standard deviation of the pulse intervals.

The standard deviation S_{τ} was calculated from the observations of pulse counts in exactly the same way as for pulses from metal points. For spruce twigs at low currents, S_{τ} was found to be similar to that for a single

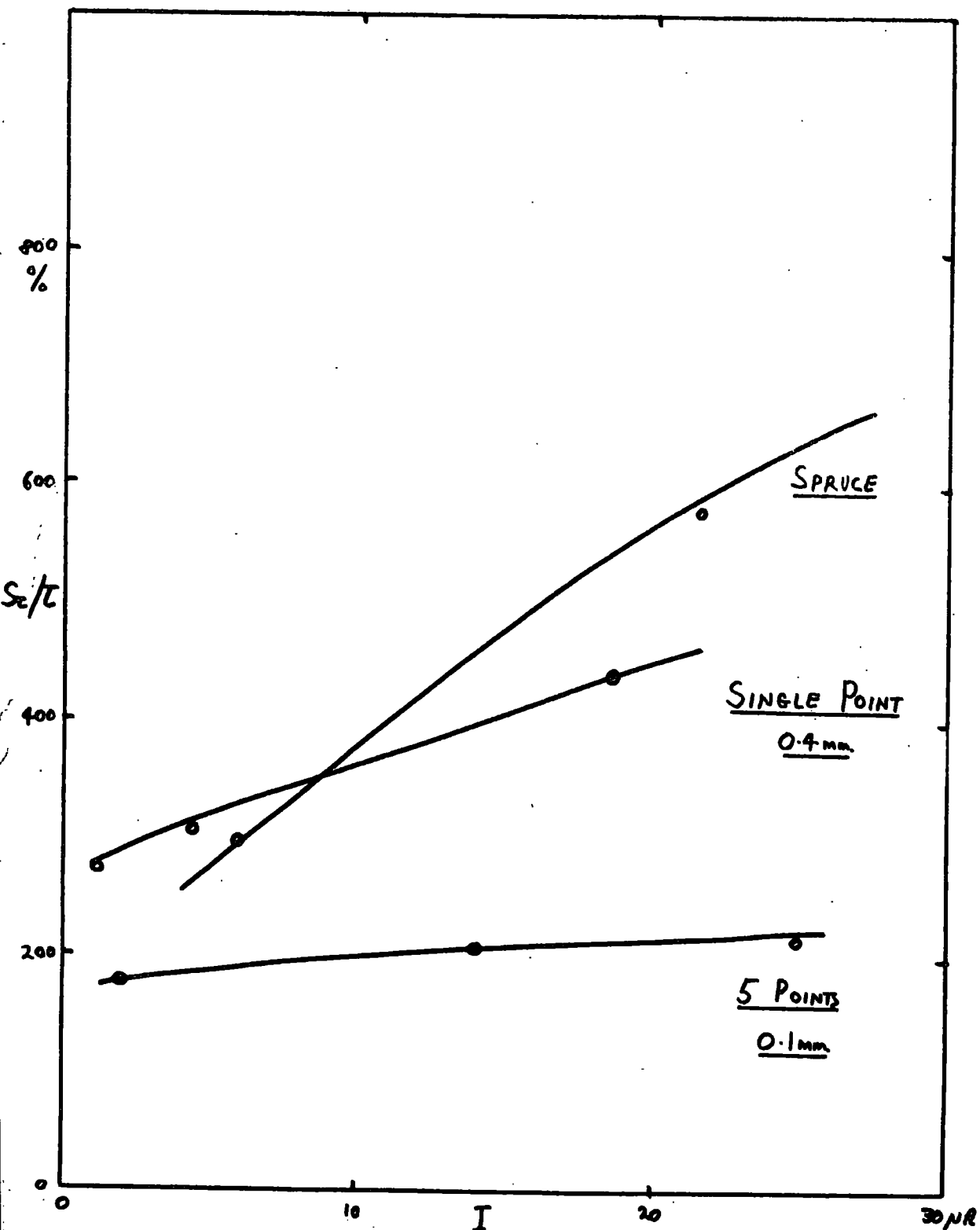


Fig. 5.4. Irregularity in Pulse Interval S_c/τ and positive current I for a Spruce twig.

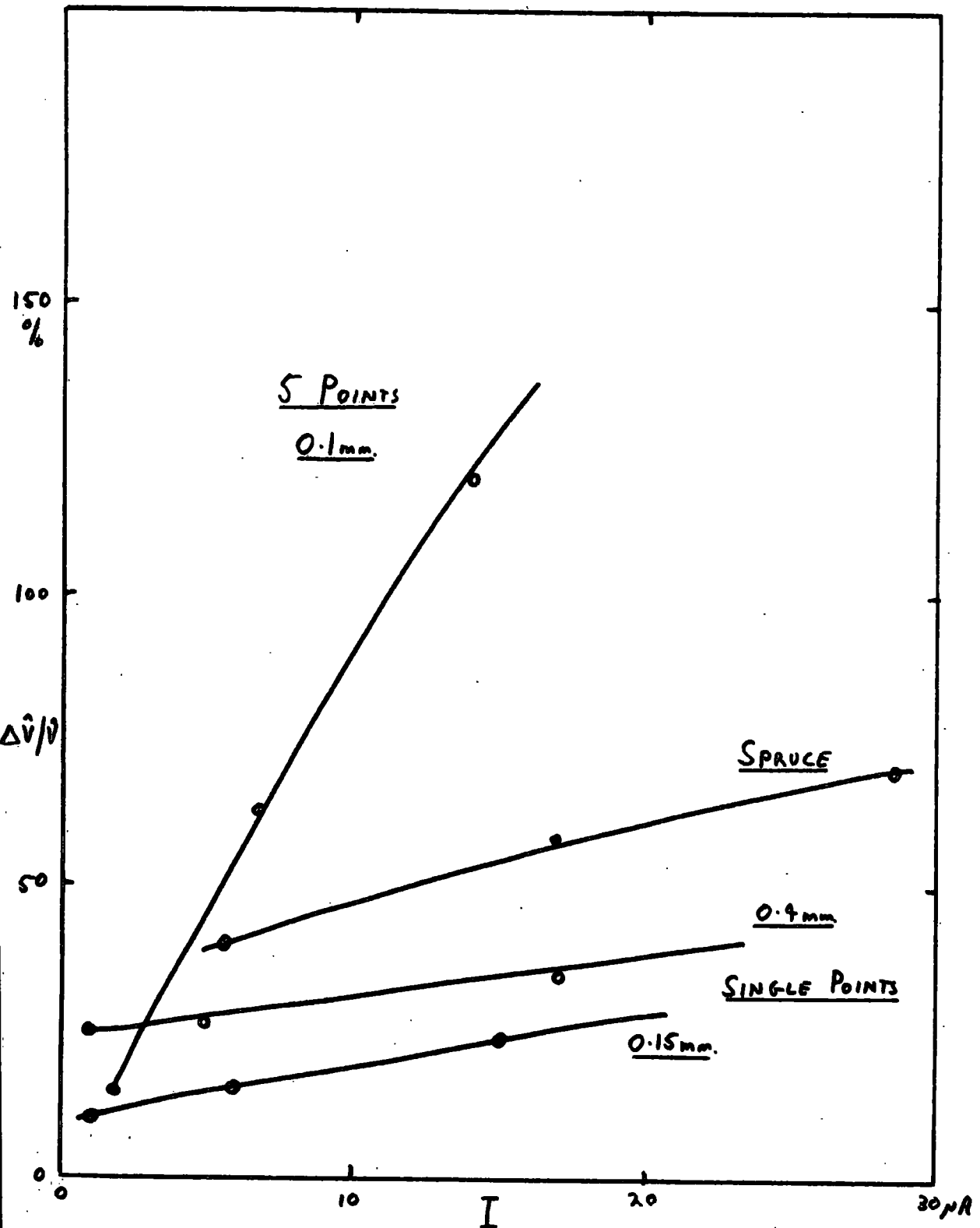


Fig. 5.5. Irregularity in pulse amplitude $\Delta V/V$ and positive current I for a Spruce twig.

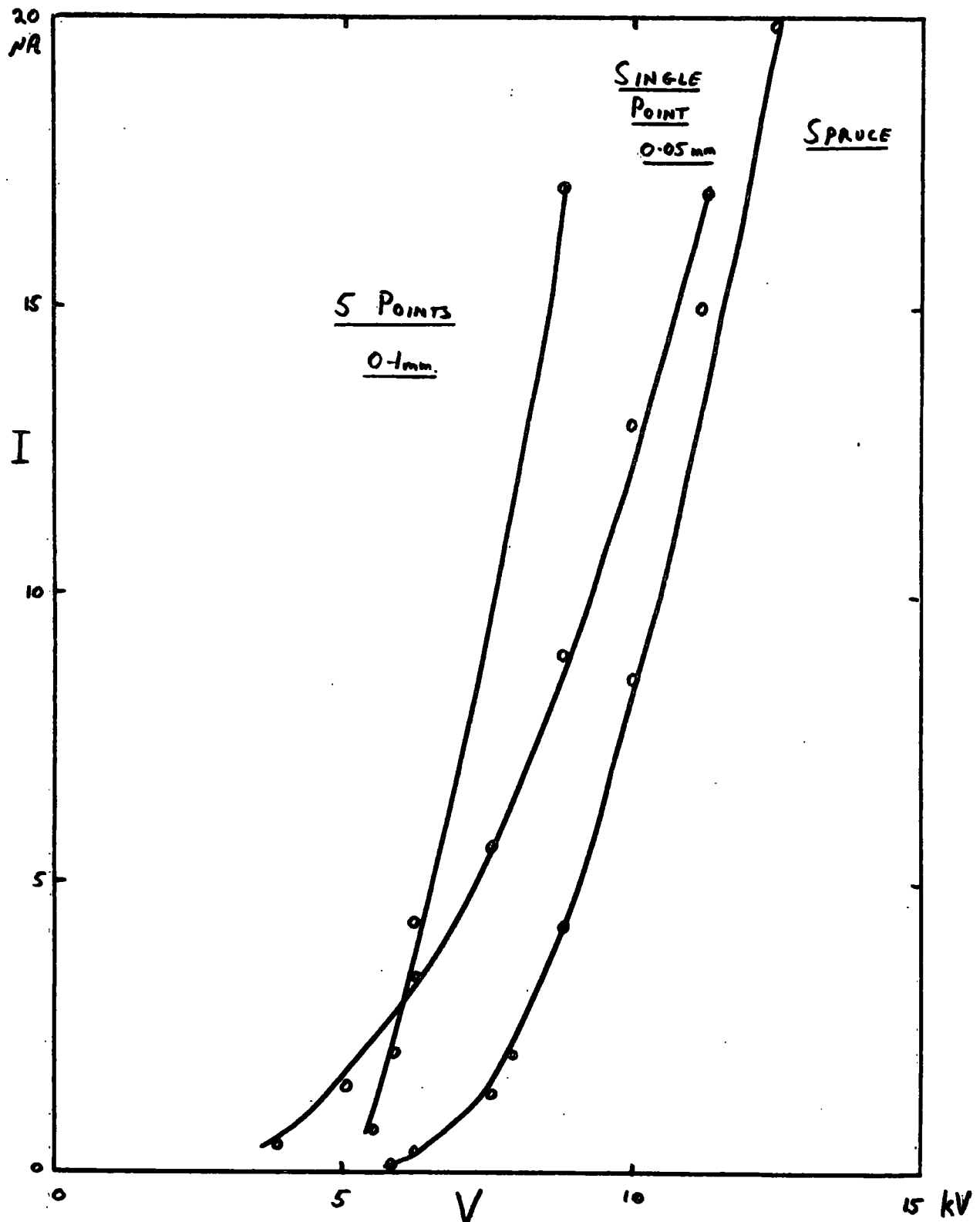


Fig. 5.6. Potential V and negative current I for Spruce twig

metal point at the same current and of the order of 300%, Fig. 5.4. However at higher values of current S_T increased to about 600%. This is considerably higher than the corresponding values of S_T for metal points.

5.4.5 The distribution of pulse amplitude

The spread in amplitude $\Delta \hat{V}/\hat{V}$, of pulses from the spruce twig is of the same order as those for metal points (Fig. 5.5). However, it is difficult to assess the integrating and attenuating effects of the spruce twig on the pulses so a more detailed comparison is probably not valid.

5.5 Results for negative currents

5.5.1 Potential - current characteristic.

A plot of V against I is shown, Fig 5.6, for the spruce twig together with the curves for a single point and multiple points. As in the case for positive currents, the slope of the curve for the spruce is, at low values of I , similar to that for a single point. At higher values of I , the slope increases and becomes similar to that for the multiple points. Again, this probably indicates that the spruce behaves, at first as a single point, and at higher potentials as multiple points.

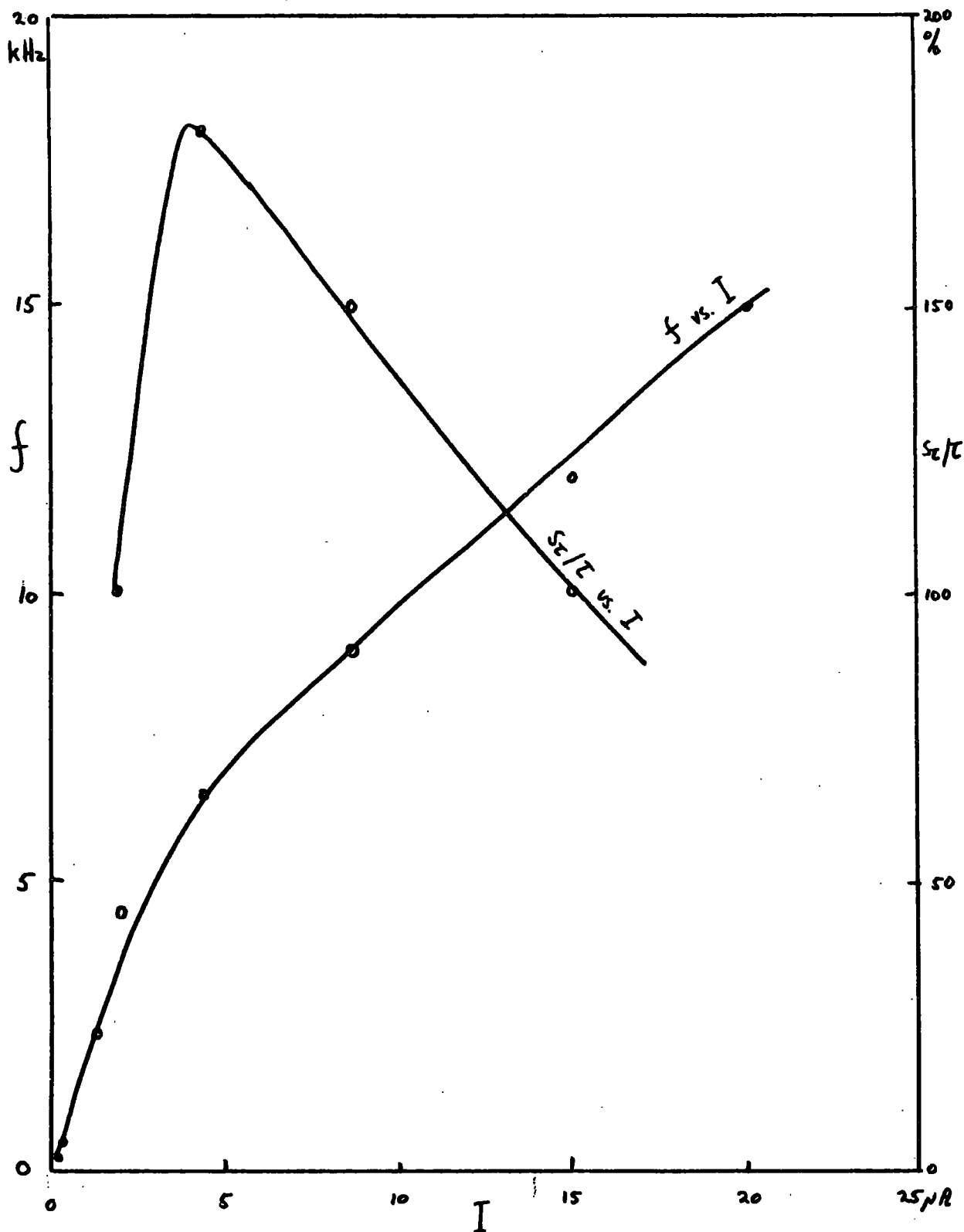


Fig. 5.7. Frequency f , irregularity of pulse interval S_r/τ and negative current I for a Spruce twig.

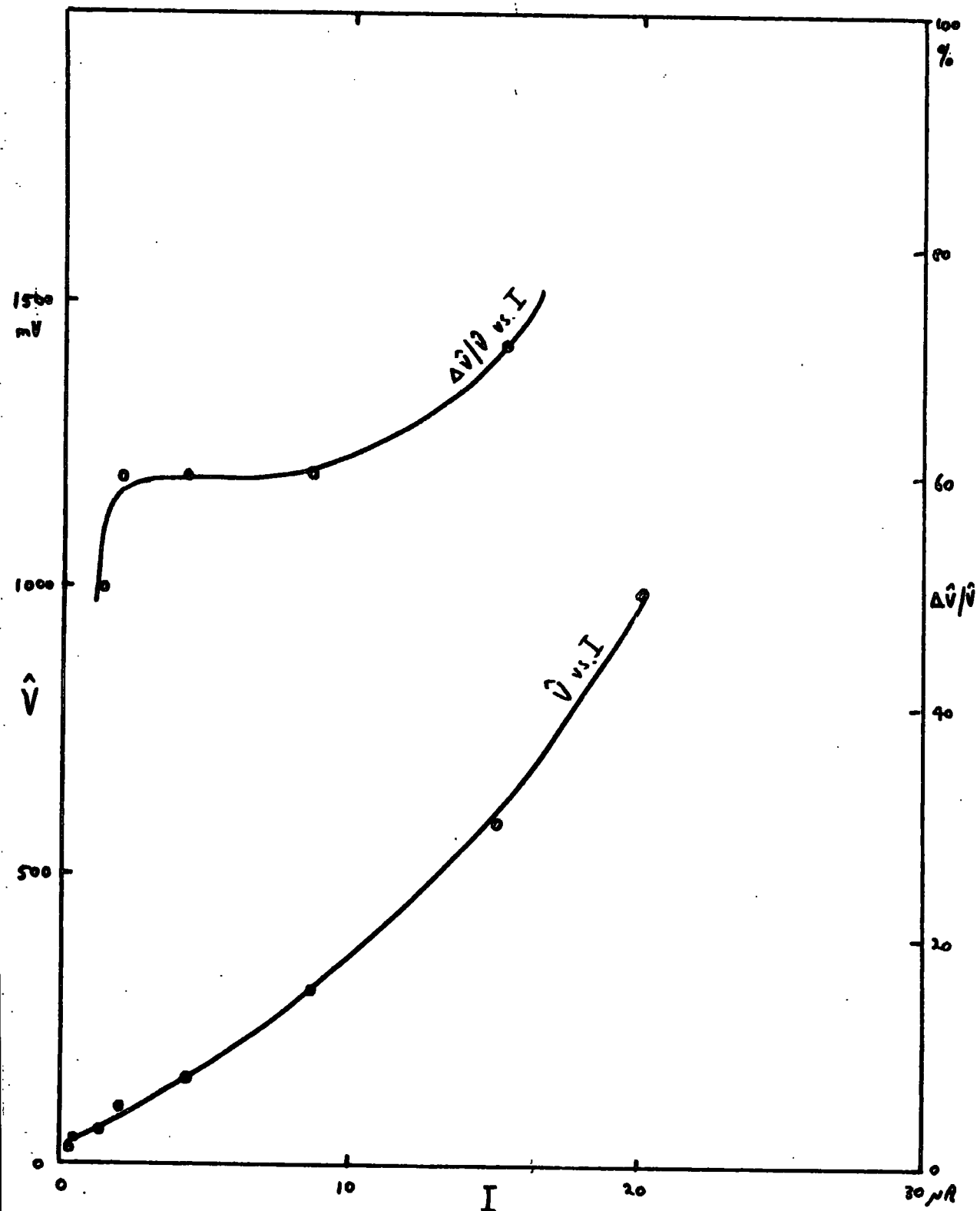


Fig. 5.8. Pulse amplitude \hat{V} , irregularity of amplitude $\Delta \hat{V} / \hat{V}$ and negative current I for a Spruce twig.

5.5.2 Pulse frequency measurements

It was found that negative currents produced by point discharge on the spruce twig were always pulsed. This is an important difference between the spruce and all the metal points, since with the latter there was often a range of current in which no pulses occurred. A graph of frequency f against current I for the spruce twig is shown in Fig. 5.7. The shape of the curve is similar to that for positive pulses but the p.r.f. is on average only one fifth of the value for the corresponding positive current. This implies that the charge per pulse may be much greater or that there is a d.c. component to the discharge. The variation of the standard deviation of the pulse intervals, S_{τ} , is also plotted against I in Fig. 5.7. S_{τ} lies in the range 100 - 200% for the current range shown. The value for S_{τ} for positive currents is 300 - 600%.

5.5.3 Pulse amplitude measurements

As in the case for positive pulses, the pulse amplitude \hat{V} increased with increasing current, Fig. 5.8. However, the amplitudes were on average about one order of magnitude greater than for the positive case. For example, at $10 \mu\text{A}$ the amplitudes were 32 mV and 350 mV for the

positive and negative cases respectively. Oscilloscope measurements showed that there was no appreciable d.c. component in the current so it can be concluded that the lower frequencies observed for negative currents are counteracted by the greater values of charge per pulse, i.e. greater pulse amplitudes. The percentage spread in pulse amplitude is also shown in Fig. 5.8. This is of the same order as the percentage spread for positive pulses.

5.6 The Capacitative Electrode

5.6.1 Electrical connection of measuring equipment to natural points

In the experiments described above, electrical connection was made to the spruce twig by means of a crocodile clip. This method would be unsatisfactory for any long term experiments, since the electrical connection would deteriorate with time. There is obviously a need for a more satisfactory method which could be used on a tree over long periods without disturbing the natural state of the tree. As it has been found in the above experiments, that both positive and negative currents through natural points are pulsed, we need only make a capacitative connection to a tree to detect point discharge currents flowing in the tree.

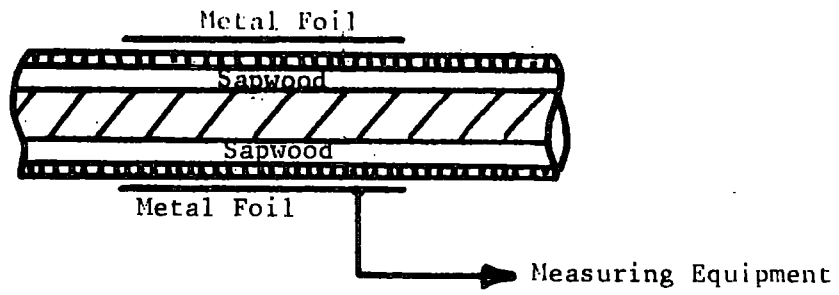


Fig. 5.9. The Capacitive electrode

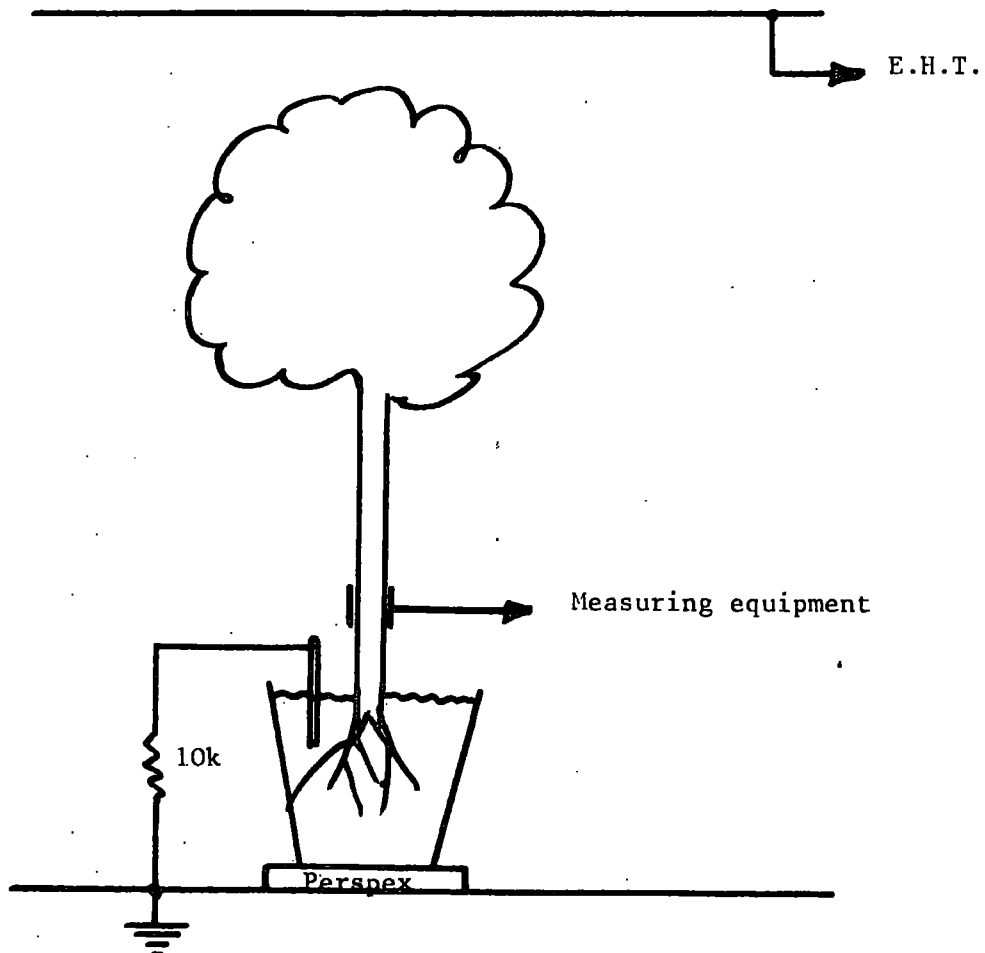


Fig. 5.10. Trial electrode on small tree

5.6.2 Design of a capacitative electrode

Consider a branch of a tree at which point discharge is occurring. If we assume that the current flows to earth along the sapwood, Fig. 5.9, then we can regard the sapwood as the inner conducting surface of a cylindrical capacitor. The bark surrounding the sapwood will be the dielectric. If a length of conducting foil is wound around the branch, this will act as the outer conducting cylinder of the capacitor. Assuming that the resistance through the sapwood to ground is not zero, it should be possible to detect point discharge pulses through this capacitative electrode. For a cylindrical capacitor, the capacitance C is given by

$$C = 2\pi \epsilon_0 K \ell / \log_e (R/r),$$

where K is the dielectric constant, ℓ is the length of the capacitor, R is the radius of the outer conducting cylinder and r is the radius of the inner conducting cylinder. If we assume $K = 3$ and $R/r = 1.3$ for a typical tree branch and let $\ell = 0.1$ m then,

$$C = 6 \text{ pF}$$

5.6.3 Performance of a trial electrode

The ideas described above were put to the test on a small spruce tree, 0.5 m in height, which was growing in a plant pot, see Fig. 5.10. The stem of the tree was about 1.5 cm in diameter. An insulating layer of P.V.C. tape was wrapped around the stem followed by a layer of aluminium foil. The cylinder of foil thus formed was 2.5 cm in length. The foil was connected to the pulse measuring equipment via a coaxial cable. The soil in the plant pot was earthed via a $10\text{ K}\Omega$ resistor which was intended to represent the resistance to ground of the sapwood in a full size tree. When artificial fields were applied to the tree, pulses in the expected frequency range were detected. The amplitude of the pulses was found to be about one tenth of that with a direct electrical connection to the sapwood. The attenuation of the pulses could be reduced by increasing the length of the electrode.

5.7 Conclusion

The above experiments show that for point discharge on a spruce twig, the pulse frequency characteristics for positive currents are similar to those for metal points. However, the pulsed nature of negative currents in the

spruce tree is completely different from that for metal points. Unlike the negative currents in the latter, there is no region of d.c. current for the spruce twigs.

A new method for detecting point discharge currents from natural points has been devised. This method relies on the fact that the discharge current is pulsed, so that a capacitative link with the tree or plant is all that is necessary to allow point discharge currents to be detected. This method has the advantage that it does not damage the tree or plant and the electrical connection to the tree will not deteriorate with time.

CHAPTER 6.

The application of the laboratory experiments to the measurement of natural point discharge

6.1 The pulsed nature of point discharge as a basis for measurement

In the past there has been no satisfactory method for measuring natural point discharge currents in trees. As a result, the global estimates of the contribution of point discharge to the transfer of charge in the atmosphere could be seriously in error. The results of the present work, described above, suggest that it might be possible to detect pulses of point discharge current in trees growing under natural conditions. If this can be done, the variations of both the frequency and the amplitude of the pulses should give a measure of the discharge current.

6.2 The capacitative electrode on full-size trees

The experiments described in 5.6 show that point discharge pulses can be detected in small branches cut from a tree, using a capacitative type of electrode. If this method is to be used on full size trees, the positioning of the electrode on the tree will obviously be important. The electrode must be sufficiently close

to the source of the point discharge so that the observed pulses are not too small to be measured. The conducting sapwood between the discharging points and the electrode will have a definite resistance. Thus the attenuation and integration of the pulses will probably increase with the distance between the discharging points and the electrode.

6.3 Measurement of positive and negative currents in trees

The laboratory experiments described in Chapter 5 show that, for both positive and negative currents, the amplitude and frequency of the pulses both increase with current. Assuming that this also happens for point discharge on full size trees, a measuring instrument is required which will respond to changes in pulse amplitude and frequency. It is also important that the instrument can distinguish between positive and negative pulses so that the sign of the current is known. If such an instrument was connected to a capacitative electrode on a tree, it should be possible to measure any point discharge current flowing in the tree.

6.4 Conclusion

If it can be confirmed that the point discharge currents in full size trees are pulsed and of a similar nature to the currents measured in the laboratory, then it should be possible to measure these currents through trees, so long as the pulses can be detected by means of a suitable electrode.

An instrument is required, which, when connected to the capacitative electrode, will give the magnitude and sign of the discharge current. This instrument should respond to changes in both pulse amplitude and pulse frequency. The calibration of such an instrument will be difficult because of the unknown effect of an individual tree on the pulse amplitudes. However, it should be possible to calibrate the measuring instrument in the laboratory, using an identical electrode on a branch cut from the full size tree.

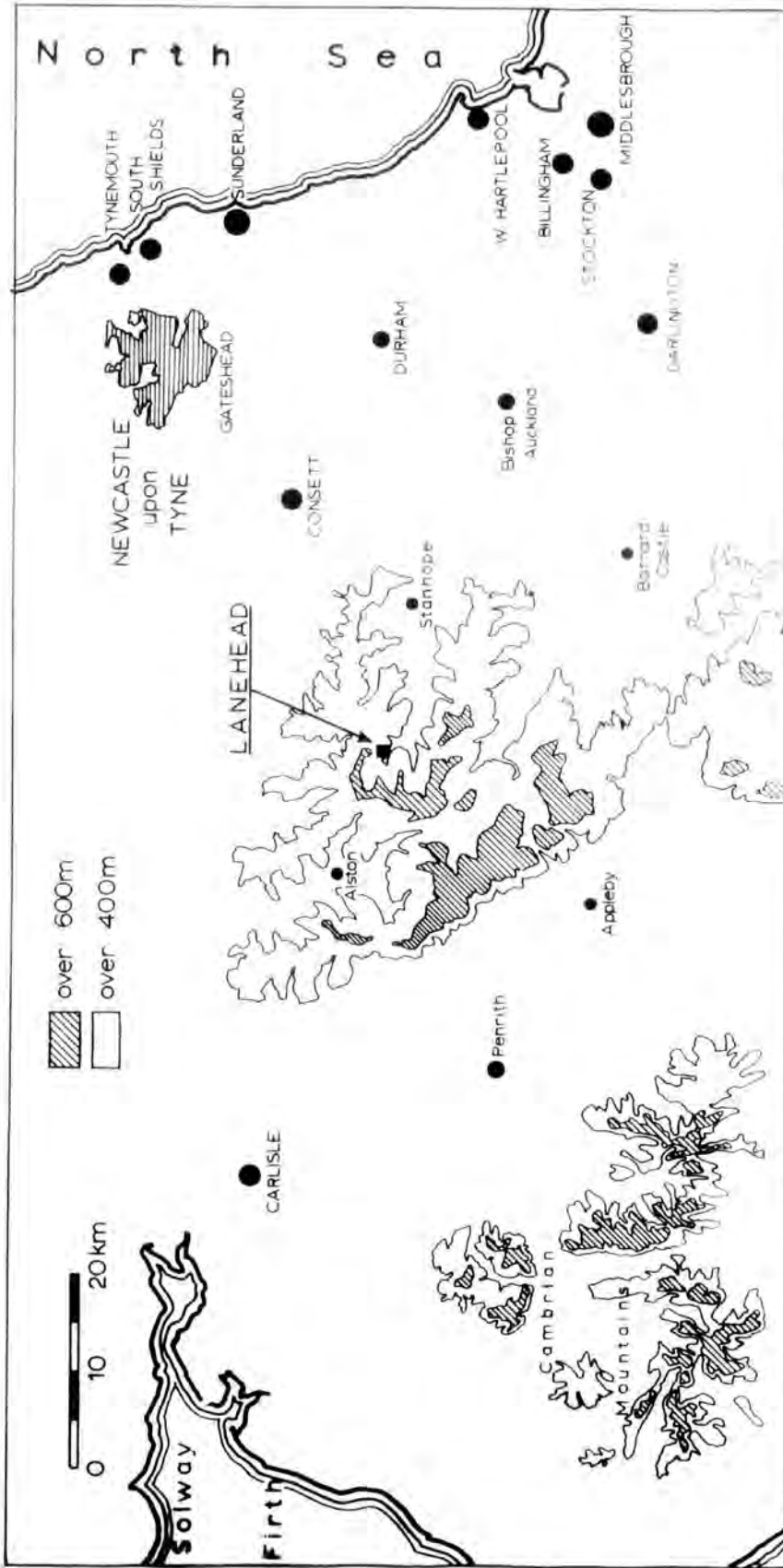
The remaining part of the present work is an account of field work carried out at Lanehead in Weardale, where the new methods, proposed above, for the measurement of naturally occurring point discharge were successfully put into practice. Measurements at Lanehead were made over a period of one year. New and important information was obtained concerning point discharge on trees under natural conditions.

CHAPTER 7.The field experiment at Lanehead7.1 Initial considerations

If it is intended that an estimate be made of the total point discharge on all trees in a given area, it is important that the trees on which measurements are made are representative of the others. This means that the trees chosen for measurements should be of the same species, height and exposure as the majority of trees in the area. For example, if the area as a whole is densely wooded, the measurements should be made on trees which are closely surrounded by others. Measurements on isolated trees would not be representative in this case. A further condition for representative measurements is that the natural state of the trees should not be disturbed by any measuring equipment. In particular it is essential that the equipment does not enhance or reduce the amount of point discharge which would occur naturally.

To obtain any reliable estimate for charge transfer in the atmosphere due to point discharge on trees, measurements must be made continuously over periods long in comparison with the intervals between successive days of point discharge.

FIG. 7.1 The North Pennines



Thus, if the period of measurement is about one year, seasonal variations in the frequency of occurrence of point discharge will be accounted for.

7.2 The site and facilities at Lanehead.

The main criteria for the choice of the site were that it should be densely wooded and also within reasonable travelling distance from Durham. Lanehead is situated 30 miles west of Durham in upper Weardale, (See Fig. 7.1). The journey by car to Lanehead takes about an hour. Durham University's Department of Geography has a field station at Lanehead and adjacent to this is a small plantation of conifers. The landscape surrounding Lanehead can be described as a typical North Pennine upland basin. The upper reaches of the river Wear open out into a series of basins, each occupied by a major headwater stream. The flat peat-covered watershed areas are typical of the gritstone uplands of England. Lanehead is 500 m above sea-level and it is quite common to have snow on the ground for six months of the year (See Figs. 7.2 and 7.3). The shallow cross-sections of the valleys and the open nature of the surrounding moorland mean that Lanehead is exposed to the full force of the wind.

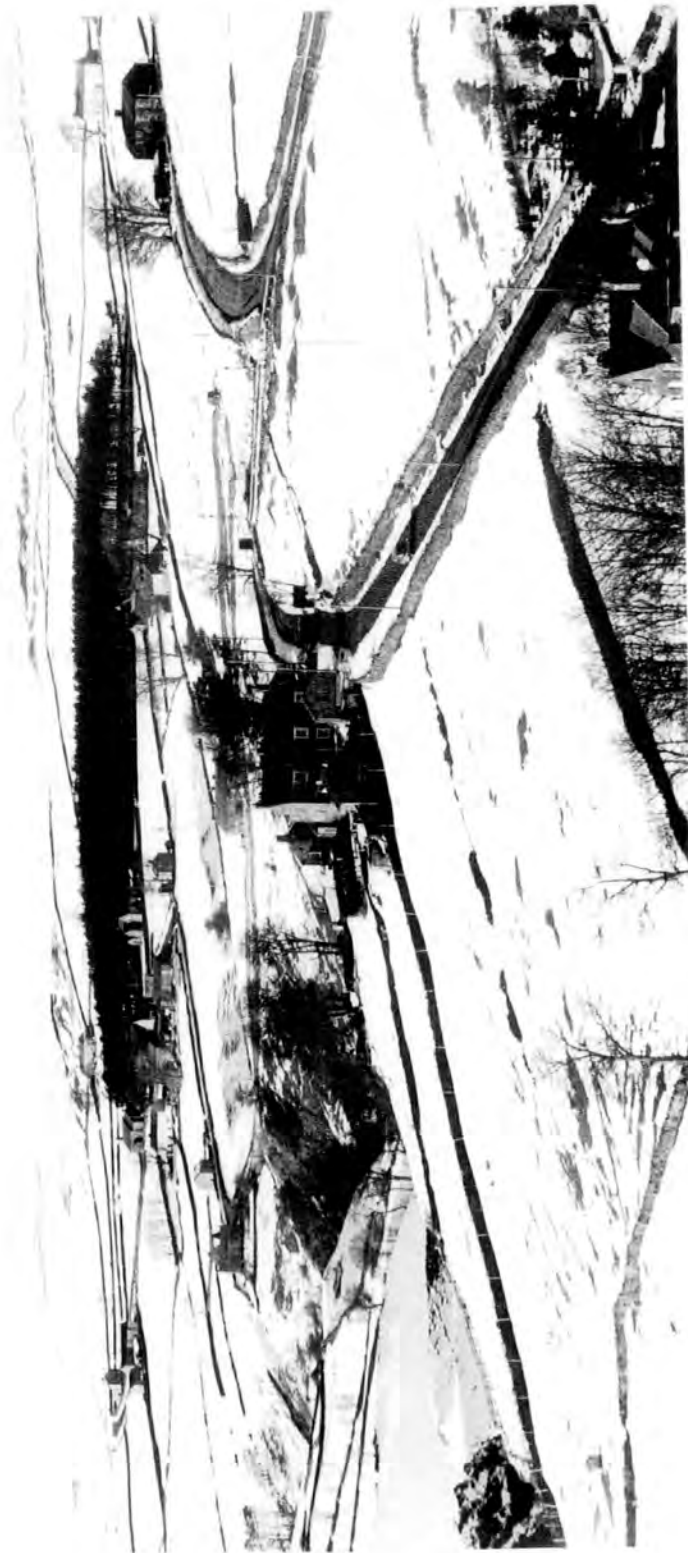


FIG. 7.2 THE FIELD STATION + PLANTATION AT LAVERHEAD FROM S.E.

The field station at Lanehead is a stone building which was, until about six years ago, the local village school. Following the closure of the school, the building and surrounding land were taken over by the Geography Department of the University of Durham. The building has been modified internally to provide the facilities necessary for the field station. There are now two dormitories to provide sleeping accommodation for about twelve people, together with a bathroom, kitchen and a study. One large classroom is now used as a laboratory. An electricity supply is available in the laboratory together with bench and cupboard space for equipment.

A fellow research student, Mr. G.T. Sharpless, has been responsible for setting up equipment at Lanehead to measure the general atmospheric electric parameters.

The plantation is situated adjacent to the field station and on its northern side. Permission to conduct experiments in the plantation was kindly given by Messrs. Smiths, Gore & Co. Ltd., Estate Agents, Corbridge, Northumberland. The trees cover an area of about 200 m by 150 m and their average height is about 18 m. The



FIG. 7.3 THE FIELD STATION AT LANE HEAD.

shallow depth of soil and the high winds at Lanehead cause trees in the plantation to be blown down fairly frequently. However, it appears that most of these trees have had their roots undermined by drainage ditches and so it is possible to select stable trees for the purpose of experiments. The conifers in the plantation are fairly uniform in both height and separation. At its northern edge the plantation is more open and there are one or two clearings. The whole of the plantation is surrounded by a perimeter wall and sheep and cattle are often allowed to graze in the plantation.

7.3 The parameters measured

7.3.1 Measurements on trees

Initially, four widely separated trees inside the plantation were used as the basis for point discharge measurements. By using capacitative electrodes on these trees it was intended that the amplitude and frequency of any pulses in the trees should be measured. At a later stage in the experiment a fifth tree on the edge of the wood was also instrumented.

7.3.2. Potential gradient

A field-mill situated outside the plantation gives a measure of the potential gradient in the region of the plantation. The output from the field mill is also used to switch on the chart recorder when the potential gradient at the field-mill increases above certain pre-set positive and negative values. In this way it is possible to use a fast chart speed and record only in periods of high potential gradient.

7.3.3. Point discharge on an elevated metal point

In the past many workers have measured the total charge brought to earth through an elevated metal point and used this result to estimate the amount of natural point discharge. In order that the results of the present work, concerning point discharge on trees, can be compared with the results obtained previously, measurements were made of the point discharge on an elevated metal point situated outside the plantation.

7.3.4. Other Parameters

Apart from the main parameters mentioned above, wind speed and direction together with wet and dry bulb temperatures were also measured. It was thought that a measure of wind speed and direction would prove useful if calculations were made on the motion of space charge originating from point discharge on the trees.

7.4 A summary of the aims of the experiment

The aims are:-

- i) The detection and measurement of point discharge currents which may pass down trees inside the plantation, without disturbing the natural conditions of the trees.
- ii) The measurement of potential gradient outside the plantation.
- iii) The measurement of point discharge currents down an elevated metal point outside the plantation.
- iv) The measurement of wind speed and direction.

- v) The measurement of wet and dry bulb temperatures.

- vi) The automatic recording of the above parameters during all periods when the measured potential gradient is high.

- vii) The estimation of the total charge brought to earth, by point discharge on all the trees in the plantation, for one year.

- viii) The determination of the relations, if any, between the measured currents and the potential gradient outside the plantation.

CHAPTER 8.

Instrumentation at Lanehead

8.1 Introduction

This chapter describes all the apparatus which was constructed and installed at Lanehead, with the exception of the point discharge detectors for the trees in the plantation. A considerable amount of time and effort was expended over the development of satisfactory detectors, and this work is described in Chapter 9.

8.2 The general difficulties of field work at Lanehead.

Before proceeding with an account of the equipment which was built and installed at Lanehead, it is relevant to include an account of the general difficulties which have been encountered there.

When the work described in Chapters 2 - 6 had been completed, the total time available for field work amounted to 16 months. It would have been very easy to spend this time simply in the development of apparatus, but, as measurements of point discharge over a period of about twelve months were needed, it has been imperative

to begin recording each parameter as early as possible. For this reason, when the equipment for one particular parameter became operational, the recording of this parameter was immediately begun. Thus the total period over which measurements were made was maximised.

Visits to Lanehead were often of two or three days duration. Single day visits were found to make inefficient use of the available time since the number of hours which remained for work, after travelling and cooking meals, was small.

The installation and testing of apparatus was often made very difficult by bad weather. In view of the shortage of time available, it was necessary to work in all but the worst weather. Much of the electronic equipment at the top of the trees was installed in the winter, when temperatures were sometimes as low as -10°C . It was necessary to climb the trees to install the equipment. Any wind causes the trees to sway about and this can be quite alarming if one happens to be working at the top of a tree. In summer, on days with little or no wind, working inside the plantation was often made unpleasant by swarms of midges and other insects.



FIG. 8.1A THE TREE ON THE N. EDGE OF THE PLANTATION.



FIG. 8.1B THE TREE INSIDE THE PLANTATION.

The ground inside the plantation is drained by a system of ditches and the movement of heavy equipment and materials into the plantation was made difficult by their presence.

Probably the most serious difficulties encountered at Lanehead were those in connection with the instrumentation of trees in the plantation. The height of the trees is about 18 to 24 m and climbing up and down these trees is quite a difficult and dangerous task. As protection against a possible fall, a safety harness and helmet were sometimes used. The trees were particularly difficult to climb due to the lack of any substantial branches growing from the trunk (see Fig. 8.1). Apart from the task of climbing them, the installation of electrodes, cables and electronic equipment at the top of trees was a difficult and hazardous operation. This was particularly so when the tree was wet or swaying in the wind.

8.3 Layout of equipment at Lanehead

The layout of equipment in and around the plantation is shown in Fig. 8.2. It was decided that it would be easier to install all the recording equipment in the

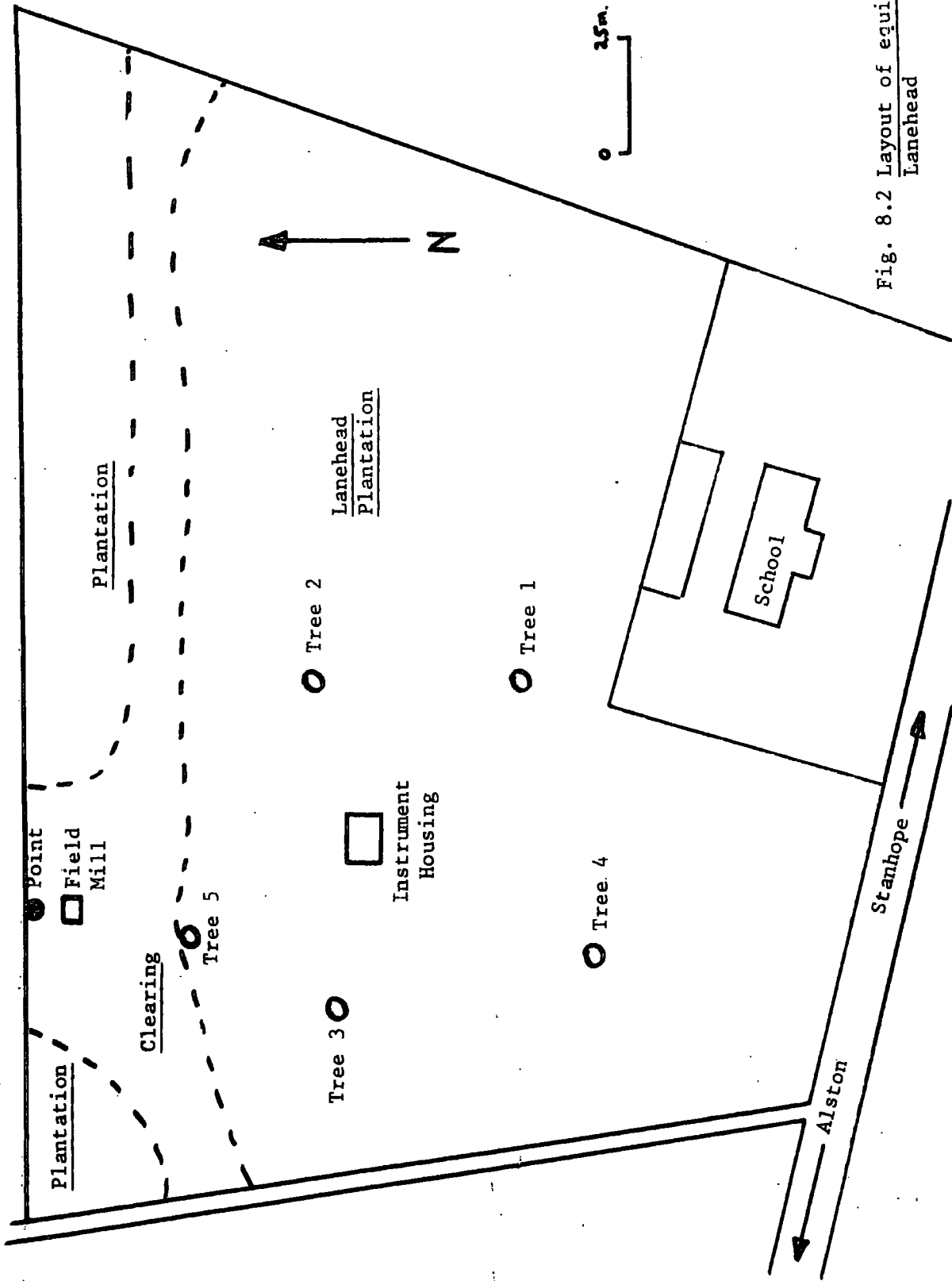


Fig. 8.2 Layout of equipment at Lanehead

middle of the plantation, rather than inside the field station building. By doing this, only a single cable to supply power is required between the field station and the instrument housing.

Initially, four trees inside the plantation were chosen for measurements. These are about 50 m apart and form an approximate square. The instrument housing for the recording equipment is situated roughly at the centre of this square. In later experiments a fifth tree on the edge of the plantation was also used for measurements. The field mill and elevated metal point are situated in a clearing at the northern edge of the plantation. The above-mentioned equipment together with the anemometer and wind vane are connected to the instrument housing via several cables.

8.4 The instrument housing

This was constructed from plywood and blockboard and is shown in Fig. 8.3. One of the sides was hinged at the bottom to give access to the inside of the box. The box was bolted to a metal framework which stands on a concrete base. The roof of the box is covered with

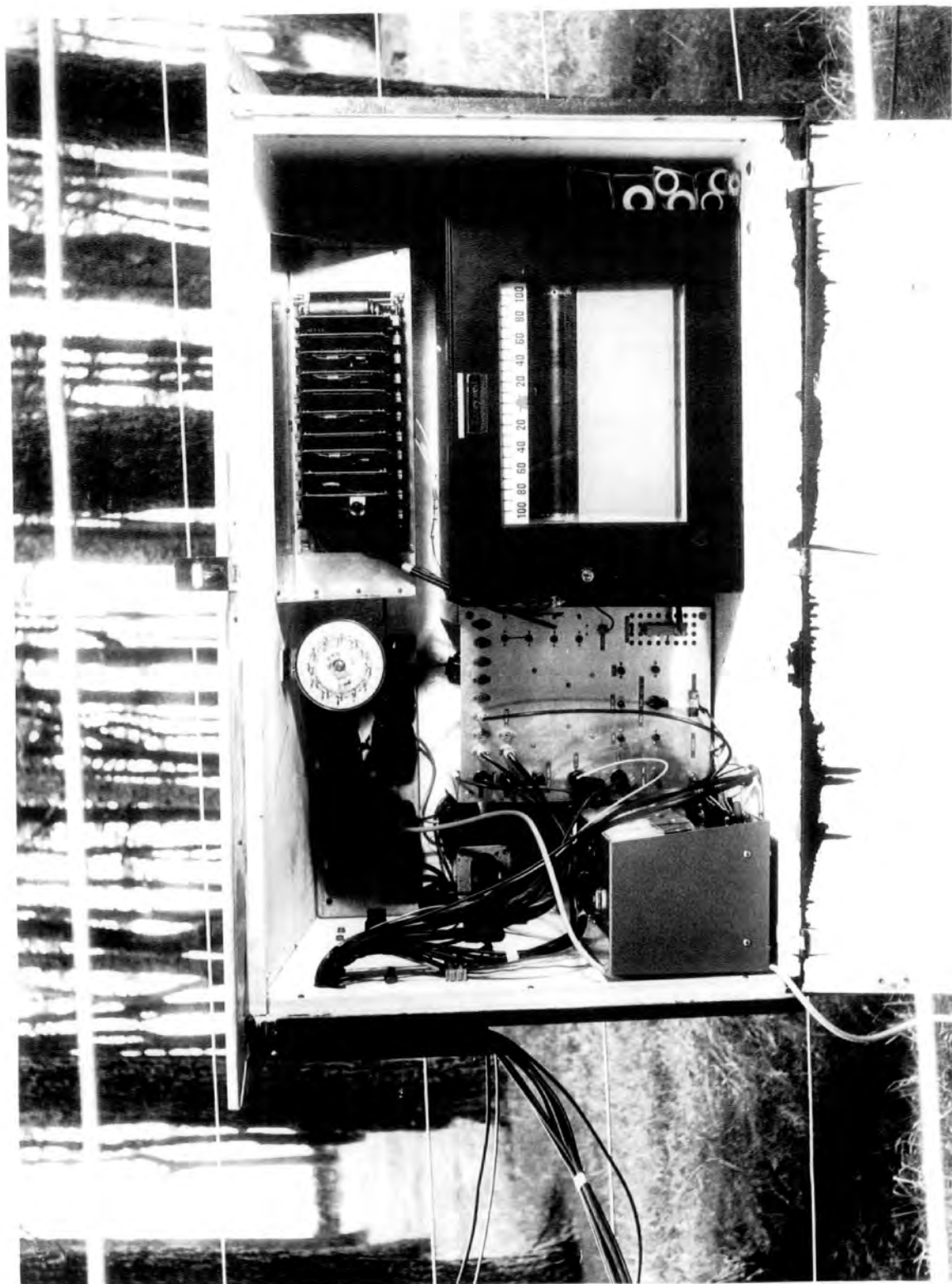


FIG. 8.3 THE INSTRUMENT HOUSING.

aluminium and the rest has been made weatherproof with several coats of paint. The metal base of the box was weighted down with several boulders to prevent the box being blown over in strong winds. A weatherproof entrance for cables was made at the left hand end of the box. The inside of the box is heated, by means of a 100W electric light bulb, to keep the air dry.

8.5 Power Supplies

A 500W isolating transformer, inside the field station building, supplies power to the instrument housing via an overhead cable running from tree to tree. In the interests of safety, the 240V a.c. mains is stepped down to 110V a.c. Inside the instrument housing the 110V line terminates at a plugboard. A second plugboard gives 240V via a small step-up transformer. The low voltage power supplies, required by the transistorised electronic equipment, are provided by two Farnell stabilised supplies Types L30 and L30T. The L30 unit gives +12V d.c. and the L30 T gives \pm 10V for the detector circuits on the trees. Both these power supply units run off 110V a.c.

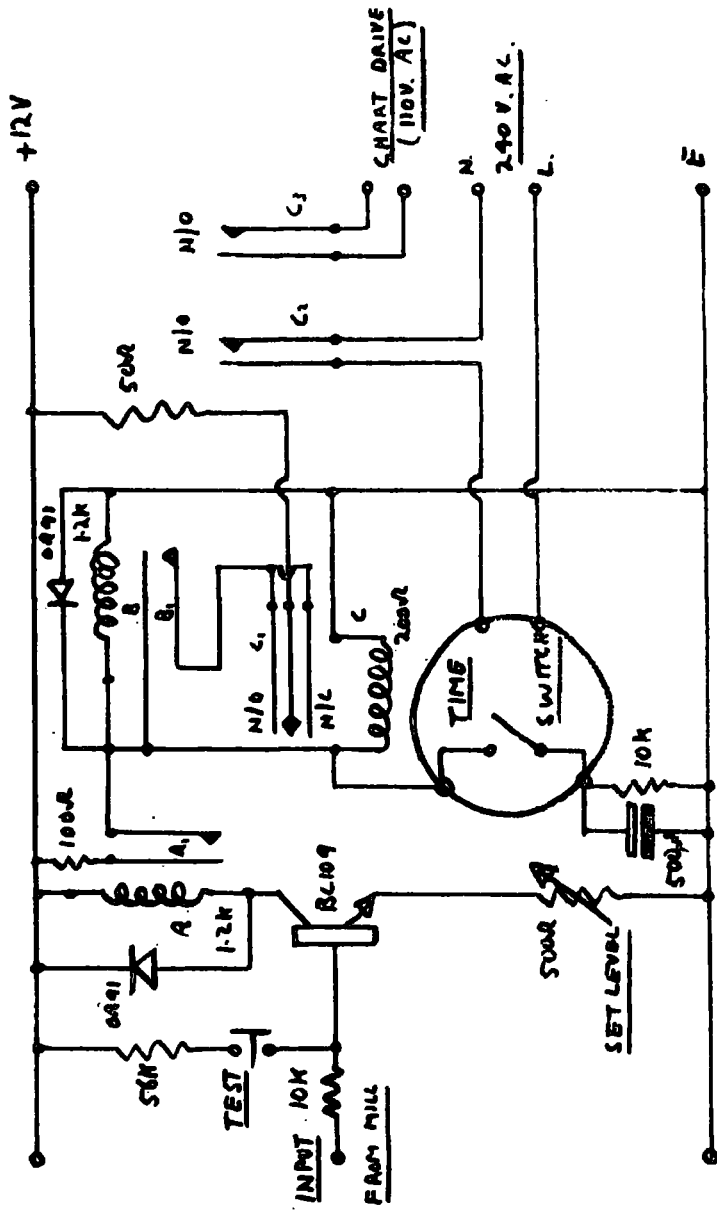


Fig. 8.4. Circuit for automatic recording system

8.6 Earthing

To begin with, difficulties were encountered when equipment was inadvertently earthed at more than one place. To prevent further trouble, it was decided that all the equipment in and around the plantation should be earthed only at the instrument housing. A length of copper pipe was driven into the ground adjacent to the instrument housing and this provides a satisfactory earthing point.

8.7 The automatic recording system

A sixteen-channel potentiometric chart recorder, Honeywell-Brown Type BY/153/X/67 forms the basis for the recording system. This instrument is of the centre-zero type and gives full scale deflection for $\pm 2.5\text{mV}$. The supply required to run the recorder is 110V a.c. A chart speed of 15 inches per hour is used during recording. The recorder amplifiers are left running continuously and the chart drive is switched on only during periods of high potential gradient, using the relay system shown in Fig. 8.4. This circuit, when triggered by the field mill, causes the chart drive to be switched on for a period of at least two hours.

Fig. 8.5. Schematic diagram of field mill amplifier

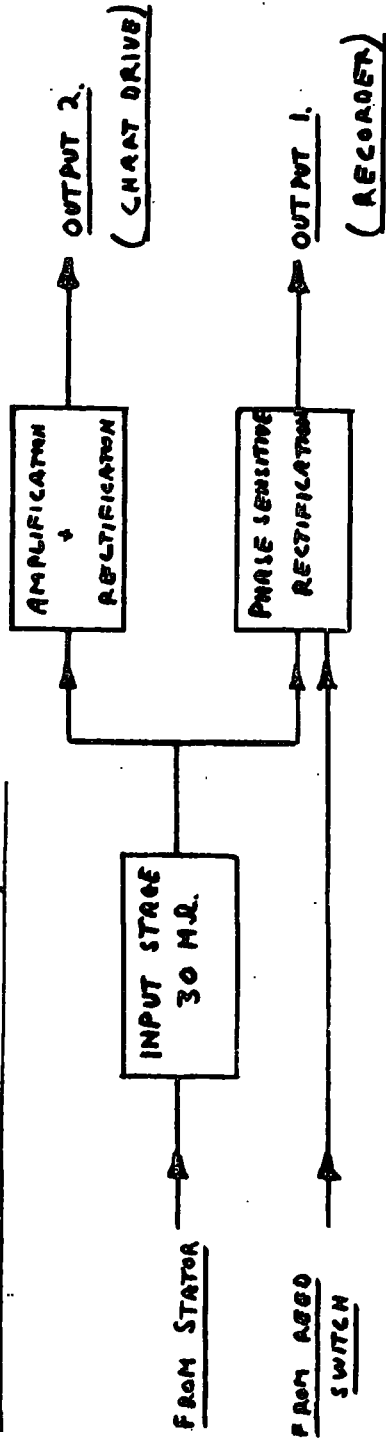
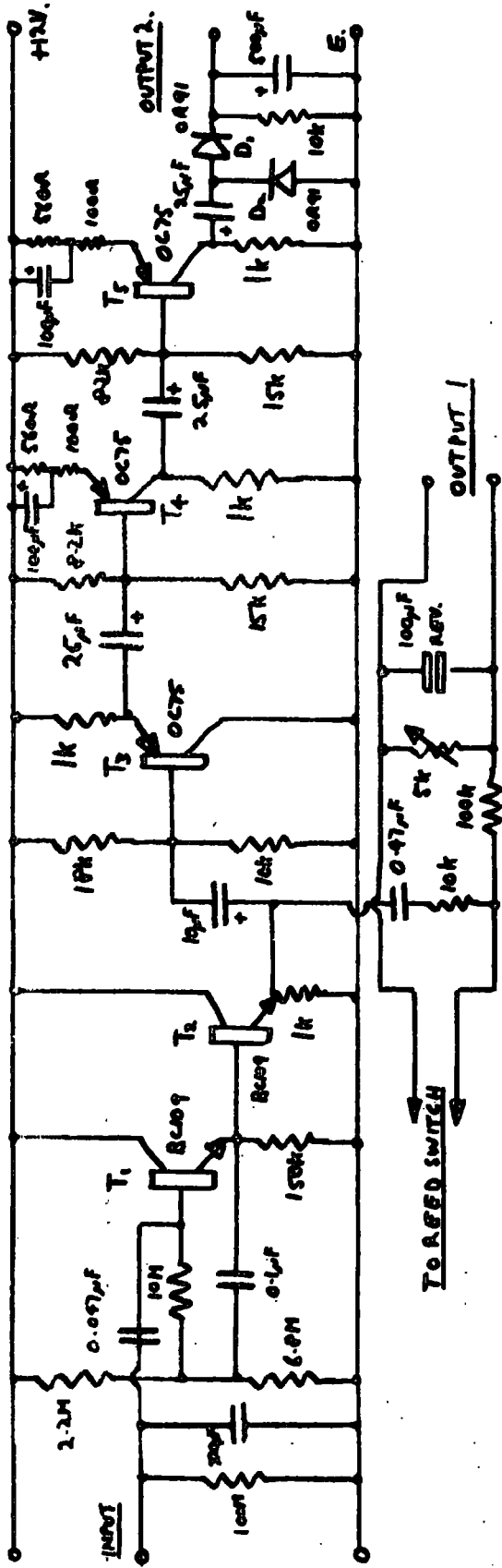


Fig. 8.6. The circuit diagram for the field mill amplifier.



Thus, if the potential gradient falls to or passes through zero during this time, the chart drive will not be switched off. At the end of the two hour period the chart drive is switched off, unless the relay system is again triggered. Thus, recordings are made only during periods of high field, so saving much chart. A single chart gives 100 hours of recording time and so it is only necessary to travel out to Lanehead to change the chart at intervals of one or two weeks.

8.8 The field mill

The field mill in this experiment serves two purposes. First of all, it gives a measure of the potential gradient outside the plantation on its northern side. Secondly, it provides a second d.c. voltage output proportional only to the magnitude of the potential gradient. This output is used to trigger the relay circuit which switches on the recorder chart drive. The electronic circuit for the field mill is shown schematically in Fig. 8.5 and in detail in Fig. 8.6. The design of the field mill itself is conventional, Fig. 8.7. The four-bladed rotor is earthed and the stator, which is of the same shape, is connected to the input of

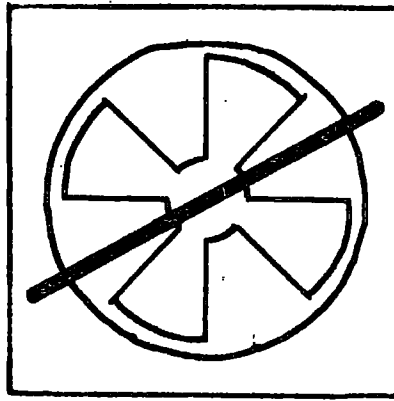


Fig. 8.7. Plan view of field mill showing rotor and supporting bar for the reed switch.

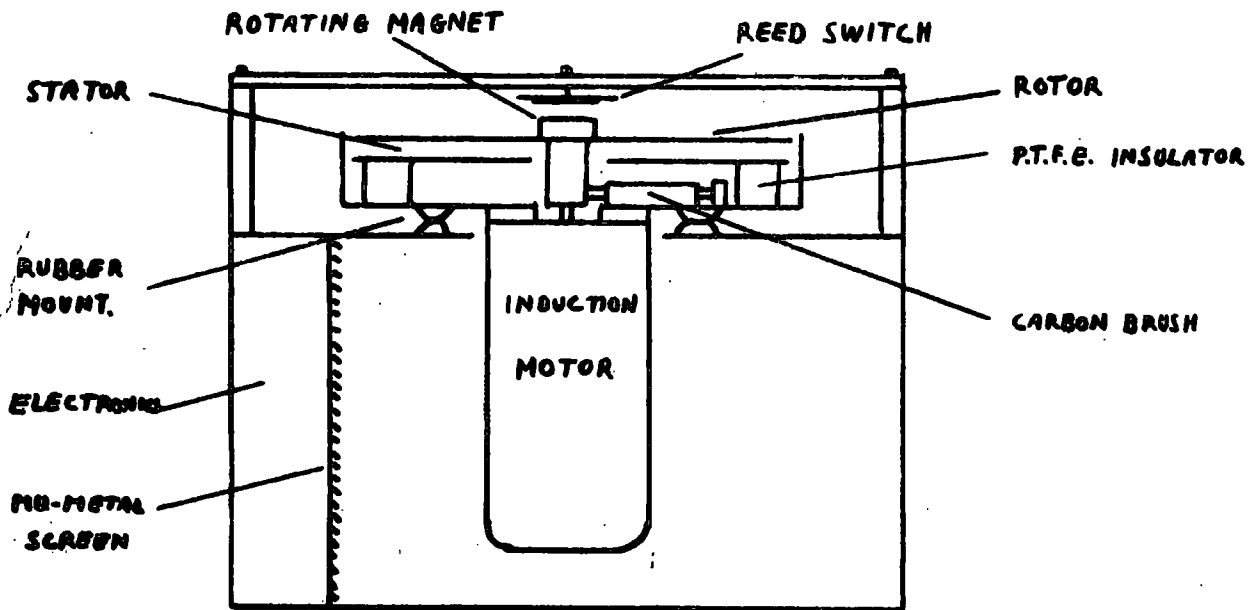


Fig. 8.9. Section through the field mill

the field mill amplifier. Sign discrimination for the potential gradient is achieved by applying phase-sensitive rectification to the output from the amplifier.

A general description of the operation of the field mill electronics may be helpful. The first two stages, involving T_1 and T_2 , provide a high input impedance of about $30\text{ M}\Omega$. This can be achieved using transistors which have a high current-gain at low currents. The technique known as "bootstrapping" is also used to increase the input impedance. The capacitor across the input of the amplifier is necessary to ensure that the amplitude of the field mill signal is independent of the motor speed. In fact, the condition for this has been shown by GROOM (1966) to be

$$WCR \gg 7$$

where W is angular frequency of the field mill signal, C is the input capacitance and R is the input resistance.

The a.c. signal produced at the output of the emitter-follower T_2 goes to the phase sensitive detector. Essentially, a reed switch driven by a rotating magnet attached to the field mill rotor, causes the a.c. signal

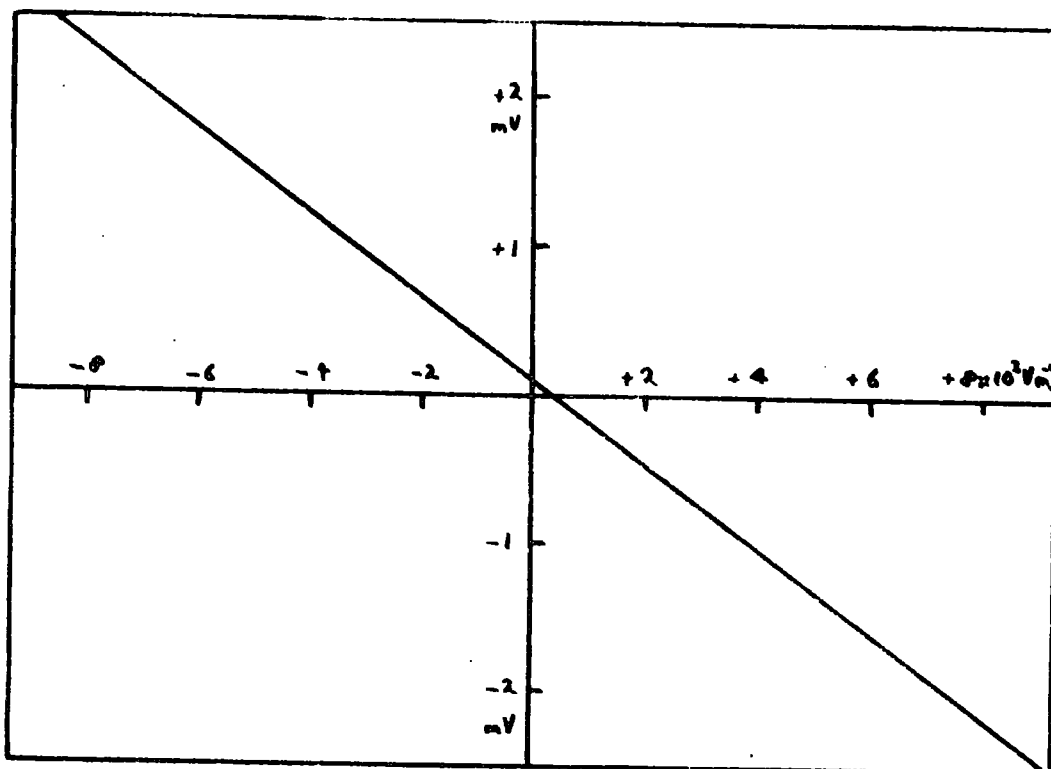


Fig. 8.8. Field mill calibration curve (Output 1)

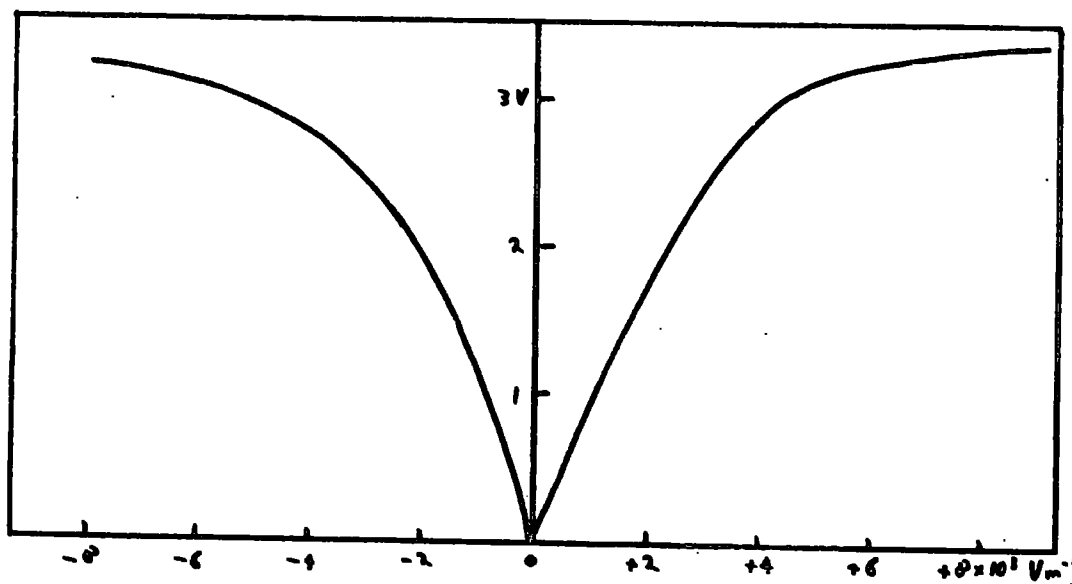


Fig. 8.10. Field mill output 2 characteristic



FIG. 8.11 LOCATION OF FIELD MILL + METAL POINT ON N. SIDE OF PLANTATION.

to be chopped in phase with the rotation of the rotor. Thus the switching of the reed switch can be adjusted so that the sign of the output from the mill is the same as the sign of the potential gradient. The calibration curve for the field mill, assuming an exposure factor of unity, is shown in Fig. 8.8. The construction of the field mill is shown in Fig. 8.9. The output from T_2 also undergoes a.c. amplification by T_3 , T_4 and T_5 , followed by rectification by D_1 and D_2 . This provides the output for the chart drive control. The characteristics of this output are shown in Fig. 8.10.

The field mill is mounted in an inverted position at the top of a metal tower 2.5 m in height (see Fig.8.11) The tower is situated at the centre of a clearing on the northern side of the plantation. The overall exposure factor of the field mill was found by comparing its output with that from a calibrated mill of exposure factor 1.2, situated well outside the plantation. The exposure factor was found to be 1.00 ± 0.05 . This value is partly determined by the screening effect of the surrounding trees. Full scale deflection on the recorder represents a potential gradient of $\pm 8750 \text{ Vm}^{-1}$ when the field mill amplifier is adjusted to maximum sensitivity.

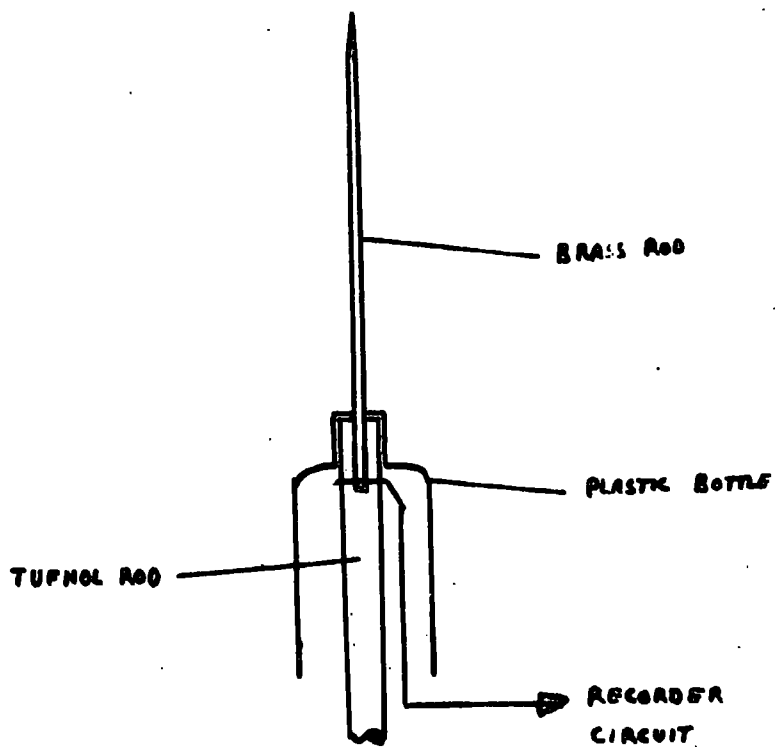
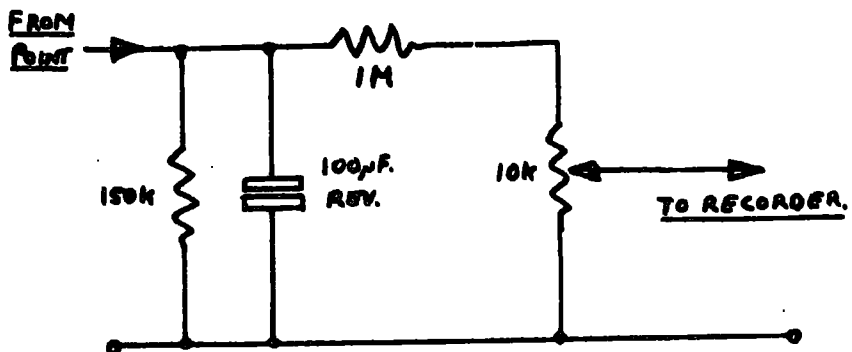


Fig. 8.12. Details of the elevated metal point.

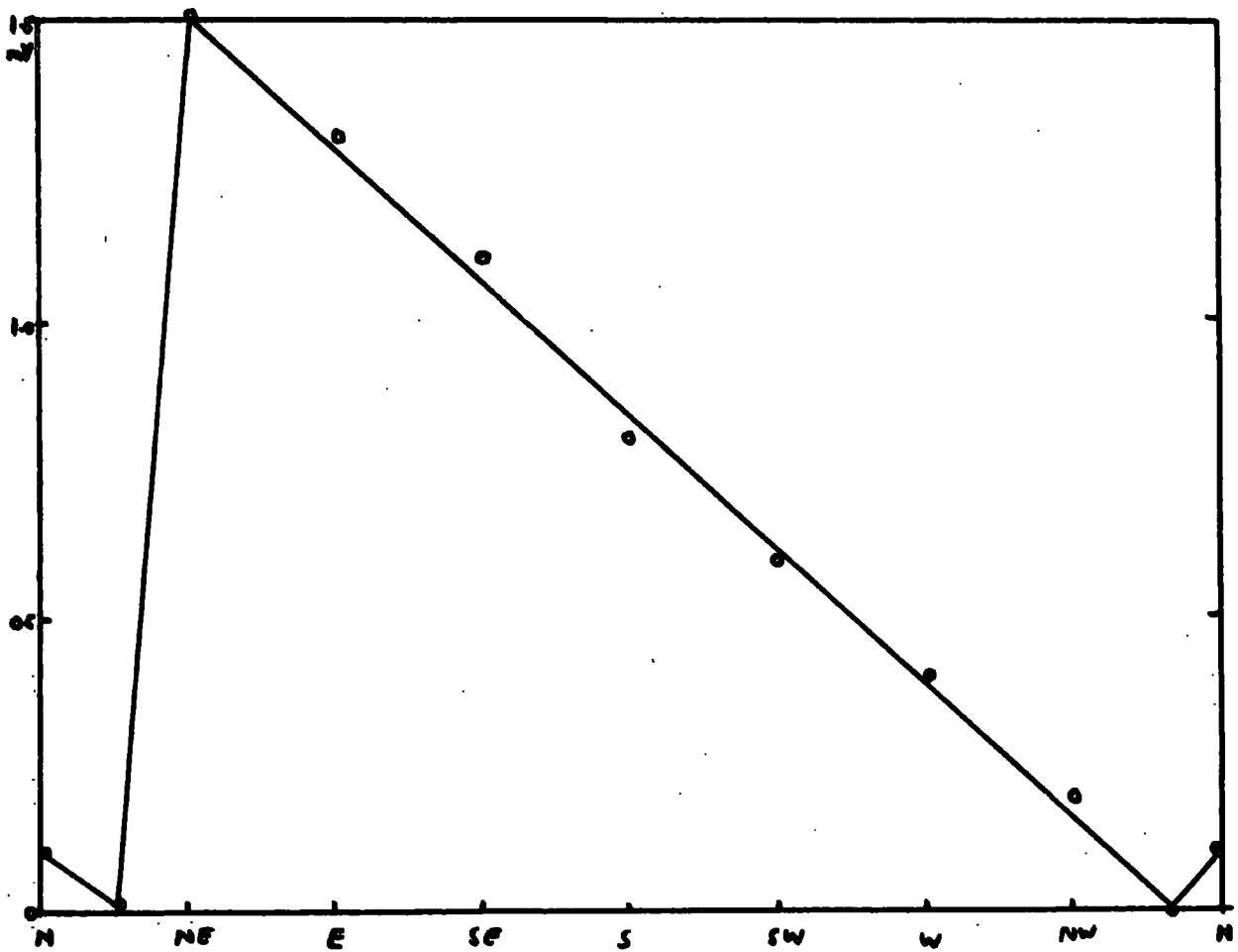
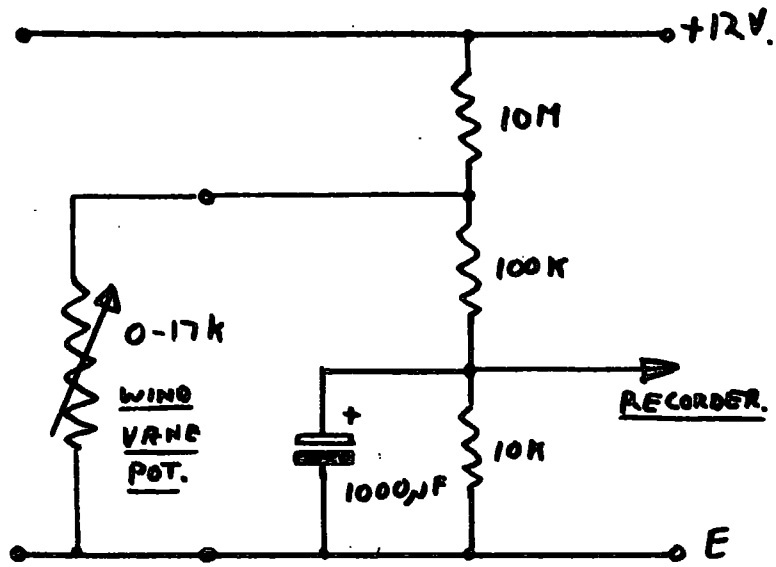


Fig. 8.13. The circuit and calibration curve for the wind vane.

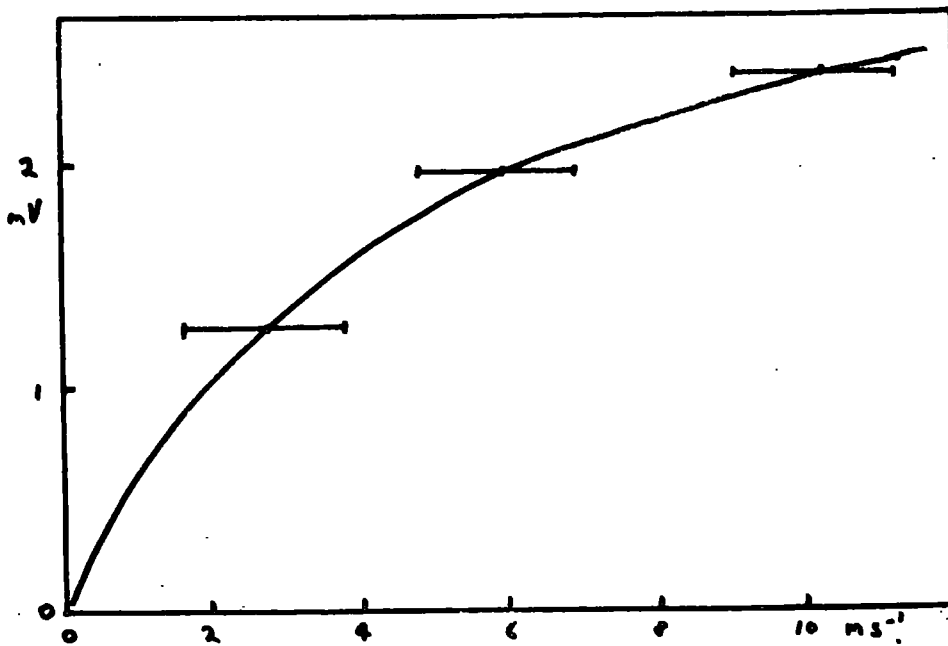
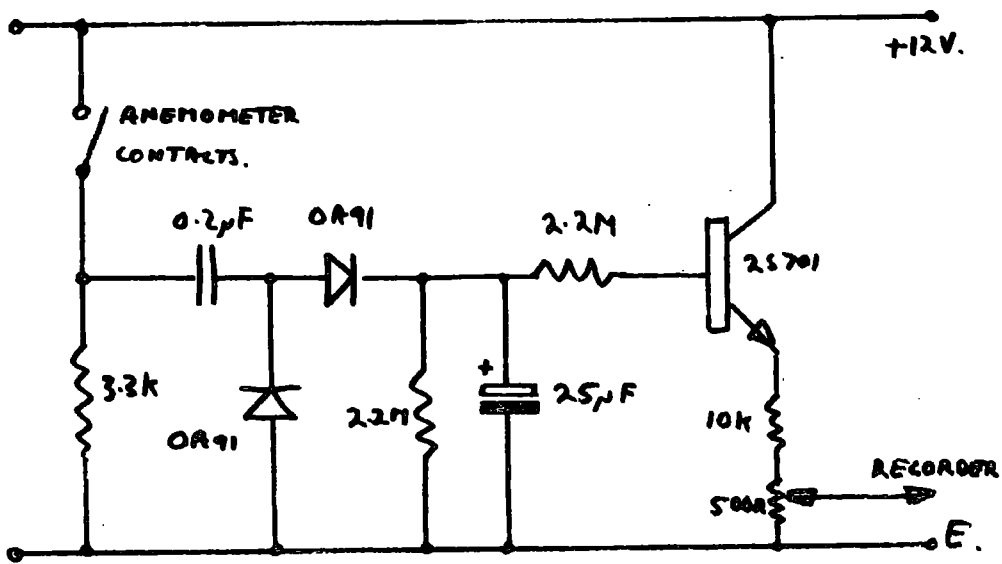


Fig. 8.14. The circuit and calibration curve for the anemometer

8.9 The elevated metal point

This was situated at the northern boundary wall of the plantation. The height of the point is 4 m. The precautions taken to prevent insulation breakdown are shown in Fig. 8.12, together with the circuit diagram for the recorder input.

8.10 Windspeed and direction

A wind vane driving a potentiometer and a cup anemometer operating a reed switch by means of a permanent magnet, are mounted on a Clark mast about 3 m above the ground inside the plantation. Measurements of wind direction were found to be more meaningful when made in the centre of the plantation compared with measurements made at the edge of the wood. The anemometer was only intended to give a very approximate measure of wind speed. The circuitry and calibration curves for the wind vane and anemometer are shown in Figs. 8.13 and 8.14.

8.11 Wet and dry bulb temperature

Aspirated thermistors mounted on the side of the instrument housing give the wet and dry bulb temperatures, see Fig. 8.15. The temperatures measured give an

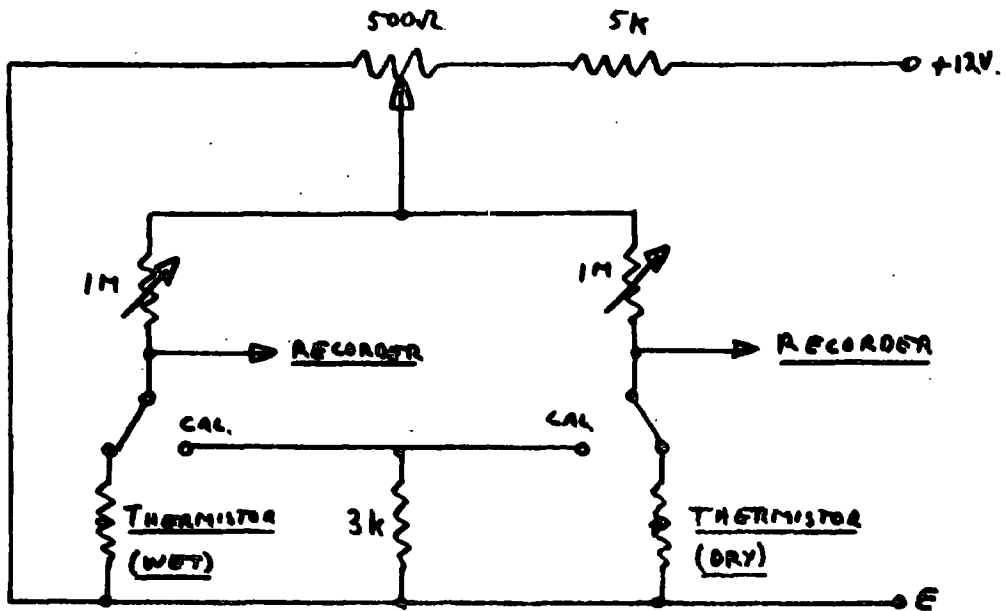


Fig. 8.15. The thermister circuit

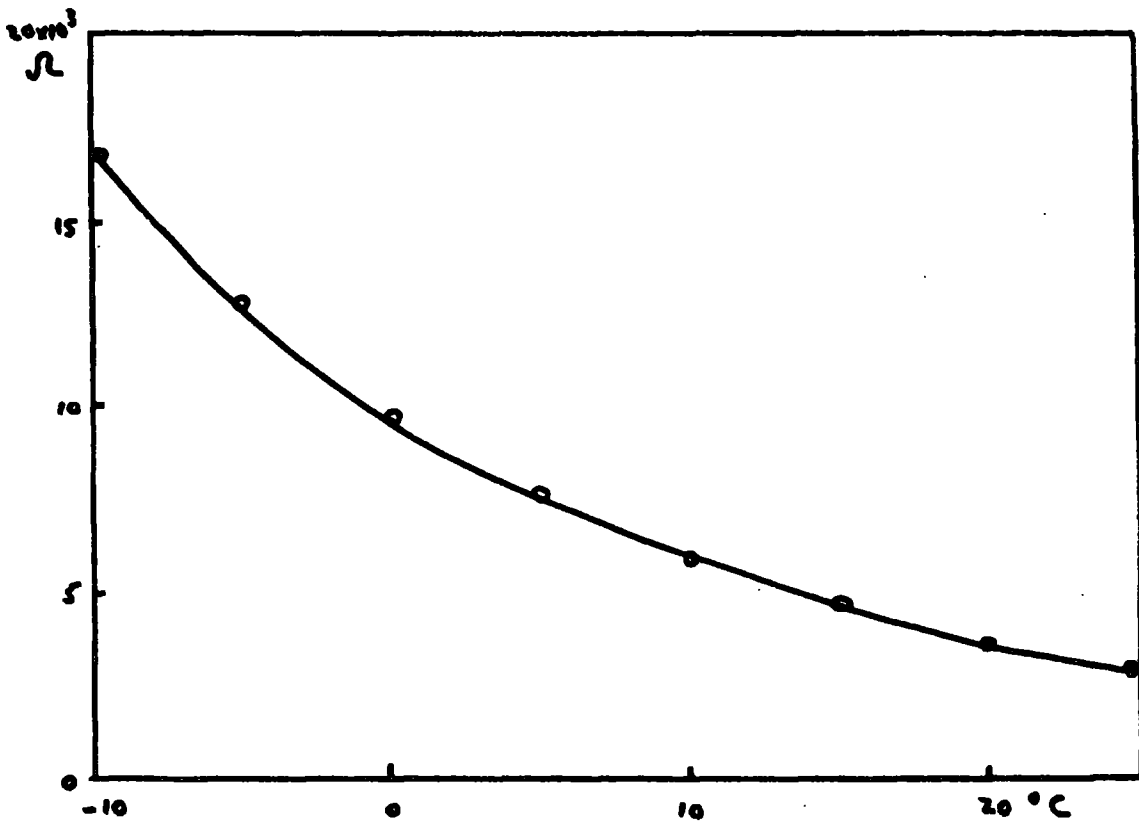


Fig. 8.16. Typical calibration curve for the thermister

indication of the humidity and are also useful in the identification of breaks in recording. The calibration curves are shown in Fig. 8.16.

8.12 Allocation of recording channels

The table below shows the channels allocated to the various parameters measured. The time for the recording of each channel is 2.4 s so one complete cycle takes about 40 s.

Channel	Parameter
6, 14	Potential gradient
5, 13	Elevated point current
1, 9)
)
2, 10)
)Measurements from four trees
3, 11)
)
4, 12)
7	Wind direction
8	Wet bulb temperature
15	Wind speed
16	Dry bulb temperature

CHAPTER 9.

The detector for point discharge on trees

9.1 Introduction

This chapter is an account of the development of a detector which would give reliable measurements of point discharge currents in the tree on which it was installed. The predominant cause of difficulties in this development work was always the presence of various types of electrical noise in the trees. By constructing various forms of detector, it gradually became possible to identify the causes of the electrical noise. One by one the various forms of noise were eliminated, until, in the final form of the detector, the signal-to-noise ratio had been sufficiently increased for reliable measurements of point discharge to be made.

9.2 Initial considerations on electrode design

The length and position of the cylindrical capacitative electrode determines the voltage amplitude of any point discharge pulses which are detected. The capacitance of a cylindrical capacitor C is given by

$$C = 2\pi\epsilon_0 k L / (\log_e (R/r))$$

where R is the radius of the outer conducting cylinder, r is the radius of the inner cylinder and ℓ is the length of the capacitor. The dielectric constant of the medium between the conducting cylinders is equal to K and ϵ_0 is the permittivity of free space. It was shown in Chapter 5, that, if we assume that the value of R/r is 1.3 and the dielectric constant of the wood and bark on a tree is about 3, then the capacitance per unit length of electrode is about 600 pFm^{-1} .

To obtain a rough estimate of the voltage amplitude of the pulses that we might expect at the electrode, we can consider the following example. Let the height of the tree be 20 m and the resistivity of the tree trunk be $5 \text{ k}\Omega\text{m}^{-1}$. Let the input impedance of the measuring equipment connected to the electrode be about $2 \text{ k}\Omega$ and assume that the electrode is positioned two thirds of the way up the tree trunk. If the measuring equipment is installed at the bottom of the tree, the shunt capacitance of the coaxial cable between the electrode and the measuring equipment will be about 500 pF. If we take a value of 50 mV for the amplitude of the point discharge pulses at source, we can now draw the equivalent circuit of the tree and measuring equipment (See Fig. 9.1).

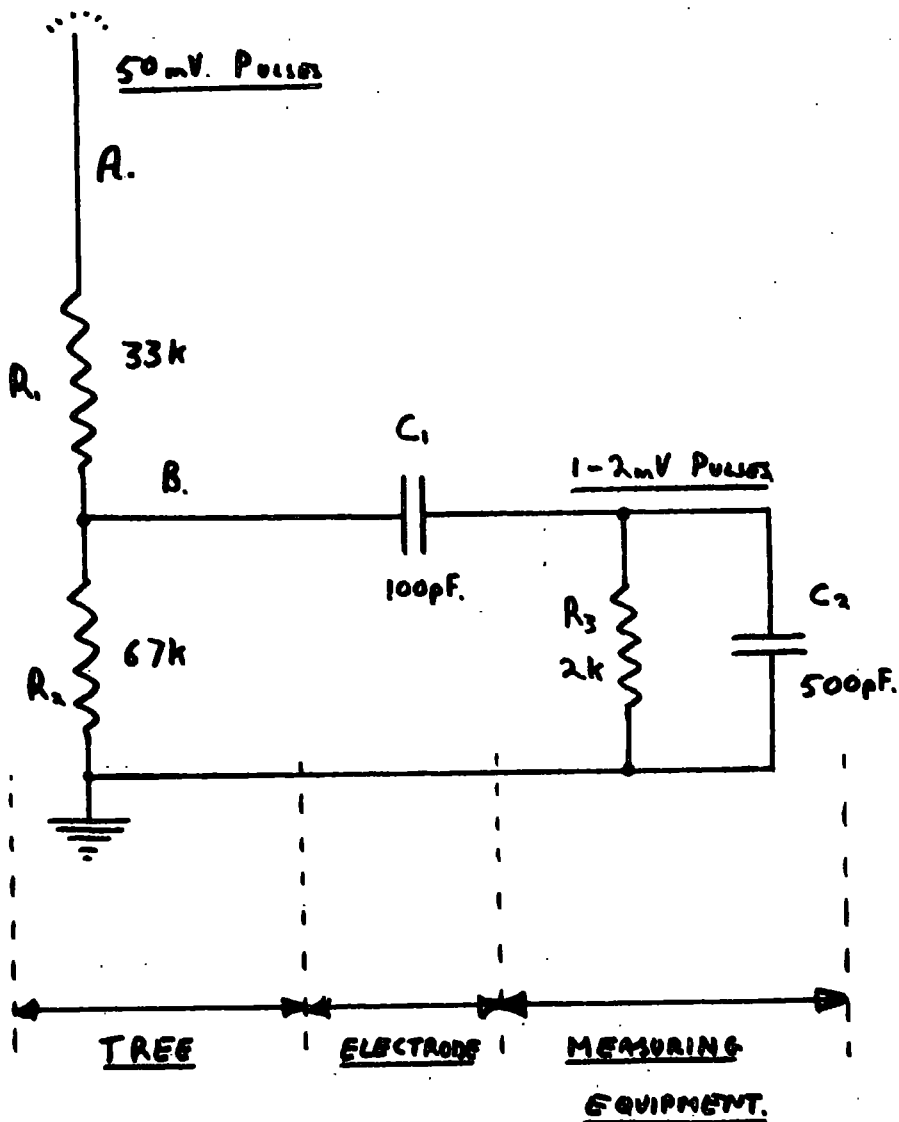


Fig. 9.1. Simplified equivalent circuit for tree, electrode and measuring equipment.

The electrode capacitance is taken as 100 pF. With reference to the diagram, it can be seen that the amplitude of pulses at B will be attenuated compared with the pulse amplitude at A. After the pulses have passed through the electrode C_1 to the measuring equipment at C they will be further attenuated. The amplitude of the pulses at point C, in this example, works out to be about 1mV. Although this example is an oversimplification of the true case, it does show that the effect of the trunk resistance, above the electrode, is to cause considerable attenuation of the pulses. It can be therefore concluded that the electrode should be positioned as high as possible up the tree trunk, to reduce the attenuation of the pulses to a minimum.

9.3 Construction of the electrodes on four trees

The electrodes used were constructed by winding about 50 turns of coaxial cable around the tree trunk. A close-wound coil was thus formed and electrical connection for the electrode was made to the outer sheath of the coaxial cable. The four trees have heights ranging from 18 to 23 m and the electrodes were fixed as high up the trees as possible. This was about two-thirds of the tree height, as this represented the maximum height to which it was possible to climb. A coaxial line from each of the four electrodes leads to the instrument housing.

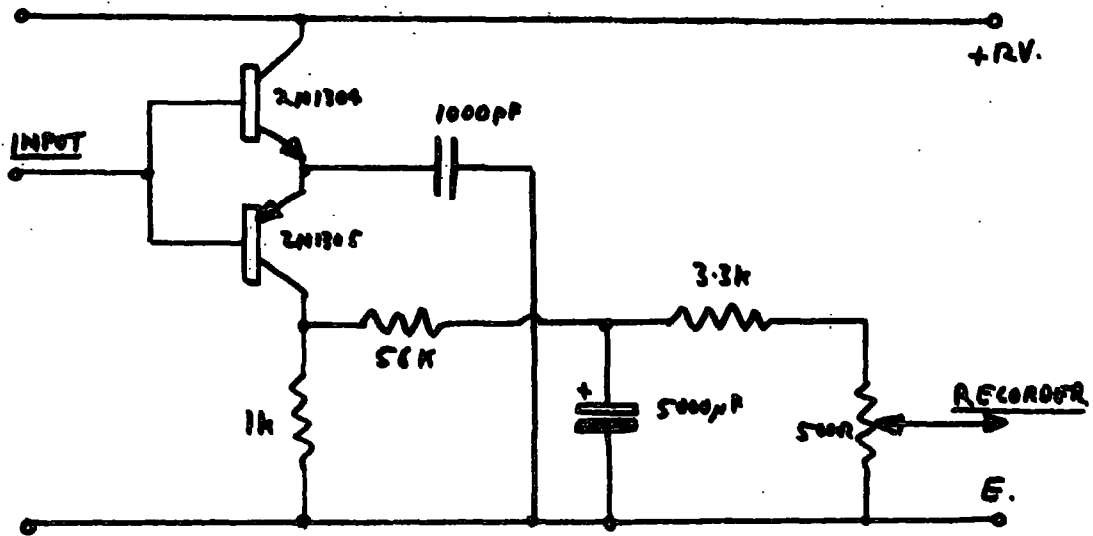


Fig. 9.2. The frequency meter circuit

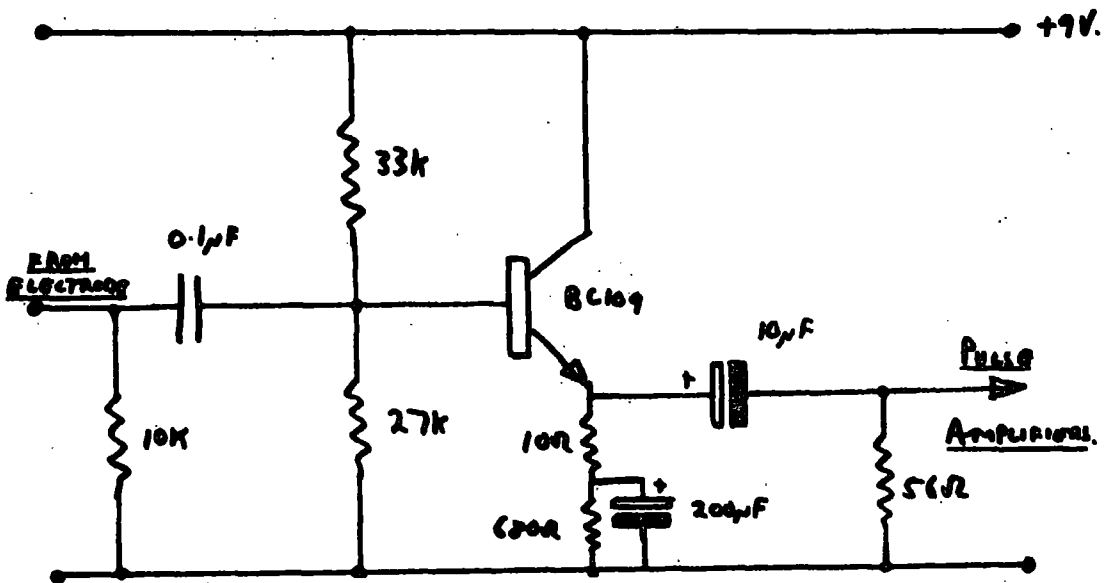
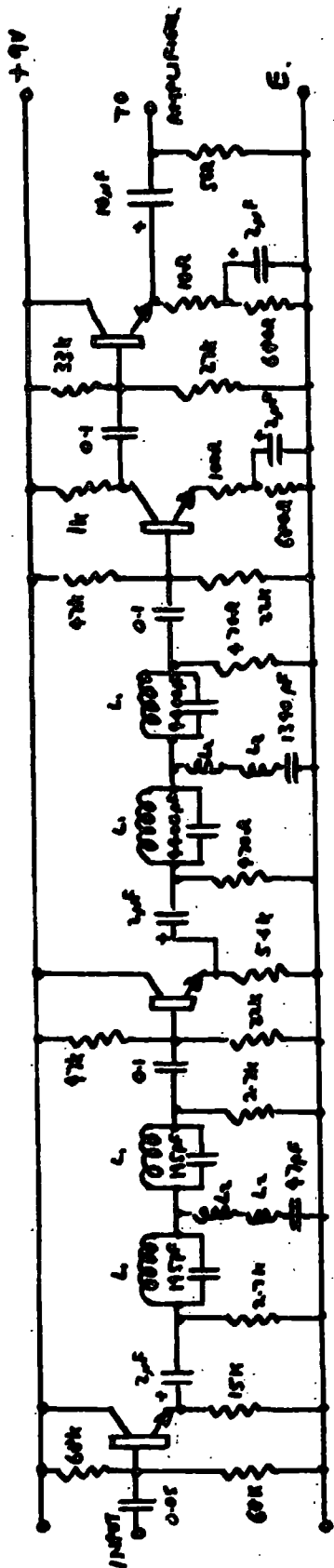


Fig. 9.3. The head-amplifier circuit

9.4 Early versions of the detector

The signals from the four tree electrodes were each amplified at the instrument housing. A voltage gain of 1000 was provided by transistor pulse amplifiers. The circuit adopted for these wideband amplifiers was designed by Racal Research Ltd using computer techniques to maximise the stability. (Design Electronics June 1967). After voltage amplification the signals from each of the four trees passed into a simple frequency measuring circuit (Fig. 9.2). The results with this system were discouraging because the recorder remained off-scale most of the time as a result of a high noise level. The noise was thought to be caused by the relatively high line impedance of $2\text{ k}\Omega$. This would allow earth signals to be picked up from the sheaths of the coaxial cables running from the trees to the instrument housing. Also amplifier noise was found to be appreciable when the impedance across the input was as high as $2\text{ k}\Omega$. The line impedance was consequently reduced to 25Ω and battery driven transistorised head amplifiers were installed at the bottom of each tree to feed into the lines (Fig. 9.3). The electronic circuits and batteries were housed in waterproof polythene boxes. The lifetime of the batteries was about 1000 hours. The noise level



ALL TRANSISTORS BC107

L₁ MAXI @ DP2 RED.

L₂ MAXI @ DP2 BLUE.

Fig. 9.4. Circuit diagram for the selective radio-frequency filter

was now considerably reduced but unfortunately the recorder still remained off-scale. A careful examination of the noise on an oscilloscope indicated that there were two definite frequencies present in the otherwise random waveform. These frequencies were found to be about 200 and 1000 kHz. It was found that the trees were acting as aerials and picking up the BBC programmes, Radios 2 and 4.

9.5 The addition of a selective radio frequency filter

To overcome this problem a selective radio frequency filter was designed (see Fig. 9.4) and incorporated into each of the head amplifiers on the trees. The filters were of the "constant k" type and it is important that these filters are terminated at each end by their own characteristic impedance. The surrounding circuitry was thus designed accordingly. Using these filters the amplitudes of the two radio signals of 200 and 1200 kHz were reduced, relative to all other frequencies, by factors of 13 and 20 respectively. The recorded output now remained on scale for most of the time and was approximately constant during clear weather in daylight. However,

at night or when the sky was clouded the recorded output showed large variations. In periods of high potential gradient the recorded tree signal often correlated with the potential gradient. At first, it was thought that this was caused by point discharge. It later became clear that this was not so, and the real cause of correlation was the change of radio noise level as storm clouds passed over Lanehead. If the noise level had remained constant, measurements of point discharge would have been possible as the apparatus described above was thought to be adequately sensitive. However, this was not the case and it was decided that completely different techniques would have to be used.

9.6 The new approach

It was concluded from the above experiments that the reasons for failure so far were twofold. In the first case, the electrodes on the trees were not near enough to the source of the pulses. Thus, the attenuated pulses needed considerable amplification and, as the signal-to-noise ratio was low, no conclusive measurements could be made. Secondly, a more selective measuring instrument



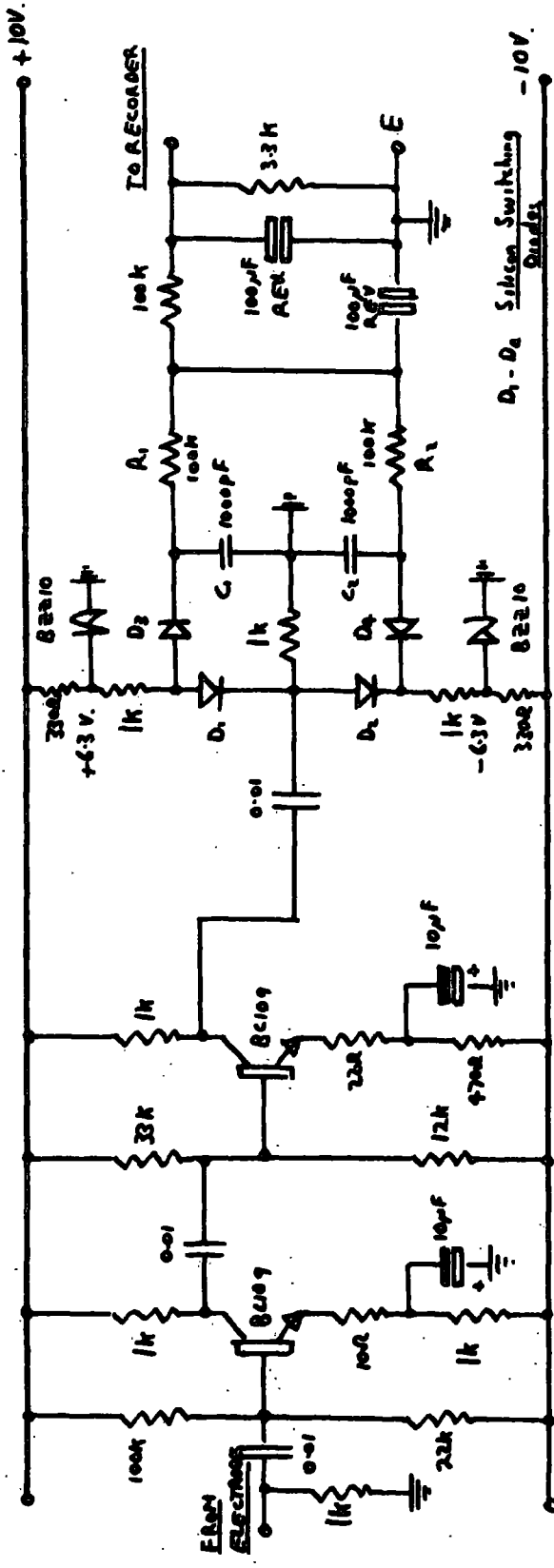


Fig. 9.5. Circuit diagram for the point discharge pulse detector

was required. If the measuring equipment can be made to respond only to non-symmetrical pulsed waveforms, and not to symmetrical waveforms such as a sine wave, then much of the noise including the radio signals would be eliminated. A new form of detector was accordingly designed to meet the above requirements. The circuit is shown in Fig. 9.5 and consists of two stages of voltage amplification followed by the diode detector stage. When correctly balanced the circuit gives no output for symmetrical waveforms such as a sine wave. Positive pulses give a positive d.c. output and negative pulses give a negative output. Thus with this detector the sign of the point discharge current will be given directly whereas, using previous methods the sign would have to be deduced from the potential gradient. The values of R_1C_1 and R_2C_2 determine the pulse frequency coverage of the detector. Thus, assuming that R_1C_1 and R_2C_2 are equal, we have,

$$f_{\max} R_1C_1 \approx 5$$

where f_{\max} is the highest frequency which can be measured.

The new detector was installed in a weatherproof box 2 m from the top of a tree on the northern edge of the plantation. This tree was chosen for two reasons. First the tree was fairly exposed and would probably begin to discharge at a lower potential gradient than the four trees previously used. Secondly, it was possible with difficulty to climb to the very top of this tree. Four electrodes 0.25 m in length were attached to the top branches of this tree and connected to the input of the detector. These electrodes are made from aluminium foil and are positioned about 1.5 m below the highest point of the tree on four separate branches. Two cables, one for the output and one for the power supply, were taken to the instrument housing. The noise level with this detector was now reduced to only 10% of full scale on the recorder. However, in periods of high potential gradient reaching about $\pm 7000 \text{ Vm}^{-1}$ no indication of point discharge was given.

9.7 Further improvements

It had been assumed, up to this point that the resistivity of the tree branches did not vary appreciably with the diameter of the branch. Laboratory tests, on



FIG. 9.6A POINT DISCHARGE PULSE DETECTOR - THE ELECTRODE.

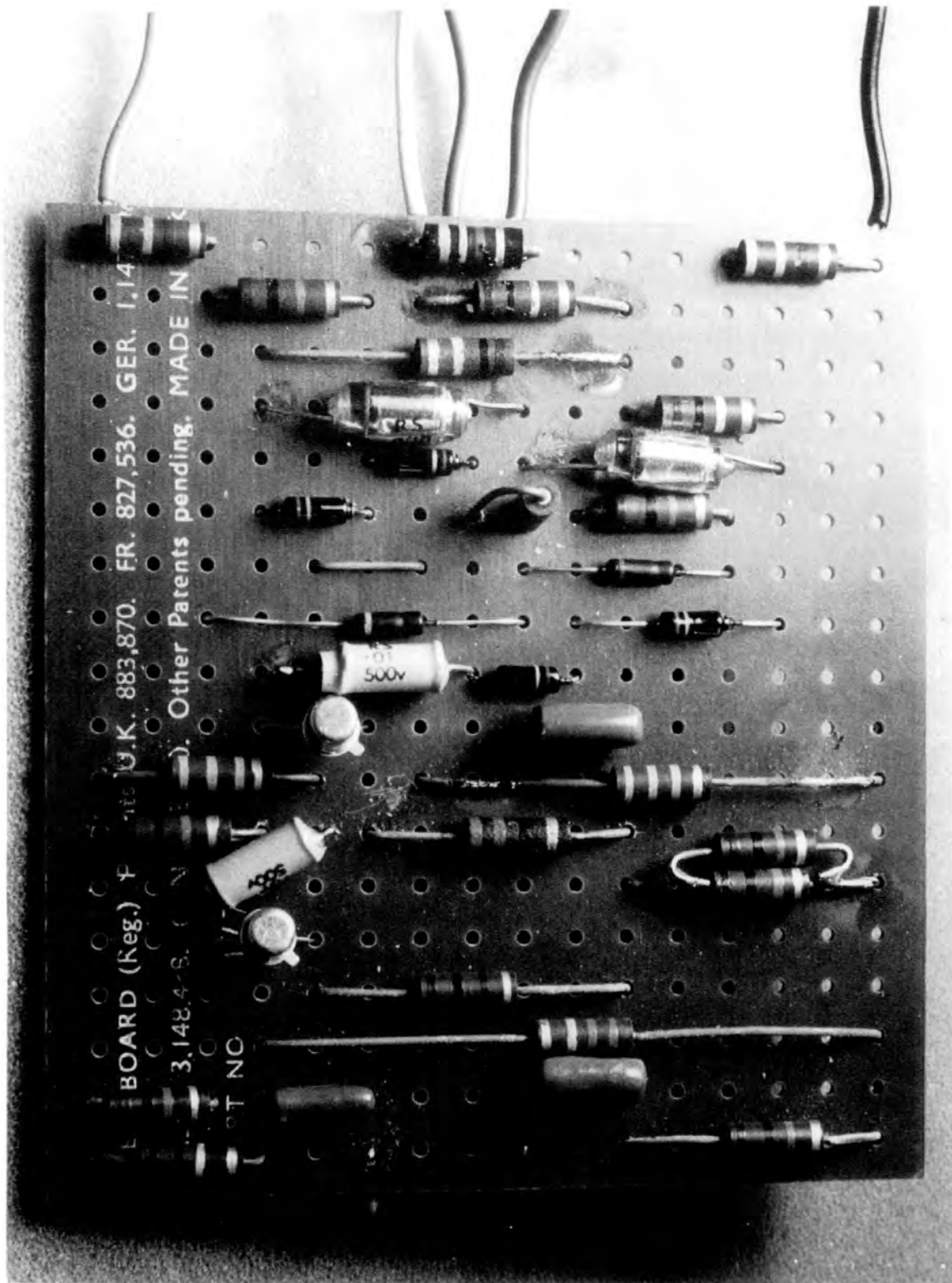


FIG. 9.6B POINT DISCHARGE PULSE DETECTOR - THE ELECTRONICS.

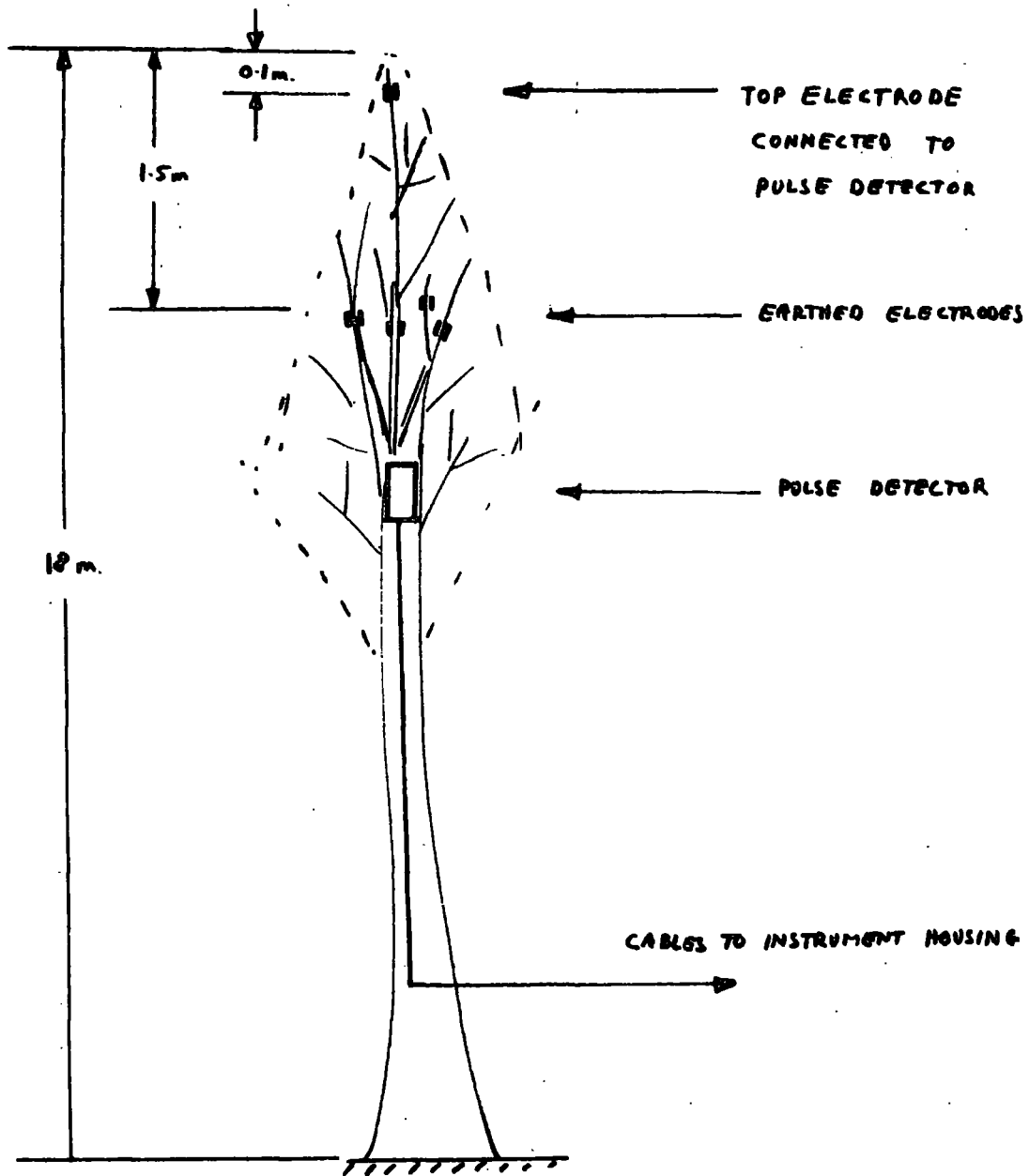


Fig. 9.7. Electrode arrangement for tree at the edge of the plantation.

branches cut from the trees confirmed that this is true for all but the thinnest branches. However, it is found that the resistivity of the twigs forming the very end of a branch is very much higher than that for the rest of the branch. With this new information, an electrode was formed on one of the top branches of the tree and at a distance of only 15 cm from its end. The electrode was again made from aluminium foil and was 10 cm in length on a branch with a diameter of approximately 1 cm (See Fig. 9.6). The four electrodes lower down the tree were connected to earth to reduce the level of noise reaching the top electrode (See Fig. 9.7).

9.8 First successful measurements of point discharge pulses

In the final form of detector and electrode described above, the noise level is less than 5% of full scale on the recorder. The only occasions when the noise level increases beyond this value are in the hours of darkness. Investigations showed that this is caused by the tree behaving as an aerial and picking up atmospheric noise. An account of the measured characteristics of this form of noise is given in Chapter 10. Shortly after the installation of the detector high potential gradients were recorded over a period of a few hours.

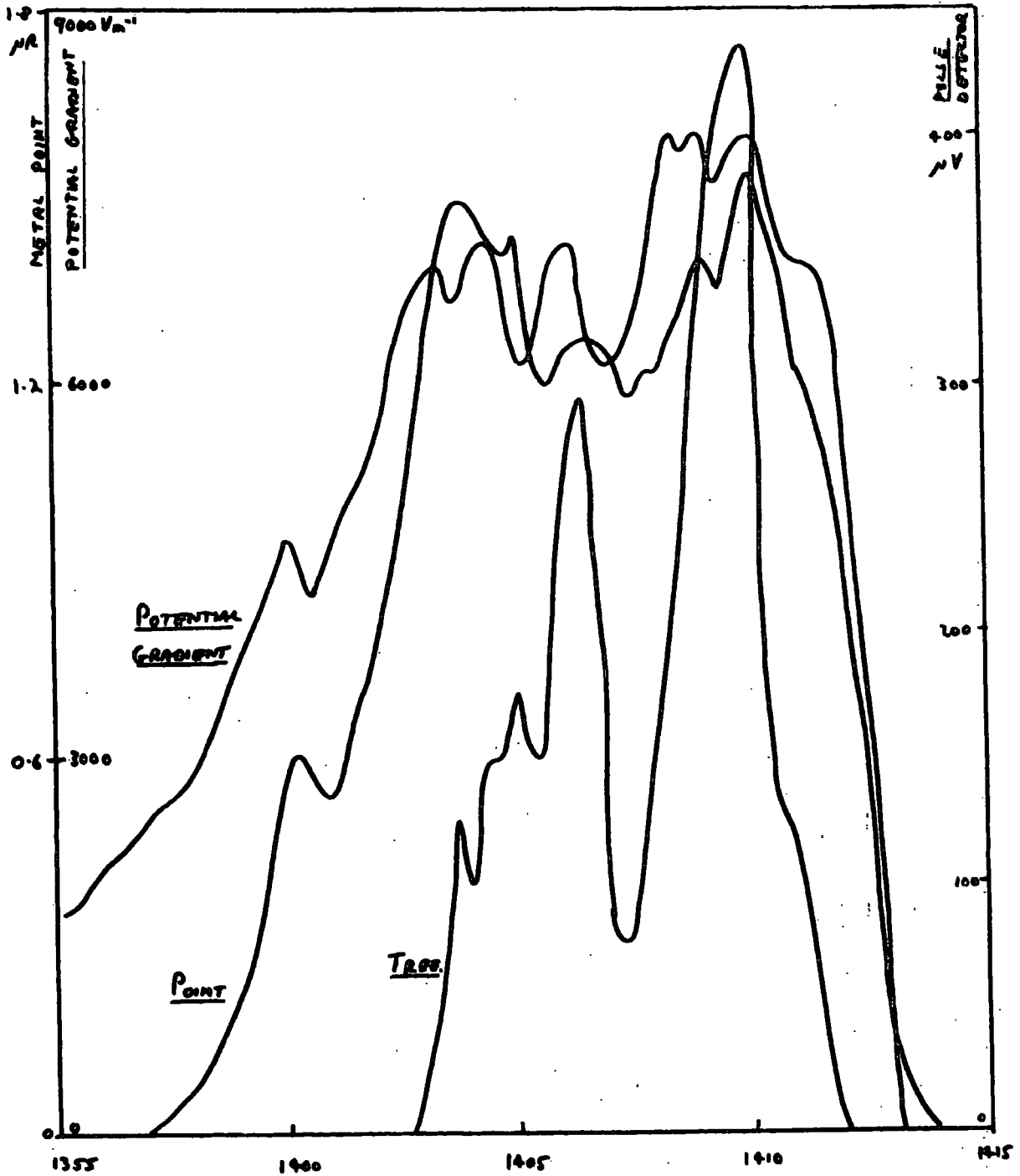


Fig. 9.8 Negative point discharge currents and potential gradient on 20th June, 1968.

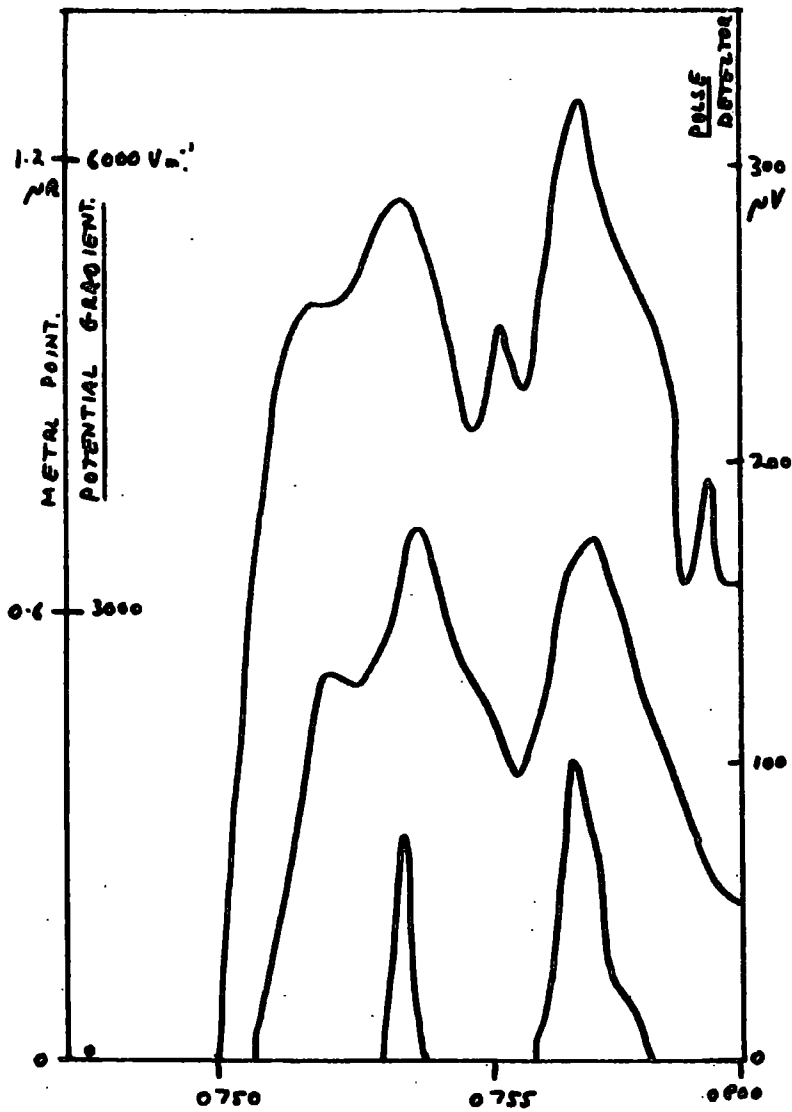


Fig. 9.9. Positive point discharge currents and potential gradient on 21st June, 1968

A clear indication of point discharge was given by the recorded output from the detector (see Figs. 9.8 and 9.9) From the record it can be seen that the tree did not begin to discharge until the measured potential gradient was about $+6000 \text{ Vm}^{-1}$.

9.9 Performance and calibration of final form of detector

It was decided that the only practicable way to calibrate the detector and electrode system was to try to simulate the top two or three metres of the tree in the laboratory. A branch was cut from one of the trees in the plantation and erected in the laboratory. The lower end of the branch was placed in a beaker of dilute salt solution to give a good electrical connection to the branch. An aluminium foil electrode was formed close to the end of the branch and connected to an identical pulse detector. A galvanometer connected between the salt solution and earth gave the current through the branch. Artificial fields were applied to the branch and the relation between the point discharge current and the detector output is shown in Fig. 9.10. The resistance to earth from the bottom of the branch was varied from zero to $1 \text{ M}\Omega$ and this was found to have little or no

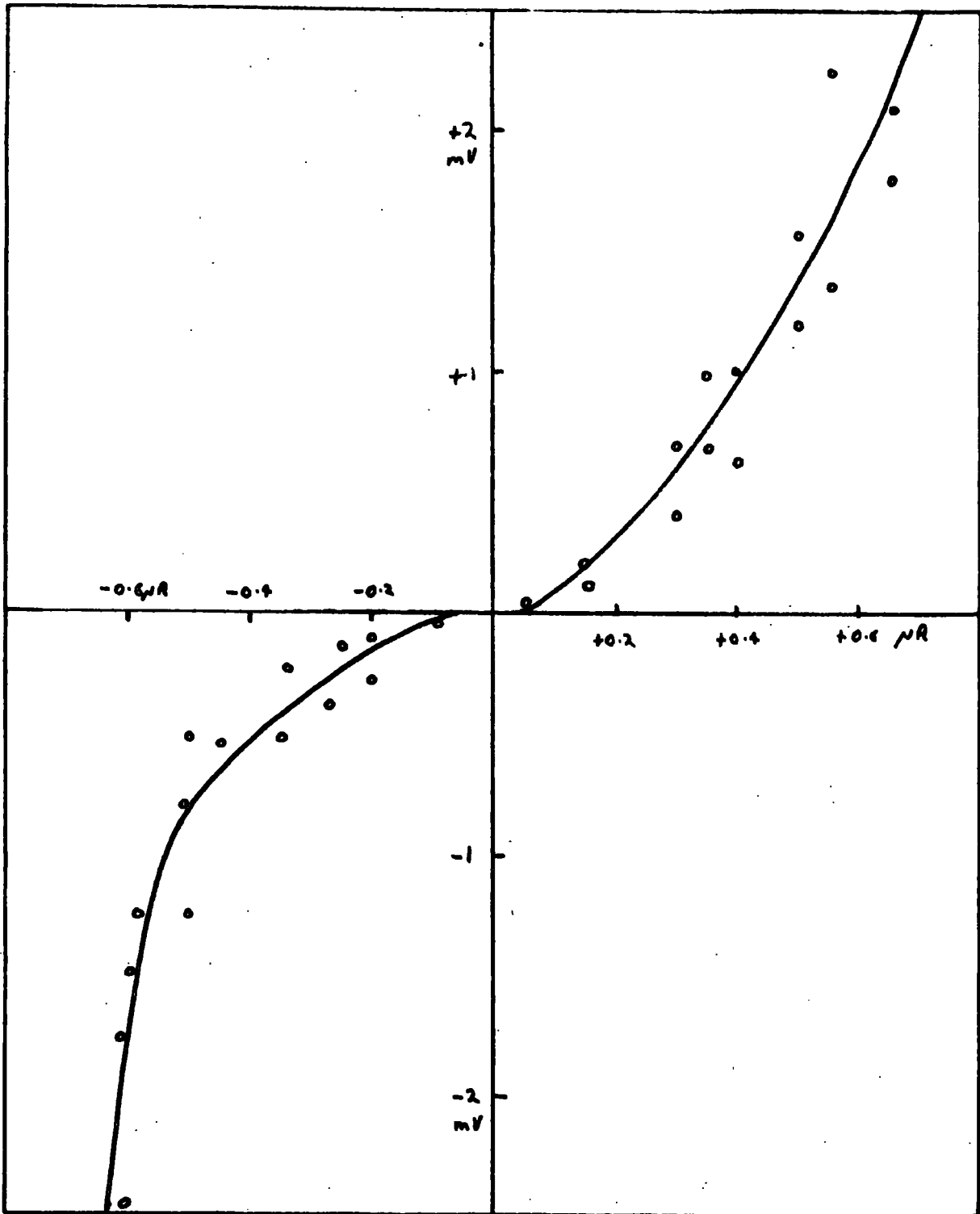


Fig. 9.10 Calibration curve for point discharge pulse detector.

effect on the calibration curve. It is therefore concluded that this curve should still hold to some extent for the case of a full size living tree.

9.10 Conclusion

There is no doubt that the system developed will detect point discharge on trees and give a measure of the current to an accuracy of about $\pm 30\%$. Further work is needed if accurate measurements of the point discharge current is needed. The important points about the detector are that it gives a measure of the current in a tree growing under natural conditions and the start of the discharge on the tree is clearly defined. The tree on which the first successful measurements were made was situated on the edge of the plantation. A second tree inside the plantation was later equipped with a similar electrode and pulse detector, so that a comparison could be made between relative amounts of point discharge on the two trees.

CHAPTER 10The point discharge current measurements at Lanehead10.1 Introduction

Measurements were made at Lanehead over the 11 month period of October 1967 to August 1968. During this time the potential gradient was recorded whenever it exceeded values of about $\pm 1500 \text{ Vm}^{-1}$. The point discharge current for the elevated metal point was measured for 10 months starting at the beginning of November 1967. It was not until June 1968 that the first measurements of point discharge on a tree were made. Point discharge currents in a tree at the edge of the plantation were recorded over a period of three months. A second tree inside the plantation was later fitted with a point discharge detector and gave measurements during the latter half of July and the whole of August. Thus it was possible to compare the results from the two trees during this period. It is thought that these measurements are important because they are probably the first reliable measurements of naturally occurring point discharge on trees.

Over the total period of 11 months the recorded data amounts to about 750 m of paper chart. This represents a recording time of approximately 2,000 hours.

10.2 Analysis of recorded data.

10.2.1 Objects of the analysis.

The recorded data for potential gradient and for point discharge currents through trees and a metal point has been analysed in such a way as to give the distributions in time for each of these parameters. These results are given in the form of histograms and show the frequency of occurrence of each of the stated range of values of the parameter. The data was analysed, first of all, on a monthly basis so that, for each parameter, one histogram was obtained for each month of measurements. The mean values of the parameters were calculated for each month and the total time for which each parameter was measured was also found.

10.2.2 Potential gradient measurements

The analysis of the potential gradient records was limited to those occasions when its value exceeded $\pm 2600 \text{ Vm}^{-1}$, that is $\pm 30\%$ of half-scale on the recorder. Potential gradients greater than these values were divided into ranges of width 875 Vm^{-1} . Thus the total time for which the potential gradient is in each range gives the distribution for the month. The records for each month in turn were analysed giving eleven distributions for October 1967 to August 1968.

10.2.3 Point discharge on the elevated metal point

The records obtained of point discharge currents through the metal point were analysed in the same way as the potential gradient records. In this case, however, all values of the parameter were included in the analysis. The recorded currents were divided into ranges of width $0.17 \mu\text{A}$. Ten distributions of current were obtained for the months of November 1967 to August 1968. However, during this period it has been found that the value of potential gradient at which the point began to discharge was not constant. The table below gives the values of potential gradient at which point discharge on the metal point commenced.

TABLE 10.1

MONTH	POTENTIAL GRADIENT AT ONSET OF DISCHARGE
November	1300 Vm^{-1}
December	1300
January	1750
February	1750
March	1750
April	2600
May	2600
June	2600
July	2600
August	2600

It is thought that the exposure of the point may have changed during the year as a result of modifications made to it.

10.2.4 Point discharge on trees

Analysis of the point discharge currents in the two trees gives the current distribution in the same way as for the metal point. However, in this case the currents are divided into ranges of width $0.05 \mu\text{A}$. The non-linearity of the output from the detectors with point discharge current means that the range of chart values, for each range of $0.05 \mu\text{A}$, varies with the current. Measurements were recorded from one tree on the edge of the plantation for June, July and August, 1968. A second tree inside the plantation gave measurements for half of July and August, 1968. As the periods of measurement for the trees were relatively short, the data was not analysed for each month, but for the period as a whole. Thus, the current distribution for the tree on the edge of the plantation was calculated for June, July and August. The distributions for both trees were found for the last half of July and August so that the results from the two trees can be compared.

10.3 Results for potential gradient and point discharge on the elevated metal point.

10.3.1 Monthly distributions for potential gradient and point discharge.

The distributions for potential gradient for October, 1967 to August 1968 together with the point discharge distributions for November 1967 to August 1968 are shown in Figs. 10.1 to 10.11. It can be seen that for all months except February the duration of negative potential gradients and currents is greater than that for positive values of the parameters. The maximum recorded values of potential gradient are approximately $-11,000 \text{ Vm}^{-1}$ and $+10,000 \text{ Vm}^{-1}$. So that the differences in the results for each months can be seen more clearly, values of the mean potential gradient and point discharge current have been calculated for both signs of current and potential gradient. The mean values for potential gradient together with the total periods of high potential gradient are given in 10.3.3. The purpose of the monthly distributions, apart from giving the mean values, is to give the data necessary for calculating the distributions of potential gradient and point discharge for the total period of ten to eleven months. These distributions are given below in 10.3.2.

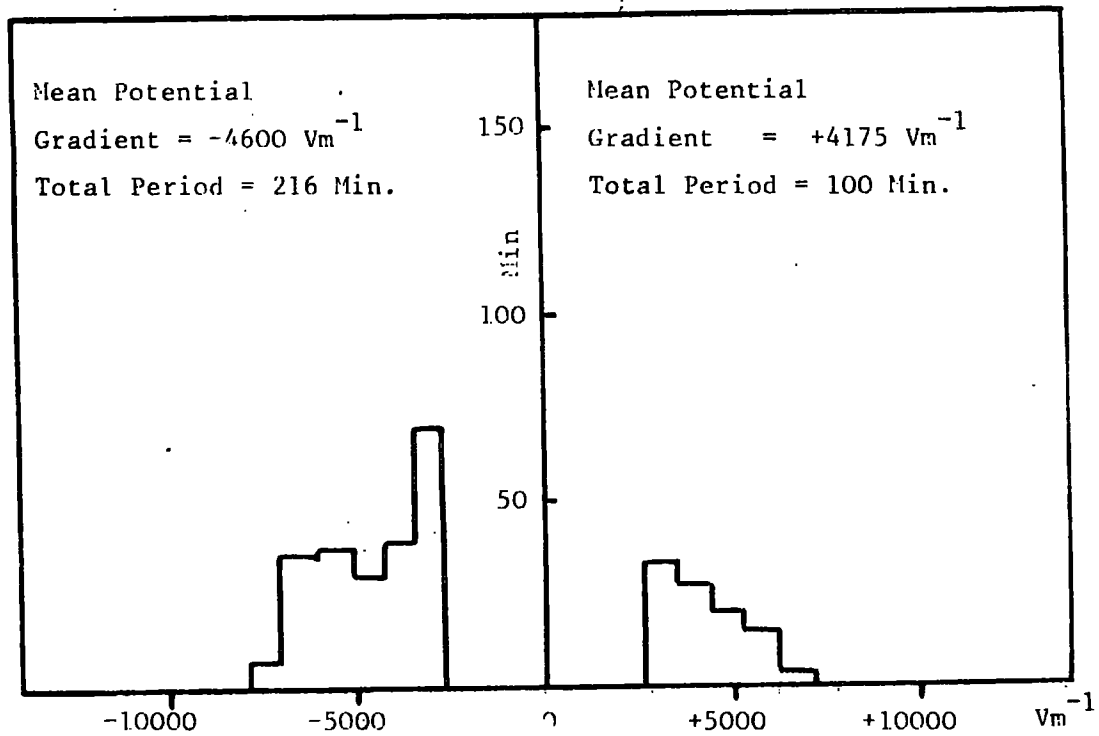


Fig. 10.1 Potential gradient for October 1967

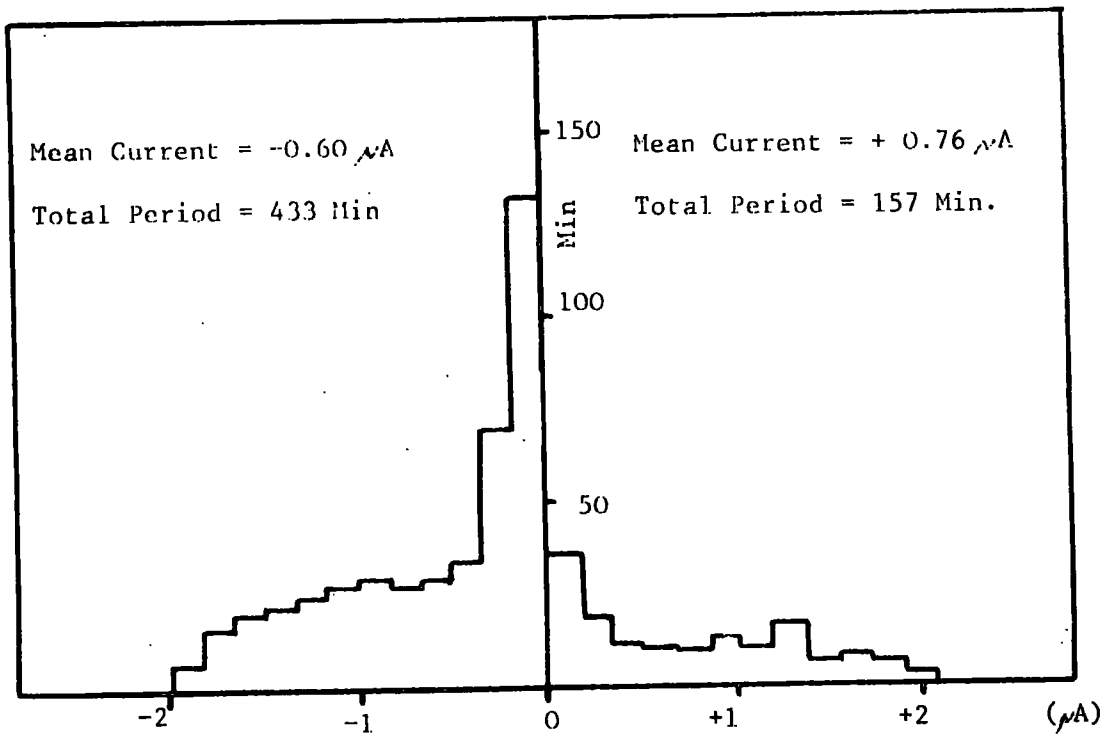
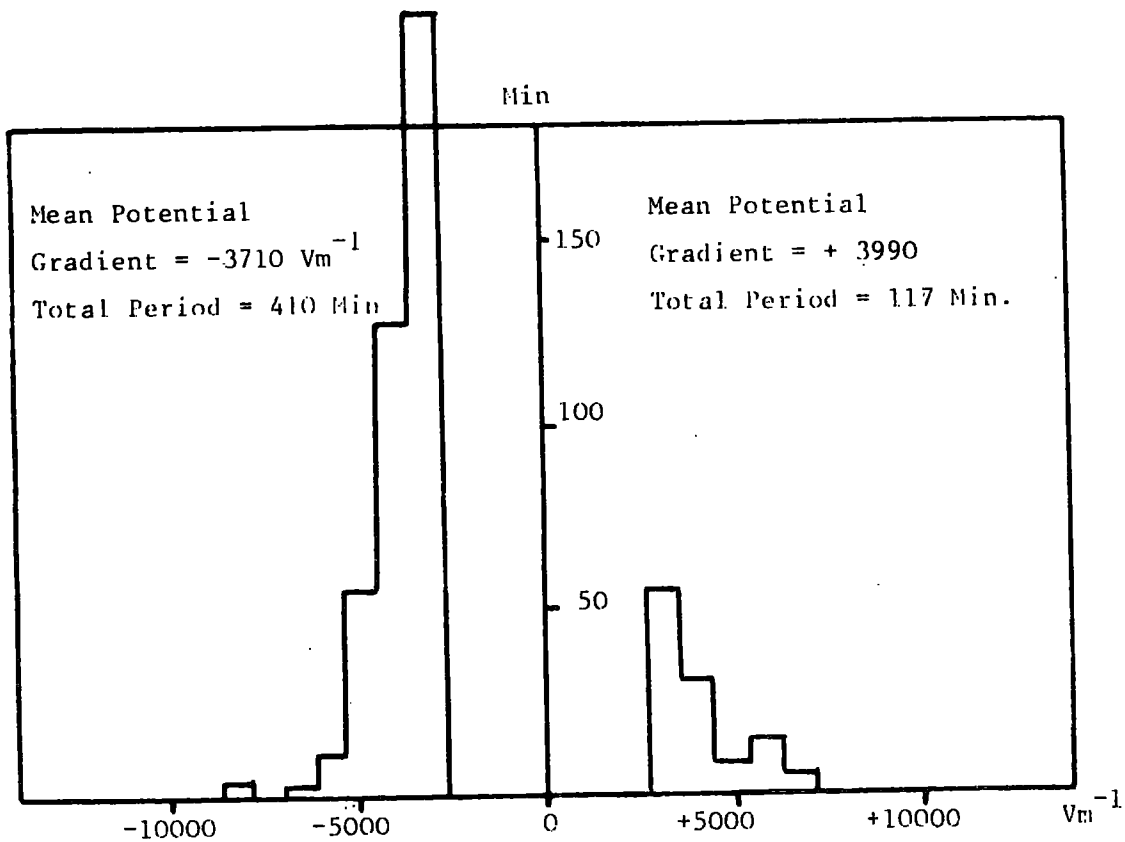


Fig. 10.2 Potential gradient and point discharge on metal point
November, 1967.

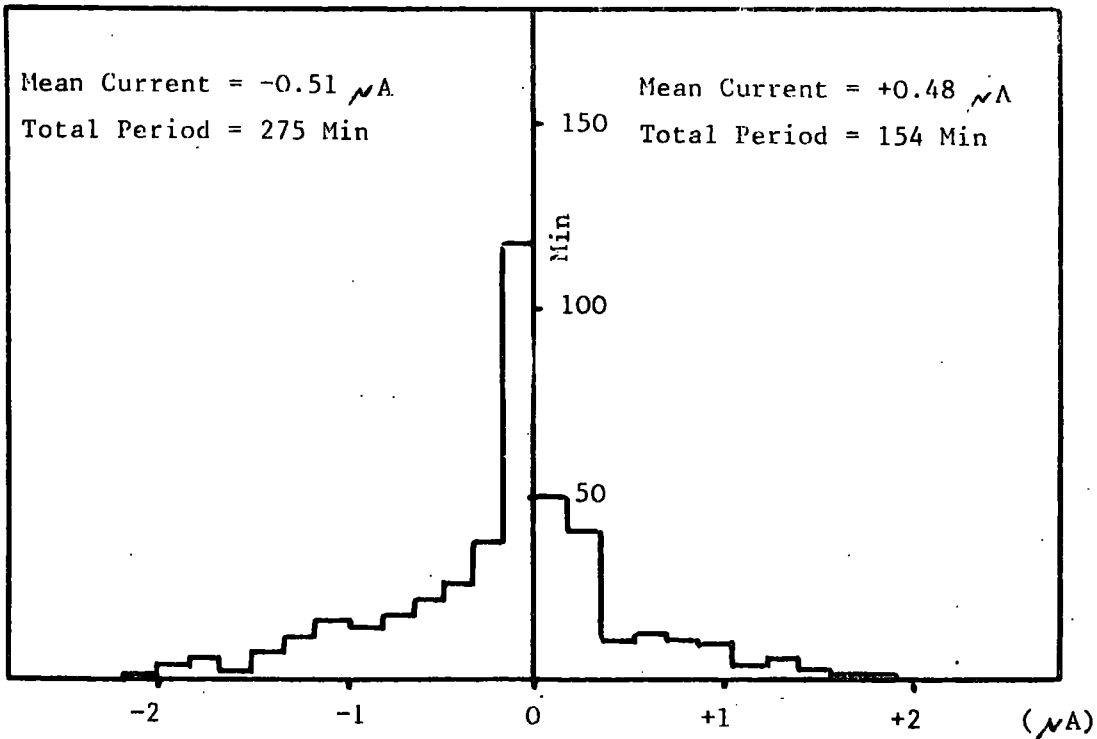
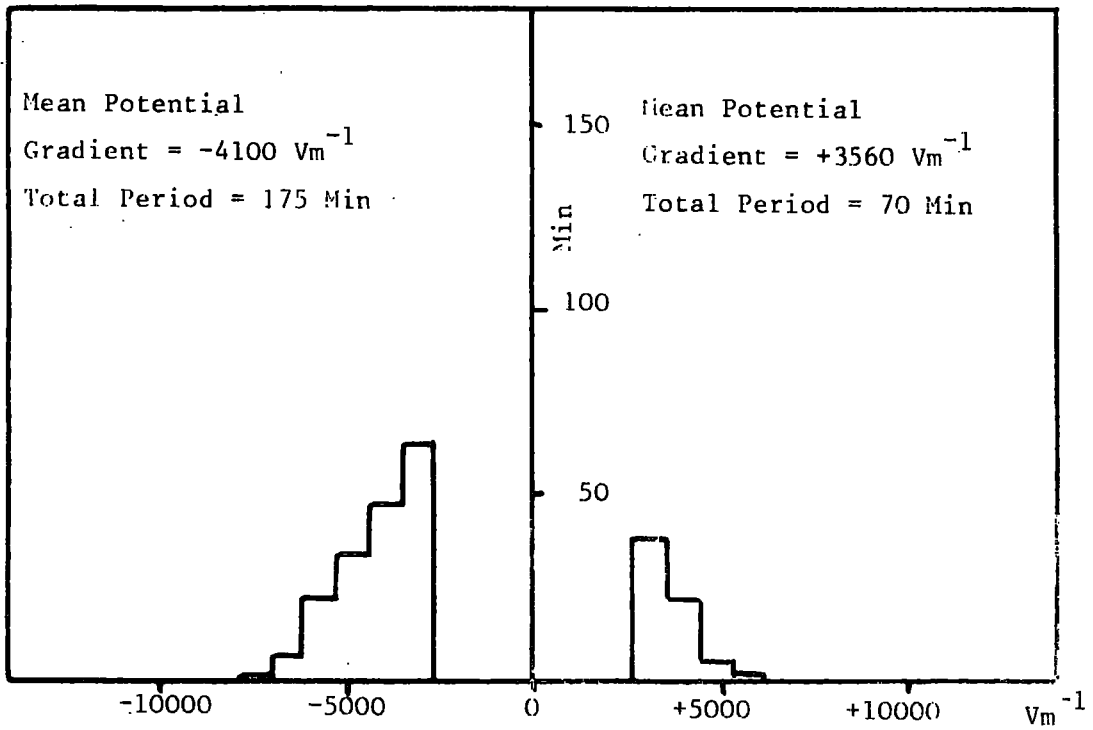


Fig. 10.3 Potential gradient and point discharge on metal point
December, 1967

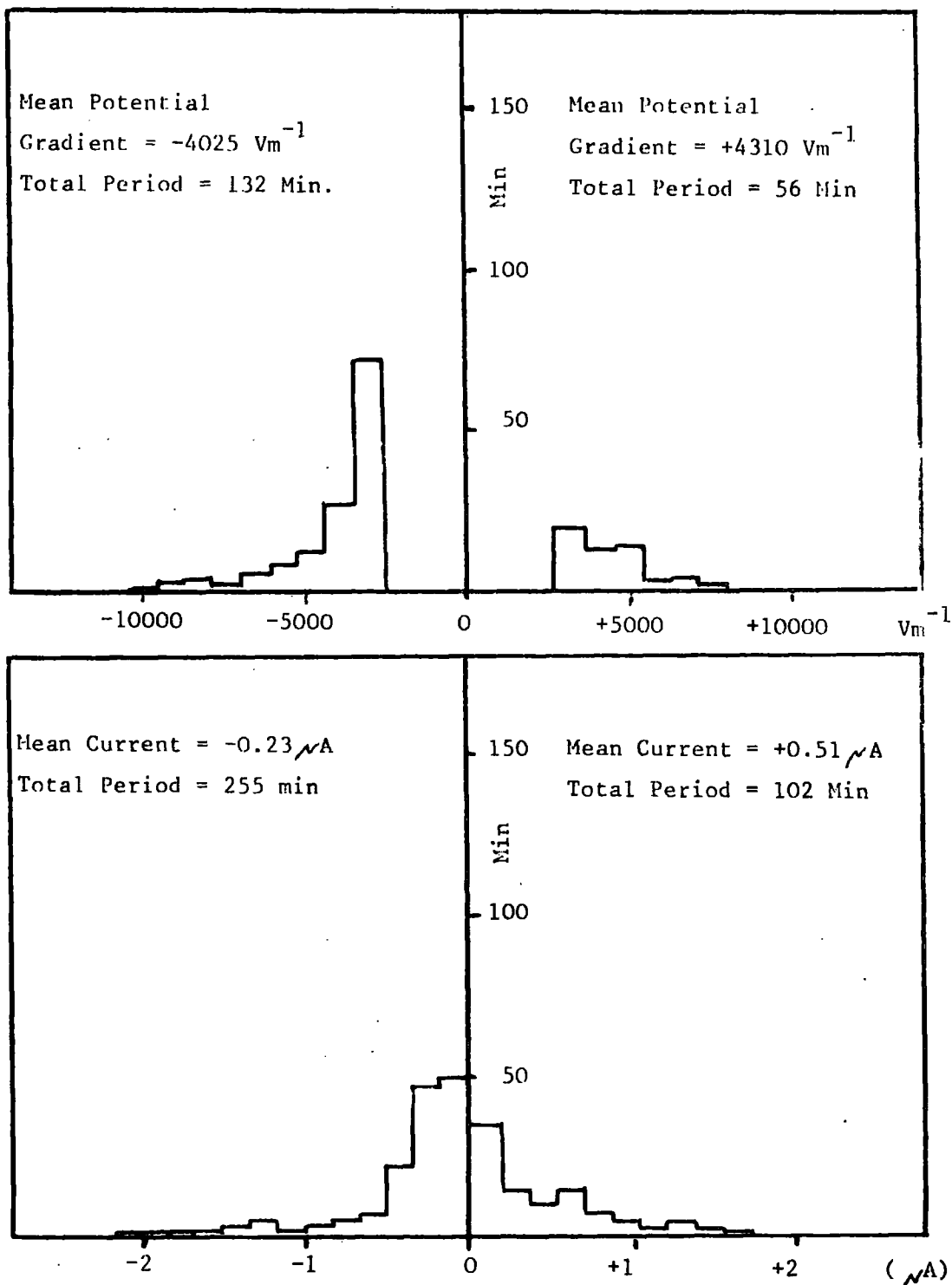


Fig. 10.4. Potential gradient and point discharge on metal point
January, 1968.

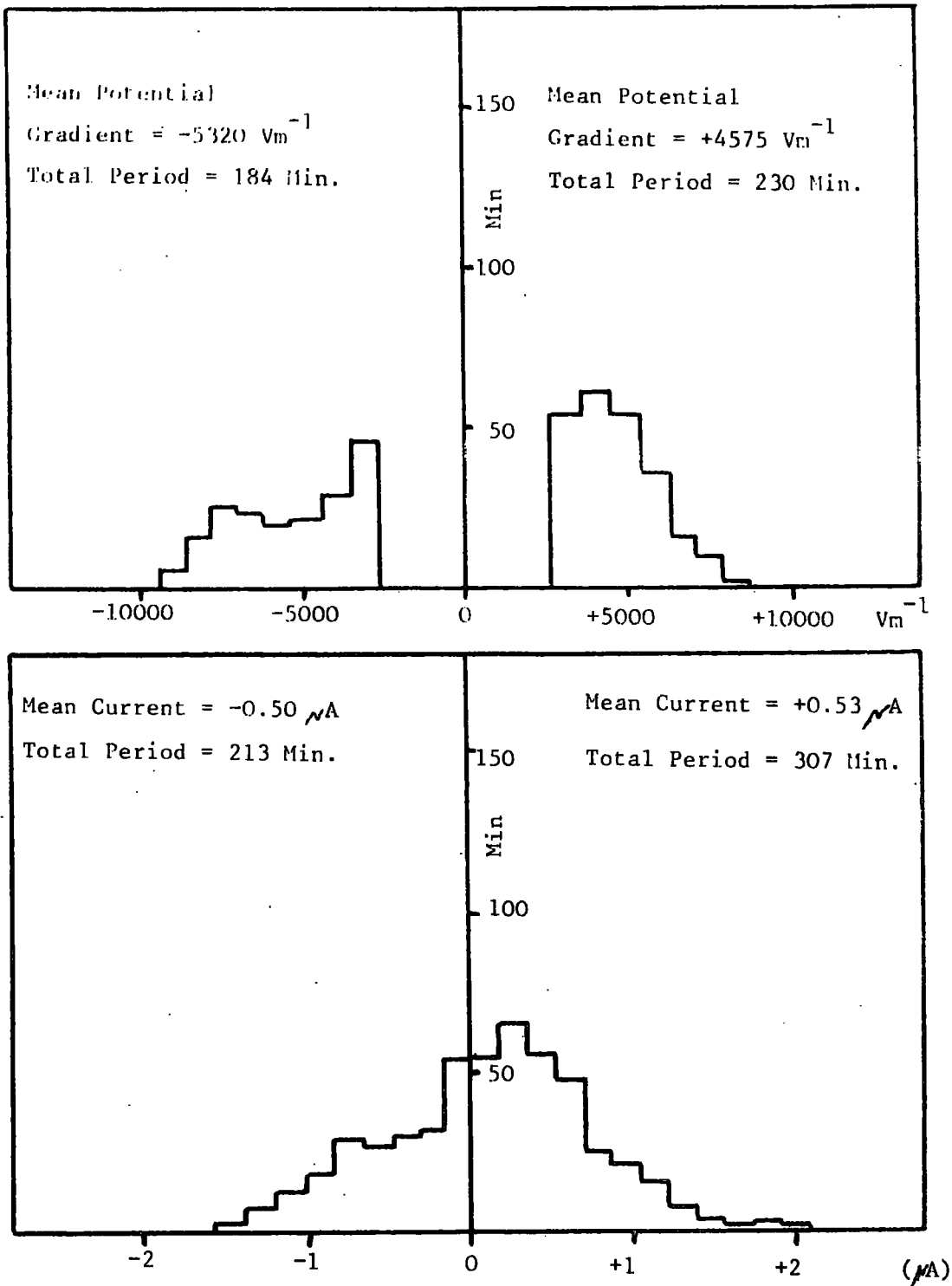


Fig. 10.5 Potential gradient and point discharge on metal point
February, 1968

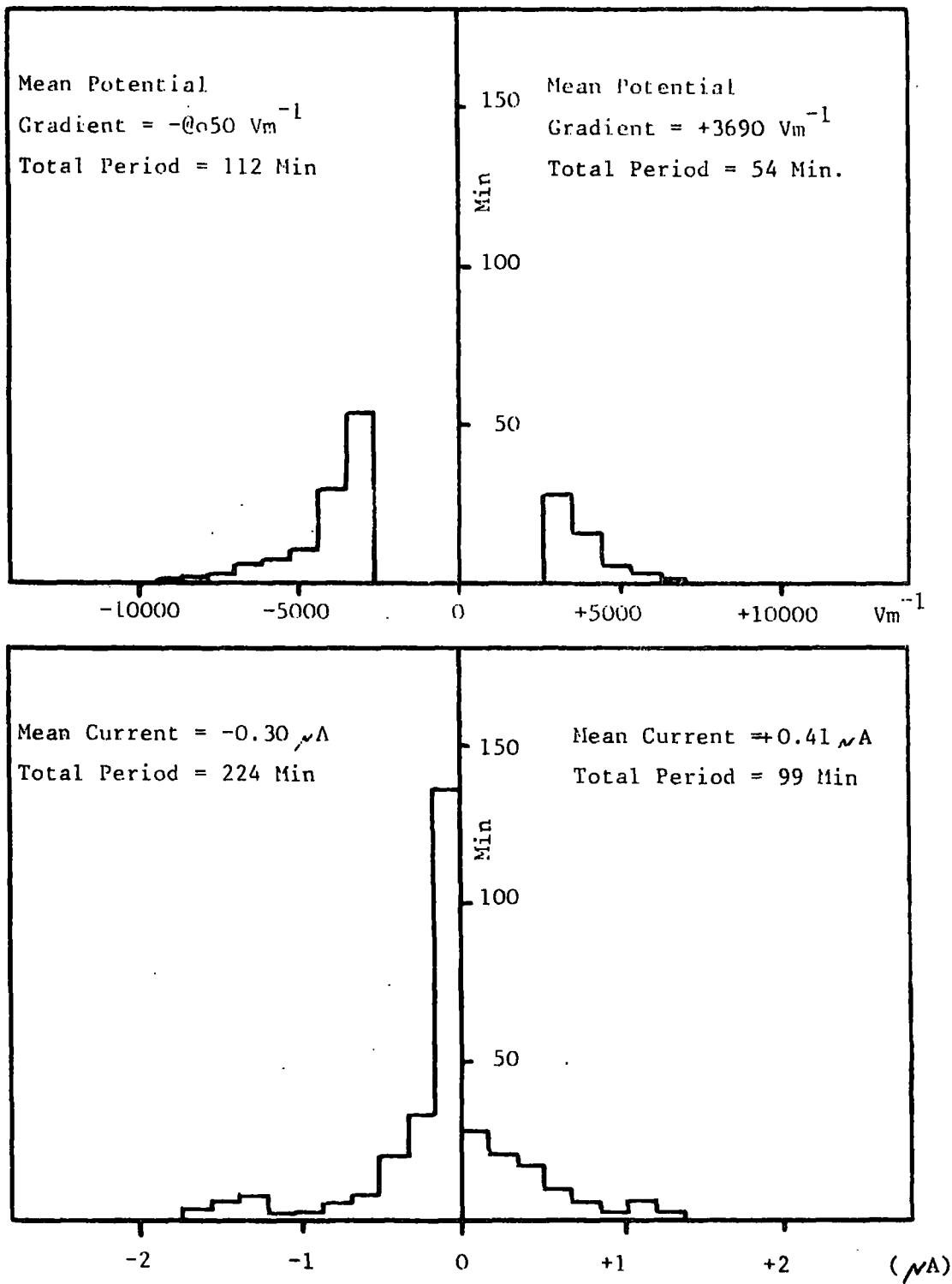


Fig. 10.6 Potential gradient and point discharge on metal point
March, 1968

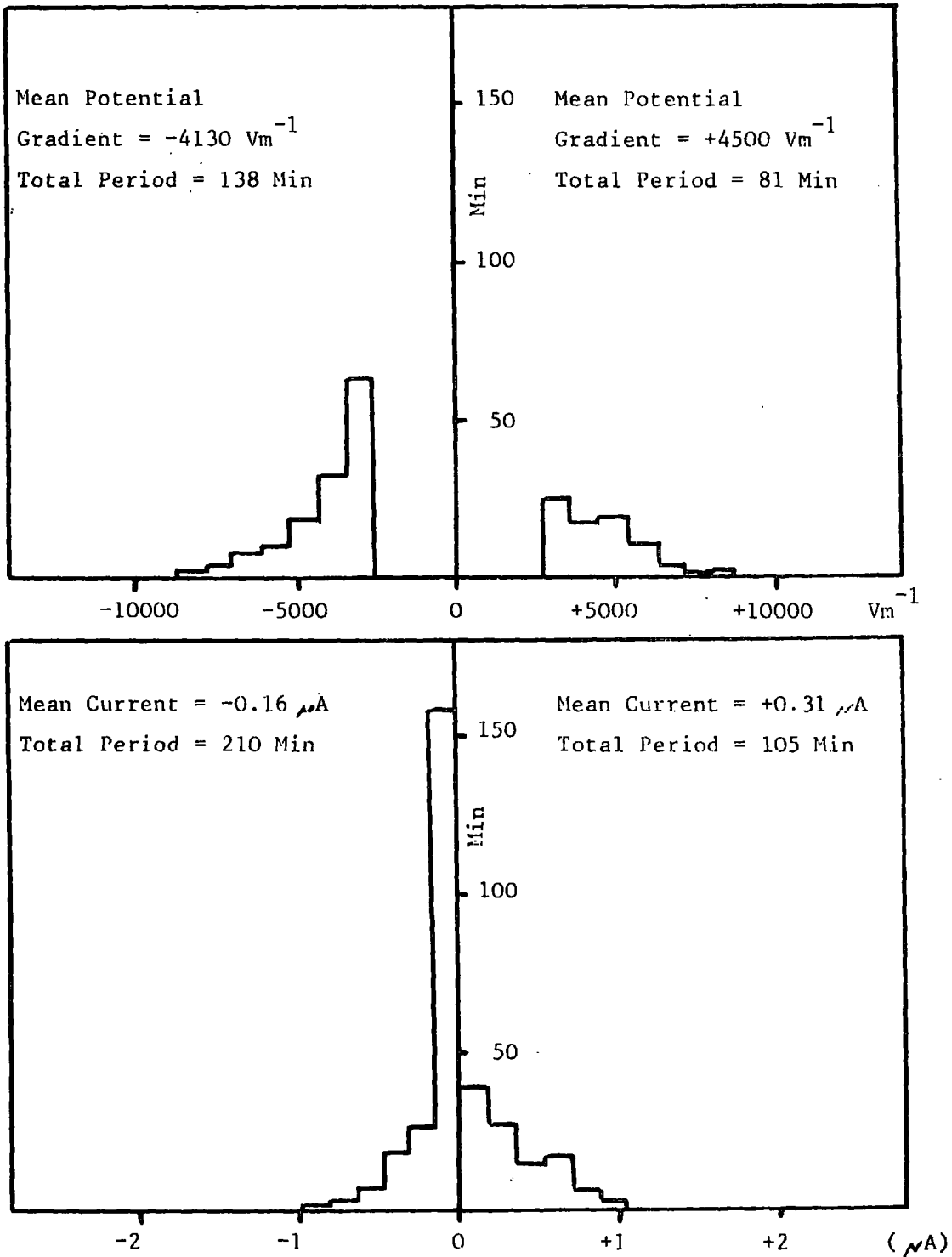


Fig. 10.7 Potential gradient and point discharge on metal point
April, 1968

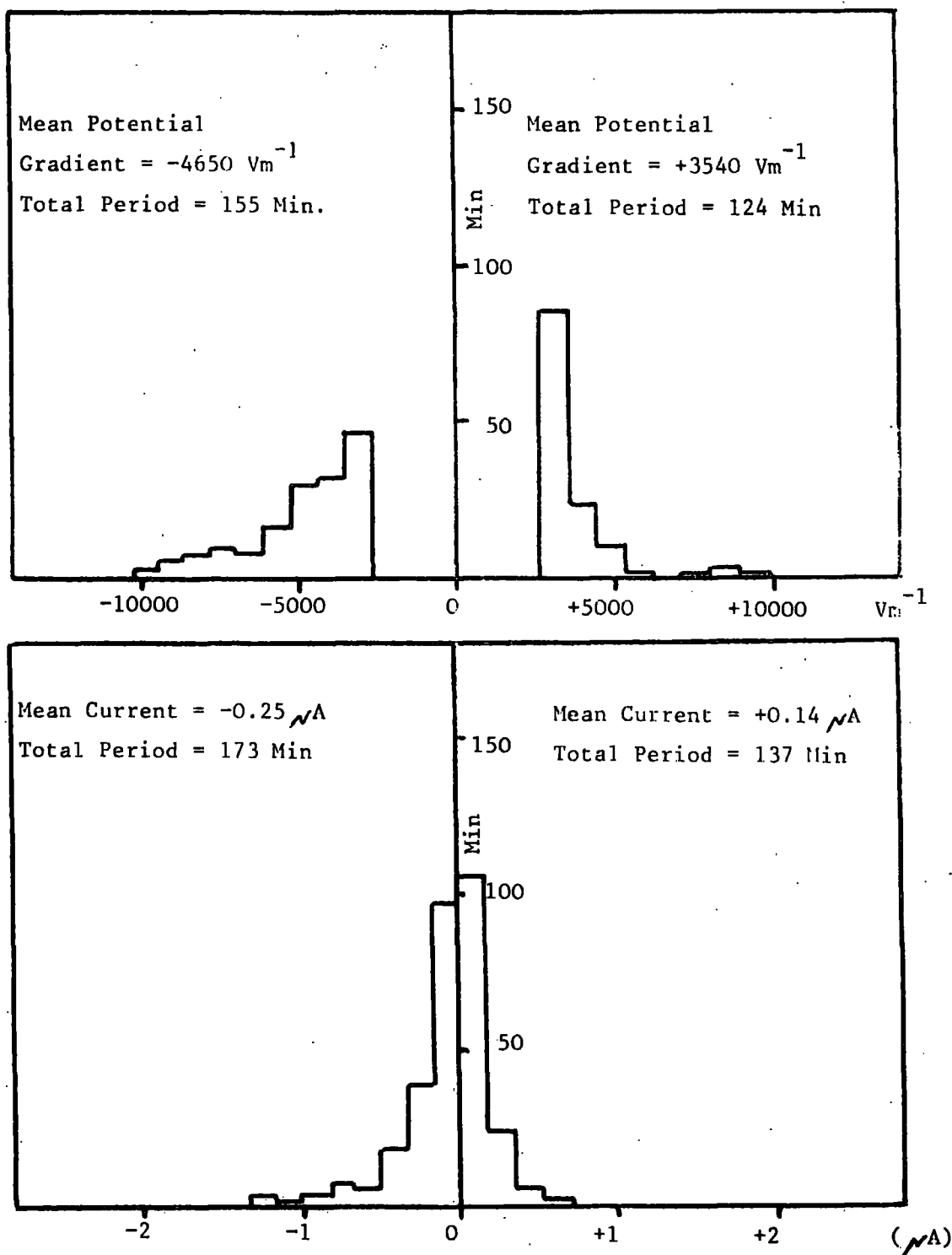


Fig. 10.8 Potential gradient and point discharge on metal point
May, 1968.

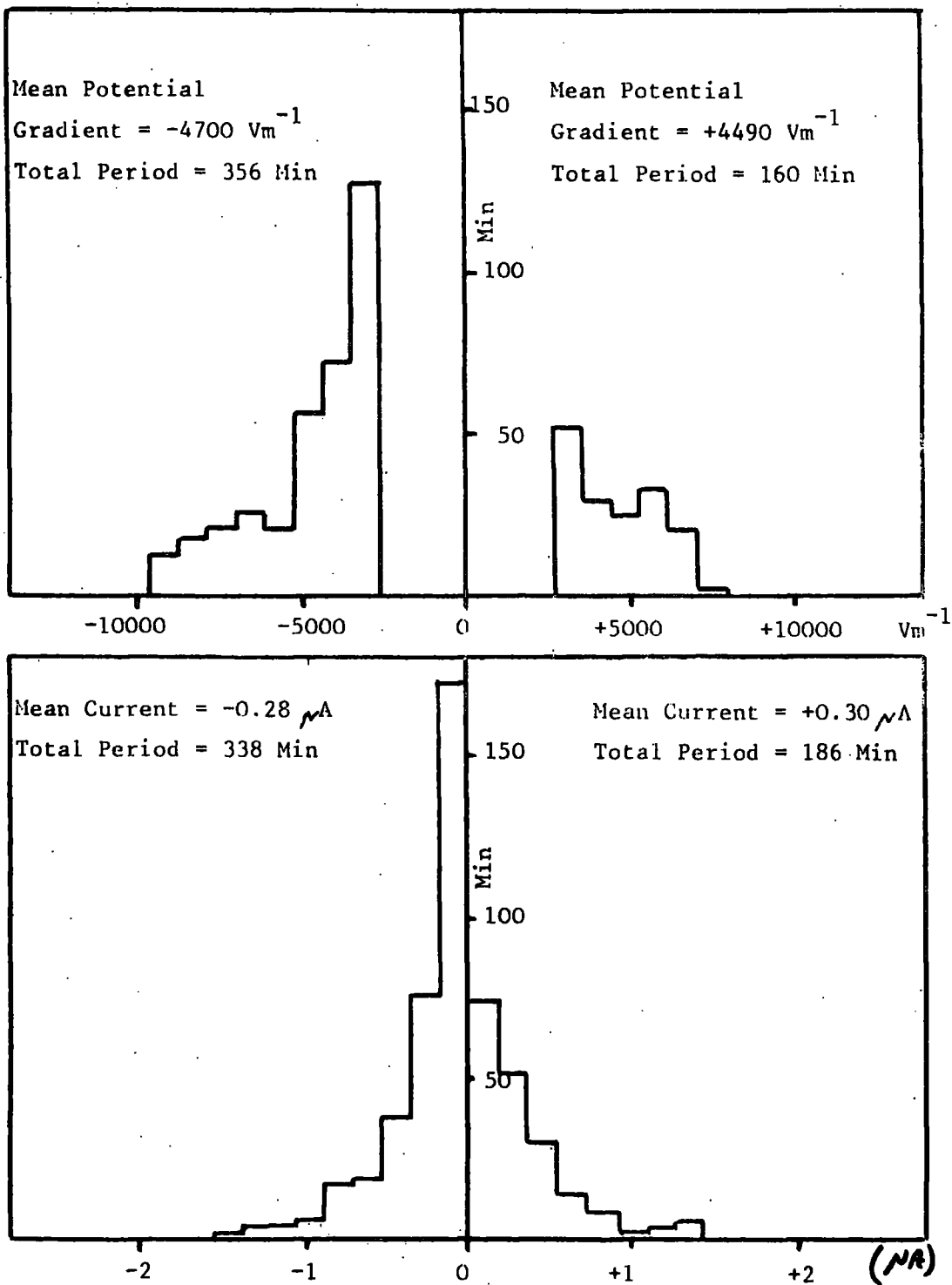


Fig. 10.9 Potential gradient and point discharge on metal point
June, 1968.

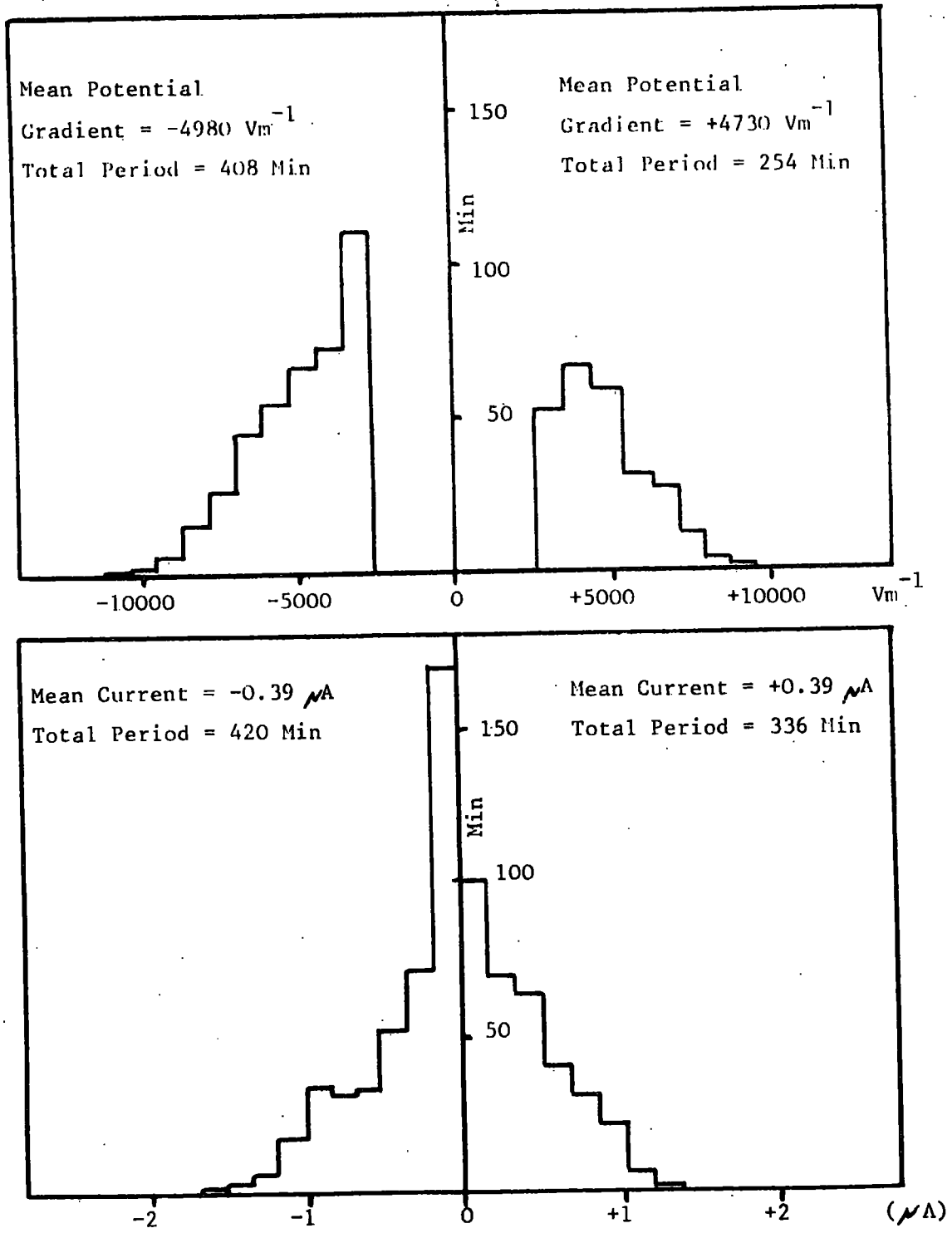


Fig. 10.10. Potential gradient and point discharge on metal point
July, 1968.

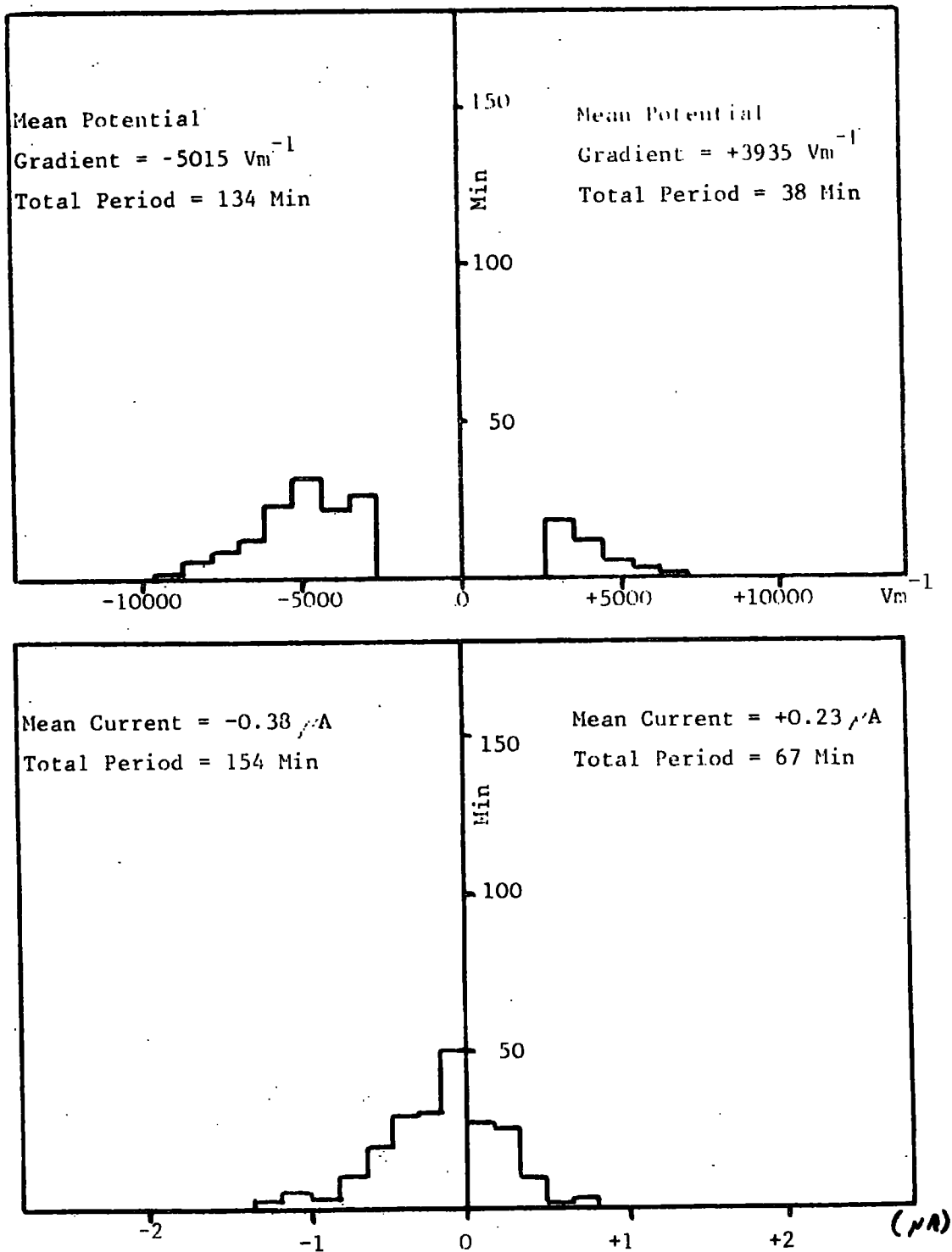


Fig. 10.11. Potential gradient and point discharge on metal point
August, 1968

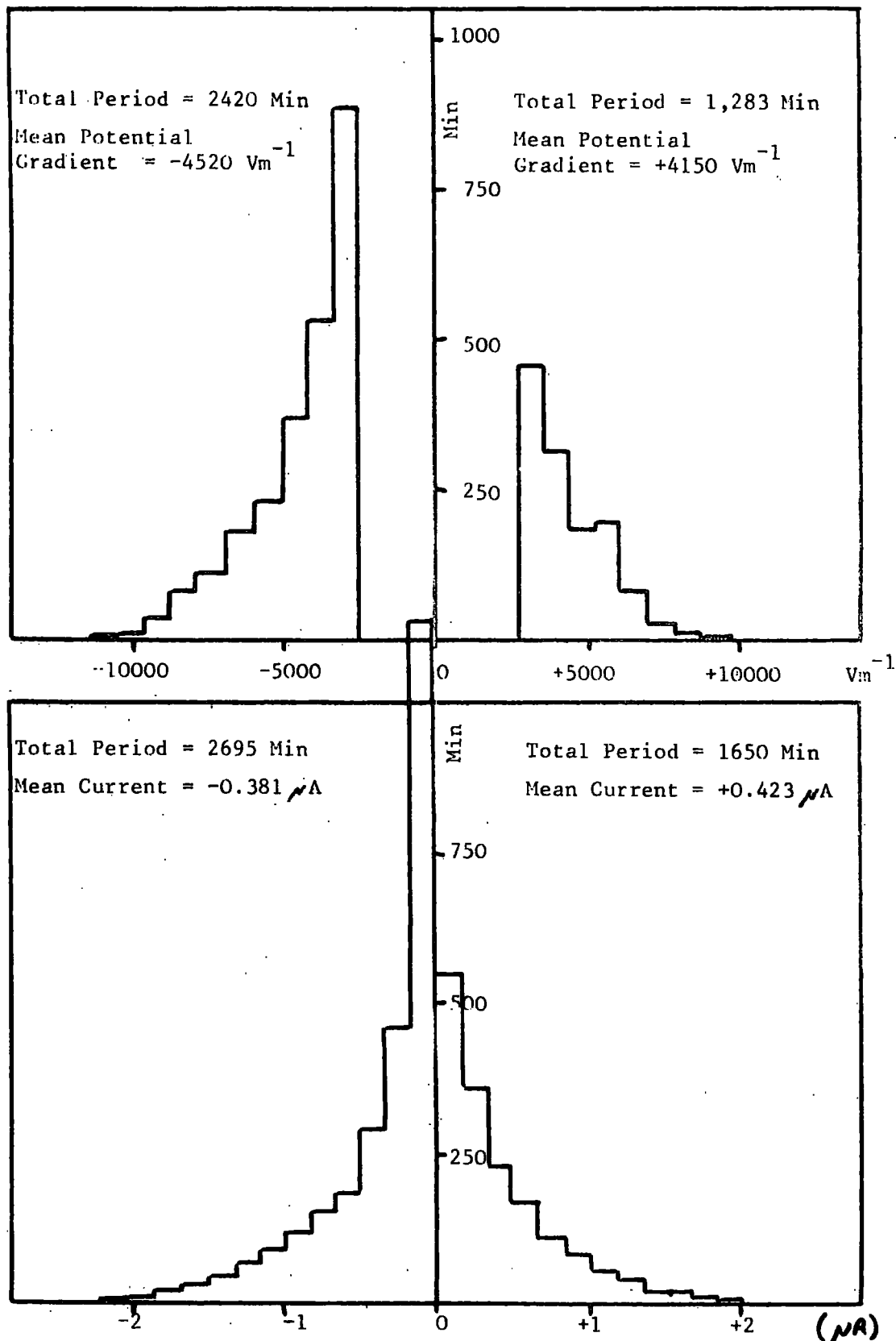


Fig. 10.12. Potential gradient (11 months) and point discharge on metal point (10 months) for October 1967 to August 1968

10.3.2 Potential gradient and point discharge distributions
for the total period.

These distributions are shown in Fig. 10.12. The distribution for potential gradient shows the durations of positive and negative potential gradients. In fact the potential gradient was negative for about 40 hours and positive for about 20 hours. The mean potential gradients are -4520 Vm^{-1} and $+4150 \text{ Vm}^{-1}$. It should be explained here that these are the mean values for potential gradients in excess of $\pm 2600 \text{ Vm}^{-1}$. The distribution for the point discharge currents through the metal point shows the greater prevalence of negative currents. The mean values of $-0.38 \mu\text{A}$ and $+0.42 \mu\text{A}$ are of similar magnitudes but it is the duration of these currents which differ greatly. If the total positive and negative charges brought to earth are calculated the values obtained for the ten-month period are -0.062 C and $+0.042 \text{ C}$. Thus the net charge transfer is -0.02 C , and the ratio of negative to positive charge transferred is 1.48. The value of -0.02 C for the total charge transfer, is low compared with the values found by WORMELL (1930) and WHIPPLE and SCRASE (1936). However, this difference is probably caused by the use of a point only 4m in height and one situated in a clearing on the edge of

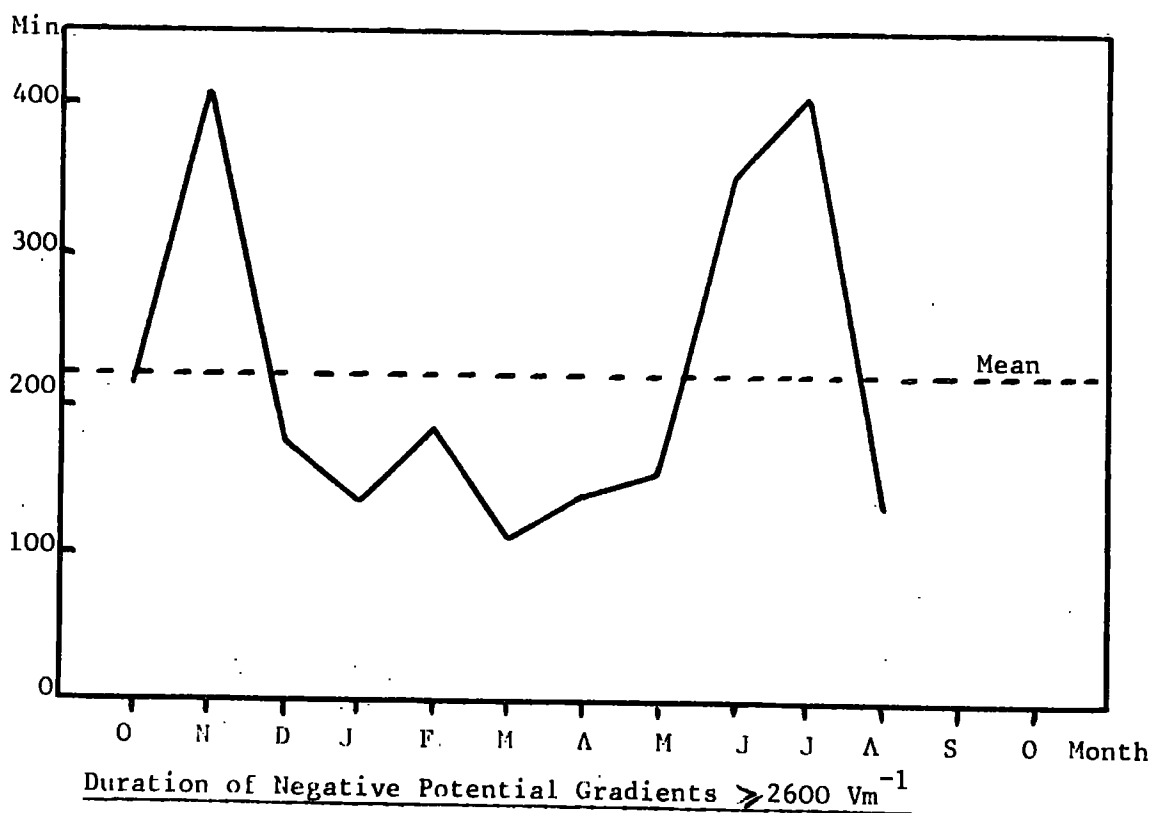
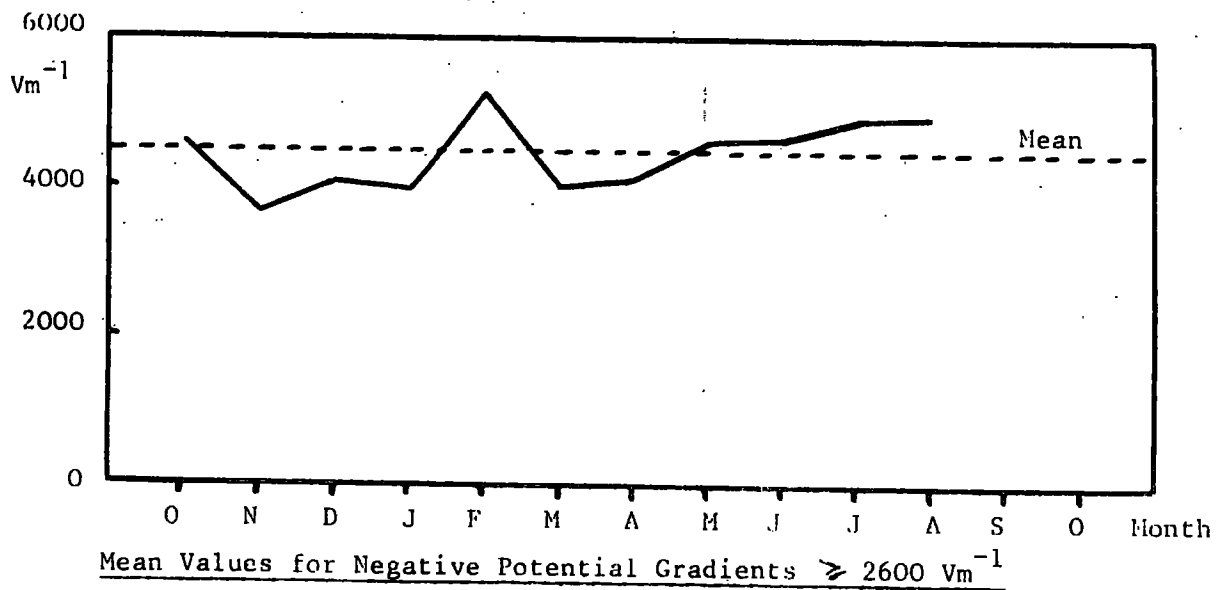
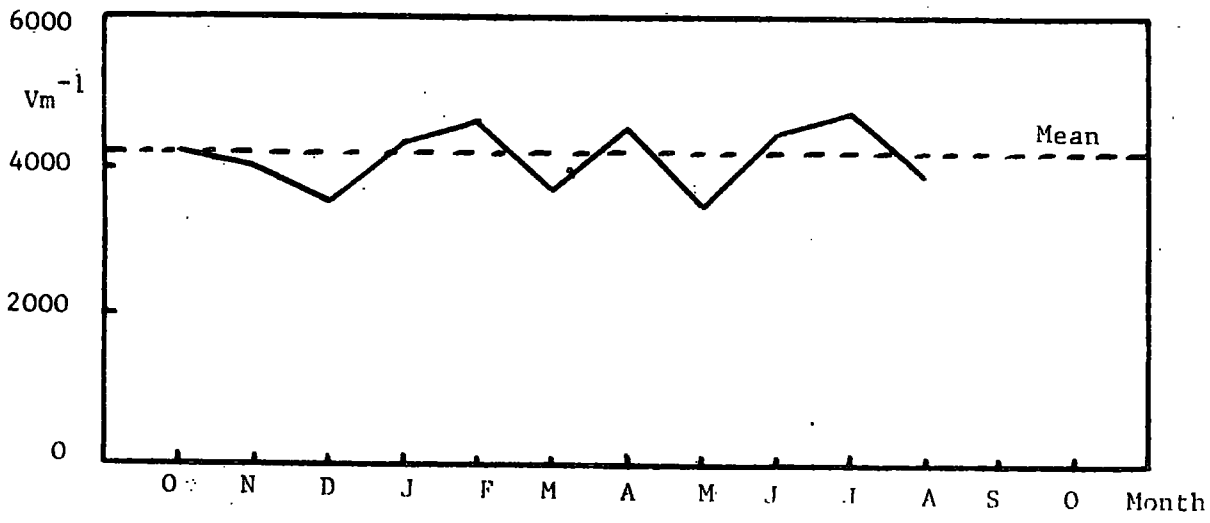
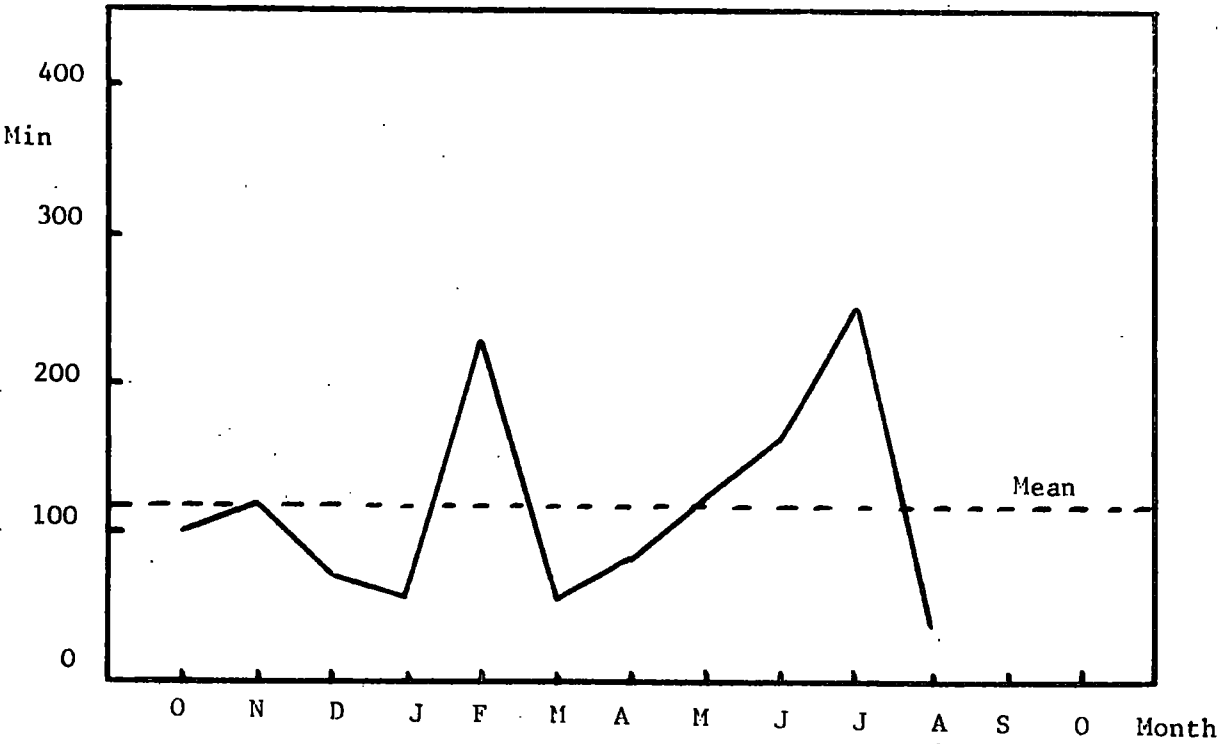


Fig. 10.13.



Mean Values for Positive Potential Gradients $\geq 2600 \text{ Vm}^{-1}$



Duration of Positive Potential Gradients $\geq 2600 \text{ Vm}^{-1}$

Fig. 10.14.

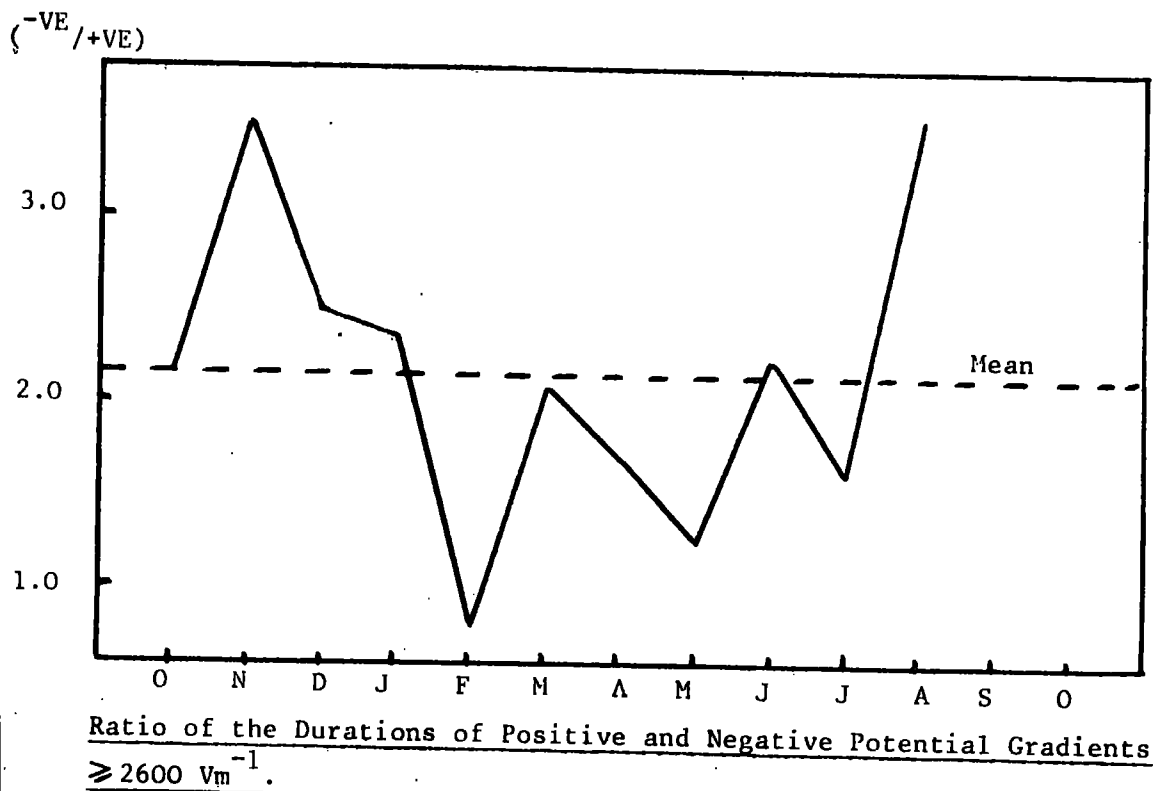
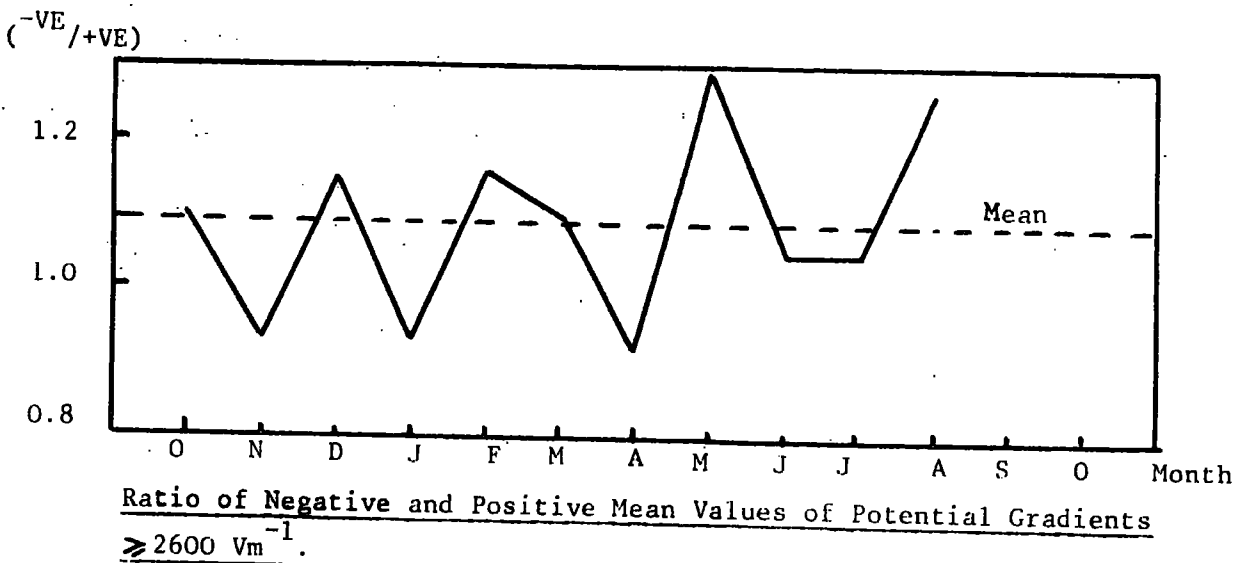


Fig. 10.15

the plantation. The ratio of negative to positive charge, found here to be 1.48, is similar to the values found by WORMELL (1930) and CHALMERS and LITTLE (1947).

10.3.3 The duration and mean values of the potential gradient

As the exposure of the metal point was found to have varied during the year, mean values of point discharge current cannot be compared. However, the variations of mean potential gradients and the durations of the potential gradients for each month are shown in Figs. 10.13 and 10.14. From these diagrams it can be seen that the highest mean values of both positive and negative potential gradients occurred in February and July. The months which had the longest periods of high negative potential gradients were November and July. The longest periods of positive potential gradient occurred in February and July. Fig. 10.15 shows the ratios of the mean values of positive and negative potential gradients and also the ratios of the corresponding durations.

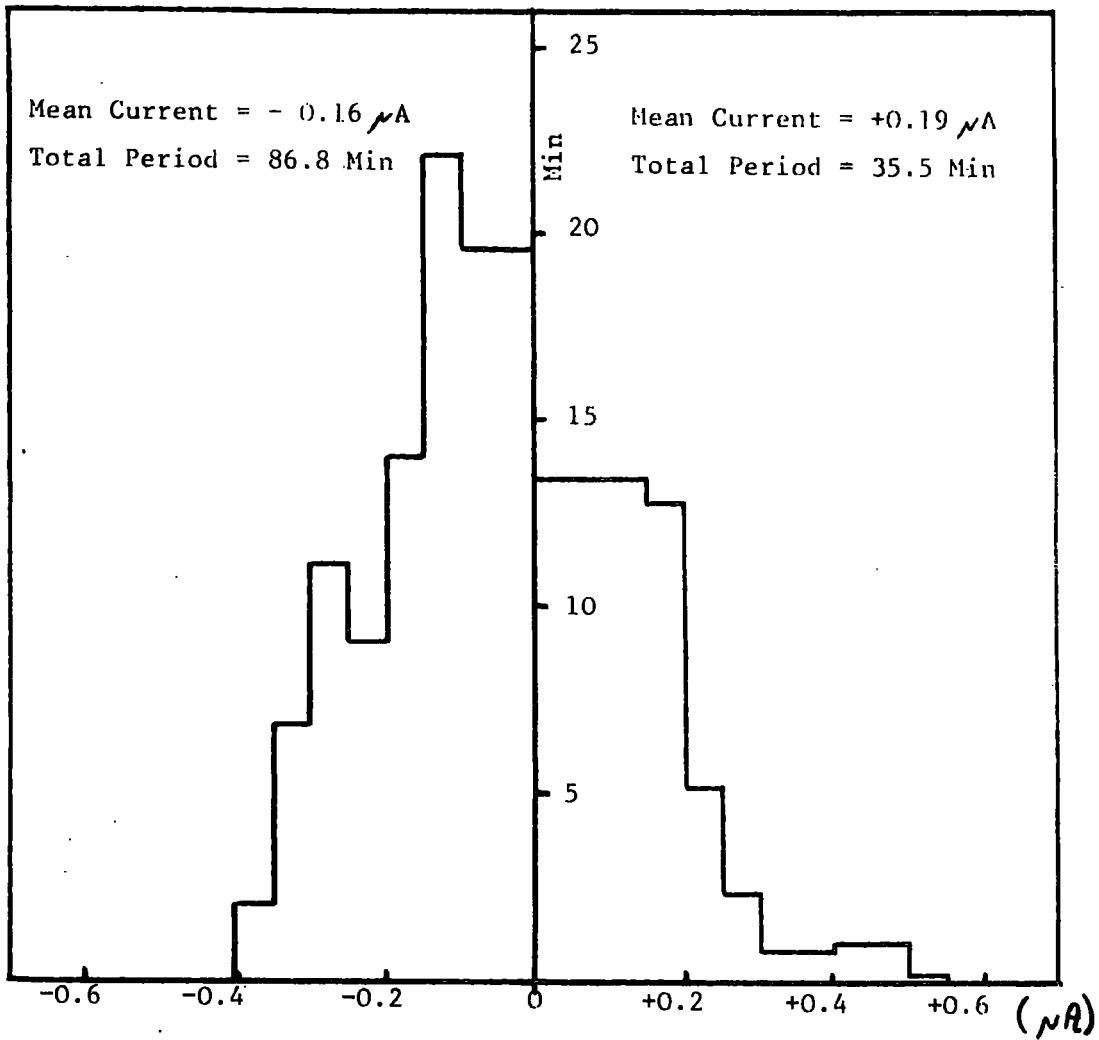


Fig. 10.16 Point discharge currents for a tree on the edge of Plantation during June, July and August, 1968.

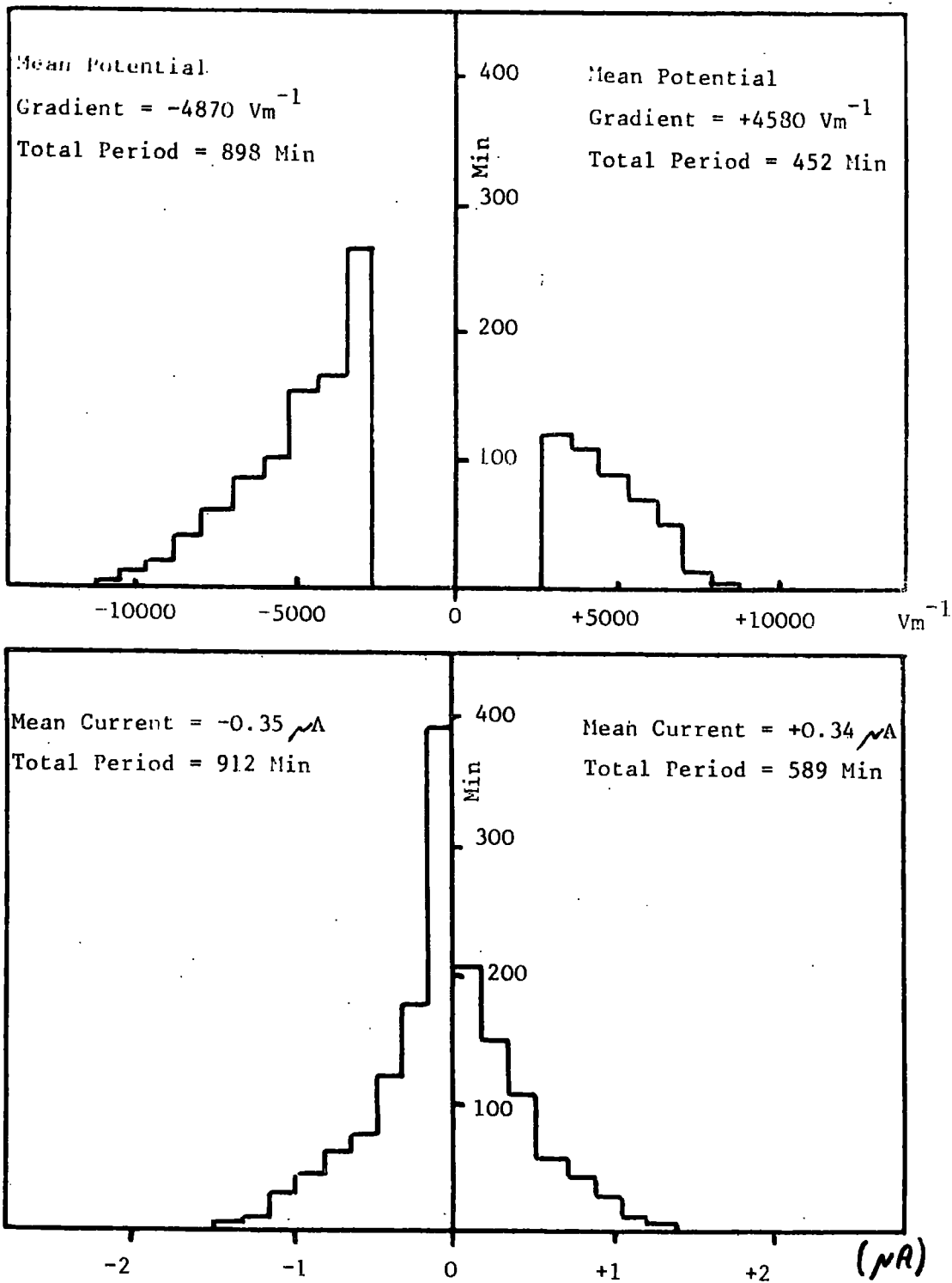


Fig. 10.17. Potential gradient and point discharge on metal point for June, July and August, 1968.

10.4 Results for point discharge on trees

10.4.1 A single tree on the edge of the plantation.

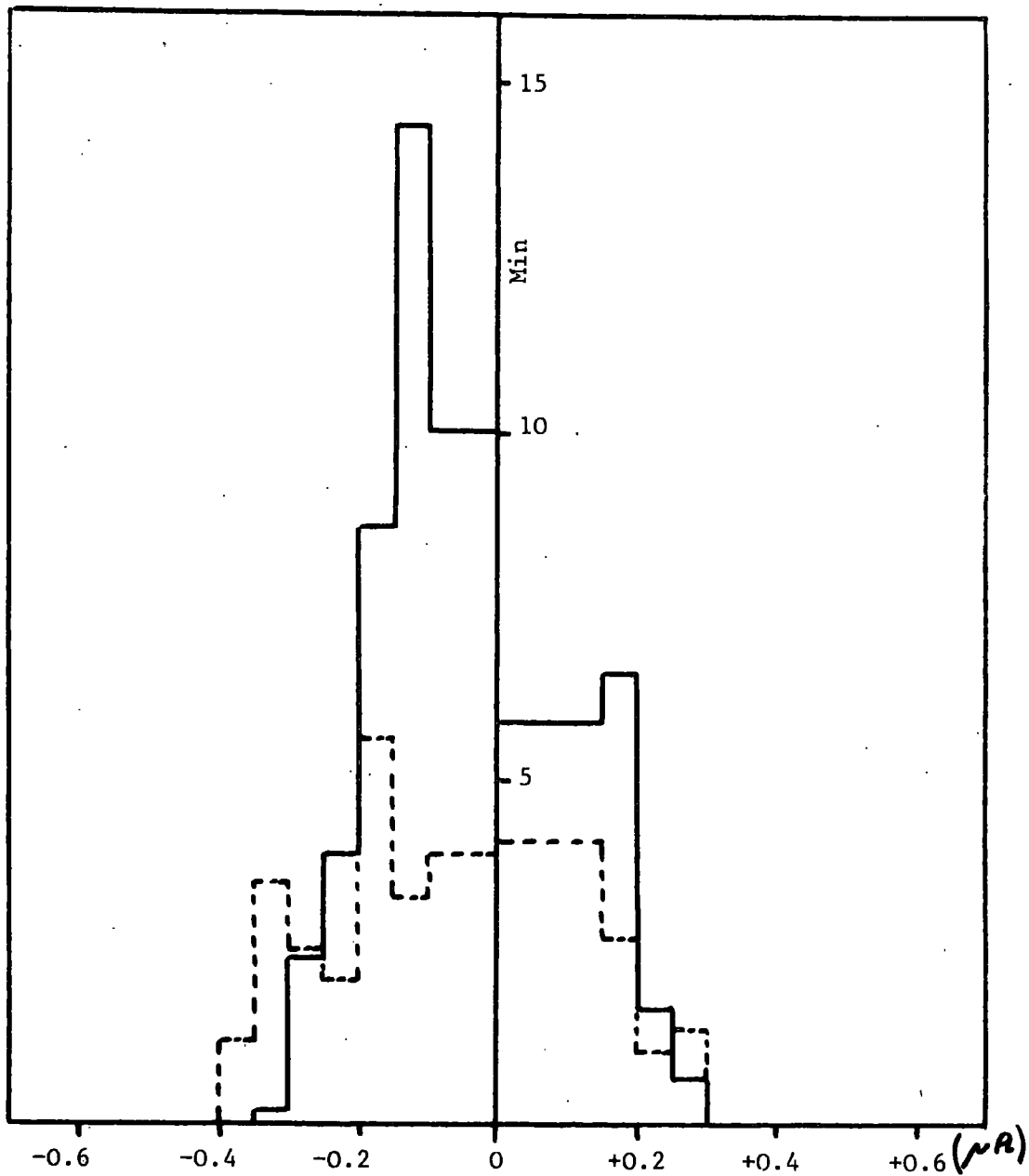
Fig. 10.16 shows the distribution for the point discharge currents in the tree during June, July and August, 1968. For comparison the potential gradient and metal point current distributions for this period are shown in Fig. 10.17. It can be seen that the mean currents for the tree are about half those for the metal point. However, the most striking difference is in the periods of point discharge. The total duration of point discharge on the tree is only about one tenth of the corresponding duration for the metal point. To make a more exact comparison between the tree and the point the relevant quantities are shown in Table 10.2 overleaf.

TABLE 10.2

Comparison between point discharge currents through the metal point and the tree on the edge of the plantation for June, July and August,

1968

	METAL POINT		TREE	
	Positive	Negative	Positive	Negative
Mean current μA	0.34	-0.35	0.19	-0.16
Total duration of current, min.	589	912	36	87
Total charge, $\text{C} \times 10^{-4}$	120	-190	4.05	-8.3
Net charge transferred in 3 months, μC	-7,200		-430	
Ratio of negative to positive charge transferred.	1.60		2.06	



— Tree inside plantation
 - - - Tree at edge of plantation

Fig. 10.18. Point discharge currents in two trees during July and August, 1968

10.4.2 Point discharge on a tree inside the plantation.

Measurements of the point discharge currents in a tree inside the plantation were made for a period of one and a half months from the middle of July, 1968. The results are shown in Fig. 10.18. The distribution drawn in dotted lines is the current distribution for the tree at the edge of the plantation during the same period. Both the trees are similar in height to those immediately adjacent to them and certainly no higher. The tree at the edge of the plantation is 17m in height. The tree inside the plantation is 21.5m in height.

Table 10 3, overleaf, shows the relevant quantities for comparison for the two trees. It is surprising that there was more point discharge on the tree inside the plantation. However, it can be seen that the net charge transfer is 30% greater than the value for the tree at the edge of the plantation.

Comparison between point discharge currents through the tree on
the edge and the tree inside the plantation for part of July
and the whole of August, 1968.

	TREE AT EDGE		TREE INSIDE	
	Positive	Negative	Positive	Negative
Mean current μA	0.15	-0.18	0.15	-0.14
Total duration of current, min.	9.3	22.1	14.7	39.5
Total charge $\text{C} \times 10^{-4}$	0.84	-2.40	1.32	-3.32
Net charge transferred in $1\frac{1}{2}$ months, μC	-155		-200	
Ratio of negative to positive charge transferred	2.86		2.52	

10.5 Signals other than point discharge pulses received by the trees.

It was mentioned in Chapter 9 that the noise level in the final form of the detector is about 3% of full-scale deflection on the recorder. For the majority of the time the noise is constant at this level. This noise is caused by B.B.C's Radios 2 and 4. When the transmitters for these stations are switched off, the noise level measured falls practically to zero. Thus a useful time check is obtained late at night and early in the morning by looking for step changes amounting to about 3% of full-scale, in the otherwise steady record.

A second form of noise which occurred only at night was identified as atmospheric noise. Particularly on nights with clear skies the recorded noise level would begin to increase from its steady value of 3% at about dusk. By midnight it could be as high as 50% of full-scale. As daybreak approached, the noise level would decrease to its steady values of 0 or 3%. The shape of the pulses from the tree during these periods of noise and their repetition frequencies were observed one night on an oscilloscope. The pulses often occurred in short bursts which gradually died away and the pulse repetition rate was typically

in the range 10 - 75 kHz. From these observations it was concluded that the noise increase was almost certainly caused by atmospherics. A full description of atmospherics and their characteristics is given in MALAN (1963). As a result of the higher noise level occurring on some nights, a small proportion of the measurements made in high potential gradients could not be analysed to give the current in the trees.

The only other form of noise that is known to affect the detector is caused by a close lightning discharge. At the instant of a flash the recorded output from the tree detector increases by about 50% of full-scale in a negative direction. These deviations are very short and can therefore be easily recognised.

CHAPTER 11Discussion of the results of the Lanehead Field experiment11.1 The techniques of measurement of natural point discharge.

Various methods have, in the past, been tried for measuring natural point discharge currents in trees. The discussion below shows that all these methods have severe limitations and that these are overcome or avoided in the present work to give what is thought to be the first reliable measurements of natural point discharge on trees. Before proceeding with this discussion, a brief summary of the techniques, which have been used for measuring point discharge on trees at Lanehead, may be useful. These measurements rely on the fact that point discharge currents in trees flow as a series of pulses. Positive currents flow as positive pulses and negative currents as negative pulses. These are detected in the tree as voltage pulses using a capacitative electrode close to the end of the discharging branch. The pulses are subsequently amplified and their sign, amplitude and repetition frequency give a measure of the current. Two ~~two~~ trees which have been instrumented in this way are part of a plantation of conifers at Lanehead. One tree is on the edge of the plantation and the other is inside. The trees are all of uniform height. The potential gradient and point discharge current are measured outside the plantation.

In general, the limitations of previous methods of measurement of point discharge have been caused either by the use of indirect methods of detection of the currents or by trying to detect the currents in the tree at too great a distance from their source. MAUND and CHALMERS (1960) attempted, with little success, to estimate point discharge currents in trees from measurements of potential gradient at the ground both upwind and downwind of the trees. The difference between the potential gradients resulting from the space charge produced at these two points should give a measure of any point discharge on the trees. They found that there was probably no point discharge on a 12 m high sycamore tree in leaf in potential gradients up to 7000 Vm^{-1} . MAUND and CHALMERS concluded that if there was any current it was certainly less than $1 \mu\text{A}$. MILNER and CHALMERS (1961) compared the observed currents from a metal point in the top branches of a 15 m high tree with currents from by-passing electrodes in a similar tree nearby. The current from the tree was observed to be about only one tenth of the point current. The threshold value of potential gradient at which discharge on the tree commenced was found to be about 1000 Vm^{-1} . However, point discharge was observed on only one isolated occasion. Also, it is known that electrochemical action

between the electrode and tree can give spurious currents which vary with the state of the tree. ETTE (1966) and JHAWAR and CHALMERS (1967) have shown that this method using electrodes does not measure the total current down the tree. ETTE (1966) showed that, in periods of rapidly changing potential gradient of the order of $500 \text{ Vm}^{-1} \text{ s}^{-1}$, such as might occur in a thunderstorm, the resulting displacement current in a tree can be of the same order as the point discharge current. CHALMERS (1962), using the metal point and electrode system of MILNER and CHALMERS (1961) observed the currents in the point and tree during a thunderstorm. He found that, whereas the metal point current closely followed the potential gradient measured at the ground nearby, the current in the tree showed a completely different behaviour. It was concluded by CHALMERS that the results could be explained if the tree behaved as a resistance-capacitance element with a time constant of about 90s. In view of the theoretical predictions of ETTE (1966) it is probable that the large peaks in the observed tree current, which coincided with lightning flashes, were caused in part by displacement currents in the tree.

In the present work, the method used for the measurement of point discharge currents in trees does not suffer from any of the above limitations. The currents are detected, close to their source, by a direct method. The electrode used, being a capacitative link only, does not give spurious currents due to electrochemical action at the tree-electrode interface. Finally, any displacement currents in the trees, caused by rapid field charges, are not detected by the measuring system as this is only sensitive to pulses with rise-times as short as those of point discharge pulses.

In the past, for lack of a better method, most estimates for the amount of point discharge on natural objects such as trees in a given area have been derived from measurements of point discharge on elevated metal points. The first estimates for charge transfer in the atmosphere due to point discharge were made by WORMELL (1930), WHIPPLE and SCRASE (1936) and later by LUTZ (1944) and CHALMERS and LITTLE (1947). In all this work, currents in the metal point were converted to a current density over the surrounding area by assuming a value for the effective separation of similar points in the area. The necessity for making this last assumption imposes a severe limitation on the reliability of these

estimates because the effective separation of points cannot be found in practice (see CHALMERS (1943)). The difference in behaviour between metal points and trees in high potential gradients was first observed by MILNER and CHALMERS (1961) and CHALMERS (1962). JHAWAR and CHALMERS (1967) showed that for a small tree in artificial potential gradients, the relation between point discharge current and potential gradient is a cube law, whereas for a metal point the relation is a square law. In order that the differences in behaviour of trees and metal points could be compared under natural conditions, point discharge measurements from a metal point were included in the Lanehead field experiment and a discussion of these measurements is now given.

The measurements of point discharge on the tree at the edge of the plantation and on the metal point outside the plantation over a 3 month period are shown in Figs. 10.16 and 10.17. A summary is given in Table 10.2. The tree on the edge, rather than the tree inside the plantation, has been chosen for comparison with the point so that a 3 month rather than a $1\frac{1}{2}$ month period can be considered. The tree inside the plantation gave slightly longer periods of point discharge, but the difference is small compared with that between the point and the tree on the edge of the plantation.

The different amounts of point discharge on the two trees are discussed below in 11.2. The heights of the metal point and the tree on the edge of the plantation are 4 m and 18 m respectively. The horizontal distance between them is about 30 m. The potential gradient is measured 2.5 m above ground level at a position 20 m from the tree and 10 m from the point (see Fig. 8.2). An examination of the results shows that the magnitudes, of the mean currents in the tree and point, differed only by a factor of two, the values being -0.35 and $+0.34 \mu\text{A}$ for the point and -0.16 and $+0.19 \mu\text{A}$ for the tree. However, the most outstanding difference between the metal point and the tree is in their respective periods of point discharge. For the point the total period was 1500 min. compared with 125 min for the tree; a ratio of 12 : 1. This difference is presumably caused by the higher potential gradient needed to initiate point discharge on the tree. The metal point began to discharge at approximately 2600 Vm^{-1} during the period under consideration, whereas the records show that point discharge began on the tree at $7000-8000 \text{ Vm}^{-1}$. An examination of the potential gradient distribution shown in Fig. 10.17 shows that the periods of time for which the potential gradient was greater than $+8000 \text{ Vm}^{-1}$ correspond to the observed periods of discharge for the tree, these being

87 and 36 min for negative and positive currents respectively. It is concluded that the reason for the higher potential gradients needed to initiate point discharge on the tree is, mainly, that the points of the foliage on the tree are less sharp than the metal point. The laboratory experiments in Chapter 5 showed that, for both signs of potential gradient, the plate voltage at the onset of point discharge was 100% greater for spruce twigs, compared with the corresponding voltage for a sharp metal point. It may also be that the top branches of the tree are less exposed to high potential gradients than the metal point, despite their greater height. If we now consider the net charges transferred it can be seen that these are $-72 \times 10^{-4} \text{C}$ and $-4.3 \times 10^{-4} \text{C}$ for the metal point and tree respectively. Thus, the charge transferred by the tree is only 6% of that for the metal point, even though the tree is over four times as high. In view of this result, it can only be concluded that estimates of charge transfer by point discharge, using metal points of heights greater than 4m, are almost certainly in error.

In conclusion, it is thought that the techniques used in the present work offer the most reliable method yet devised for measuring point discharge on trees. However, improvements in the instrumentation are needed so that it can be installed lower down the tree and yet still measure the point discharge current. This would considerably reduce

the difficulties involved in the installation of electrodes. Thus it would then be possible to equip large numbers of trees with point discharge detectors and possibly make simultaneous measurements at more than one site.

11.2 The transfer of charge by point discharge on trees at Lanehead.

Measurements of point discharge on one tree on the edge of the plantation at Lanehead were made for three months. A second tree inside the plantation gave measurements during the second half of the above period. The behaviour of the two trees is compared below, and certain assumptions are made, so that an estimate of the amount of point discharge, for the whole plantation, can be obtained for the three month period. The mean monthly values of high potential gradients, in this period, are then compared with those for the rest of the year and the total charge transferred to earth for the plantation in one year is thus estimated. The significance of the resulting mean annual current density, for point discharge at Lanehead, is discussed. To conclude, the role of point discharge in some aspects of atmospheric physics is discussed in the light of the results of the present work.

The measurements, for the two trees in the plantation, made over a period of 1½ months are shown in Fig. 10.18 as distributions of current with time. The relevant quantities resulting from these measurements are compared for the two trees in Table 10.3. It is evident that the mean positive and negative currents measured in the two trees during this period were more or less the same and equal approximately to $+0.15 \mu\text{A}$ and $-0.16 \mu\text{A}$. However, the tree inside the plantation discharged for 75% longer than the tree at the edge. This implies that the former tree starts to discharge at lower measured values of potential gradient than the latter. The net charges transferred were $-1.55 \times 10^{-4} \text{C}$ and $-2.00 \times 10^{-4} \text{C}$ for the tree on the edge and the tree inside the plantation respectively. This difference can probably be explained in terms of the different shapes and exposures of the top sections of the trees. The tree inside the plantation is 21.5m high compared with 18 m for the tree at the edge. However, both trees are of the same heights as the trees immediately adjacent to them. The answer is probably, that, as the taller tree is the more pointed, its topmost branches will begin to discharge at lower potential gradients than those necessary for the other tree, despite the presence of surrounding trees. The question now arises as to the number of discharging branches at the top of a tree.

The positioning of the electrodes is such that they will detect only point discharge pulses produced at the top of the branch on which they are fitted. This means that there will probably be point discharge occurring on other parts of the tree. Trees with flatter tops may have a larger number of discharging branches. This offers an explanation of the unexpected result that the tree at the edge apparently gave less point discharge than the tree inside the plantation. The tree at the edge has a relatively flat top and the branch selected for the electrode is similar in exposure to seven or eight others. In the case of the tree inside the plantation the branch with the electrode is the highest and there are only two or three other branches on the tree which approach this height. Thus, to find the point discharge current for a tree we must know the total current from all branches.

If we now consider, not two trees, but the plantation as a whole, it should be possible to estimate the mean annual current density due to point discharge. To do this we must know:-

- i) The average number of branches per tree which discharge,
- ii) The average amount of point discharge per branch, and
- iii) The area of the plantation and the total number of trees.

The area of the plantation is about $3.75 \times 10^4 \text{ m}^2$ and there are about four trees per 100 m^2 . Thus the total number of trees is about 1500. A subjective assessment of typical trees in the plantation suggests that the average number of branches on each tree which might discharge is about 5. To find the average charge transferred to earth for each branch in a year, we have to take a value for the three month period when measurements were made and then estimate for the preceding nine months. The average high potential gradients measured in the 11 month period of October 1967 to August 1968 are within 5-10% of the average values for the three month period of June, 1968 to August 1968. Thus, there is reasonable justification in taking the three month period as being representative of the year as a whole if we allow for the different duration of high potential gradients in these periods. The net charge transferred, in one branch of the tree on the edge, was less than that for the tree inside. However, it is probably a more realistic value because this tree is more typical in shape than the tree inside the plantation. In three months the net charge transferred to earth through one branch of the tree on the edge of the plantation was $-4 \times 10^{-4} \text{ C}$. We can now estimate the net charge transferred in one year for the plantation. The

value obtained is $450 \text{ C km}^{-2} \text{ yr}^{-1}$. However, if only two branches on each of half the total number of trees discharge the value is $90 \text{ C km}^{-2} \text{ yr}^{-1}$. The latter value is probably an underestimate, whereas the former may be an overestimate. For the purpose of discussion let us take the value $270 \pm 180 \text{ C km}^{-2} \text{ yr}^{-1}$. Measurements on a greater number of trees are clearly necessary if the amount of point discharge is to be found to closer limits than those given above. However, it is interesting that the value found is of the same order as those previously estimated from measurements of point discharge on elevated metal points. CHALMERS and LITTLE's (1947) value for Durham is $-90 \text{ C km}^{-2} \text{ yr}^{-1}$. CHALMERS' (1949) estimate for Kew is $-125 \text{ C km}^{-2} \text{ yr}^{-1}$ and WORMELL (1953) found a value of $-170 \text{ C km}^{-2} \text{ yr}^{-1}$ for Cambridge. In view of the present degree of uncertainty of the value for the plantation at Lanehead, any further comparisons would have little meaning.

From the measurements made at Lanehead, there are several important conclusions to be drawn and these are now summarised below. First of all it has been found that trees at Lanehead do not begin to give point discharge until the measured potential gradient is greater than $7000\text{-}8000 \text{ Vm}^{-1}$.

This is in agreement with the conclusions of MAUND and CHALMERS (1960). The results also show that a tree inside the plantation gives similar amounts of point discharge compared with a tree on the edge. However, as a result of the high potential gradients necessary to initiate point discharge on trees, the amount of charge flowing to earth in the three month period was found to be only $4.3 \times 10^{-4} \text{C}$ for the tree compared with $72 \times 10^{-4} \text{C}$ for the metal point. A further consequence of the above is that space charge will originate at the trees in the plantation only on rare occasions. However, the work of OGDEN (1967) and the space charge measurements of BENT, COLLIN, HUTCHINSON and CHALMERS (1965) suggest that point discharge on isolated trees can occur at lower potential gradients. Thus, under these conditions significant space charge concentrations may originate from isolated trees.

In conclusion it should be emphasised that the site at Lanehead is by no means unique. In fact there are thousands of square kilometers along the pennines with landscapes similar to that of Lanehead and its surroundings. The fact that Lanehead is about 500 m above sea-level, and consequently that much closer to cloud base, means that potential gradients may be a little higher than at sea-level

but again this is not uncommon. In fact, CHALMERS (1952) argued that the nature of the ground surface does not influence the amount of point discharge. This is considered to be governed only by the rate of separation of charge in the storm cloud above. The experimental verification of this theory would make a big step forward in the understanding of natural point discharge.

CHAPTER 12Suggestions for further work12.1 The improvement of measuring equipment

If the design of the point discharge detector could be improved so that the capacitative electrode can be positioned lower down the tree, the task of installing the equipment on the trees would be much easier. It would then be practicable to instrument a large number of trees instead of the two used in the present work.

It would be an advantage to have the detectors as self-contained units each with their own means of recording the amount of point discharge. Thus, no external power supplies or recording system would be needed, and so experiments over a large area could be conducted.

Whilst it is thought that the detection of point discharge pulses offers the best approach to the measurement of point discharge on trees, it may be possible to detect the pulses in a different way by using an aerial to pick up the radio frequency interference produced by point discharge. This approach may prove to be the most practicable if experiments on a large scale are envisaged.

12.2 Further experiments

The continuation of the experiment at Lanehead, with improved equipment on a larger number of trees, will give a more accurate estimate of the amount of point discharge than has been made in the present work. In particular, it would be useful to determine the average number of branches which discharge per tree. As the measurements in the present work are limited to two trees, it has not been possible to see the effect on discharging trees of space charge produced at trees upwind. With measurements from several trees throughout the plantation, it would be possible to compare the amounts of point discharge on upwind and downwind trees.

Before any estimates of point discharge can be made for large areas, it is necessary to know to what extent the nature of the ground surface determines the amount of point discharge. It is suggested that, to begin with, measurements are made for different types of trees, as it seems likely that deciduous trees give less point discharge than conifers. (See MAUND and CHALMERS (1960)). Further experiments could include an investigation of the possibility of point discharge on grass and other vegetated terrain. There is also the question of to what extent point discharge occurs

over the surface of the sea and over desert areas. It was mentioned in 11.2 that CHALMERS (1952) argued theoretically that the amount of point discharge on the ground below a storm cloud is independent of the nature of the ground surface. The experimental verification of this result would be difficult but it would mean that large scale estimates of the amount of point discharge could be made with a much higher degree of certainty.

REFERENCES

1. AMIN (1954). "Fast time analysis of intermittent point-plane corona in air". American Journ. Appl. Phys. 25, 210, 358, 627.
2. BENT, R.B., COLLIN, H.L., HUTCHINSON, W.C.A. and CHALMERS, J.A. (1965). Space charges produced by point discharge from trees during a thunderstorm, J. Atmosph. Terr. Phys. 27, 67-72.
3. BROOKS, C.E.P. (1925). The distribution of thunderstorms over the globe, Geophys, Mem., Lond. 24 .
4. CHALMERS, J.A. (1943). The separation of electricity in clouds, Phil. Mag. 34, 63-7.
5. CHALMERS, J.A. and LITTLE, E.W.R. (1947). Currents of atmospheric electricity, Terr. Magn. Atmos. Elect. 52, 239-60.
6. CHALMERS, J.A. (1949). Atmospheric Electricity, Clarendon Press, Oxford.
7. CHALMERS, J.A. (1952). The relation between point discharge current and field, J. Atmosph. Terr. Phys. 2, 292-300.
8. CHALMERS, J.A. (1952). Point discharge currents. J. Atmosph. Terr. Phys. 2, 301-5.
9. CHALMERS, J.A. (1953). The charge on the ionosphere, J. Atmosph. Terr. Phys. 3, 345-6.
10. CHALMERS, J.A. (1953). The effective separation of discharging points, J. Atmosph. Terr. Phys. 3, 346-7.
11. CHALMERS, J.A. and MAPLESON, W.W. (1955). Point discharge currents from a captive balloon, J. Atmosph. Terr. Phys. 6, 149-59.
12. CHALMERS, J.A. (1962). Point-discharge currents through a living tree during a thunderstorm. J. Atmosph. Terr. Phys. 24, 1059-63.
13. CHALMERS, J.A. (1967). "Atmospheric Electricity". Second edition 1967. Pergamon Press.

14. CHAPMAN, S. (1956). Electrostatic Field Measurements, Corona Discharge and Thunderclouds, CAL Report 68, Cornell Aeronautical Lab., Buffalo, N.Y.
15. CLARK, J.F. (1958). The fair weather atmospheric electric potential and its gradient, Rec. Adv., pp. 61-73.
16. DAVIS, R. and STANDRING, W.G. (1947). Discharge currents associated with kite balloons, Proc. Roy. Soc. A, 191, 304-22.
17. DESIGN ELECTRONICS (1967). "Computer aided Design" June, p.64.
18. ETTE, A.I.I. (1966). Estimation of displacement currents in trees. J. Atmosph. Terr. Phys. 28, 831-838.
19. ETTE, A.I.I. (1966). Measurement of electrode by-passing efficiency in living trees, J. Atmos. Terr. Phys. 28, 295-302.
20. FEINBERG, R. (1966). Handbook of electronic circuits. Chapman & Hall.
21. FISCHER, H.J., (1962). Die Elektrische Spannung zwischen Ionosphäre und Erde, Thesis. Tech. Hochsch, Stuttgart.
22. FRANKLIN (1752). Phil. Trans. Roy. Soc. 47, 289.
23. GISH, O.H. and WAIT, G.R. (1950). Thunderstorms and the earth's general electrification, J. Geophys. Res. 55, 473-84.
24. HEAVISIDE, O. (1902). Telegraphy I. Theory, Encycl. Brit. 10th Edn., 33, 213-8.
25. HUTCHINSON, W.C.A. (1951). Point-discharge currents and the earth's electric field. Quart. J.R. Met. Soc. 77, 627-32.
26. ISRAEL, H. (1953). Bemerkung zum Energieumsatz im Gewitter. Geofis. Pur. Appl. 24, 3-11.
27. JHAWAR, D.S. (1967). The relation of point discharge to other parameters. J. Atmosph. Terr. Phys. 30, 113-123.

28. JHAWAR, D.S. and CHALMERS, J.A., (1967). Point discharge currents through small trees in artificial fields. *J. Atmosph. Terr. Phys.*, 29, 1459-1463.
29. KELVIN, LORD. (1860). Atmospheric electricity, Roy. Instn. Lect.; Pap. on Elec. and Mag., pp. 208-26.
30. KENNELLY, A.E. (1902). On the elevation of the electrically conducting strata of the earth's atmosphere, *Elect. World. N.Y.* 39, 473.
31. KIRKMAN, J.R. and CHALMERS, J.A. (1957). Point discharge from an isolated point. *J. Atmosph. Terr. Phys.* 10, 258-65.
32. KRAAKEVIK, J.H. (1961). Measurements of current density in the fair weather atmosphere, *J. Geophys. Res.* 66, 3735-48.
33. LARGE, M.I. and PIERCE, E.T. (1955). The fine structure of natural point discharge currents, *Quart. J.R. Met. Soc.* 81, 92-5.
34. LARGE, M.I. and PIERCE, E.T. (1957). The dependence of point-discharge currents on wind, as examined by a new experimental approach, *J. Atmosph. Terr. Phys.* 10, 251-7.
35. LOEB, L.B. (1965). Electrical coronas: Their basic physical mechanisms. Univ. California Press.
36. LUTZ, C.W. (1941). Über die Spitzentladung bei Gewittern und Schauern, *Beitr. Geophys.* 57, 317-33.
37. LUTZ, C.W. (1944). Über den Beitrag der Spitzentladung zur Aufrechterhaltung der negativen Erdladung. *Beitr. Geophys.* 60, 9.
38. MALAN, D.J. (1963). *Physics of Lightning*. The English University Press Ltd.
39. MILNER, J.W. and CHALMERS, J.A. (1961). Point discharge from natural and artificial points (II), *Quart. J.R. Met. Soc.* 87, 592-6.
40. MAUND, J.E. and CHALMERS, J.A. (1960). Point discharge from natural and artificial points, *Quart. J.R. Met. Soc.* 86, 85-90.

41. OGDEN, T.L. (1967) Durham Ph.D Thesis.
42. PIERCE, E.T., NADILE, R.M. and McKINNON, P.J. (1960). An Experimental Investigation of Negative Point-plane Corona and its Relation to Ball Lightning. Tech. Rep. Contract AF 19(604)-7342, Avco Cpn., Wilmington, Mass.
43. SCHONLAND, B.F.J. (1928). The interchange of electricity between thunderclouds and the earth. Proc. Roy. Soc. A, 118, 252-62.
44. SCRASE, F.J. (1933). The air-earth current at Kew Observatory, Geophys. Mem., Lond. 58.
45. SIMPSON, G.C. and ROBINSON, G.D. (1940). The distribution of electricity in thunderclouds II. Proc. Roy. Soc. A. 177, 281-329.
46. STERGIS, C.G., REIN, G.C. and KANGAS, T. (1957). Electric field measurements in the stratosphere, J. Atmosph. Terr. Phys. 11, 77-82.
47. TOWERS, T.D. (1965). Elements of Transistor Pulse Circuits. Iliffe Books Ltd.
48. TRICHEL, G.W. (1938). The mechanism of the negative point to plane corona near onset, Phys. Rev. 54, 1078-84.
49. WHIPPLE, F.J.W. and SCRASE, F.J. (1936). Point discharge in the electric field of the earth. Geophys. Mem., Lond. 68, 1-20.
50. WILSON, C.T.R. (1925). The electric field of a thundercloud and some of its effects, Proc. Phys. Soc., Lond. 37, 32D-37D.
51. WORMELL, T.W. (1930). Vertical electric currents below thunderstorms and showers, Proc. Roy. Soc. A., 127, 567-90.
52. WORMELL, T.W. (1953). Atmospheric electricity; some recent trends and problems, Quart. J.R. Met. Soc. 79, 3-50.

